FAST PYROLYSIS OF BIOMASS IN A CIRCULATING FLUIDISED BED REACTOR

IOANNIS PHILIPPOS BOUKIS

Doctor of Philosophy

THE UNIVERSITY OF ASTON IN BIRMINGHAM

June 1997

The University of Aston in Birmingham

FAST PYROLYSIS OF BIOMASS IN A CIRCULATING FLUIDISED BED REACTOR

IOANNIS PHILIPPOS BOUKIS

1997

SUMMARY

The objective of this work was to design, construct, test and operate a novel circulating fluid bed fast pyrolysis reactor system for production of liquids from biomass. The novelty lies in incorporating an integral char combustor to provide autothermal operation.

A reactor design methodology was devised which correlated input parameters to process variables, namely temperature, heat transfer and gas/vapour residence time, for both the char combustor and biomass pyrolyser. From this methodology a CFB reactor was designed with integral char combustion for 10 kg/h biomass throughput.

A full-scale cold model of the CFB unit was constructed and tested to derive suitable hydrodynamic relationships and performance constraints. Early difficulties encountered with poor solids circulation and inefficient product recovery were overcome by a series of modifications.

A total of 11 runs in a pyrolysis mode were carried out with a maximum total liquids yield of 61.50 % wt on a maf biomass basis, obtained at 500°C and with 0.46 s gas/vapour residence time. This could be improved by improved vapour recovery by direct quenching up to an anticipated 75 % wt on a mositure-and-ash-free biomass basis.

The reactor provides a very high specific throughput of 1.12 - 1.48 kg/hm^2 and the lowest gas-to-feed ratio of 1.3 - 1.9 kg gas/kg feed compared to other fast pyrolysis processes based on pneumatic reactors and has a good scale-up potential. These features should provide significant capital cost reduction.

Results to date suggest that the process is limited by the extent of char combustion. Future work will address resizing of the char combustor to increase overall system capacity, improvement in solid separation and substantially better liquid recovery. Extended testing will provide better evaluation of steady state operation and provide data for process simulation and reactor modeling.

Key words: biomass; reactor; design; circulating fluidized bed; pyrolysis liquids; fast pyrolysis;

Acknowledgments

I would like to thank several people who helped and assisted me during the execution of this work. I am indebted to them all and especially to:

Prof. A.V. Bridgwater for his continuous support, guidance and sincere efforts for the completion of this work. I am particularly grateful for his superior patience and for always being there to provide constructive comments through stimulating discussions and helping remove barriers and problems even though everything looked dark and obscured by clouds.

Dr. K. Maniatis for his valuable technical suggestions, friendship, good-fellowhip, stimulating discussions as well as his unyielding efforts to provide good engineering basis for this work and trying to make me read between the lines.

Prof. Sp. Kyritsis for his valuable comments, moral support and good sense of humor as well as for providing the space to carry out this work at the Agricultural University of Athens.

Dr. Ch. Sooter for being supportive to this work, especially during the difficult initial period.

Mr. D. Kasinas, Mr. B. Giannopoulos for the electrical work and particularly Mr. Efstathios Karahisaridis (Bokas) for setting up the data acquisition system and providing excellent support during the painstaking layout of this work.

Mr. Lukas Gabriel who assisted during the construction, commissioning, maintenance and experimentation of this work and Mr. Dionissios Papavasiliou for the gas analysis.

Mr. I. Varotsos and Mr. G. Giannakopoulos for the construction of the reactor and related equipment.

My colleagues in the Centre for Renewable Energy Sources, in particular Maria Zacharopoulou and Mrs. I. Siadima for helping me in editing a large part of this work.

My parents, Philippos and Alexandra for their help and support in many ways.

My dearest wife, Rebecca who was always there to help and support me through her perpetual care, love and encouragement and Philippos for his patience and his inspiring smile.

CONTENTS

List of figures

Chapter 4

Chapter 5

Chapter 9

Chapter 10

List of tables

Chapter 5

Chapter 6

Chapter 7

Chapter 8

Chapter 9

CHAPTER 1: BACKGROUND

1.1 Introduction

Biomass makes a significant contribution to today's primary energy supply, perhaps as much as 10%, but much of it is squandered by inefficient use. Furthermore, biomass is often exploited on an unsustainable basis at great cost to the environment. New approaches, centered on modern technology, are required to enable the full potential of this resource to be unlocked.

Biomass energy utilization as a modern energy technology has its origins in the early 1970's. The cause was that due to the two oil embargoes during the 1970's, the energy supply had been disrupted. The subsequent fluctuations in all energy prices forced many industries to examine alternative feedstocks, such as wood wastes, agricultural residues and other low-grade feedstocks. This gave those industries a level of control over their energy needs, and sparked the development of new, more efficient technologies to wring more energy from biomass feedstocks.

However, the commercial attractiveness of biomass systems was begun to be realised to be poor in the late 1980's in conjunction with the low oil and natural gas prices prevailing. Thus, the economic attractiveness of biomass-to-energy systems was seriously questioned. On the other hand, extensive use of biomass was once more justified due to globally increasing environmental concern. Although no firm evidence of global warming can yet be identified, it is widely believed that an augmented "greenhouse effect" could have a severe impact on the world economy, and there is a growing support for precautionary action directed at reducing the CO_2 emissions from fossil fuels. Moreover, biomass is essentially sulphur-free, its enhanced exploitation reducing SO_x emissions and, hence, the negative impacts of acid rain deposits.

Besides the growing environmental concern, additional driving forces for the extensive, rational use of biomass for energy purposes, such as positive socioeconomic impacts, local energy security, industrial competitiveness and a favourable public attitude towards renewables may be quoted.

The biomass grown for energy purposes in carbon storage forests could theoretically provide an indefinite flow of commercial energy. The exploitation of biomass grown on such a fully sustainable basis is essentially carbon neutral to the atmosphere, as the carbon released by burning the fuel is balanced by the carbon fixed photosynthetically in new tree growth.

Moreover, biomass exploitation for energy purposes has a series of socioeconomic advantages listed below:

- energy independence on a regional scale, leading to the decrease of the extensive oil import market in the majority of the European Union countries
- valorisation of forestry and agricultural residues
- reduction of agricultural surpluses, which is of extreme importance in the European Union to comply with the Common Agricultural Policy
- increase in income for rural areas and a reduction in urbanisation rates
- exploitation of marginal lands in rural areas leading to employment increase
- provision of innovative technological choices for development in rural societies
- revitalization of the farm sector.

However, in spite of the advantages referred to above, some conversion processes would be desirable before using biomass as an energy source. This is due to the fact that solid biomass fuels have a low-energy density, particularly in the raw state, so commercial opportunities in kilns or boiler applications are limited to locations close to the point of biomass production by energy market economics, particularly transport costs. Among the different approaches to overcome these limitations, one of the most convenient ones is biomass conversion from solid, raw and bulky feedstock to easily stored and transported liquid fuels.

There are two main routes for converting biomass into liquid fuels; biologically by utilizing the enzymatic action of bacteria and yeast, Figure 1-1 (Coombs, 1986), or thermochemically which is the conversion of biomass by heat and chemical reaction, Figure 1-2 (Bridge, 1990). Biological conversion processes are best suited to wet feedstocks (moisture content >40 % wt) and incorporate low temperature biological actions, such as fermentation and digestion, which are best suited for sugar- or carbohydrate-rich feedstocks, such as sugarcane, sweet sorghum or corn. Thermochemical conversion processes are on the other hand particularly suitable for relatively dry (moisture content <20 % wt) feedstocks rich in lignin, which is the main constituent of woody biomass and withstands enzymatic action. Thus, thermochemical

conversion methods achieve a better utilisation of biomass energy content than biological conversion methods, providing better valorisation of the vast quantities of both woody biomass and the majority of agricultural wastes and forest residues (Grassi, 1989).

Biomass

Figure 1-1: Conversion of biomass to liquids (ethanol) via a biological route (Coombs, 1986)

Figure 1-2: Conversion of biomass to liquids (pyrolysis liquids) via a thermochemical process (Bridge, 1990)

An additional disadvantage for the biological conversion methods, as far as liquids production is concerned, is that they are carried out in long periods covering time intervals from some hours to some days, while thermochemical conversion routes are carried out in seconds or minutes. Another requirement for biological conversion is that each component of biomass must be processed separately. The above restrictions do not apply to thermochemical conversion and therefore, the latter ones are considered the most promising route for producing liquids from biomass.

Out of the four main thermochemical processes of biomass conversion listed in Table 1-1, pyrolysis is one of the most promising ones, being developed to directly convert biomass into liquid fuels, liquefaction (at high pressure) being an alternative route. Liquefaction may also be possible indirectly via gasification followed by reforming of synthesis gas to methanol.

Table 1-1: Thermochemical conversion technologies and products (Bridgwater and Bridge, 1991)

Technology	Primary Product	Example of application
Pyrolysis	Gas	Fuel gas
	Liquid	Liquid fuel substitution
	Char	Solid fuel of Slurry fuel
Gasification	Gas	Fuel gas
		Methanol or gasoline (indirectly)
Liquefaction	Liquid	Liquid fuel substitution
Combustion	Heat	Heating

As already mentioned, much of the present interest in thermochemical conversion activities centres on liquid products due to their high energy density, in comparison with the raw feedstock which reduces the cost of storage and transport, Table 1-2.

Table 1-2: Some characteristics of biomass and fuel derivatives from thermochemical conversion methods (Bridgwater and Bridge, 1991)

Energy carrier	Bulk density (kg/m^3)	Heating value (GJ/t)[1)]	Energy density(GJ/m^3)
Straw	~100	20	2
Woodchips	~400	20	8
Pyrolysis Liquids	~1200	23	27
Char	~300	30	9
Char-water slurry	~1000	15	15
Char-oil slurry	~1500	24	28

1) on a moisture and ash free (maf) feedstock basis

Liquid products potential is, hence, considered very important for premium conventional, liquid fuel substitution in a variety of applications, such as:

- heating, i.e., substitution of heavy fuel oil in boilers and furnaces (Gust, 1997)
- electricity generation and hence substitution of heavy or lighter fuel oil in stationary internal combustion/diesel engines (Leech, 1997) and gas turbines (Patnaik, 1997)

- transportation fuels indirectly via high pressure hydrotreating (Baldauf, 1997; Kaiser, 1997) or zeolite upgrading (Diebold *et al.*, 1988).

Besides the much higher energy density, the justifications for the transformation of biomass to liquid fuels via thermochemical conversion methods also incorporate:

1. A liquid fuel fits very well to the existing infrastructure for conventional liquid fossil fuels, so that minor equipment modifications at low cost are required to pump, transport, store and utilize pyrolysis liquids in industrial burners, furnaces, modified diesel engines or gas turbines, provided proper handling of pyrolysis liquids (i.e. storage at low temperatures, proper mixing and prolonged contact with air is avoided).
2. Storage costs are, as said, minimal so that seasonal harvesting and conversion are more feasible than for example gasification, where the product (gas) has to be processed immediately on site.
3. As for pyrolysis liquids, which are composed of a very complex mixture of oxygenated hydrocarbons, their upgrading to high-value-added chemicals, like phenols or anhydrosugars, in a secondary processing plant may also prove a viable commercial activity in the near future. These components can be utilized pure or blended with other materials, or serve as precursors for the production of many other fine and speciality chemicals, reducing significantly the cost for their production via traditional, complex synthetic chemistry pathways.

1.2 Biomass fast pyrolysis

Biomass pyrolysis is the thermal degradation in the complete absence of an oxidising agent, or with such a limited supply that gasification does not occur to an appreciable extent (Bridgwater and Evans, 1993). Compared to gasification, relatively low temperatures of 400-800°C are employed. Gas, liquid and solid char are produced, the relative proportions of which depend very much on the reaction parameters of temperature and reaction time as well as of the rate of heat transfer to biomass feedstock. The process of pyrolysis and the products derived are described in detail in Chapter 2.

According to the discussion held above, a suitable biomass transformation process should proceed via a thermochemical route maximising the amount of the desired energy carrier, considered to be a liquid product, at the expense of the solid char and pyrolysis gas, which are then considered as reaction byproducts. Among the various thermochemical processes

studied and assessed in the past for the transformation of biomass to liquids, fast pyrolysis (IEA, 1988), that is the conversion of biomass feedstocks at atmospheric pressure to liquids in a fraction (fast) of a second, presents a number of significant advantages compared to other liquefaction processes incorporating high pressures (high-pressure liquefaction) or requiring a significant number of intermediate steps (methanol synthesis via gasification).

Biomass fast pyrolysis is today practised in a variety of reactor configurations incorporating some form of external heat provision to the biomass feedstock. However, significant advantages could be achieved, when fast pyrolysis is carried out in a reactor configuration directly utilizing the high energy content of byproduct char, in order to cover pyrolysis thermal requirements.

1.3 Purpose of this work

The above considerations, namely fast pyrolysis of biomass in a reactor configuration incorporating utilisation of char energy content in a rational way, in order to provide the heat requirements for the pyrolysis process, was the main objective of this thesis.

More specifically, during this work, sponsored by the European Commission Directorate General XII JOULE (Joint Opportunities for Unconventional or Long-term Energy) Programme, a new reactor technology was developed in order to obtain information on the potential of internally utilizing the char content in an appropriate reactor scheme in the range of 8-12 kg/h.

Among the different approaches for biomass pyrolyzers adopted over the years, critically reviewed and evaluated in the course of this thesis, it has been concluded that a circulating fluidised bed with integral char combustion should be an ideal candidate reactor configuration to meet the main objective on reactor design set above.

In order to carry out this major output, some key steps were necessary, namely:

1. Understand the complex and transient nature of the biomass pyrolysis process and interaction of the reactions, pathways and effects of process parameters on product yields and other essential characteristics for reactor design and optimisation.
2. Design and construct a novel, bench scale fast pyrolysis plant for the fast pyrolysis of biomass, in order to produce liquid fuels. According to the discussion above, the thermal

requirements of the pyrolysis process will be covered by the internal utilization of the byproduct char energy content.

3. Operate the bench scale plant to identify the key problems associated with reliable reactor operation, taking all the necessary measures to correct or improve them.
4. Establish the effect of key process parameters on the performance of the biomass fast pyrolysis reactor system.
5. Derive relationships and models for performance prediction and control of the proposed circulating fluidised bed.
6. Produce a design methodology for a scaled-up pilot plant.

1.4 Structure of this thesis

This thesis involves the design, construction and operation of a novel circulating fluidised bed fast pyrolysis reactor for the production of pyrolysis liquids from biomass, providing for autothermal operation through the integral utilisation of char energy content. The construction of a product recovery system is also included.

In order to gain insight on the process fundamentals a thorough review of the principles of biomass fast pyrolysis is undertaken, Chapter 2, and a review of reactor systems designed to maximise liquid yields is performed, Chapter 3, leading to new concept for a novel reactor configuration, comprising of a Circulating Fluidised Bed (CFB). Detailed sizing of the proposed CFB reactor components is undertaken in Chapter 4. The construction and testing of a cold reactor model to gain experience from reactor operation and establish relationships between key reactor operating parameters is described in Chapter 5. Sizing of peripheral and auxiliary CFB reactor equipment is performed in Chapter 6, and a detailed description of the CFB biomass fast pyrolysis plant, as first built, is described in Chapter 7. Problem identification and remediation procedures adopted as well as commissioning experiments are described in Chapter 8, while the actual experimental work and reactor operation is described in Chapter 9. Reactor stability issues and proposed control strategies are further referred to in Chapter 10. Finally, the conclusions of this thesis and recommendations for future work ar given in Chapter 11.

The structure of this thesis is depicted in Figure 1-3, below:

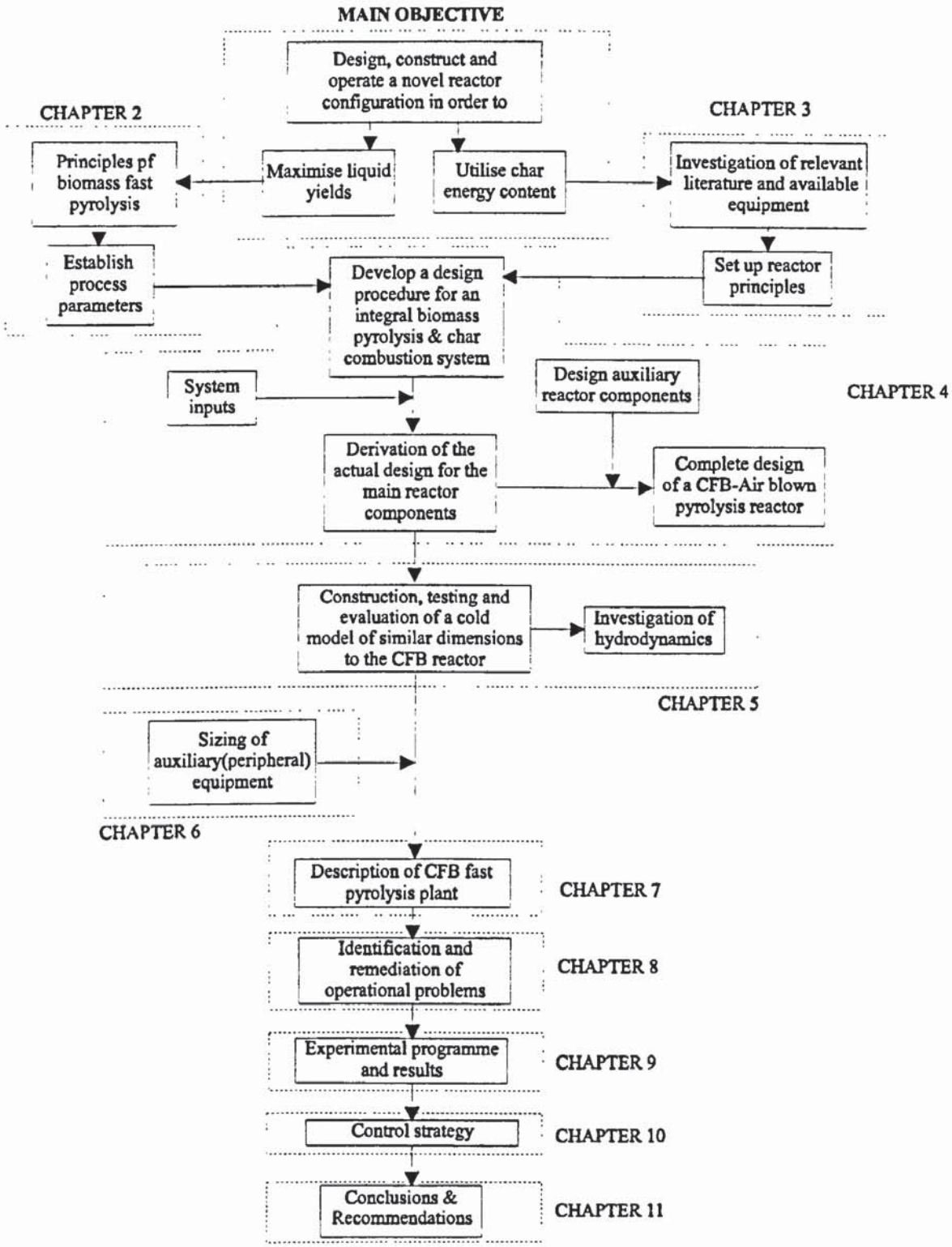

Figure 1-3: Structure of this thesis

CHAPTER 2: THE PRINCIPLES OF BIOMASS FAST PYROLYSIS

2.1 Introduction

Biomass includes wood, grasses and agricultural crops and may be defined as a renewable source of fixed carbon in the short term (Beenackers and Bridgwater, 1989). Biomass typically has three main constituents: cellulose, hemicellulose and lignin with minor constituents including resins, ash and extractives. It is not necessary to describe and review the wood physical structure here, as this has minimal effect on the primary thesis objectives. The reader may find excellent summaries in the relevant literature (Browning, 1963; Wenzl, 1970; Sjöström, 1981).

The high percentage of volatile matter in biomass feedstock favours higher yields in liquid and gaseous products, compared to coal, so that biomass conversion could play an important role in meeting the growing need for high quality fuels and chemicals. Biomass can be converted to different types of fuels (solid, liquid or gas) by a variety of thermochemical processes, see Chapter 1. While conventional pyrolysis processes such as slow pyrolysis and carbonisation transform biomass into a variety of low value products, including gases, tars and solid char, this process could be modified to give high yields of specific liquid product species through understanding of the selective material and energy transformations, explored and understood through the discipline of chemistry, and careful reactor design using appropriate heat transfer mechanisms, investigated and studied through the discipline of process engineering.

In particular, fast pyrolysis of biomass has been shown to give very high yields of pyrolysis liquids (also termed pyrolysis oil, biofuel oil, bio-crude or simply bio-oil), which can further be burnt with minimum retrofitting in existing oil fired burners (Freel and Huffman, 1995), used for power generation in diesel engines (Solantausta *et al.*, 1995) or gas turbines (Andrews *et al.*, 1995), upgraded by zeolites (Diebold *et al.*, 1988) or hydrotreatment (Elliot and Baker, 1986) to diesel and gasoline grade transportation fuels or be used as feedstock for specialty and commodity chemicals (Radlein, 1997).

In the following, the review is focused on mechanisms, chemical pathways and kinetics of biomass pyrolysis in order to define fast pyrolysis in terms of the requirements for process

conditions (temperature and residence times) and the most appropriate chemical pathway in order to maximize the desired product yields. A review of biomass pyrolysis kinetics is also given in order to provide a sound basis for reactor dimensioning. Finally, fast pyrolysis is characterized in terms of heat transfer requirements in order to achieve the necessary heating rates so that the desired product distribution is obtained.

2.2 Pyrolysis and fast pyrolysis

The pyrolysis of biomass to produce gases, liquids and char is an ancient process. Once a source of bulk chemicals (acetone and methanol in the Lambiotte process)), biomass pyrolysis is practiced now as a method for producing pyrolysis liquids and specialty chemicals (e.g. the RTP process, Section 3.6). Pyrolysis liquids were until recently considered essentially by-products of the char production, a slow process operated at temperatures about 350-450°C.

Pyrolysis may be defined as the thermal decomposition of organic materials occurring in the absence of oxidant (air or oxygen), although some researchers consider oxygen-deficient thermal degradation of biomass feedstock to be a true pyrolysis process, as long as the primary products are liquids or solids (Soltes *et al.*, 1981; Graham *et al.*, 1982). This process may also include partial gasification (Antal 1980c; Bridgwater and Beenackers, 1989; Bridgwater and Bridge, 1991).

Carbonisation has been used for centuries to produce charcoal, tars, alcohols and other solvents and is usually carried out in batch processes using kilns or retort furnaces (Tillman, 1977; Luengo and Censig, 1991). Conventional pyrolysis is similarly characterized by a low feedstock heating rate (less than 10°C/s), low temperatures (less than 500°C) and relatively extended gas/vapor and solids residence times (greater than 50 s for the gas, while solids residence times may vary from minutes to days). The slow devolatilization of the feedstock and the subsequent coking and recombination reactions in the vapor phase, usually termed secondary reactions, result in tar and char as the primary products (Shafizadeh and Fu, 1973; Graham *et al.*, 1982). The secondary reactions are allowed to occur in the reactor, after primary pyrolysis has taken place, due mainly to the prolonged gas/vapor and solids residence times. Pyrolysis at high heating rates, termed as fast, flash, rapid or ultra pyrolysis, according to heating rates, reactor temperature and residence times, substantially changes the proportions of gas, liquid and solid products.

Fast pyrolysis for liquids production is a rapid heating rate process (>100°C/s) occurring at moderate temperatures (typically 400-600°C) and very short gas/vapor product residence times (typically less than 2 s). Fast pyrolysis can give high yields of liquid oil products at the expense of char and gas. Vapor residence times are normally less than 2 s (Shafizadeh and Fu, 1973; Graham *et al.*, 1982; Scott and Piskorz, 1982). Until recently, fast pyrolysis was differentiated (Graham *et al.*, 1984) from flash pyrolysis with respect to temperature (greater than 600°C), vapor residence time (less than 0.5 s) and end product, this process primarily aiming to maximize the production of high-quality gases (i.e. olefins and other hydrocarbons) at the expense of char and condensable liquids (Reed *et al.*, 1980; Deglise *et al.*, 1981). Over the past five years, the distinction between fast and flash pyrolysis has largely disappeared (Dave *et al.*, 1979; Bridgwater and Double, 1989; Bridgwater and Bridge, 1991), so that in the following, the term fast pyrolysis will be used to describe any thermal process characterised by:

- high heating rates (>1000°C/s)
- reactor temperatures greater than 450°C
- short vapor residence times (<2 s)
- rapid product quenching.

Other work has attempted to exploit the complex degradation mechanisms by carrying out pyrolysis in unusual environments. The characteristics of the main modes of pyrolysis are summarised in Table 2-1, and variants are summarised in Table 2-2.

Table 2-1: Characteristics of pyrolysis processes (from Bridgwater and Bridge, 1990)

Variant	Residence Time	Heating Rate	Temperature (°C)	Major product
Carbonisation	hrs-days	very low	400	charcoal
Conventional	5-30 min	low	600	liquids, charcoal & gas
Slow	0.5-5 s	fairly high	650	liquids
Fast (liquid)	<1 s	high	< 650	liquids
Fast (gas)	<1 s	high	> 650	chemicals & fuel gas
Ultra	<0.5 s	very high	1000	chemicals & fuel gas
Vacuum	2-30 s	medium	400	liquids
Hydro-pyrolysis	<10 s	high	< 500	liquids & chemicals
Methano-pyrolysis	<10 s	high	> 700	chemicals

Table 2-2: Pyrolysis Technology Variants (Bridgwater and Bridge, 1991)

	Carbonisation	Slow	Fast (liquids)	Fast (gases)
Parameters				
Temperature, °C	300-500	400-600	450-600	700-900
Pressure, bar	1	0.1-1	1	1
Maximum throughput achieved, dry t/h	5	1	0.05	0.10
Products (dry basis on dry feed)				
Gas yield, % wt	up to 150	up to 60	up to 30	up to 80
HHV, MJ/Nm^3	3-6	5-10	10-20	15-20
Liquid yield, % wt	up to 25	up to 30	up to 70	up to 20
HHV, MJ/kg	20	20	24	22
Solid yield, % wt	up to 40	up to 30	up to 15	up to 15
HHV, MJ/kg	30	30	30	30

As seen from the tables presented above, the relative yields of gas, liquid and char products depend strongly on the pyrolysis method and process parameters, such as heating rate, gas residence time, temperature and pressure. The influence of these parameters will be discussed in more detail in the following sections.

2.3 Primary pyrolysis of lignocellulosic components

The pyrolysis of biomass involves very complex organic chemistry, which is not at all well understood. Biomass is composed primarily of cellulose, hemicelluloses, which are polysaccharides in nature, and lignin, which is a polymer formed from phenylpropane units. The difficulties in studying the phenomenon of pyrolysis can be traced partly to the great chemical and structural diversity of the materials coupled with their low thermal stability. These properties result in a complex array of products on decomposition which themselves are also thermally sensitive. Moreover, small differences in feedstock properties and reaction conditions may cause large changes to the product spectrum. In the following, the three biomass constituents are characterized with respect to their primary pyrolytic behaviour.

If biomass is completely pyrolysed, resulting products are about what would be expected by pyrolyzing its three components separately, although synergistic effects are evident (Browne,

1963; Antal, 1980a). In the following, a review of cellulose, hemicellulose and lignin decomposition mechanisms and pathways during pyrolysis is presented.

2.3.1 Cellulose pyrolysis

Cellulose, the principal wall component in woody tissues, is a biopolymer of anhydroglucose units, connected to each other by glycosidic bonds. Of all lignocellulosic components, the thermal decomposition of cellulose has been best characterized. Until 1980, research was related to flame retardants and fire research, e.g. as reviewed by Shafizadeh (1968) and by Byrne *et al.*,(1966). It was Madorsky, as reviewed in Byrne *et al.*,(1966), who first proposed two pathways for cellulose decomposition: the first preserving the cellulose chain hexose units by depolymerisation, and the second leading to fragmentation of the monomers by dehydration and condensation reactions. This is further referred as the two-competing pathways mechanism for cellulose pyrolysis.

According to this first adopted concept for cellulose pyrolysis mechanism, described in detail by Kilzer and Broido (1965), cellulose pyrolysis proceeds by two reactions as above, namely dehydration, evolution of light gases (CO_2, CO, etc.) and charring at low temperatures (<280°C) and the depolymerisation producing tar, primarily levoglucosan, the characteristic monomers tar unit. The cellulose pyrolysis pathway is depicted in Figure 2-1.

Figure 2-1: The two competing pathways mechanism for cellulose decomposition (Kilzer and Broido, 1965)

To account for the ultimate formation of the char residue and to highlight the structure of "dehydrocellulose", Kilzer and Broido proposed that cross-linking reactions of the cellulose chains take place. This occurs exothermically in the region of 220°C with evolution of water, which is the product of etherification between C_4 and C_6 of adjacent cellulose chains. The structure of this "dehydrocellulose" was thought to involve a tedrahydro-5-hydroxy-methylfurfural, which yield upon decomposition 5-hydroxy-methyl furfural and water by subsequent rearrangement (Weinstein and Broido, 1970), Figure 2-2.

Figure 2-2: Mechanism of cross-linking and dehydration (Weinstein and Broido, 1970)

Byrne *et al.*,(1966) accepted the hypotheses made by Madorsky and Kilzer and Broido and using gas-liquid chromatography tried then to actually identify specific chemical intermediates in the two competing pathways mechanism. Byrne confirmed the presence of 19 carbonyl compounds, determining that hydroxyacetaldehyde (glycol aldehyde) and glyoxal are the most important and abundant intermediates and correctly reporting that anhydrosugars and carbonyl compounds are produced by competing and not sequential reactions. However, Byrne accepted the two-competing pathways mechanism proposing, in error, that the volatile, carbonyl compounds formation is a reflection of the low temperature, i.e. less than 300°C, pathway proposed by Kilzer and Broido (1965). This proposal is wrong, since the experiments in this paper were carried out at 420°C, the product yields and composition being therefore not representative of the lower temperature route. Moreover, recent research (Piskorz *et al.*, 1986), reviewed later in this section, has confirmed that the carbonyl-forming reactions compete with anhydrosugar-forming reactions at elevated temperatures.

A three-competing reactions pathway for pyrolysis of cellulose was proposed some years later by Shafizadeh (1968). According to this hypothesis, each pathway was postulated to depend upon the pyrolysis temperature, Figure 2-3. The first pathway dominates at lower temperatures (<280°C) and involves cellulose dehydration reactions, which result in a reduction in cellulose degree of polymerisation (DP) by bond scission, the elimination of water, formation of char and the evolution of carbon oxides. The reduced DP solid substrate, which is formed after bond scission, and which precedes char formation, is often referred to as "anhydrocellulose" or "dehydrocellulose", and does not occur with any marked specificity nor does it yield valuable products.

Figure 2-3: Three-competing reactions cellulose pyrolysis pathway (Shafizadeh, 1968)

At about 300°C a second major degradation pathway competes significantly with dehydration. This pathway, known as depolymerisation or fragmentation predominates with increasing temperature (Shafizadeh *et al.*, 1979) and is accomplished by transglycosylation, a rapid chain cleavage of the glycosidic bonds accompanied by free hydroxyl group substitution and rearrangement of the monomers to levoglucosan (1,6-anhydro-β-D-glucopyranose). Transglycosylation takes place when the molecule has gained sufficient flexibility (activation) and produces besides levoglucosan, its furanose isomer and larger randomly linked oligosaccharides, as shown in Figure 2-4 (Shafizadeh and Fu, 1973). Shafizadeh reports levoglucosan yields of up to 40 % wt from vacuum pyrolysis, while similar yields have been obtained by fast pyrolysis at atmospheric pressure. Diebold (1986) summarises the levoglucosan formation mechanism as a chain cleavage followed by a subsequent rearrangement of the resulting anhydroglucose monomers to levoglucosan.

The inter- and intra-molecular transglycosylations shown in Figure 2-4 are accompanied by dehydration. Levoglucosan and other less abundant primary tars may undergo secondary vapor phase reactions resulting either in repolymerization of stable heavy syrups (secondary tars) or cracking to lighter fragments and carbon black. These fission and disproportionation secondary reactions, which are taking place in the vapor phase, are further discussed in Section 2.4.

According to this model, depolymerisation is favoured at temperatures between 300 and 500°C, while for high heating rates fast pyrolysis results in a mixture of low-molecular gaseous or volatile products, the formation of which was attributed by Shafizadeh (1968) to fission, dehydration, disproportionation, decarboxylation and decarbonylation reactions. The volatile products assumed were primarily carbonyl compounds, namely hydroxyacetaldehyde, furaldehydes and glyoxal.

Figure 2-4: Detailed decomposition of cellulose to decomposition products at higher temperatures (Shafizadeh and Fu, 1973)

Although Shafizadeh earlier proposed a third cellulose pyrolysis pathway at high temperatures, forming carbonyl compounds and competing to tar formation, he described only two of the primary pyrolysis pathways in most of his publications (Shafizadeh, 1982b), not being fully convinced that the third pathway was in fact a competing reaction. He believed that the low-molecular mass volatiles were produced from anhydrosugars in subsequent vapor phase ring cleavage reactions rather than from competing reactions from direct fragmentation of the cellulosic ring. Thus, Shafizadeh and co-workers (Bradbury *et al.*, 1979) lumped the formation of those products into the second, depolymerisation reaction pathway, in a modified Kilzer and Broido two-competing reactions pathway, Figure 2-5.

Figure 2-5: Two-competing reactions cellulose pyrolysis pathway (Shafizadeh, 1979)
(1º indicates primary and 2º secondary pyrolysis reactions)

Moreover, various attempts to determine the kinetic rates of the two competing reactions postulated initially by Kilzer and Broido and later by Shafizadeh's group for the pyrolysis of cellulose, led Bradbury *et al.*,(1979) to the postulation of a reaction, which precedes the formation of char and volatile condensable organics (levoglucosan), due to an observed induction period. The intermediate from this initial reaction was called "Active" and was found (Broido *et al.*, 1973) to have a much lower DP than the initial cellulose feedstock, indicating the existense of a liquid or plastic state during pyrolysis. In the model proposed by Shafizadeh's group and presented in Figure 2-5, developed to obtain chemically meaningful data (further discussed in detail in Section 2.6.2), it was assumed that the initiation reactions led to the formation of an "active cellulose", which subsequently decomposes by two competitive first order reactions, one yielding anhydrosugars (levoglucosan) and the other char and a gaseous fraction.

The confirmation that the third pathway, originally referred to by Shafizadeh (1968), is in fact a primary competitive pyrolytic mechanism has been the integrated result of recent research, particularly by researchers at Waterloo University (Piskorz *et al.*, 1986; Piskorz *et al.*, 1989; Radlein *et al.*, 1991; Scott *et al.*, 1992), and other North American groups (Antal, 1983; Evans and Milne, 1984, 1985; Richards, 1987). Thus, the existence of carbonyl compounds, such as hydroxyacetaldehyde, as primary intermediate products has been confirmed and Shafizadeh's three-competing reactions pathway of cellulose pyrolysis has been enhanced and clarified. High yields of hydroxyacetaldehyde derive primarily from direct fragmentation, i.e. via ring cleavage of the cellulose polymer chain.

Although, as discussed above, evidence of a second competing pathway at high temperatures was probably known to Shafizadeh through kinetic studies, the volatiles and gases identified were attributed to secondary decomposition products derived by cracking of anhydrosugars at elevated temperatures, rather than primary products from direct fragmentation of cellulosic rings. The low-molecular weight products were supposed to form by fragmentation of principal intermediates like levoglucosan and cellobiosan (Pouwels *et al.*, 1989) according to a mechanism, which could be rationalized in terms of a sequence of dehydration, retroaldolisation and decarbonylation reactions. Various researchers (Shafizadeh and Fu, 1972; Schulten and Gortz, 1978) showed that similar low molecular weight products can be formed by secondary pyrolysis, indicating that the second cellulose pyrolysis pathway, i.e. the modified Kilzer-Broido reaction scheme shown in Figure 2-5, was reasonable.

This was initially accepted by Piskorz *et al.*,(1986) but then rejected after a landmark study conducted by Richards (1987), who argued that it is more likely that hydroxyacetaldehyde forms directly from cellulose by a plausible mechanism involving dehydration followed by a Diels-Alder reaction, Figure 2-6.

Figure 2-6: Hydroxyacetaldehyde formation according to Richards (1987)

Data published by Piskorz *et al.*,(1989), showing the variation of hydroxyacetaldehyde yields with temperature, are compatible with the mechanism suggested by Richards (1987). This is also compatible with earlier evidence provided by Hopkins and Antal (1984), according to which there exists a pathway for the direct fragmentation of cellulose to low molecular weight products. These postulations are in agreement with the initial, earlier proposal of Shafizadeh (1968). The wide acceptance of the three-competing pathways mechanism provides a simple yet elegant model of cellulose primary pyrolysis, shown in Figure 2-7, and provides a basis to relate and integrate the results from a broad range of biomass pyrolysis studies, both fast and slow.

According to the proposed Waterloo Model, (Piskorz *et al.,* 1991) cellulose decomposes by three major parallel pathways with one or another being dominant according to temperature, intrinsic effects, i.e. cellulose morphology, DP and presence of alkali cations as well as the reaction process parameters such as temperature, heating rate and pressure.

A more or less similar model for cellulose pyrolysis is accepted by Graham (1993), slightly modified by the fact that the initial activation step is common to all of the three subsequent primary steps.

Figure 2-7: The Waterloo model proposed for cellulose decomposition pathways (Scott *et al.*, 1991)

It is important to note that in these very similar models the initial "activation" step is once more involved. This step was previously discussed under the work of Bradbury *et al.*,(1979).

Although the available mechanisms for cellulose pyrolysis do not fully illustrate the exact way chemical reactions occur, a definitive reaction pathway, namely the Waterloo reaction pathway, has been generally accepted. This pathway clearly exhibits that cellulosic biomass can be converted to the following generic products via three competing primary pyrolysis reactions:

1. Dehydration products (char, H_2O and gas).
2. Depolymerisation products (primary anhydrosugars).
3. Fragmentation products (carbonyls, acids and alcohols).

The first reaction pathway is heterolytic and dominates (according to the Waterloo model) at low heating rates and low temperatures. Once the dehydration and condensation reactions go to completion, the cellulose is reduced to char, gases and water. The second and third pathways are homolytic and predominate at high heating rates and elevated temperatures (>350°C). There is convincing evidence that temperature, as well as the presence of small amounts of inorganic substances (cations) and biomass morphology (crystallinity and DP), greatly affect selection of the two homolytic pathways.

Using untreated Avicel cellulose (to account for catalytic effects) Piskorz *et al.*,(1989) have looked at the effects of reactor temperature on liquid product yields, which showed that hydroxyacetaldehyde yields decreased from a maximum at about 600°C to a minimum at about 400°C, with a corresponding increase in levoglucosan yield reaching a maximum at 400°C, Figure 2-8. This evidence further verifies the fact that the depolymerisation and fragmentation of cellulose at elevated temperatures are true competing reactions, the former one predominant between 300 and 450°C, while the latter one being favoured at temperatures exceeding 450°C.

Figure 2-8: Variation of hydroxyacetaldehyde and levoglucosan yields with temperature for Avicel cellulose (Piskorz *et al.*, 1989)

It has already been mentioned that small amounts of inorganic substances can cause profound changes in the thermal behaviour and product spectrum of cellulose pyrolysis. This phenomenon was established long ago when many of the earlier experiments used untreated cellulosic biomass, which had its inherent cationic composition preserved. Piskorz *et al.*,(1989) has shown that cationic substances (particularly alkali or alkaline earth cations) in very small quantities (<0.5 % wt) will favour fragmentation by retarding depolymerisation.

These substances are normally associated with natural cellulose and other biomass materials and, if present, depolymerisation reactions are negatively affected, a fact already known to

Arsenau and Stanwick (1971), who reported that alkali salts resulted in diminished levoglucosan yields. These conclusions are in agreement with many other studies, for example that of Shafizadeh *et al.*,(1979) on the effects of additives, including bases like NaOH, Lewis acids like HCl and neutral salts like NaCl. Pan and Richards (1989) were able to show that K^+ has a much stronger influence than Ca^{2+} on the fragmentation reactions on cellulose and hemicellulose and that direct addition of as little as 0.01 % wt of NaCl to pure cellulose can almost halve the pyrolytic yield of levoglucosan.

Finally, the morphology (crystallinity and DP) also affect the pathway selection although to a lesser degree than the presence of cations and the temperature range. It has been reported that levoglucosan yields increase with X-ray crystallinity index while char yields decrease (Cabradilla and Zeronian, 1976). Weinstein and Broido (1970) indicate that less crystalline regions of cellulose undergo more rapid thermal degradation. Graham (1993) claims that low DP and reduced crystallinity expose more end-sites favouring depolymerisation.

Although extended research has been conducted to determine chemical reactions occurrence during cellulose pyrolysis, a definitive reaction pathway has not as yet been generally accepted. From the reaction pathways presented, the Waterloo model, i.e. the three competing primary pyrolysis reactions scheme, best explains the range of products formed during cellulose pyrolysis and accounts for the effects of temperature, heating rate, ash and degree of polymerisation.

2.3.2 Hemicelluloses pyrolysis

Hemicellulose has received less attention due to its lower abundance, variety of constituents (e.g. xylan, galactoglucomanan, etc.), high reactivity and rapid degradation at low temperatures, decomposing within the range of 200 to 260°C (Browne, 1963), since it shows a much greater variety in structure and consequently is much less well-defined than cellulose. Hemicellulose also shows lower thermal stability, presumably on account of its lack of crystallinity and much lower DP. According to other researchers, hemicellulose decomposition is initiated at temperatures as low as 120°C (Ramiah, 1970; Wenzl, 1970; Antal, 1980a). A degradation pathway similar to that of cellulose is proposed, which occurs in two steps: dehydration reactions are important at temperatures less than 280°C and are replaced by rapid depolymerization as the temperature is increased (Beall and Eichner, 1970; Shafizadeh, 1968). Dehydration is characterized by random cleavage of the C-O bonds

producing branched-chain anhydride fragments, water-soluble acids, char and light gases (Browne, 1963; Beall and Eickner, 1970; Antal, 1980a).

In the case of high temperature hemicellulose pyrolysis, a characteristic intermediate, the analogue of hydroxyacetaldehyde or levoglucosan in cellulose pyrolysis, is assumed to exist from kinetic data, and is thought to be furan or furfural derived from hemicellulosic pentosans like arabinose, readily found in softwoods xylans (Antal, 1980b; Browne, 1963). These derivatives from softwoods hemicellulose pyrolysis are difficult to isolate due to their extremely rapid formation and decomposition. Several xylan decomposition products have been identified, a recent compendium being that of Pouwels *et al.,* (1987). There is preliminary evidence that anhydroxyloses or substituted anhydroxyloses are the more significant compounds in terms of potential yields (Heulleur, 1988, in Piskorz *et al.,* 1991).

It should also be mentioned that xylan degradation is subject to similar fragmentation effects to those observed for cellulose in the presence of inorganic impurities, since xylan possesses ion-exchange sites, which make it particularly susceptible to uptake of impurity cations.

2.3.3 Lignin primary pyrolysis

The mechanisms and kinetics of the primary pyrolysis of lignin have not yet been extensively investigated and a major characteristic pyrolysis product has not been identified (Beall and Eickner, 1970; Shafizadeh and Chin, 1976; Antal, 1980b). This is primarily attributed to the complex structure of lignin, which varies significantly as a function of species and method of preparation. Lignin is, in general, more thermally stable than other components and is readily partially depolymerized. Under similar pyrolysis conditions lignin produces more char and a higher fraction of aromatics in the liquid product than cellulose or hemicellulose (Browne, 1963; Ramiah, 1970; Shafizadeh, 1982a), which is known as pyrolytic lignin. Researchers at the University of Waterloo claim that this pyrolytic lignin is rich in phenolic, methoxy- and propenyl compounds, and it can be easily recovered from pyrolytic liquids as a brown powder of relatively low molecular weight readily soluble in methanol, organic acids and other solvents. Further pyrolysis gives rise to phenols, catechols, xylenols, etc., and char from aromatic monomers and produces carbon oxides, hydrocarbons, aqueous acids and char from the straight carbon chain (Browne, 1963).

Antal (1985) proposes a primary lignin pyrolysis pathway consisting of three parallel reactions, similar to cellulose pyrolysis, Figure 2-9. Antal's lignin pathway is similar to

Shafizadeh's first proposed cellulose pathway with each pathway being related to the temperature. Antal (1980d; 1985) speculates that rapid pyrolysis may initially result in the formation of monomeric units, joined by ether linkages, patterning to some extent the depolymerisation of cellulose by the cleavage of the glycosidic bonds.

Figure 2-9: Antal's proposed lignin reaction pathway (Antal, 1985)

At low temperatures dehydration is assumed to be the main reaction (pathway 1), while at higher temperatures pathway 2 dominates and a variety of lignin monomers is formed. It should be noted that these two pathways are not well differentiated as far as temperature is concerned, unlike cellulose pyrolysis, Figure 2-1, nor are the monomers of a single type intermediate due to the complexity of lignin structure (phenylpropane units). It has been proposed that primary pyrolysis occurs with the cleavage of the straight carbon chains which connect the aromatic units. Suggested pathways 4 and 5 become evident at high temperatures (> 500 °C) due to monomers degradation in the vapor phase. Antal notes that experimental evidence suggests there may be competitive dehydration and decarboxylation reactions in pathway 5. The two remaining pathways, 3 and 6, are believed to exist at very high heating rates, where char is formed by condensation reactions. However, this proposed pathway is highly controversial since experimental evidence (Graham, 1993) exhibit a substantial decrease in char yield as heating rate and temperature are increased.

A modified lignin pyrolysis pathway, proposed by researchers at the Massachussets Institute of Technology (MIT) for milled wood lignin, is presented below in Figure 2-10.

Figure 2-10: MIT proposed lignin reaction pathway (Nunn *et al.*, 1985)

By this modified lignin pyrolysis model the formation of CO from pathway 5, i.e. from the vapor phase secondary cracking of the volatile matter at temperatures above 700°C, is confirmed. The increase in permanent gases yield, predominantly CO, occurs at the expense of liquid yield. Moreover, Nunn *et al.*,(1985) have shown that low molecular weight oxygenates (formaldehyde, methanol and acetaldehyde) are also formed at low temperatures (below 500°C) in conjuction with water and CO_2, as direct products of dehydration pathway 1, as also correctly proposed by Antal (1985).

2.3.4 Discussion on the primary decomposition of lignocellulosics components

An important concept arising from the above discussion is the realisation that thermal pyrolysis is not necessarily the random and largely uncontrollable reaction it was once believed to be. In fact, selectivity of cellulose to fragmentation yielding carbonyls (mainly hydroxyacetaldehyde) on the one hand, or depolymerisation to monomeric anhydrosugars (mainly levoglucosan) on the other at elevated temperatures (>350°C) can be as high as 70 to 80 % wt for either of these conversion steps (Graham, 1993).

It may also be concluded that, as far as the primary decomposition of the three major biomass constituents is concerned, this can be summarised as follows (Shafizadeh and Chin, 1976):

- hemicellulose is the most reactive component depolymerising between 225 and 325°C
- lignin is the most thermally stable component decomposing gradually between 250 and 500°C
- cellulose is intermediate in terms of its reactivity, decomposing between 325 and 375°C. Decomposition is initiated at a higher temperature than lignin but occurs rapidly within a much narrower range.

2.4 Secondary pyrolysis reactions of lignocellulosic components

The secondary reactions, i.e. the evolution of products not directly from the cellulosic ring, occur either in the vapor phase, or involve gas-solid reactions between vapor phase components with char.

These reactions are considered are considered very important since they lead to cracking of pyrolysis product vapors to non-condensible gases, seriously reducing the yields of pyrolysis liquid products (Diebold and Benham, 1980; Bohn and Benham, 1984; Graham *et al.*, 1985).

Five general secondary reactions are known to be significant in conventional pyrolysis and gasification, and these are evaluated with respect to their relative significance in fast pyrolysis processes. These reactions include (Graham *et al.*, 1984):

- cracking reactions
- reforming reactions
- the water-gas shift reaction
- the carbon-carbon dioxide (Boudouard) reaction and
- the carbon-steam reaction.

The thermal decomposition of heavy vapor phase hydrocarbons to smaller fragments is known as cracking. During this endothermic reaction, C-C, C-O and C-H bonds are broken or rearranged resulting in shorter carbon chains, ring cleavage, the production of hydrogen and carbon oxides and the formation of unsaturated components, such as olefins and alkynes. Although the specific chemical pathway is not fully characterized, vapor phase cracking predominates at temperatures exceeding 700°C and occurs on a millisecond scale (Roman *et al.*, 1981; Diebold and Scahill, 1983; Roy *et al.*, 1983).

Reforming is a broad class of endothermic reactions of hydrocarbons with steam at elevated pressures, which results in isomerisation, hydrogenation and eventual fragmentation to CO_2 and hydrogen free radicals. It has been demonstrated, however, that at the temperatures, residence times, and relatively low pressures characterised by fast pyrolysis, reforming is completely insignificant (Hoffman *et al.*, 1983).

The water-gas shift reaction:

$$H_2O + CO \rightleftharpoons H_2 + CO_2$$

is a reversible reaction of steam with carbon monoxide to produce hydrogen and carbon dioxide. This exothermic reaction is faster than the reaction of carbon-steam and carbon-carbon dioxide (Roman *et al.*, 1981; Desrosiers, 1981), and contributes to the final product distribution in pyrolysis processes. It should be noted here that in the absence of an appropriate shift catalyst, iron or nickel, the forward step (i.e. the production of hydrogen and carbon dioxide) is faster than the reverse step at temperatures below 810°C (Walawender *et al.*, 1984).

The carbon-steam and carbon-carbon dioxide (Boudouard) reactions are similar with respect to rate, mechanism and degree of endothermicity. The former reaction:

$$C + H_2O \rightleftharpoons CO + H_2$$

proceeds at a negligible rate below 830°C. This reaction is thought to play a minor role in fast pyrolysis and is reported (Hallen *et al.*, 1984) that only by catalysis participate significantly in the pyrolysis process.

The latter reaction:

$$C + CO_2 \rightleftharpoons 2CO$$

is hardly detectable below 850°C and is also thought to play only a minor role in fast pyrolysis.

From the above discussion it may be concluded that as long as the temperature of the pyrolysis environment is kept lower than approximately 650°C, gas/vapor residence time is lower than approximately 2 s and care is taken that heterogeneous reactions incorporating gases and solid char are avoided, secondary reactions will not be significant. The decomposition of primary, high molecular weight organic vapors to low molecular weight permanent gases will then be kept at minimum levels.

2.5 General biomass pyrolytic pathways

Biomass pyrolysis involves very complex chemical reactions, the sequence and kinetics of which, and hence the expected yields of the products, depend on a large number of variables. These variables are heating rate, temperature, gaseous environment, pretreatment and extent and catalytic effects of inorganics (Shafizadeh and DeGroot 1977; Basu and Stangeby, 1981; de Jenga *et al.*, 1982). If the influence of the above variables on the mechanism and kinetics of pyrolytic reactions were known or could be predicted, the pyrolysis conditions could be controlled in order to reduce the side reactions and enhance the formation of the desirable products.

Fundamental research over the past two decades has attempted to identify the major competitive and consecutive reactions which may occur during the thermal pyrolysis of biomass (Kilzer and Broido, 1965; Shafizadeh, 1968, 1980, 1982b; Soltes and Elder, 1981;

Milne and Soltys, 1983). Recently, the processing parameters have moved towards shorter residence times and very high heating rates in an attempt to maximize gas or liquid products at the expense of solids (charcoal). Although modeling is primarily based on cellulose pyrolysis, these results appear to be consistent with those obtained in processes using wood and other biomass (Antal 1980a, 1980b; Roy *et al.*, 1982). A more detailed discussion of the pyrolysis of lignocellulosic components is given above in Section 2.3.

Several pathways have been established which explain most of the observed phenomena during rapid pyrolysis of biomass. The first general mechanism hypothesis proposed is attributed to Diebold (1980), who was initially interested in the production of olefinic gases from biomass and was apparently the first researcher to attempt to identify fast pyrolysis reaction mechanisms within the framework of general pyrolysis reactions. Diebold's model is presented in Figure 2-11 and was formulated from a consensus of pyrolysis specialists at a workshop sponsored by the former (now National Renewable Energy Laboratory/NREL) Solar Energy Research Institute (SERI, 1980).

Figure 2-11: Biomass pyrolysis global mechanism (SERI, 1980)

Interest at that time was directed to the production of olefins and the pathway leading to olefin formation is shown as the horizontal sequence of reactions within the rectangular box of Figure 2-11. According to this first comprehensive reaction scheme, a primary liquid (termed perhaps incorrectly then as primary "tar") is formed via an "active" intermediate on the biomass surface at low temperatures. These characteristic primary oil precursors are shown to be of special interest to the development of a fast pyrolysis process (Shafizadeh, 1968; Nunn *et al.*, 1982; Diebold and Scahill, 1982) and once formed on the biomass surface,

are subsequently vaporized promoting olefin production when subjected to high temperatures, high heating rates and low vapor partial pressures. The sequence of the desirable reaction pathways includes thermal cracking, see Section 2.3.4, to produce very active transient oxygenated fragments (now known to be carbonyls, organic acids, alcohols and depolymerized lignin), which are rapidly cracked to form hydrogen, carbon oxides, olefins and other hydrocarbons.

The undesirable pyrolysis pathways reported depict, according to this scheme, the conversion of primary pyrolysis "tars" to two types of secondary tars: the high-pressure liquefaction product (L), which has been widely studied, and the vapor phase derived tar (V or L). However, neither of these secondary tar formation pathways addresses the change in tar composition as it is held at high temperatures without high pressure. Thus, according to this desired pathway only transient oxygenated fragments and gases are produced from primary tar at high temperature and low pressure. Extended reaction times allow the olefins and related products to react in the vapor phase and form particulate carbon (carbon black) and permanent, low molecular mass, equilibrium gases. To preserve the olefins, the pyrolysis pathway must be interrupted by rapid quenching of the intermediates before equilibrium can occur.

A simpler set of global kinetics was later proposed by Diebold and Scahill (1984) to gain insights to ablative pyrolysis of biomass, Section 3.7. As shown in Figure 2-12, this simpler model used chain-cleavage reactions to form a plastic "active" state, primary vapors, secondary vapor derived tar and gases, and dehydration reactions leading to direct production of char from biomass and water. However, this pathway does not have a step accounting for the formation of secondary char from secondary gas/vapor phase reactions which are known to occur (Zaror *et al.*, 1985).

Figure 2-12: Biomass global pyrolysis reaction scheme (Diebold and Scahill, 1984)

Reference to an "active" intermediate, typical of cellulose pyrolysis, has already been done in Section 2.3.1. This "active" cellulose intermediate was found (Broido, 1973; Bradbury *et al.*, 1979) to have a much lower DP than the cellulose feedstock, indicating depolymerization of feedstock macromolecules to form viscous primary oil precursors, formed with almost no byproducts and having consequently an elemental structure similar to wood (Diebold, 1986). Scanning electron microscopy experiments (McGinnes *et al.*, 1974, 1976) showed that, after pyrolysis, the cellulose walls thickness was reduced and that the fine cell wall structure had become blurred so as to have a fused appearance. This wood particle size shrinkage, analogous to that exhibited by heat-shrinkable polyethylene tubing during the application of heat, is an indication that wood must have passed through a viscous, plastic state of some sort. The existence of this depolymerized, highly viscous plastic phase has been confirmed and exploited by Diebold (1980) as a basis for the design of an ablative fast pyrolysis reactor.

The complete series of pyrolysis pathways, presented by Evans and Milne in 1985, was confirmed later by the same researchers (Evans and Milne, 1987) and is shown in Figure 2-13. In this series of reactions, vapors formed in biomass primary pyrolysis under high pressure appear to have the same composition as the vapors obtained directly from low-pressure pyrolysis (Evans and Milne, 1987a, 1987b), i.e. a composition very similar to wood. Under high pressure conditions, the direct formation of a liquid product mixture is due to the transformation of wood to a "plastic" state, similar to that reported by Diebold (1986), at the temperatures and pressures involved, an hypothesis also confirmed by Lèdè *et al.*,(1985). At low pressures and under direct-contact fast pyrolysis conditions, the products pass, as discussed above, into a liquid state ("molten plastic state"). This glass transition is associated with the onset of "rubbery" flow caused by slippage of biopolymers.

Primary and secondary tars exhibit quite different behaviour. Primary vapors, produced by chain cleavage of the cellulose polymer, have a high oxygen content and are quite soluble in water. The secondary tars are thermally stable, aromatic compounds which are insoluble in water. Molecular beam-mass spectroscopy has shown that the constituents of the secondary tars are not present in the primary vapors, but rather are formed from the primary vapors (Evans, 1984, 1985).

Figure 2-13: Biomass pyrolysis global mechanism (Evans and Milne, 1987)
(PNA = PolyNuclear Aromatics)

According to this model, biomass is pyrolysed at low pressures to primary oils which are further converted sequentially to give oxygenates, aromatics, polycyclic aromatics and, eventually, soot. This series of reactions correlates well with the progression of chemicals earlier identified by Elliott (1985) and shown in Figure 2-14.

Figure 2-14: Chemical components progression in biomass tars (Elliott, 1985)

As already discussed, biomass fast pyrolysis is a fast reaction occurring at moderate to high temperatures (450-600°C). The understanding of such a gas-solid reacting system can only be achieved by carefully considering the strong interplay between chemical kinetics, transport processes and structural variations, which take place as the reaction progresses.

The principal sequential reactions in the overall fast pyrolysis pathway have become apparent from a review of the available literature (Section 2.3), an analysis of the possible generic chemical reactions and the consensus of pyrolysis experts. Due to the recent work of Piskorz *et al.*, Diebold and Richards described previously, it may be claimed that mechanistically, biomass fast pyrolysis consists of activation, fragmentation or depolymerisation and

cracking. Preservation of valuable products (liquid or gaseous) will occur if rapid vapor quenching is exerted before vapor-phase secondary cracking is allowed to proceed to any appreciable extent.

If non-treated biomass is considered, then the pathways of fast pyrolysis are limited, involving the competing steps of depolymerisation and fragmentation, taking into account the process parameters as well as the intrinsic nature of the feedstock pyrolysed. The global wood pyrolysis mechanisms described above do not determine intermediate products and reactions and may only serve as speculative, since more information on the fast pyrolysis of cellulose and particularly lignin and hemicellulose, is required to allow for the further development of reaction mechanisms.

2.6 Biomass fast pyrolysis kinetics

Biomass fast pyrolysis has been defined in terms of the requirements for process conditions, such as temperature and vapor residence time as well as the selected chemical pathway.

The complexity of the pyrolysis process implies that there are numerous homogeneous and heterogeneous reactions occurring either simultaneously and/or consecutively depending on the reactor conditions. Kinetic modelling is further investigated as an attempt to represent the overall kinetics as individual and distinct reaction pathways, in order to primarily assess the effects of the interaction of parameters on the yields and compositions of the final products.

Due to the complexity discussed above, biomass fast pyrolysis kinetics investigation is a difficult task and a series of simplifications must inevitably be introduced in order to predict true kinetics by simplified reaction patterns, such as those presented in Sections 2.3 to 2.5.

Thus, kinetic modeling is utilised for several end results, such as:

1. The development of a diagnostic tool in order to evaluate the importance of the process parameters on the products.
2. The prediction of the effects of process parameters, i.e. heating rate, reactor temperature, particle size, gas/vapor residence time on the product yields and characteristics in order to aid optimisation of the pyrolysis process.
3. The development and establishment of better reactor design techniques.
4. The optimisation of the parameters for the desired end product.

The kinetic investigations of wood pyrolysis can generally be separated into three major groups:

1. Models considering an overall decomposition rate of wood to char and volatiles. These one-step models are employed when an overall reaction is used to describe degradation of solid biomass by experimentally measuring the weight loss of wood sample as a function of time and temperature and are reviewed in Section 2.6.1.
2. One-stage, multi-reaction models used to correlate reaction product distribution. These models propose stepwise degradation of biomass to a variety of primary vapor products, char and several gaseous species and determination of rate constants for their formation and are reviewed in Section 2.6.2.
3. Two-stage, semi-global models are used when kinetic investigations aim to determine rate constants for both primary pyrolysis reactions and secondary reactions of the volatile products and are reviewed in Section 2.6.3.

A great number of investigations on wood pyrolysis kinetics have been carried out since 1950, and it is beyond the scope of this work to treat them individually. Excellent recent reviews have been given by Mok (1984), Lidén (1985), Bridge (1990), Graham (1993) as well as Peacocke (1994).

A summary of these three approaches to kinetic modeling follows.

2.6.1 Overall decomposition rate expressions and constants

A very common technique employed to study pyrolysis kinetics is the Thermo-Gravimetric Analysis (TGA), which can be combined with Differential Thermal Analysis (DTA) or Differential Scanning Calorimetry (DSC) to also permit estimation of the heat of reaction.

Since TGA only correlates the weight loss of a wood sample as a function of time and temperature and as there is usually no provision for volatile pyrolysis products collection, only an overall decomposition rate of wood is obtained.

The global thermal degradation process can then be described by a simple model:

$$\text{Biomass} \longrightarrow \text{Char}_{(S)} + \text{Volatiles}_{(V)}$$

The rate of the above reaction is usually described to follow a first order reaction, while the rate coefficient is assumed to follow an Arrhenius' law dependence on temperature:

$$\frac{dW}{dt} = -k(W - W_f) = -k_o \exp[-E/(RT)](W - W_f)$$

(Eq. 2-1)

where

W	initial weight fraction	[kg]
W_f	final (non-degradable) weight fraction	[kg]
k	rate coefficient	[s^{-1}]
k_o	pre-exponential (frequency) factor	[s^{-1}]
E	activation energy	[kJ/kmole]
R	universal gas constant (=8.314)	[kJ/kmole K]
T	temperature	[K]
t	time	[s]

The Arrhenius kinetic parameters, E and k_o, are derived by obtaining best fit curves through the experimental data and solving the Arrhenius rate law using a least squares method. The kinetic constant for first order reactions is then used to predict the change in mass or composition of the original material by the equation:

$$\Phi = \Phi^*[1 - e^{-kt}]$$

(Eq. 2-2)

where

Φ	yield at time t	[% wt]
Φ^*	maximum attainable yield at temperature T (K)	[% wt]

As discussed by Lidén (1985), Vovelle *et al.*,(1987) and Bridge (1990), kinetic parameters exhibit a considerable scatter even for similar feedstocks and similar conditions, due to a number of reasons:

1. The assumption that the steady-state temperature is used as the overall reaction temperature (Williams and Besler, 1994).
2. The use of too simple a kinetic model (since researchers were quite often unaware of the basic primary pathways).
3. The ignorance of the importance of the feedstock quality (i.e. morphology, DP, inorganic composition, impurities, etc.).
4. The failure to appreciate the significance of heating rate (and its role in determining whether fast or slow pyrolysis reactions would occur) especially when kinetic modelling has been performed with large biomass samples.

All models used to predict weight loss cannot be applied for the prediction of product distribution, since complicated procedures are required. Moreover, these models assume complete decomposition of a wood sample with infinite reaction times and equilibrium conditions, a severe limitation when kinetic investigation of biomass fast pyrolysis is to be investigated and strict residence times constraints be met.

More recent investigations employed techniques different from TGA, which is not a suitable method for fast pyrolysis studies, since the heating rate is too low and significant heat limitations to overcome charring reactions exist in the particles undergoing pyrolysis. Electrical heating of filter cellulose as paper was used by Lewellen *et al.*,(1977), who were the first to show that, irrespective of detailed molecular mechanism, the residence time of the volatiles in the solid matrix is a critical parameter in pyrolysis. Although Shafizadeh *et al.*,(1979) also reported an overall decomposition rate, a model with different rate constants for different groups of products was suggested.

2.6.2 Multiple product rate expressions and constants

Interest in specific products of biomass pyrolysis has led to stepwise modelling, which describes the change of wood to intermediates and final products, as shown in Figure 2-15.

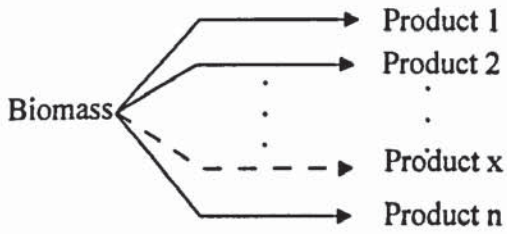

Figure 2-15: Biomass decomposition to different products

The experimental procedure is more cumbersome, since more final products must be determined and measured for the closure of the mass balance.

A method of stepwise modeling describing cellulose pyrolysis by a simple, three reaction model, was proposed by Bradbury *et al.*,(1979), Figure 2-16, to account for the variations in product yields.

Figure 2-16: Bradbury's kinetic model for cellulose pyrolysis (Bradbury *et al.*, 1979)

According to the above model the following expressions are derived:

$$-\left(\frac{dW_{cell}}{dt}\right) = k_i[W_{cell}]$$

$$-\left(\frac{dW_A}{dt}\right) = k_i[W_{cell}] - (k_v + k_c)[W_A]$$

$$-\left(\frac{dW_{Cl}}{dt}\right) = 0.35k_c[W_A]$$

(Eqs. 2-3)

where

W_{cell}, W_A, W_V, W_C and W_G	the normalized weights of cellulose, "active cellulose", volatiles, char and gases respectively
0.35	the char fraction, W_C /(W_C + W_G), assumed constant for the range of temperatures (259-341°C) investigated
k_i, k_v, k_c	rate constants of activation and decomposition to volatiles - char+gases reactions respectively

In the above model, it is assumed that a first-order "initiation reaction" leads to the formation of "active cellulose", an intermediate with high activation energy. The exact nature of this intermediate is not known, but Diebold (1986) reports that it has a much lower DP than the initial cellulose feedstock and is considered to be in a liquid or "plastic" state, a feature already discussed in Section 2.4. This intermediate is subsequently decomposed by two competitive first-order reactions, one yielding volatiles and the other char and a gaseous fraction. Bradbury's model suggests that cellulose macromolecules are not directly converted to low molecular weight volatile products, gases and char but undergo intermediate physical and chemical changes such as glass transition, a hypothesis also supported by Back (1973) and Salmén and Back (1977), and depolymerization to DPs of around 200 (Shafizadeh and Bradbury, 1979). It has also been used by Arsenau (1971), who showed that at higher

temperatures and shorter times, the formation of volatiles would proceed much more rapidly than the concurrent char forming step.

It is important to note that Bradbury's kinetic equation was developed for the two-pathway model, Figure 2-5, before the third primary pathway was rediscovered, by researchers at the University of Waterloo, and confirmed. It is very likely that empirical kinetic parameters, like k_v, associated with the "volatilization" pathway represent the combined kinetic parameters of the primary depolymerisation and fragmentation pathways suggested by the Waterloo model, Figure 2-7.

This general type of modelling, Figure 2-15, was also tested by Nunn *et al.*,(1982), in rapid pyrolysis of wood in an electrical screen heater reactor, where high conversion of the wood to volatile products was obtained in very short solids residence times and moderate temperatures, liquid, referred to as "tar" by Nunn *et al.*,(1982), being the major pyrolysis product (liquid yields 55 % wt in 627°C being reported). Yields of several individual products (except liquid) were correlated with a single, first order decomposition model. In this model, the rate of formation of a product i at time t, is given by the expression:

$$\frac{d\Phi_i}{dt} = k_{oi} \exp[-E_i / (RT)](\Phi_i^* - \Phi_i) \qquad \text{(Eq. 2-4)}$$

where

Φ_i	the obtained yield of product i at time t (s)	[% wt]
Φ_i^*	the ultimate attainable yield of product i	[% wt]
k_{oi}	the pre-exponential factor for product i	[s^{-1}]
E_i	the activation energy for product i	[kJ/kmole]

Although liquid species and light oxygenates evolution kinetics were not analyzed with this model, since single-reaction first order kinetics alone cannot predict a maximum in yield, statistically satisfying correlations of laboratory data were obtained. This model was found to be a useful tool for comparing different data sets, correlating data and performing engineering calculations.

A thorough study of Nunn's stepwise modeling has also been conducted by Hajaligol *et al.*,(1982), who used an electrical screen heater reactor for studying the separate effect of temperature (300-1100°C), heating rate (100-15000°C/s), pressure (1 atm and above) and solids residence time (0-30 s) on the yields, compositions and rates of formation of products

from the rapid pyrolysis of 0.101 mm (101 μm) thick sheet of cellulose. During the experimentation, special care was given to exclusion of secondary reactions on the screen heater and within the sample. Under the operating conditions specified above, increasing the sample thickness to 0.2 mm (200 μm) had no significant effect on weight loss or total yield of tar and volatiles.

It was concluded furthermore that enhanced secondary cracking due to the increased tar and volatiles residence time together with limitations due to internal heat and mass transfer, caused a decreased tar yield in samples thicker than 0.4 mm (400 μm). Preliminary kinetic modeling assumed that the cellulose decomposes directly to each reaction product i by a single, independent reaction pathway, designated by:

$$\text{Cellulose} \xrightarrow{k_i} \text{Product i}$$

It was also assumed that the kinetics of this process can be modeled by the unimolecular first order reaction described above by Nunn *et al.*,(1982).

Thurner and Mann (1981) studied pyrolysis of oak sawdust using the model suggested by Shafizadeh and Chin (1977), which was based on the three-competing pathways mechanism for cellulose pyrolysis assuming wood decomposition into gas, char and tar described by three parallel first-order reactions, Figure 2-3. Rate constants were also calculated, over the range 300-400°C considering sample temperature variation. Thurner and Mann furthermore concluded the reaction to be chemically controlled for particles smaller than 2 mm. Similar modelling approaches using the kinetics proposed by Bradbury *et al.*,(1979), have been adopted by other researchers, e.g. Salazar and Connor (1983), Simmons and Lee (1985), Samolada and Vasalos (1991), and Varhegyi *et al.*,(1994) with reasonable agreement between experimental and predicted results.

2.6.3 Primary and secondary pyrolysis rate expressions and constants

This kind of approach is the most difficult, because the rate of formation of a number of products must be measured as a function of time. Not only is the residence time of solids in the reactor important, but also the residence time of volatiles.

In spite of its complexity, this approach seems the most appropriate to study since it more closely approaches the true reaction pattern, and simpler models will probably fail to predict liquid yields as they do not consider the importance of volatiles residence time.

Kosstrin (1980) reported that the modeling of biomass pyrolysis behaviour must account for secondary reactions, referring primarily to cracking and carbon deposition on particles and the associated conversion of part of the oils to char and gases. This requirement arises because of the decrease of the oil yields at increasing temperatures, whereas they are expected to increase with increasing temperatures, according to existing models predicting liquid yields. It is clear that vapors cracking by secondary reactions must be considered to explain the observed pyrolysis liquids yield decrease. The overall reaction mechanism considers a series of primary reactions, each of which is acted upon by a series of secondary reactions. According to this scheme, char is assumed to be formed as the solid biomass residue of the primary reactions and as deposited solid material in the course of secondary reactions.

Recent kinetic models, which account for the secondary decomposition of primary pyrolysis tars have been proposed by Lidén (1985), Gorton and Knight (1984) and Diebold (1986) as described below. They all assumed that the production of primary vapors (oil or tar) from wood and the subsequent decomposition of them are first-order reactions, with respect to the vapors the yield of liquid products being estimated as a function of the pyrolysis temperature and the residence time of volatiles in the reaction zone. Lidén (1985) and Diebold (1986) proposed similar kinetic models, the reaction scheme shown in Figure 2-17, below.

Figure 2-17: Reaction scheme used by Lidén (1985) and Diebold (1986)

The expressions used to estimate liquid yields are listed below (Bridge, 1990):

$$\Phi_L = \Phi_L^*[1-\exp(-k_L\tau_{sL})](\frac{1-\exp(-k_{3L}\tau_g)}{k_{3L}\tau_g})$$

$$\Phi_D = \Phi_D^*(\frac{1-\exp(-k_{3D}\tau_g)}{k_{3D}\tau_g})$$

(Eqs. 2-5)

where

Φ_L, Φ_D	actual (observed) liquids yield according to Lidén (L) and Diebold (D) respectively	[% wt]
Φ_L^*, Φ_D^*	theoretical (ultimate) tar yield	[% wt]
k_{3L}, k_{3D}	reaction rate constant for the oil decomposition step	[s^{-1}]
τ_g	mean residence time of volatiles in the reactor	[s]
τ_{sL}	residence time of solids according to Lidén	[s]
k_L	overall wood decomposition rate constant	[s^{-1}]

If $k_L\tau_{sL}$ is at least 10 times larger than $k_{3L}\tau_{gL}$, the second term in the expression proposed by Lidén (1985) is very close to unity, so that this expression can be reduced to one similar to Diebold's. The constants k_{3L} and k_{3D} follow Arrhenius' law:

$$k_{3L} = 4.28 \times 10^6 \exp(-\frac{107500}{RT})$$

$$k_{3D} = 1.55 \times 10^6 \exp(-\frac{87634}{RT})$$

$$\Phi_L^* = 0.703,\ \Phi_D^* = 0.78 \text{ or } 0.76$$

(Eqs. 2-6)

The reaction scheme proposed by Gorton and Knight (1984) is shown in Figure 2-18 below.

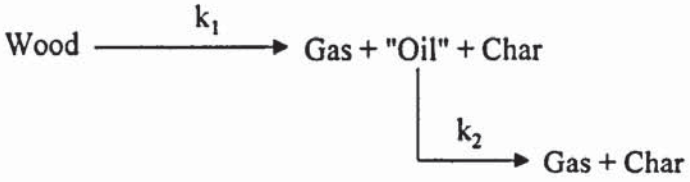

Figure 2-18: Reaction scheme proposed by Gorton and Knight (1984)

while their kinetic expression is as follows:

$$\Phi_G = \frac{k_{1G}\Phi_G^*}{k_{2G} - k_{1G}} \exp(-k_{2G}\tau_g)$$

(Eq. 2-7)

where

$$k_{1G} = 1.483 \times \exp(-\frac{21380}{RT})$$

$$k_{2G} = 23.12 \exp(-\frac{7060}{RT})$$

$$\Phi_G^* = 0.811$$

(Eqs. 2-8)

The kinetic models of Lidén and Diebold were tested by Scott *et al.*,(1987) and described successfully the yield of liquid product from about 450 to 850°C. These results showed that the predicted liquid yields agreed with achieved yields within ±10% for the temperature range 500-700°C with residence times of up to 1 s.

Similarly, Vassalos *et al.*,(1988) found that using Lidén's parameters, a better fit of ±20% for the liquid yield for the particle size range 300 - 425 μm was obtained, while using Diebold's parameters, a better fit of ±10% for the liquid yield for the particle size range 500-600 μm was given. Gorton and Knight's model did not predict satisfactorily liquid yields for either particle size range. The variation observed between predicted values and the experimental results were attributed to the exclusion of water yield in the reaction mechanism, the different residence times used, and the type and size of biomass tested.

Table 2-3 gives a comparison of the four kinetic models discussed in Section 2.6.3. These incorporate both primary and secondary decomposition steps, in terms of a common feature, namely the pyrolysis vapor decomposition rate constant.

The problem is that only a limited number of kinetic parameters have been reported for secondary cracking reactions. Kosstrin (1980) expressed these parameters on a surface basis. Converting these rate constants to a volume basis (Lidén, 1988) and taking into account the kinetic parameters given by Kosstrin (1980), Lidén (1985), Diebold (1986) and Gorton and Knight (1984), a comparison of secondary rate constants can be made, shown in Table 2-3:

Table 2-3: Comparison of secondary vapor decomposition reaction rate constants

Temperature (°C)	Kosstrin $k\ (s^{-1})$	G&K $k_{2G}\ (s^{-1})$	Lidén $k_{3L}\ (s^{-1})$	Diebold $k_{3D}\ (s^{-1})$
500	0.40	7.71	0.23	0.19*
600	1.44	8.74	1.58	0.89
700	4.03	9.66	7.23*	3.07

* extrapolations

Taking into account the differences in the feedstock and experimental procedure, the agreement is surprisingly good, emphasizing that a similar kinetic model can be expected to yield very reasonable results.

2.6.4 Summary of kinetic models

According to the discussions above (Sections 2.6.1 to 2.6.3) a sound kinetic model, which accounts for both primary and secondary pyrolysis reaction steps should be used in order to estimate correctly liquid yield from fast pyrolysis of biomass particles.

Furthermore, Lidén's model has been found (Lidén, 1985; Scott *et al.*, 1988; Vasalos *et al.*, 1988) to provide very reasonable predictions within the range of operating conditions studied, the secondary reaction rate constant comparing very well with other constants reported in the literature. Thus, this model will be used in the continuation of this thesis to provide kinetic data for reactor sizing.

2.6.5 Kinetics considerations for reactor sizing

Experiments performed by different researchers have clearly shown that the maximum yield for liquid products is obtained at temperatures around 500°C and occurs over a limited temperature range, the yield dropping off sharply on both sides. This is shown in Figure 2-19, where the liquid yield (organics, i.e. excluding water) versus temperature is correlated by two independent research groups for a variety of experimental conditions, feedstocks and equipment used. Calculations may be found in Appendix 1.

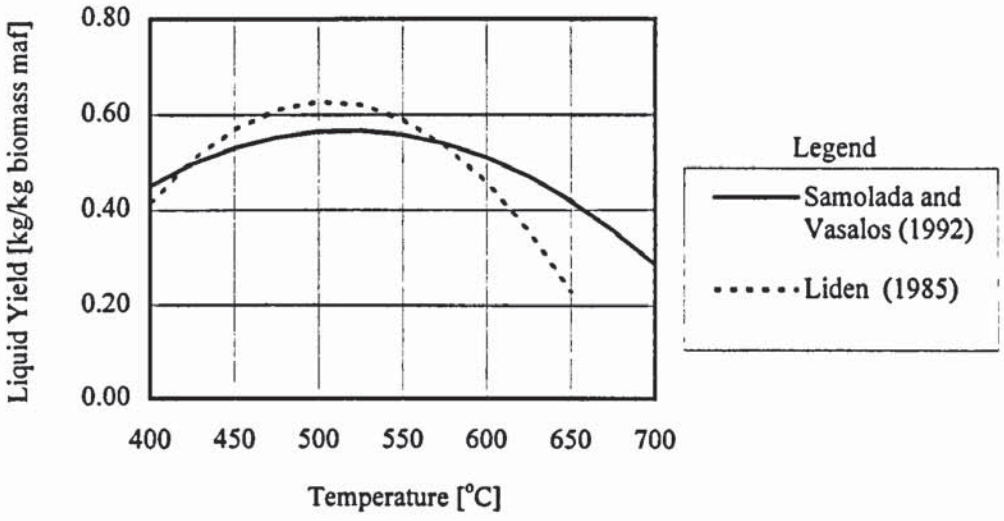

Figure 2-19: Prediction of liquid yield (organics) versus temperature

To account for the liquid yield dropping at elevated temperatures, a reliable kinetic model of biomass fast pyrolysis should incorporate both primary and secondary pyrolysis reactions, as discussed in Section 2.6.3. Such a model realistically predicts pyrolysis vapors yields at elevated temperatures.

As already mentioned in the previous sections very few kinetic models incorporating secondary reactions have been proposed in the literature and even fewer tested and verified. Of the models proposed in Section 2.6.3, that of Lidén (1985, 1988), also tested by Scott *et al.*,(1987), has been established as one of the most successful in predicting pyrolysis liquids yields over a wide range of conditions.

Lidén's model was developed through extensive experimentation of biomass fast pyrolysis in a fluidised bed bench scale reactor operated isothermally (Scott and Piskorz, 1982; Lidén, 1985), where reactor temperature is considered constant. The results from this model, shown in Appendix 1, are summarised in Figure 2-20, where the pyrolysis liquid yields versus reactor temperature for vapor residence times between 0.3-0.8 s are plotted.

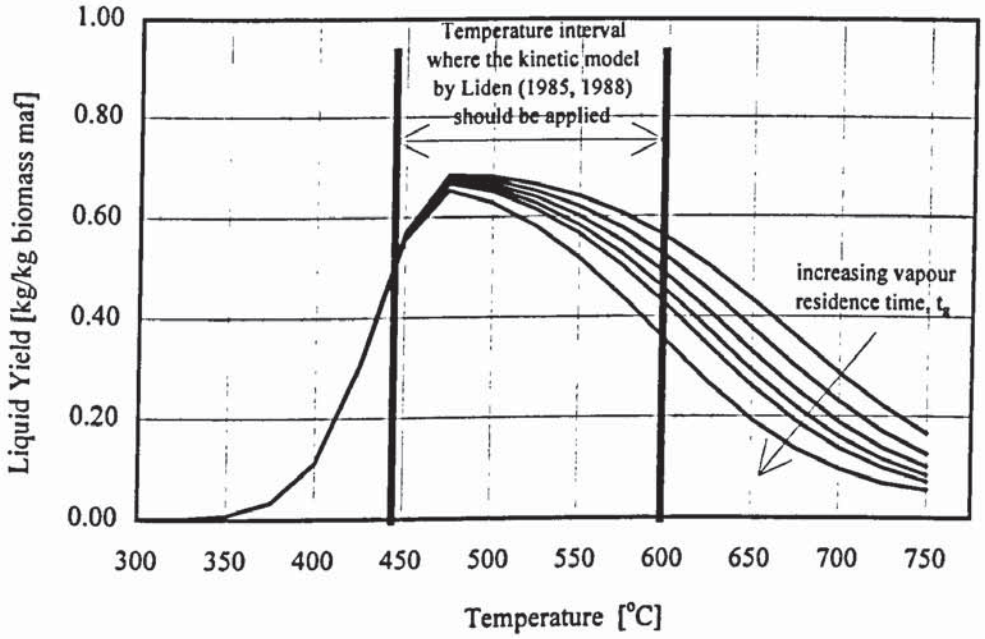

Figure 2-20: Liquid yield versus temperature for vapor residence times in the range of 0.3-0.8 s (data based on Lidén's (1985) kinetic model)

Furthermore, the effect of temperature on liquid yields estimated by different researchers for a given vapor residence time (0.5 s) and elevated (>500°C) temperatures, where secondary vapor decomposition (Section 2.4) becomes important, are presented in Figure 2-21. From this comparison it is clear that Lidén's kinetic model for secondary phase vapor cracking is the modest one in terms of the rate of liquid loss at higher temperatures. Detailed calculations may be found in Appendix 1.

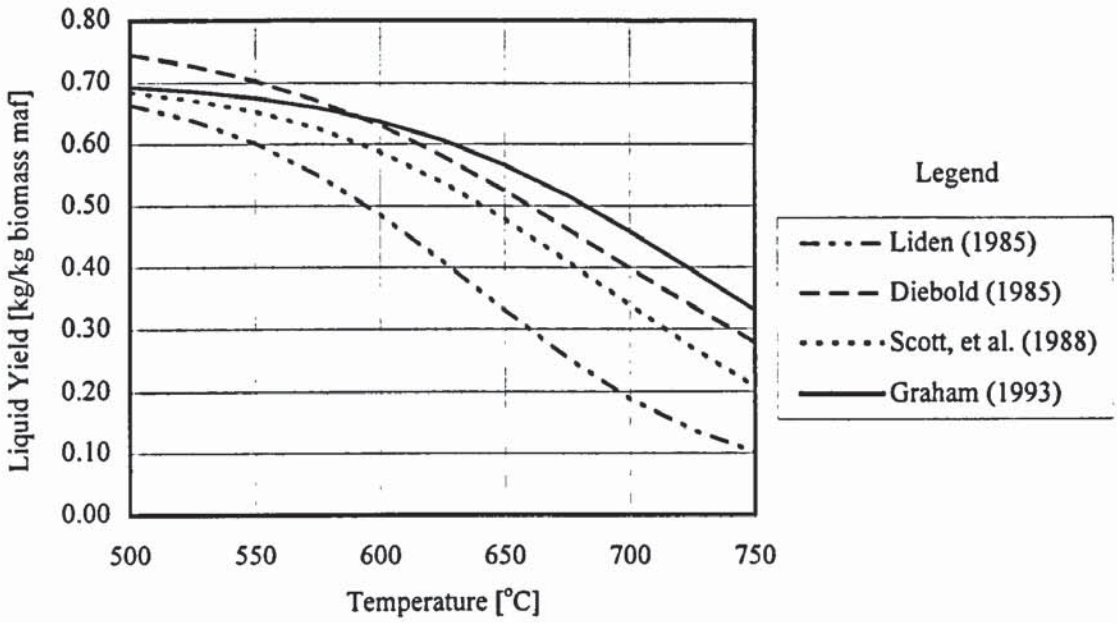

Figure 2-21: Predictions of liquid yield versus temperature for a given vapor residence time of 0.5 s according to different secondary cracking models

The secondary cracking models presented in Figure 2-21 have already been referred to in Section 2.6.3 and have been derived upon experimental data by the respective researchers. From the above discussion it may be concluded that:

1. The effect of the most important process parameters, i.e. temperature and gas/vapors residence time on liquid product yield may be accurately predicted.
2. A suitable kinetic model for biomass fast pyrolysis should incorporate both primary and secondary reactions.
3. One of the most suitable models, the results of which tend to be validated by the fact that its predictions on product yields have been successfully verified, is the model developed by Lidén (1985, 1988).
4. The model proposed by Lidén (1985, 1988) represents a very good linkage between current knowledge on biomass pyrolysis decomposition pathways and reaction kinetics.

The main result from the above study of the kinetics is that for the production of liquids in high yields, short gas/vapor residence times (less than 1 s) and low temperatures (450-550°C) are required. Moreover, for the sizing of a reactor that would be employed for the maximisation of liquid yields, a kinetic model incorporating both primary and secondary reactions should be used. One of the most successful models has been that developed by

researchers from the University of Waterloo, linking in an excellent way reaction mechanisms to experimental data.

Fast pyrolysis has now been defined in terms of reaction kinetics, the nature of desired products and specific pyrolytic reaction pathways, so that reactor design and the required reaction conditions can be derived from first principles. However, heat transfer and heating rate to biomass particles during pyrolysis, an important issue of relevance to reactor design, has yet to be considered. These issues are further discussed below.

2.7 Heat and heat transfer effects

2.7.1 Biomass fast pyrolysis and heating rates

The rapid thermal decomposition of biomass can follow either of two extremes of behaviour or an intermediate. At one extreme, the resistance to heat and mass transfer within particles is negligible, so that no temperature or pressure gradients are sustained in them. At the other extreme, if heat transfer to and through the biomass particle is inadequate, a significant temperature gradient will exist for a significant period of time from surface to center and, depending on the size of the biomass feed material, a substantial fraction will remain unreacted or follow an alternate, undesirable pyrolysis pathway (Graham, 1993).

If a large piece of biomass is fixed in a hot gaseous stream, the surface reactions might be typical of fast pyrolysis, the primary organic vapors being swept from the reacting surface and away from the reactor. However, it is very likely that a large temperature gradient would exist for a significant period of time from the surface to the centre of the particle, since biomass exhibits very low thermal diffusivity ($\sim 10^{-7}$ m^2/s) being a thermal insulator with very poor penetration at short times. Under these conditions and despite the fact that the reactor temperature lies in the fast pyrolysis regime, slow pyrolysis and secondary cracking could occur in the solid and liquid phases at or below the reacting surface.

Fast pyrolysis demands, as already discussed, a high heating rate. Hence, a minimal heating rate to the particle must be defined, such that temperature gradients in the particle do not effectively exist, that is, they exist for a period of time which is less than that required for slow pyrolysis to occur (Graham, 1993). Therefore biomass thermodynamic properties, particle sizes and reaction rates must all be included when considering heat transfer, which must be adequate to ensure that this minimal heating rate is achieved.

Graham *et al.*,(1984) applied first principles of heat transfer and empirical correlations using published thermodynamic and physical properties of wood (MacLean, 1971; Kanury, 1972; Holman, 1976; Peters, 1983) to define fast pyrolysis in terms of heating rate. Graham's analysis simply considered conduction through the wood particle given an array of heat fluxes, which were related to typical heating environments. The effect of heat transfer and particle size on heating rate is shown in Figure 2-22, which shows the time taken for a particle of a given size to reach a mean temperature, which is half that of the heat transfer environment. These isochrones indicate that fast pyrolysis requires heating environments such as fluidised beds, and small particles in the range of 100 to 1000 μm.

Figure 2-22: The effect of heat transfer and biomass particle size on heating rate (Graham *et al.*, 1984)

Based on the data derived from Figure 2-22, Graham *et al.*, (1984) defined fast pyrolysis as referring to a combination of environments and biomass particle sizes such that the mean rate of temperature rise in the centre of the particle was greater than 1000°C/s. Thus, they proposed that the sample would attain reasonable temperatures for reaction on a time scale corresponding to the "half life" of the reaction. Using a pre-exponential factor of approximately 10^9 s^{-1} and an activation energy of the order of 120 000 J/mole, they calculated that the half time of such a reaction at 500°C would be approximately 100 ms. Combining the calculations of this simple approach with the results presented in Figure 2-22, it was predicted that in a fluidised bed, the average particle size of biomass particles would have to be less than 500 μm in order to achieve fast pyrolysis at 500°C.

Other researchers have attempted to define fast pyrolysis criteria in terms of particles heating rates, as summarised by Graham (1993).

Scott and co-workers (Scott, 1986; Scott *et al.*, 1987; Scott *et al.*, 1988) outlined two criteria for quantifying fast pyrolysis definition in terms of heating rate, by employing both theoretical modeling and empirical data from two similar fast pyrolysis reactor systems, namely the Waterloo University fluidised bed reactor, Section 3.4, and the University of Western Ontario downflow transport reactor, Section 3.5.

The first criterion defines fast pyrolysis as any pyrolysis process in which the temperature at the centre of the biomass particle reaches at least 95% of reaction temperature in a time period not more than 20% of the particle residence time. According to data provided by the University of Waterloo the time estimated for a 600 μm particle to reach 450°C in a bubbling fluidised bed reactor is estimated to be 618 ms, the particle residence time in the bed being between 2 and 6 seconds. Thus, the first heating rate criterion outlined above is satisfied and fast pyrolysis conditions would prevail. However, the first heating rate criterion does not deal directly with the kinetics of fast pyrolysis reactions and their relationship to heating rates, assuming that if the particle temperature achieves fast pyrolysis temperatures within a certain fraction of its residence time, then heat transfer will not be the rate-limiting step and the requirements for heating rates will be satisfied. For example, in a slow pyrolysis process, e.g. wood carbonisation, fast pyrolysis temperatures are reached in a period of hours, while particle residence time is on the order of days. Again the first criterion set by Scott and co-workers is fulfilled, however it is clear that fast pyrolysis does not occur.

The second criterion of Scott for fast pyrolysis definition, as far as heating rate is concerned, relates chemical rate equations to expressions for biomass particle heating rates, and arrives at a model which can be effectively applied on a broad basis. On the basis of empirical data, Scott and Lidén (1985) proposed that fast pyrolysis occurs if the particle centre temperature reaches 450°C before more than 10% wt of the solid feedstock had decomposed. A heat transfer model incorporating secondary vapor-phase reactions predicts that for all particle sizes < 2 mm, the second criterion will be satisfied, excessive char production will be avoided and the optimal production of organic liquids will be obtained. These predictions have been verified during actual fluidised bed fast pyrolysis studies (Lidén, 1985).

A simplified heat transfer model was also described by Simmons and Gentry (1986). These workers, in order to provide an upper boundary for particle size in kinetic studies, estimated the regimes under which biomass particle pyrolysis would be kinetically or heat transfer limited. Simmons and Gentry assumed, furthermore, that internal heat transfer is solely by conduction. The boundary between the kinetic-controlled and heat-transfer limited regions was determined by finding the heat-up time required for the centreline temperature of a wood slab associated with 90% of the ultimate rate. This heat-up time was then compared to the kinetic time for 10% decomposition. The procedure adopted was identical to Scott's second heating rate criterion for biomass fast pyrolysis. In this way, Simmons and Gentry compared characteristic times for reaction rates versus heat-up rates and constructed an approximate boundary for particle size as a function of temperature; above this boundary, the reaction rate is strongly heat transfer dominated, and below the boundary the reaction rate is kinetically controlled. The results are illustrated in Figure 2-23 for two different values for the heat of reaction λ (J/g) from where it may be depicted that for a particle dimension (B) of 0.01 cm, corresponding to a wood slab thickness of 0.02 cm, the pyrolysis of the 200 μm particle might be investigated kinetically at temperatures around 450-500°C. Above this size limitations due to internal heat transfer would require a transport model accounting for internal conduction to be included in any kinetic interpretation.

Although the estimated limit for particle size to undergo pyrolysis in the kinetically controlled region is an order of magnitude lower than that estimated by the University of Waterloo researchers, it must be born in mind that Simmons and Gentry did not account for external heat transfer neither have they taken into account that real particles have higher surface to volume ratios and heat up faster than the estimate provided by a flat plate model.

Figure 2-23: Particle size limit versus temperature for kinetically controlled pyrolysis of cellulose (Simmons and Gentry, 1986)

Researchers at NREL/SERI (Reed *et al.,* 1980; Reed and Cowdry, 1987) initially defined biomass fast pyrolysis in terms of heat transfer requirements, relating the heat for pyrolysis and heat flux to char yields from cellulose. The results of their studies were that the biomass fast pyrolysis requires about 2000 kJ/kg of heat to be supplied to a biomass surface of at least 460°C with a heat flux somewhat above 5 x 10^5 W/m^2, which is also consistent with the findings of Graham (1984), presented in Figure 2-22. Concluding, it is claimed that according to the work undertaken at NREL a reactor system employing some form of conductive heat transfer would be necessary for a successful practical fast pyrolysis system.

Exploring the idea of conductive heat transfer to biomass reacting particles, which could overcome the stringent particle size limitations mentioned above, Diebold (1980b, 1985) demonstrated that contact (or ablative) heat transfer could result in the rapid pyrolysis of even larger biomass feedstocks. Ablation is a physical/mechanical mechanism that removes the primary depolymerisation liquids from the reacting surface at a surface regression rate that is consistent with the heat (thermal) penetration rate. In effect, at an infinitesimal distance below the reacting biomass surface, the temperature remains far below the reaction surface and very limited depolymerisation reactions occur. Diebold described ablation as "solid convective heat transfer" (accelerated conduction) and demonstrated it elegantly by

rapidly slicing through a wooden dowel with a hot nichrome wire. This type of heat transfer may be characterized by direct, intimate contact between a hot non-reacting surface moving over the reacting biomass particle surface, which was found to react, vaporize and retreat at a rate which was much faster than the rate of heat conduction, so that no temperature gradients were practically realized.

The importance of conductive heat transfer on maximisation of pyrolysis liquids is further discussed below.

2.7.2 The fast and the ablative pyrolysis regimes

In the following, a heat balance on a cold (T_o=25°C), wood particle of 1 mm as it heats up to the bed temperature T_R=500°C that maximises (Scott and Piskorz, 1982, 1984) pyrolysis liquids yields is considered. The heating rate, dQ/dt, be written as:

$$\frac{dQ}{dt} = h_t A_p (T_R - T_{wc})$$

(Eq. 2-9)

where

Q	the heat gained by the cold particle	[J]
h_t	the overall (total) heat transfer coefficient	[W/m² K]
A_p	the surface area of wood particle	[m²]
T_R	the reactor temperature	[K]
T_{wc}	the temperature in the centre of the wood particle	[K]
t	the heating time for the particle centre to reach T_R	[s]

The heat gained by the cold particle, Q, is given by

$$Q = m_p c_{pw}(T_R - T_o)$$

(Eq. 2-10)

where

m_p	the mass of the wood particle	[kg/m³]
c_{pw}	the specific heat capacity of wood particle	[J/kg K]
T_o	initial particle temperature (=25°C or 298 K)	[K]

Although the biomass (wood) heat capacity, c_{pw}, is dependent on temperature, it is generally assumed to be constant under fast pyrolysis conditions up to the point at which the biomass decomposes (Peacocke, 1994). A value of 2700 J/kg K (Lèdè *et al.*, 1985) will be used in the following.

Combining Eq. 2-9 and Eq. 2-10 and integrating gives the heating time as

$$t = \frac{m_p c_{pw}}{h_t A_p} \ln \frac{T_R - T_o}{T_R - T_{wc}} \qquad \text{(Eq. 2-11)}$$

Evaluating terms gives (considering the wood density to be ρ_w=350 kg/m^3)

$$m_p = \frac{\pi}{6} d_p^3 \rho_W = \frac{\pi}{6}(10^{-3})^3(350) = 1.83 \times 10^{-7} \text{ kg}$$

$$A_p = \pi d_p^2 = \pi(10^{-3})^2 = 3.14 \times 10^{-6} \text{ m}^2$$

Substituting these values in Eq. 2-11 and considering the temperature at the centre of the particle, T_{wc}, to be 450°C, i.e. 90 % of the reactor temperature (T_R=500°C) to fulfill the second criterion of Scott *et al.*,(1986) for fast pyrolysis definition in terms of heat transfer, Section 2.7.1, a maximum and a minimum heat-up time is obtained depending on the total heat transfer coefficient, h_t. Taking into consideration the heat transfer coefficients calculated by Lidén (1985) in a bubbling fluidised bed of small (approximately 250 μm particles Eq. 2-11 is modified to give the heat-up times, namely:

$$h_t = 100 \Rightarrow t = \frac{(1.83 \times 10^{-7})(2700)}{100 \times 3.14 \times 10^{-6}} \ln \frac{773 - 298}{773 - 723} = 3.54 \text{ s}$$

$$h_t = 300 \Rightarrow t = \frac{(1.83 \times 10^{-7})(2700)}{300 \times 3.14 \times 10^{-6}} \ln \frac{773 - 298}{773 - 723} = 1.18 \text{ s}$$

$$h_t = 510 \Rightarrow t = \frac{(1.83 \times 10^{-7})(2700)}{510 \times 3.14 \times 10^{-6}} \ln \frac{773 - 298}{773 - 723} = 0.69 \text{ s}$$

The above discussion shows the significance of the proper heat transfer environment to fulfill the fast pyrolysis criterion discussed above. For the above discussion, typical heat transfer coefficients for single phase reactors (entrained beds or cyclonic reactors - h_t=100 W/m^2 K, Kovac *et al.*, 1991), two-phase lean reactors (transported beds or Circulating Fluidised Beds - h_t=110-300 W/m^2 K, Kobro and Brereton, 1986) and dense two-phase reactors (bubbling fluidised beds - h_t=300-510 W/m^2 K, Lidén, 1985) are considered.

A non-reacting solid particle exposed to an external heat flux is heated up but not instantaneously. The heating rate is governed by the boundary layer resistance and the rate of

heat flow inside the solid. The relative importance of these two factors is measured by the Biot number, Bi, a dimensionless number which shows where the major resistance to heat transfer lies, comparing as it does the relative magnitude of the surface convection to the internal conduction resistance to heat transfer. Thus:

$$Bi = \frac{h_t d_p}{\alpha_w} = \frac{\text{interior resistance}}{\text{surface resistance}} \qquad \text{(Eq. 2-12)}$$

where

α_w wood thermal conductivity [W/m K]

The wood thermal conductivity is in fact a function of temperature but it is considered constant under fast pyrolysis conditions up to the point at which the biomass decomposes. According to Lèdè *et al.*,(1985) a value of 0.11 W/m K will be used in the following, assumed to be constant throughout the course of pyrolysis.

Substituting the values of the overall heat transfer coefficients discussed above into Eq. 2-12, three values for Bi are found for the different reactor systems considered, namely:

$$h_t = 100 \quad \Rightarrow \quad Bi = \frac{(100)(1 \times 10^{-3})}{0.11} = 0.909$$

$$h_t = 300 \quad \Rightarrow \quad Bi = \frac{(300)(1 \times 10^{-3})}{0.11} = 2.727$$

$$h_t = 510 \quad \Rightarrow \quad Bi = \frac{(510)(1 \times 10^{-3})}{0.11} = 4.636$$

In the first case, of a low heat transfer coefficient to the wood particle (Bi≈1), and the resistance to heat transfer at the surface of the particle (boundary layer) is comparable to the interior resistance, while in the other two cases (Bi>1) the resistance to heat transfer is located in the interior of the particle.

The temperature distribution within the particle is then shown in Figure 2-24 and the pyrolysis regime is referred to as the fast pyrolysis regime, where reaction rates for primary vapor formation are higher than those favouring charring, these dominating at lower temperatures, Section 2.3.1.

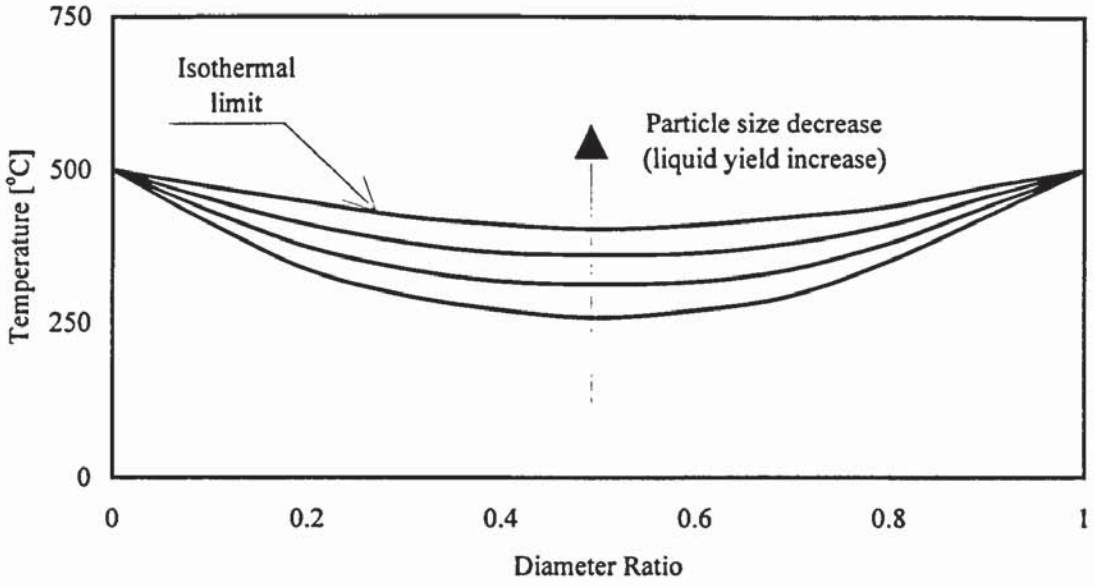

Figure 2-24: The biomass fast pyrolysis regime

Moreover, in this regime the pyrolysis reaction occurs in the whole volume of the small particle and, given the non-uniformity of the original feedstock, significant temperature gradients within the particle may be apparent. The internal temperature gradients complicate the picture, since different reactions predominate at different temperatures. As a consequence, small particles are required to reduce temperature gradients and attain a uniform temperature throughout the whole particle volume. In this regime, liquid yields increase up to the isothermal limit as particle size decreases. The isothermal limit is here considered to be the temperature in the centre of the particle, in accordance to the second criterion of Scott *et al.*,(1986) for the fast pyrolysis definition in terms of heat transfer.

As a result, and despite the existence of high heat transfer environments, where the external heat transfer resistance to biomass particles could be overcome by higher temperatures and high turbulence, the biomass low thermal conductivity would still impose significant heat transfer problems and the internal conduction resistance would prevent larger particles (>1 mm) to attain high temperatures within the narrow time limits required. Moreover, operation of pyrolysis reactor at conditions where the isothermal limit is not reached promote slow pyrolysis, carbonisation reactions. As a consequence, the released volatile products from the biomass particles interior to the bulk of the gas stream have to pass through a char matrix promoting heterogeneous gas-phase secondary reactions, Section 2.4, which crack condensable vapors further and reduce pyrolysis liquids yield.

However, as Diebold (1986) indicated in his ablative pyrolysis system, accelerated conduction by intimate direct contact between biomass particles and heated reactor walls at high pressures, Section 3.7, promotes high local heat transfer coefficients preventing undesired vapor decomposition reactions occurring in the fast pyrolysis regime.

In this way, primary pyrolysis products are mainly deposited on the biomass particle surface as a "melt", which then subsequently decomposes and gives rise to volatile products, which are not decomposed to non-condensable gases by the vapor cracking mechanism readily encountered in the fast pyrolysis regime of heat transfer, since they are evolved from the surface of the biomass particle. In effect the temperature at an infinitesimal distance below the retreating reaction surface, remains far below the reaction temperature, that is actually virgin wood, not being exposed to temperatures high enough to enhance charring reactions, which would furthermore promote heterogeneous secondary reactions resulting in primary vapor cracking and substantial decrease of liquid yields. These conditions ensure the operation of the reactor in the so-called ablation pyrolysis regime, where the reaction occurs in a very thin layer close to the surface of a big particle. Severe pressure gradients are present in the very thin outer particle layer and the temperature profile within the biomass particles resembles this, see Figure 2-25.

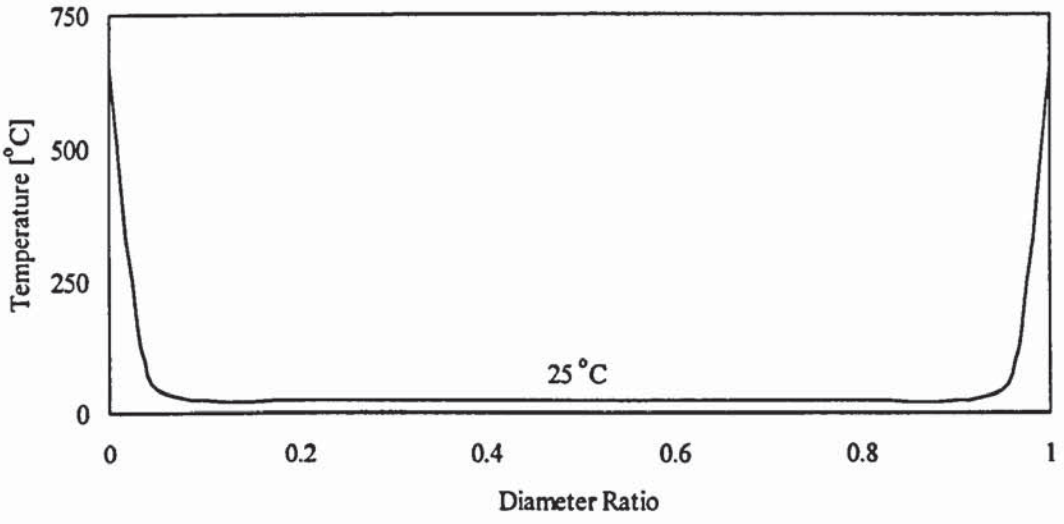

Figure 2-25: The biomass ablative pyrolysis regime

Since only the outermost layers react, particle size is immaterial, which makes operation in the ablative pyrolysis regime advantageous. The same phenomenon of the relative motion between biomass particles and a heated surface is obtained in fluidised beds and other dense phase reactors, such as transported beds, where ablation is defined as a physical/mechanical

mechanism that removes the primary depolymerised liquids from biomass reacting surface at a surface regression rate that is comparable with the thermal penetration rate, see Graham (1993).

Scott *et al.*,(1988) pointed out that once the heating rate criteria are met, all high heating rate reactors (fluidised beds, transported beds or ablative reactors) should show comparable performance, the differences in liquid yields determined solely by variations in gas/vapor residence time and temperature, the only parameters to affect the extent of secondary organic vapors decomposition, as illustrated in Figure 2-26.

Figure 2-26: Prediction of total liquid yields from maple (Scott *et al.*, 1988)

The conclusions drawn by the different research group reviewing heat transfer and related it to various practical heating environments is that for a successful, practical fast pyrolysis reactor system it would be necessary that some form of solid-solid conductive heat transfer, also termed ablation (Diebold 1985; Graham, 1993; Peacocke, 1994), be employed. As a general recommendation it should also be pointed out that a particle size of approximately 2 mm can probably successfully be pyrolysed in a fluidised bed and related high heat transfer

reactor systems for wood fast pyrolysis, such as transported beds and solid-phase heat transfer reactor systems (ablative pyrolysers).

2.8 Summary and conclusions

Biomass fast pyrolysis differs substantially from conventional pyrolysis in terms of reactor conditions, chemical mechanism, product yield and quality and heat transfer requirements.

More specifically, fast pyrolysis of biomass consists of a complex series of reactions but through extensive research in the last decade and the consensus of pyrolysis experts it may be concluded that mechanistically, fast pyrolysis consists of activation, fragmentation and cracking, similar to the Waterloo Model pathway proposed for cellulose pyrolysis, Section 2.3.1. Preservation of valuable gaseous or liquid products will occur if product quenching occurs before heterogeneous vapor-phase cracking, Section 2.4, is allowed to proceed to any appreciable extent.

The main benefits of a large number of kinetic studies, related to biomass fast pyrolysis, have been the optimisation of process parameters and the prediction of yields which, in turn, may lead to improved reactor design approaches assessing the variation in product yields with the most important process parameters, namely gas/vapor phase temperature and residence time. Through the use of several assumptions regarding the nature of biomass fast pyrolysis, the kinetic expressions derived by Lidén (1985) for both primary conversion of biomass to organic vapors and secondary cracking of vapors to gases, secondary pyrolysis products and char, seem to be the most appropriate ones for estimating the liquid yields. Moreover, the kinetic expression adopted seems to link very well the latest findings, in what concerns biomass pyrolysis mechanisms and pathways, to experimental results derived over a wide range of operating conditions for different reactor configurations.

Finally, biomass fast pyrolysis is related to heating rate, which is identified to be a crucial factor for optimizing liquid yield. The heating rate to the biomass particle must be quite high in order to by-pass the low temperature region which favours charring reactions. Different heating rate criteria have been reviewed and discussed, the main conclusion being that the planned new reactor systems must employ some form of solid conductive heat transfer (ablation) to biomass particles.

CHAPTER 3: BIOMASS FAST PYROLYSIS PROCESSES REVIEW

3.1 Introduction

Fast pyrolysis of biomass to produce pyrolysis liquids has already been defined in terms of process conditions requirements, such as temperature and gas/vapor residence time, and has been characterized in terms of heat transfer requirements. Theoretically, the process conditions necessary to carry out fast pyrolysis may be achieved in a variety of equipment, incorporating the features listed below, extensively discussed in Chapter 2:

- high heat transfer, to avoid undesired charring reactions of woody feedstocks
- moderate temperatures, where liquid product yield is maximised
- short gas/vapor residence time, to minimise the extent of secondary reactions.

Since the control of temperature and residence time may, in principle, be adjusted in a variety of reactor configurations, the crucial characteristic that most usually determines the applicability of the different reactor configurations as successful candidates for biomass fast pyrolysis is the heat transfer mechanism to the biomass particles.

According to the conclusions drawn in Chapter 2, it is evident that in a successful practical fast pyrolysis system, heat transfer must be as high as possible in order to bypass the slow heat-up, where slow pyrolysis reactions and formation of char dominate. The high heat transfer that is necessary to heat the biomass particles sufficiently quickly, imposes a major design requirement on achieving the high heat fluxes required to match both the high heating rates and the energy requirements for the pyrolysis reactions.

Each mode of heat transfer imposes certain limitations on the reactor operation and may increase its complexity. The two dominant modes of heat transfer in fast pyrolysis technologies are conductive and convective. Each mode can be maximised or a contribution can be made from both depending on the reactor configuration (Bridgwater, 1995).

A number of reactor systems are reviewed in this chapter, the main criterion for their classification being the mechanism of heat transfer to biomass particles. The selection is based on the achievements made on pilot, demonstration and commercial scale applications. Thus, the pyrolysis systems to be examined in this chapter will include relatively simple reactor configurations operational at near atmospheric conditions, in the absence of moving

parts and using orthodox chemical process industry practices. In this review, ablative, i.e. almost 100 % conductive heat transfer, fast pyrolysis systems will also be briefly discussed, since these reactors have been proven excellent candidates for biomass fast pyrolysis.

Relatively high yields of pyrolysis liquids have also been realized by vacuum pyrolysis, due to the selective withdrawal of specific reaction products from the reactor system before they can react further to secondary products. These systems are also being reviewed and evaluated in the following.

The reactor configurations to be examined are listed in Table 3-1.

Table 3-1: Fast pyrolysis reactor configurations reviewed

Reactor Type	Organisation/Country	Mode of heat transfer	Section
Upflow entrained flow bed	GTRI/USA	5-10 % Conduction 95-90 % Convection	Section 3.2
Downflow entrained flow bed	Egemin/Belgium	5-10 % Conduction 95-90 % Convection	Section 3.3
Fluidised bed 1	ERCO/USA	80-90 % Conduction 20-10 % Convection	Section 3.4
Fluidised bed 2	Univ. of Waterloo / Canada Union Fenosa/Spain	80-90 % Conduction 20-10 % Convection	Section 3.4
Transport reactor 1	Occidental Research Corporation/USA	30-40 % Conduction 70-60 % Convection	Section 3.5
Transport reactor 2	Ensyn, Inc./Canada	50-60 % Conduction 50-40 % Convection	Section 3.6
Ablative pyrolysis systems	NREL/USA Aston University /UK	10 % Convection 90 % Conduction	Section 3.7
Vacuum pyrolysis	University Laval/Canada		Section 3.8

Some considerations about the applicability of a conceptually different reactor configuration for biomass fast pyrolysis, incorporating autothermal operation by means of char energy content utilisation are further discussed in Section 3.9. More specific, the characteristic features of a novel Circulating Fluidised Bed reactor with integral char combustion are outlined and its comparison to other fast pyrolysis reactor systems critically discussed.

Finally, the main features and limitations of the different reactor configurations that have been employed to maximise the liquid yields from biomass fast pyrolysis are summarised in Section 3.9.

3.2 Upflow entrained flow pyrolysis of biomass - GTRI (USA)

3.2.1 Summary of research project and objectives

The design for the Georgia Institute of Technology-USA (later Georgia Tech Research Institute - GTRI) entrained flow pyrolysis process originated in 1978.

The main objective of the original programme was to perform laboratory studies in pyrolysis and gasification, and to design and build a Process Development Unit (PDU), to test the concept of using an entrained bed reactor to generate pyrolysis liquids from biomass. Another aim of this project was to determine the conditions required to optimise oil yields from wood, using the entrained flow pyrolyser.

In 1981, the programme was reviewed and it was decided that the project would be restricted to the development of a PDU, capable of converting about 45 kg/h of biomass, to investigate entrained pyrolysis of hardwood species, readily available in Southeastern USA. The process conditions for optimum yields of pyrolysis oils were experimentally investigated in the entrained flow PDU, which was completed in March, 1983. The results of the experimental runs on this unit (PDU-Confuguration I) demonstrated that dry oil yields of approximately 50 % wt based on a moisture-and-ash-free (maf) feed basis could be obtained. In 1984, modifications were made for design changes and the unit (PDU-Confuguration II) was operated to verify the adequacy of the modified design. In 1987 finally, the design was further amended to include the modification of the unit (PDU-Confuguration III), to improve pyrolysis liquids collection and quality. Due to the modifications and amendments employed, the performance of the GTRI entrained flow pyrolyser was substantially improved and liquid yields of up to 60 % wt have been reported. During this period identification of upgrading catalysts was undertaken and their evaluation was carried out, but the results of the tests were inconclusive and the data from the test were not reported (Kovac *et al.*, 1991).

In 1989, the GTRI project was discontinued due to shrinking programme budgets and the retirement or moves of the key staff.

3.2.2 Description and operation

In the following the description and operation of PDU Configuration III, which resulted from modifications to the previous PDU Configurations I and II referred to above, will be undertaken. For a detailed analysis of this reactor evolution development, the reader may consult the work of Kovac *et al.*, (1991).

Pyrolyzer operating conditions are given in Table 3-2.

Table 3-2: Final GTRI pyrolyzer operating conditions (Configuration III)

Feedstock	Oak Hardwood
Moisture	5-7 % wt
Particle Size	0.25-2.0 mm
Feed Rate	7-23 kg/h (on a maf biomass basis)
Reactor Diameter	0.15 m
Reactor Temperature	550-650 °C

A flow diagram for the final GTRI PDU configuration (Configuration III) is given in Figure 3-1 and its operation is described below (O'Neil *et al.*, 1989).

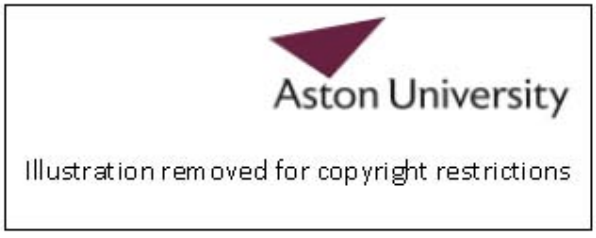

Figure 3-1: Flow Diagram-GTRI, Configuration III (Kovac *et al.*, 1991)

Propane (1) and air (2) supplied by a blower were burned stoichiometrically in an inert gas generator, and the combustion products were cooled with a water spray (3), the gases being saturated with water vapor. The exit stream from the generator was split into two streams, the first (4) providing moderating gas for the first burner, while the other (5) providing conveying gas for the feed particles (6). Propane (7) also fueled a second burner, operated stoichiometrically with air (8). The mixture, consisting of moderating gas, conveying gas, burner combustion products and wood particles, moved upwards through the pyrolysis reactor tube. The resulting mixture (9) consisted of non-condensable gases, water vapor (entering moisture plus combustion and pyrolysis products), pyrolysis vapors and char. Almost all of the char particles (10) were removed in the cyclone the stream (11) leaving the cyclone consisting of condensable gases, water and pyrolysis vapors and some char fines.

This mixture was directed toward the first jacketed cyclone (12). A liquid (water or other solvent) was sprayed upstream of the cyclone inlet, so that the mixture could be quenched rapidly. Three additional sites were available for the injection of quench spray liquid. These sites were upstream of and at the exit of the second jacketed cyclone, and upstream of the first demister. The mixture (13) then entered the second cyclone (14), the pyrolysis vapors and some water vapor being condensed. The condensed phases (15) were removed via sumps and collection receivers, and the exiting mixture (16) consisting of non-condensable gases, water vapor, light organics and aerosols passed through two demisters connected in series (17) and (18), removing most of the aerosols. The resulting mixture (19) consisted mainly of non-condensable gases, water vapor and remaining aerosols enters the flare where it was combusted, the products of combustion (20) being exhausted to the atmosphere.

The results from a number of experimental runs is shown in Table 3-3.

Table 3-3: GTRI product yields (modified reactor - Configuration III)

Run No.	3/10	3/12	3/16A	3/16B	3/18
Temperature, °C[1]	475	524	525	523	504
Yields (% wt on maf feed)					
Organic Liquids	51.8	53.8	56.8	57.1[2]	60.0[2]
Char	10.0	8.4	9.6	9.3	12.1
Water	not reported				
Total Gas	13.0	34.3	5.6		

[1]reference temperature K-type thermocouple located at the entrance of the reactor
[2]hexane used as the quench spray fluid

3.2.3 Products

The organics derived from the GTRI entrained flow pyrolysis reactor are highly oxygenated with no phase separation. They have an initial boiling point range from 70 to 90°C. They are heat sensitive and will decompose when heated to temperatures greater than 185-195°C. The liquids are acidic, have an acrid odour and also exhibit corrosive properties with some metals. A typical analysis is shown in Table 3-4.

3.2.4 Special features and problems

The GTRI entrained system successfully produced several hundred kg of pyrolysis liquids. The liquid yields ranged from 31 to 60 % wt (on a maf feedstock basis) depending on the reaction conditions. In spite of the extended experimental programme undertaken by GTRI, several problems could still be identified which include:

- accumulation of tarry material in the first stages of the air-cooled condenser (a problem removed after the quenching of hot vapors, practiced in Configuration III)
- proper design of high temperature pyrolysis vapors cooler/condenser to avoid premature water condensation
- lack of operational experience on recycled product gas for reactor heating.

A reactor model has been devised and tested (Gorton *et al.*, 1990) that predicts that liquid yields of approximately 70 % wt for a particle residence time of 1.05 s are achievable

although the maximum experimental pyrolysis liquids yields did not exceed 60 % wt. It should be noted here that in the GTRI upflow entrained mode of operation, the particle residence time equals gas residence time. In order to further increase the liquids yield the particle residence time should be reduced substantially. This can be accomplished by an increased flowrate, by a shorter reactor, or both (Kovac *et al.*, 1991).

However, the main problem of the GTRI entrained fast pyrolysis system is the method of heat transfer, which is provided almost entirely by convection between hot entraining gases and biomass particles. Inadequate heat transfer was exceptionally dominant during the initial development of the GTRI entrained flow pyrolyser, which led to significant decrease of biomass throughput from 40-50 kg maf biomass/h (Configuration I - Knight *et al.*, 1983) to 7-23 kg maf biomass/h (Configuration I - Kovac *et al.*, 1987). Since the heat fluxes attained with gases alone are inferior to those readily encountered in two-phase heat transfer systems, where conduction with hot solids is the dominating mode of heat transfer, extensive residence times are required in order to avoid incomplete pyrolysis.

As a result of the higher gas/vapor residence times needed to ensure adequate heat transfer to biomass particles, additional secondary reactions/cracking are taking place in the vapor phase, which subsequently lowers the liquid yield and hence the performance of the pyrolysis system (Knight *et al.*, 1984). The results from the GTRI experience emphasize the importance of reaction severity in terms of heat transfer and the decisive role this factor plays on determining product yields.

3.3 Downflow entrained flow pyrolysis of biomass - EGEMIN (Belgium)

3.3.1 Summary of the project and objectives

The aim of this process was the production of pyrolysis liquids by fast pyrolysis of fine wood particles in a 200 kg/h vertical downflowing entrained flow pilot plant. The Egemin plant was commissioned in October 1991.

The idea originated from the concept of a cyclonic reactor, investigated in the early and mid 1980s by Lédé and coworkers at the University of Nancy-France, who operated a cyclonic reactor for pyrolysis at wood flowrates up to 0.35 kg/h (Lédé *et al.*, 1985; Martin *et al.*, 1986).

3.3.2 Description and operation

The feedstock consisted of small (<2.5 mm, with 90 % being smaller than 1.6 mm) wood particles. Feed moisture and ash contents were 16 and 0.57 % wt respectively. Wood was transferred from a storage silo to a small buffer hopper before being fed into the reactor using a water cooled screw provided with a nitrogen purge, Figure 3-2. Wood particles were entrained into the downflowing reactor (height 1.2 m, diameter 0.4 m) in a stream of hot gases at between 700 and 800°C produced by a 90 % substoichiometric propane burner, diluted with nitrogen to limit the temperature. The reactor was designed to achieve an average particle residence time of 0.6 s, mainly determined by the velocity of the carrier gas.

Figure 3-2: Flow diagram of the Egemin fast pyrolysis process (Baeyens *et al.*, 1994).

Pyrolysis products left the reactor at approximately 490°C and passed through a cyclone, where most of the char was retained. Char recycle - dashed lines in Figure 3-2 - was never practiced although the system was designed for it. The gaseous stream was then quenched in a venturi scrubber using pyrolysis liquids as the scrubbing medium. The gas entry temperature to the venturi scrubber was approximately 400°C and the scrubber liquid exit temperature was 55°C during normal operation. The recycled pyrolysis liquids were cooled with a water cooled heat exchanger. Mineral oil was used to start up the scrubbing system. The pyrolysis liquids were allowed to accumulate in the disentrainment tank (decanter) and were drained at the end of the run.

Approximately 75-80 % of the pyrolysis liquid products were collected by the scrubber, most of the remainder being collected from the fan drain. Gas separated from the liquid products left the venturi scrubber disentrainment tank through a demister (fibre mist eliminator) using a recycle compressor. The liquid product collected from the fan was highly viscous compared with that collected by the venturi scrubber, which was partly attributed to water and light organics being evaporated and partly to higher gas/vapor residence times. The non-condensable gases were flared, but still contained a small amount (up to 5%) of aerosols.

A mass balance is given in Table 3-5 (Maniatis *et al.*, 1993). The gas mass flow rate was not measured and was obtained by difference. The pyrolysis liquids measured were collected from the primary collection vessel, the secondary collection vessel and the drain of the fan.

Table 3-5: Mass balance for Egemin biomass fast pyrolysis process

Streams	Mass flowrate (kg/h)	Yield (% wt)
Input		
Wood (dry)	84.0	-
Outputs		
Organics	33.5	39.9
Gas (by difference)	13.6	29.0
Char	24.4	16.2
Water	12.5	14.9

3.3.3 Special features and problems

During the operation, a number of problems were encountered (Maniatis, 1995) which led to the low yields of pyrolysis liquids:

- the preheating of the carrier gas and its dilution with nitrogen to adjust the temperature was not controlled very well, resulting in relatively large temperature variations (± 50°C)
- the inlet of the gases and the entrained biomass particles in the reactor was not tangential, resulting in poor flow patterns in the cyclonic upper part of the reactor
- the cyclone had, due to operation at less than design efficiency, low efficiency, resulting in high carryover of char fines to the liquid condensation unit and hence to the liquid product collected
- the cooling of the liquids was not rapid enough, due to the accumulation of char fines in the heat exchanger which resulted in a gradual blockage and reduced heat removal
- the collection of the liquids and their separation from the gas stream proved inefficient, resulting in liquids being collected at 3-4 different points.

However, the main problem encountered with the Egemin reactor configuration was poor heat transfer characteristics. As a result, the feed was not completely pyrolysed, particularly at feed rates in excess of 100 kg/h, which needs to be compared to the system design capacity of 200 kg/h. The heat transfer to the biomass particles, mainly by convection from the gas phase, proved insufficient at the short residence times employed. An elemental analysis of the product char showed high quantities of hydrogen and oxygen, which also indicate incomplete reaction as already discussed (Maniatis *et al.*, 1993). Smaller particles would help to reduce this problem. The hot, partially pyrolysed wood continued to pyrolyse in the cyclone and char collection pot, potentially contaminating the primary fast pyrolysis products with secondary ones. To solve this problem, Egemin proposed a recycle loop for the partially reacted feed which is analogous to the recycle loop in the NREL vortex ablative reactor (Stevens, 1994b).

3.4 Fast pyrolysis in a bubbling fluidised bed (ERCO-University of Waterloo-Union Electrica Fenosa)

3.4.1 Introduction

Fluidised bed reactors have been used extensively in industry for a variety of gas-solids reactions such as combustion and gasification. In the early 1970's, fluidised bed reactors were developed for the pyrolysis of coal, Municipal Solids Waste (MSW) and biomass, ranging from pilot plants to commercial demonstrations. Energy Resources Co., Inc. (ERCO) of Cambridge, Massachusetts, undertook an extensive experimental programme on biomass

rapid pyrolysis in a classical bubbling fluidised bed to investigate the effect of secondary reactions and the role they play in the determination of the final product yield. Moreover, ERCO developed an analytical model to predict the yield of liquid fuels from biomass.

Meantime, a similar programme was initiated in 1980 in the University of Waterloo, with the main objective of establishing conditions for maximising liquid yields from biomass, particularly from forest and agricultural wastes. The initial bench scale continuous unit was based on a coal fast pyrolysis technology developed at CSIRO in Australia (Scott, 1995).

A continuous fluidised bed bench scale fast pyrolysis unit, operating at atmospheric pressure and feed rates of about 100 g/h, was employed (Scott and Piskorz, 1982). Extensive pyrolysis tests with hybrid aspen-poplar sawdust (105-250 μm), were carried out in a nitrogen atmosphere, over a temperature range of 400-600°C. Results indicated that at an apparent vapor residence time of 0.5 s, high organic liquid yields of up to 65 % of the dry wood weight fed were obtainable from hardwoods such as aspen-poplar and maple, while yields of 40-60 % wt could be obtained from agricultural wastes such as wheat, straw, corn stover and bagasse (Scott and Piskorz, 1982).

Using the results obtained from the bench scale unit, a larger process unit of 2-3 kg/h was designed, constructed and tested (Scott and Piskorz, 1984). Yields from hardwoods as high as 65-70 % wt of the dry wood fed were achieved at optimal conditions, i.e. temperatures of about 500°C, while agricultural wastes, such as wheat straw, gave significantly lower liquid yields (45-50 % wt) with higher optimal temperature (550-600°C). Based on the experience gained from this process, known as the Waterloo Fast Pyrolysis Process (WFFP), a 200 kg/h unit for Union Electrical Fenosa in Spain was designed, constructed and tested and plans are underway to further scale up this unit (Cuevas, 1996).

3.4.2 Description and operation

Operating conditions for ERCO's bubbling fluidised bed are presented in Table 3-6.

No further data are known about ERCO's fluidised bed process except the fact that this is an incomplete combustion process, where a portion of the char is burned to provide the heat necessary to carry out pyrolysis thermal requirements (Kosstrin, 1980a). There is no reference about the superficial velocities of the gas but it is believed that they are an order of magnitude higher than the minimum fluidisation velocity of the inert heat carrier (sand). A flow diagram of the 3 kg/h process unit at the University of Waterloo is shown in Figure 3-3 (Scott and Piskorz, 1984).

Figure 3-3: Flow diagram for the University of Waterloo biomass fast pyrolysis process (Scott and Piskorz, 1984)

All forms of biomass tested were air dried, hammer milled and screened to -595 μm (-30 mesh) particle size. The feed material was then conveyed from a hopper by a variable speed twin screw feeder, at the end of which the biomass particles were pneumatically swept off the screw discharge by a flow of recycled product gas and were conveyed into the reactor. The feed injection point was within the fluid bed itself. The reactor fluidising material was sand, and the fluidising agent (recycled product gas) was preheated in the inlet line by controlled electric heaters. In addition, the reactor was wrapped with heating coils, allowing extra heat to be added electrically either to the bed of sand or to the freeboard space.

All pyrolysis products were swept from the reactor to a cyclone. The char was separated in the cyclone and the product gas and vapors passed to two vertical condensers in series, which had the pyrolysis gas/vapor inside the tubes and where the liquids were collected. Every tube had a clean-out plug at the top and a condensate collection pot at the bottom. The first condenser, where heavier organics are collected, could be operated at temperatures up to 100°C, while the second condenser, where light chilled organics are obtained, uses water at near 0°C as the cooling medium. The gas from the condensers then passed through two filters to remove mist and then was directed to a recycle compressor. A regulated gas flow was taken from the compressor discharge and used to fluidise the reactor bed and to convey feed into the reactor, while the excess was vented through a gas analyzer and gas meter as product gas. The product gas was analyzed for CO and CO_2 in an on-line infra-red gas analyzer-recorder. Samples of the product gas were also taken periodically and analyzed by gas chromatography.

The gas flow rate (and hence bed velocity), reactor configuration as well as sand and biomass feed particle size, were selected so that the sand or biomass feed was not eluted from the bed, while the low density char formed after pyrolysis was conveyed out of the reactor (entrained) into the cyclone. In this so called "blow-through" mode of operation, which results in a negligible amount of char present in the bed, there is no need for sand circulation or entrainment.

The successful demonstration of a high liquid yield producing process resulted in a delivery of a number of similar units, designed and constructed by the University of Waterloo, for research purposes at universities and research centres worldwide, including NREL, University of Stuttgart, Technical Research Centre of Finland and Aston University. These systems range from 0.1 to approximately 2 kg/h. It was recognised that indirect cooling was an inefficient and ineffective way to collect pyrolysis vapors and alternative product recovery units were provided in some of the above systems. Thus, in the Aston University, 1.5 kg/h bench scale unit, the shell-and-tube heat exchangers were replaced by a quench unit, where product vapors come in direct contact with recycled pyrolysis liquids, Figure 3-4. The unrecovered pyrolysis vapors are further collected in a demister, are passed through a cotton wool filter and finally a molecular sieve column, to remove any water, before they are metered and released through the vent (Peacocke, 1995).

Figure 3-4: Flow diagram for the Aston University variant of WFPP (Peacocke, 1995)

3.4.3 Results

The highest pyrolysis liquids yield from sawdust for ERCO process was 40% wt, obtained at 510°C and about 2 s residence time, while char and gas yields were 30% and 20% respectively (Kosstrin, 1980a).

As far as the WFPP is concerned there are distinct differences between the liquids derived from woody feedstocks and those derived from agricultural residues (Scott and Piskorz, 1984). The liquid products derived from wheat straw appears to have a lower viscosity and a significantly higher pH of 3.2 to 3.8 than did the liquids derived from hardwoods, which had a pH of 2.3 to 2.8. On the other hand, liquid elemental analyses were very similar for the liquids derived from wheat straw and those from the hardwoods.

Table 3-7 shows the experimental yields of products from selected runs (Piskorz *et al.*, 1987), for four different woods. High organic liquid yields are characteristic of all four materials when undergoing fast pyrolysis in WFFP. The liquids are highly oxygenated, single-phase, homogeneous fluids, which pour readily, and which contain from 13 % to 16 % wt water depending on the feed material, its moisture content and the reaction temperature employed.

Table 3-7: Pyrolysis yields from different woods at optimal conditions

Feedstock	Brockville Spruce	White Maple	Red Poplar	IEA Poplar
Temperature, °C	504	500	508	504
Moisture content, % wt	5.2	7.0	5.9	4.6
Particle top size, μm	1000	1000	590	1000
Gas apparent residence time, s	0.47	0.65	0.47	0.48
Feed rate, kg/h	2.10	1.91	1.98	1.85
Yields, % wt of maf wood				
Total liquids	72.6	78.1	76.9	78.4
• Organic liquids	62.9	66.5	67.9	66.2
• Water	9.7	11.6	9.8	12.2
Char	16.5	12.2	13.7	7.7
Total gas	12.0	7.8	9.8	11.0
• H_2	0.02	0.02	0.01	0.01
• CO	4.95	3.82	4.12	4.44
• CO_2	6.14	3.37	4.89	5.75
• CH_4	0.45	0.38	0.36	0.37
• C_2H_4	0.22	0.17	0.16	0.13
• C_2H_6	0.06	0.03	0.04	0.05
• Others (C_3,C_4)	0.19	0.04	0.21	0.27
Mass balance closure (%)	101.1	98.1	100.4	97.1

Over the past ten years the WFPP has been developed to the point at which a semi-commercial demonstration plant becomes feasible. A 200 kg/h pilot plant, based on results from the PDU, was constructed in Spain (Carrasco, 1990). This plant, now operating under the Spanish utility Union Electrica Fenosa, completed the commissioning phase in 1994 and extensive testing is now underway to maximize its performance. Plans have been announced for a scale-up to a demonstration plant of 2 tonnes maf biomass/h (Cuevas, 1996).

3.4.4 Special features and problems

Fluidised bed reactors have proved successful for biomass fast pyrolysis. In addition to their flexibility and thermal stability they exhibit a number of advantages mainly in terms of operation simplicity and heat provision.

The deep fluidised bed system developed by ERCO achieves rapid heating rates and a controlled elevated temperature, however it is limited by a relatively long average residence time that is beyond the optimal level for maximum yields of liquids, as discussed in Section 2.5. Extensive gas backmixing is inherent in this type of fluidised bed and contributes to a

broad residence time distribution of gas and vapors and, hence, poor control of product selectivity.

The main features of the WFPP, the shallow (i.e. low height-to-diameter ratio, lying in the order 2-3) fluidised bed process, are:

- the "blow-through" method of operation (char and sand separation is thus avoided in a subsequent step)
- the use of recycle gas for fluidisation
- the external supply of heat to carry out the pyrolysis reaction (preheating the fluidising gas, externally heating up of the reactor).

The most critical design feature in the WFPP is the method of heat transfer used and the resulting constraints this puts on the reactor design and, more specifically, its ability to achieve economical scale-up for industrial applications. Since heat is mainly provided to the biomass by the incoming fluidising gas, large gas flows are required to sustain the pyrolysis reaction. This leads, in turn, to quite a large fluidised bed area in order to obtain a smooth fluidisation and operate in the "blow-through" mode. Thus, the gas velocity at the entrance of the fluidised bed reactor should be less than 0.3 m/s at reaction temperature approximately 500°C (McKeough *et al.*, 1988) in order to ensure continuous entrainment of the pyrolysis solid product (char), while the heat carrier is to be maintained in the bed.

The low gas velocities employed impose yet another limitation in reactor scale-up, since the height of the reactor should be quite shallow to achieve the narrow range of gas residence times allowable for optimal pyrolysis liquids production. In large and shallow fluidised bed reactors, it becomes necessary to introduce the solid biomass through multiple feed points to achieve a relatively even distribution throughout the reactor, which introduces another complication in reactor design and operation. These problems are reflected to the fact that although designed to operate at a biomass throughput of approximately 200 kg/h, the pilot plant is currently operating at maximum 160 kg/h, i.e. a reduction by 20 % (Cuevas, 1996).

Another problem arises from the fact that in order to meet the plant energy demands, and more specifically the heat for pyrolysis, the incoming fluidising gas should be heated to approximately 800°C. For a commercial process, this heat for pyrolysis still has to be provided internally, by exploiting the energy content of the byproduct char and pyrolysis gas, in order to achieve economic operation of an industrial process. In this case, additional

equipment, such as an air-blown gasifier to produce fuel gas from the char or a gas furnace for subsequent char combustion, will still be needed (Beckman *et al.*, 1990), that will not only increase the complexity of the plant but may also have a negative impact on plant overall economics.

The main conclusions drawn for the WFPP are:

- a fluidised bed system for biomass fast pyrolysis proves superior in performance comparing to entrained flow systems
- the "blow-through" mode of operation proved to be an effective way to remove char from the bed, so that undesired secondary gas-phase reactions are not taking place and pyrolysis products are successfully preserved in the freeboard
- the operation at higher capacities might prove difficult, due to the inherent difficulty to scale-up shallow fluidised bed systems
- the energy requirements of the process must be met externally by proper heating of the recycle gas to elevated temperatures.

3.5 Indirect char combustion to provide the heat for pyrolysis in a transport reactor (Occidental Research Corporation - USA)

3.5.1 Introduction

During the early 1970s a process for solid waste pyrolysis was developed by Garret Research and Development as an extension to the liquefaction of coal. Initial theories were tested in a 1.5 kg/h laboratory test unit, on different types of wastes including lignocellulosics, such as Douglas fir bark, rice hulls and grass straw. The effects of pyrolysis temperature, feed moisture content and particle size on product yields and quality were determined in order to derive optimum conditions for subsequent reactor scaleup. The results of the laboratory study indicated that total pyrolysis liquids yield based on dry reactor feed were in the range of 40-50 % wt (Bogley *et al.*, 1977).

Based on the data derived from the laboratory unit, a 4 tonnes/day pilot plant was completed in March 1971 and tested up to March 1975 (Levy, 1975). With this unit, Garret Research and Development (which by that time had been acquired by Occidental Petroleum and renamed Occidental Research Corp.) was able to verify the theoretical principles established in the laboratory unit and to process enough material to allow definition of design parameters

for a full size plant. The pilot plant results confirmed that a moisture free pyrolysis liquid yield of approximately 43 % wt on a maf basis at 480°C could be obtained from the pyrolysis of Douglas fir bark, while yields from rice hulls and straw were somewhat lower at 30.2 and 33.3 % wt respectively (Bogley *et al.*, 1977).

Finally, a project was launched to scale-up the pilot plant technology initially using Municipal Solid Waste (MSW) processed to Refuse Derived Fuel (RDF) at a 200 tonnes/day demonstration plant in San Diego County, California. This project was divided into three major phases: design, construction and evaluation. However, difficulties occurred in finding a site for the project and as a consequence the construction phase, originally planned for August 1975, did not begin until February 1976 and the final phase of the project, a one year testing and evaluation period, scheduled to begin September 1976. The pyrolysis runs actually began in August 1977 and continued until mid-March 1978, after which plant staffing was substantially reduced. During the pyrolysis operation, five unsuccessful attempts were made to pass an EPA acceptance test of 72 hours of consecutive pyrolysis operation, which (if successful) would have resulted in additional funding. Various parts of the non-pyrolysis systems continued in operation, such as the front-end preprocessing units and the glass and aluminum recovery systems, until staffing of the demonstration facility was completely discontinued at the end of July 1978 (Acres American Inc., 1979).

3.5.2 Description and operation

The pyrolysis system of OFPP was composed of a complex network of recirculating loops that incorporated the char and pyrolytic gas produced during the fast pyrolysis process. The RDF was comminuted to a fluff prior to feeding and was fed pneumatically to the bottom of a 6.8 m vertical, refractory-lined reactor vessel (essentially a lined steel pipe), where it was pyrolyzed under 510°C, 83 kPa conditions for 0.3 s gas residence time (Acres American Inc., 1979). A schematic of the OFPP is shown in Figure 3-5.

A series of cyclones removed char and ash, which were pneumatically transported to the ash stripper (essentially a sand/char pot), a vertical, refractory-lined vessel operating at identical conditions to the pyrolysis reactor. Char collected in this vessel entered a cold recirculation loop and was pneumatically transported by high pressure recycle gas to the char burner, where any unburned organics were combusted at 730°C, 83 kPa. Subsequently, the hot ash and char were separated from the flue gases and were recycled, along with high pressure

recycle gas to the pyrolysis reactor, where it was used as the direct heating medium at an ash/waste feed weight ratio of 5 (Bogley *et al.*, 1977).

The pyrolysis vapors were quickly transported to a quench venturi, where intimate mixing with light fuel oil terminated further cracking, condensing much of the vapor into a "pyrofuel" mixture. The pyrofuel and quench oil fractions were subsequently separated in a decanter. Noncondensable pyrolytic vapors were cleaned in an acid scrubber at 54°C and then either compressed in low (205 kPa) and high (308 kPa) pressure centrifugal compressors for use as an inert transport medium or combusted in the afterburner for process heat purposes.

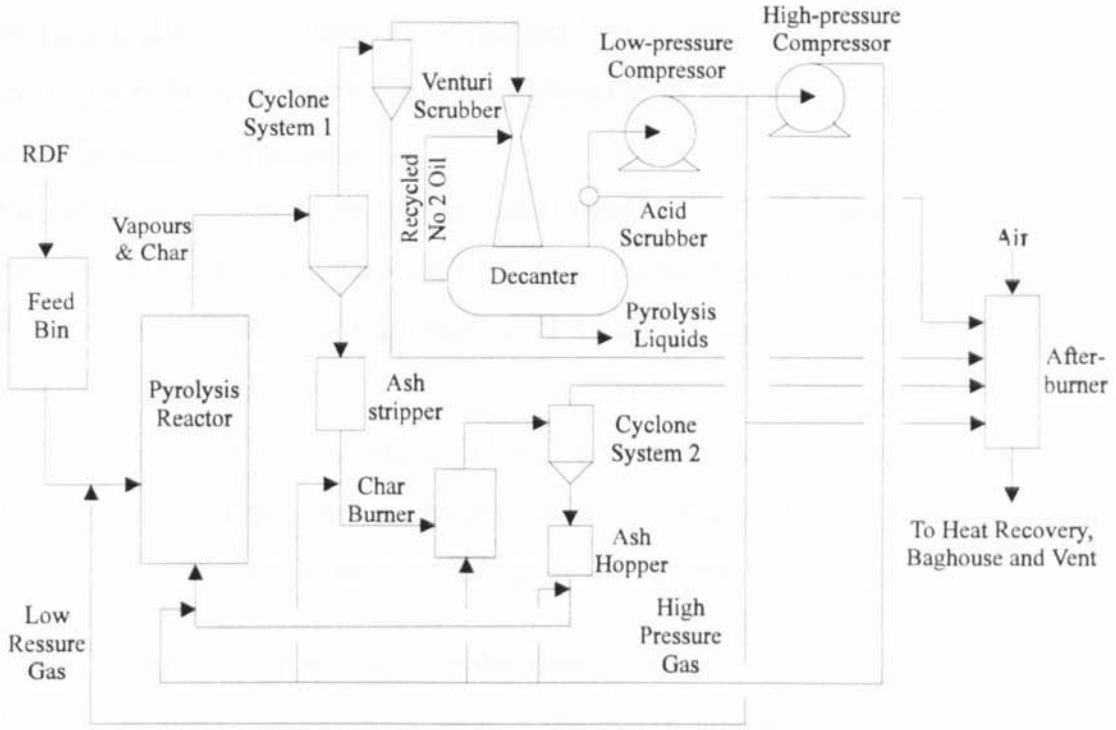

Figure 3-5: Flow diagram of OFPP-RDF fast pyrolysis process

3.5.3 Special features and problems

The OFPP had a large number of developmental problems. The total time of operation from was 140 hours, due to the excessive mechanical problems and breakdowns experienced throughout the plant. Processing rates never reached greater than 40 % of design values.

Major problems in the char recirculation system were encountered, as the quantity and quality of internally produced solids (char and ash) necessary to meet heat transfer purposes were never reached. In spite of this, the recirculation of char and its direct contact with pyrolysis vapors, promoted heterogeneous reactions resulting, to secondary gas-phase cracking of primary pyrolysis products, leading to the formation of excess water and non-condensible

gases, as discussed in Section 2.4. Likewise, sufficient amount of clean, pyrolytic recycle gas could not be produced to replace the temporary use of nitrogen gas for transport purposes and of light fuel oil for various process heating purposes.

As a result of the excessive vapor cracking, the properties of the small amount of pyrofuel produced did not approach product expectation, since its characteristics did not resemble those of a marketable fuel. Moisture content, originally predicted to be 14 %, averaged 52 %. The resultant volumetric heating value was only 27 % of heavy fuel oil, as opposed to the projected 64 %.

In conclusion, although the concept of indirect heat transfer by utilization of byproduct char proved to be right in the pilot plant, its application in the case of the demonstration plant failed for the following reasons:

- char and ash are not the proper heat transfer medium since, on the one hand, heterogeneous char-vapor secondary reactions promote gas formation (Section 2) and, on the other hand, char is not an easy solid to handle and circulate around an extended recirculation loop system
- gas-solid separation in the complicated cyclone system was not effective, as large amounts of solids remained entrained in the gas stream, eventually depositing in the decanter and deleteriously affecting the recovery of the remaining pyrolysis products.

However, it must be kept in mind that the above conclusions are based on short-term, non-steady state, reduced capacity runs. Few of the major equipment items were at full design load conditions during data collection. Upstream inadequacies (e.g. insufficient shredding and drying) passed on to the downstream processing units, making their original designs inadequate for processing the "undesigned-for" feed characteristics. Difficulties in meeting the EPA acceptance test of pyrolysis operation were often due to unit inabilities and not system inabilities.

Similar to OFPP dual-bed systems for the energy exploitation of solid wastes incorporating circulating solids and indirect char combustion to provide the heat for pyrolysis include the Tsukishima Kikai and the AIST-Ebara pyrolytic processes, developed in Japan. Unlike OFPP, these systems operate at higher temperatures (750-800°C) and longer vapor residence times, producing medium calorific value gas and smaller amounts of secondary tars (Kuester, 1981). The dual-bed concept was also exploited during the development of the Battelle

Columbus biomass gasification process (Paisley *et al.*, 1989), which uses a hot sand phase, instead of char, as the heat transfer medium and thus it is possible to separate the endothermic gasification reactions from the exothermic combustion ones. The reactions in the gasifier produce a medium calorific value gas and char which, along with the sand, is separated from the product gas and is transferred to the combustor, where char is consumed to reheat the sand, which then returns to the gasifier.

3.6 Rapid thermal processing in transport reactors (University of Western Ontario-Ensyn, Inc. - Canada)

3.6.1 Introduction

In the early 1980s, a group of chemical engineers at the University of Western Ontario (UWO) initiated the development of a rapid pyrolysis/cracking process, which was then termed "Ultrapyrolysis" (UP). The primary objectives of the UP program was to produce high value petrochemical feedstocks like ethylene as well as other valuable chemical intermediates (i.e. unsaturates) and saturated hydrocarbons at the expense of solid and liquid products.

In 1984 two of the original Ultrapyrolysis development engineers from the UWO formed Ensyn, Inc., in order to carry on process development at a larger scale, in order to produce non-equilibrium chemicals and pyrolysis liquids in quantities large enough to fuel applications of industrial interest, such as furnaces, diesel engines and gas turbines.

3.6.2 Description and operation

An Ultra-Rapid fluidised reactor was designed and constructed. This early investigation (Bergougnou *et al.*, 1983) incorporated a steady-state, semi-continuous reactor system rated at 0.3 kg/h and led to the further development of a 1.0 kg/h hot pilot plant, which produced high olefin yields with little or no char formation (Mok *et al.*, 1985).

Over 500 runs were carried out using the Ultrapyrolysis system with reactor temperatures in the range 650-1000°C and gas residence times of 50-900 ms. The feedstocks used were Avicel cellulose (a 100 μm microcrystalline cellulose powder), IEA poplar, red maple and lignin. For cellulose, it was found that the asymptotic total gas yield increased from 28 % to 88 % wt as the temperature is increased from 650 to 900°C.

The major components of the Ultrapyrolysis process are illustrated in Figure 3-6. Rapid mixing and heat transfer are carried out in two conical vessels known as vortical contactors or Vortactors. The first was termed a Thermovortactor and allows heat to be transferred from hot particulate solids (thermofor) to the biomass (Berg *et al.*, 1986). The second vortactor, termed a Cryovortactor, allowed fast quenching of the products by the transfer of heat to cold solids (cryofor).

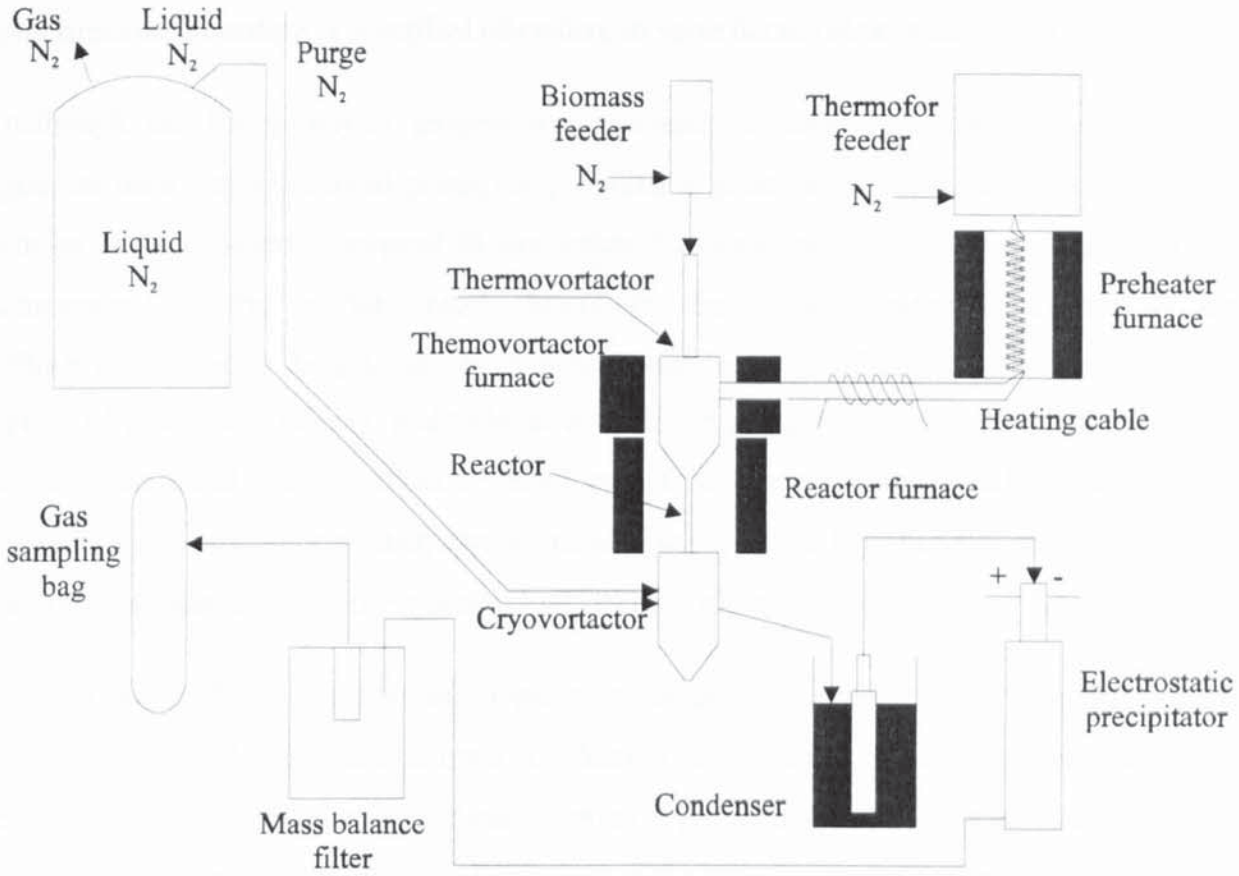

Figure 3-6: Flow diagram - University of Western Ontario Ultrapyrolysis system

Thermofor (sand), cryofor (liquid nitrogen) and biomass feeders were employed in the system. During Ultrapyrolysis experiments, these units were all fluidised-bed type, pneumatic transport feeders, which essentially "pumped" the fluidised solids through a transport line. The thermofor feeder sent cold (i.e. at room temperature) particulate solids to a double preheater coil assembly, where they were heated to the reaction temperature, then on to the Thermovortactor. The cryofor and biomass feeders delivered their solids directly to the Cryovortactor and Thermovortactor, respectively.

The fast pyrolysis of biomass was initiated in the Thermovortactor and continued in a plug-flow entrained bed downflow reactor. The reactor was simply a 1 m length of Inconel 601

pipe, which was housed in an electrical resistance oven. The mixture of hot solids and biomass passed from the Thermovortactor, through the entrained flow reactor, to the Cryovortactor. Products which were initially cooled to about 300 to 350°C in the Cryovortactor were cooled to room temperature in a cyclonic condenser heat exchanger. Solids and condensable were deposited in the filter, and the entire non-condensable product gas was collected in the gas collection bags. The Ultrapyrolysis flow scheme and experimental procedure is described elsewhere in more detail (Mok *et al.*, 1984).

Although the Ultrapyrolysis process was primarily developed for the maximization of gaseous fuels, its operational principles provided a good basis for further development of similar reactor systems designed to maximize the liquid products yields by reducing the temperature of the reactor vessel. Moreover, the severe limitations existed in the Ultrapyolysis reactor design, such as excessive wear (erosion) of the reactor walls and "dead spots" of incomplete mixing, had to be overcome and provision had to be made for scale-up to a commercial size. Process development and significant modifications of the Ultrapyrolysis process were then carried out by Ensyn, Inc., a firm incorporated in 1984 and gave rise to "Rapid Thermal Processing" (RTP) pilot plants.

The generic RTP process has been reported to consist of several reactor systems ranging from 0.3 to 1000 kg/h feedstock input (Graham *et al.,* 1990). The common denominator of each system is the rapid mixing (and resulting rapid heat transfer) and precise control of relatively short gas/vapor residence times, one of the most important process parameters. To date, at least three reactor systems have been developed one of which is a downflow transported bed, while the others two are upflow transported beds. The optimum process residence time is the critical parameter for selecting the reactor configuration.

The RTP-1 pilot plant, rated nominally at 10 kg/h and representing a scale-up of more than 30 times the Ultrapyrolysis plant capacity, was designed, built and tested at Ensyn's Ottawa facility (Graham *et al.,* 1990). At the heart of the plant is a simple downflow jet reactor system which, like its predecessor, uses hot solids to rapidly heat the carbonaceous feedstocks materials. This unit was developed to investigate a broad range of residence time, and was capable of operating within a residence time range of 50 to 1500 ms (from heat-up to quench), and from 400 to 900°C. Figure 3-7 illustrates the principal components of the 10 kg/h RTP-1 unit (Bridgwater and Bridge, 1990).

Figure 3-7: Ensyn RTP-1 pilot plant (10 kg/h)-Downflow design (Bridgwater and Bridge, 1990)

Hot solids (sand) were fed from a number of heat carrier feeders to the mixer where they were injected towards the centre of the vessel. The feedstock was delivered from a feeder to the top of the reactor where it was injected into the cloud of turbulent hot solids. Extremely rapid heating of the feed material was achieved as the feed and hot sand particles were quickly and thoroughly mixed. After the fast, intimate mixing was complete, the feed and solid heat carrier passed though a tubular reactor whose length was adjusted to control the processing time. The sand flow rates were adjusted to maintain the desired reaction temperature and to ensure isothermal conditions. The products were rapidly cooled in a quencher and the solids were removed in a drop-out vessel (solids catch-pot). Two condensers, an electrostatic precipitator and filter system were used to separate the liquids from the gaseous products (Graham *et al.*, 1990).

A second unit, termed RTP-2a rated at 30 kg/h, was assembled (1988) and tested (early 1989). The reactor was an upflow configuration with the mixing section at the base. Residence times varied between 850 ms and 1.5 s. Temperatures were in the range of 450 to 650°C. Successful operation of the 30 kg/h flow system, gave rise to the basic design parameters for a similar 100 kg/h (nominal) upflow RTP plant, the RTP-2b. This system, which is shown in Figure 3-8 (Graham *et al.*, 1990), was constructed in mid-1989 and incorporated complete recirculation of the heat carrier streams in a reactor system capable of operating between 450 and 600°C at residence times in the range of 600 to 1100 ms.

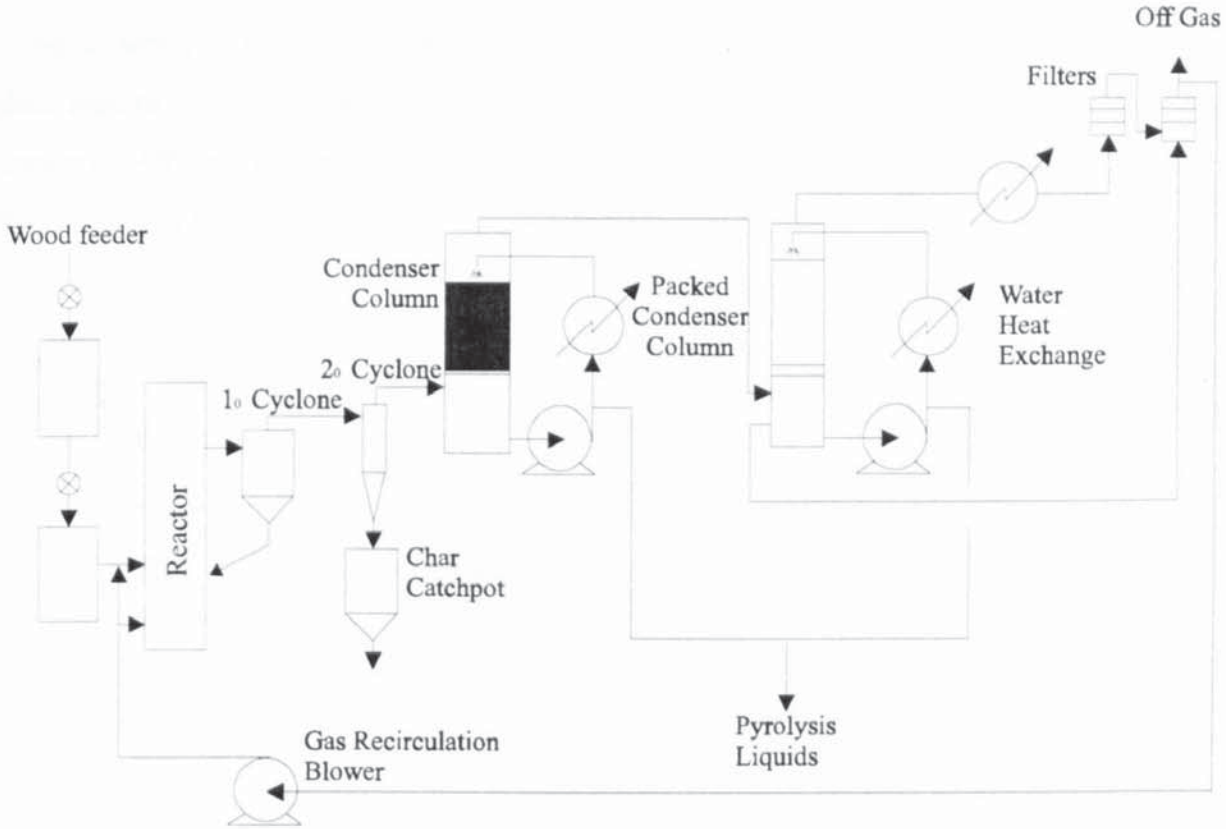

Figure 3-8: Ensyn RTP-2b demonstration plant (100 kg/h) - Schematic diagram

The RTP-2b plant consisted of a lock-hopper surge bin, the lock achieved by a pinch valve. Wood was conveyed via a metering screw to a mechanical feed screw system and injected near the base of the reactor into the mixing section in which streams of heat carrier (particulate sand) were conveyed pneumatically by a portion of recycled product gas. The particulate heat carrier was stripped from the pyrolysis vapors in a primary cyclone, reheated and recirculated to carry heat to the fresh feedstock. The char and inorganic fines (ash and attrited heat carrier) were removed in a secondary cyclone, which was coupled to the in-plant recovery system from where the char was transported to a combustor for process heat generation. A bank of condensers, filters and demisters was used to condense and recover

the product, and to clean up the product gas prior to recirculation. This was a very critical part of the whole process since effective removal and recovery of the liquid product eliminated problems associated with the recirculation blower, which often failed, in early trials, when exposed to a high aerosol of condensable loading in the gas stream.

Ensyn has also provided the Thermal Research Centre of ENEL, Italy's National Power Utility, with a turnkey RTP plant, designed to process 15 tonnes/day of 15 % wt moisture content woody biomass (IEA, 1994). The the detailed design of this project was completed in mid-1994 and construction commenced in early December 1994. The plant was commissioned in Canada in late spring 1995 and then disassembled, shipped to Italy and delivered to ENEL by late 1996. Commissioning and operation of the plant was scheduled for early 1997 and is now under way. A simplified diagram of this plant is given in Figure 3-9 (Trebbi and Rossi, 1993).

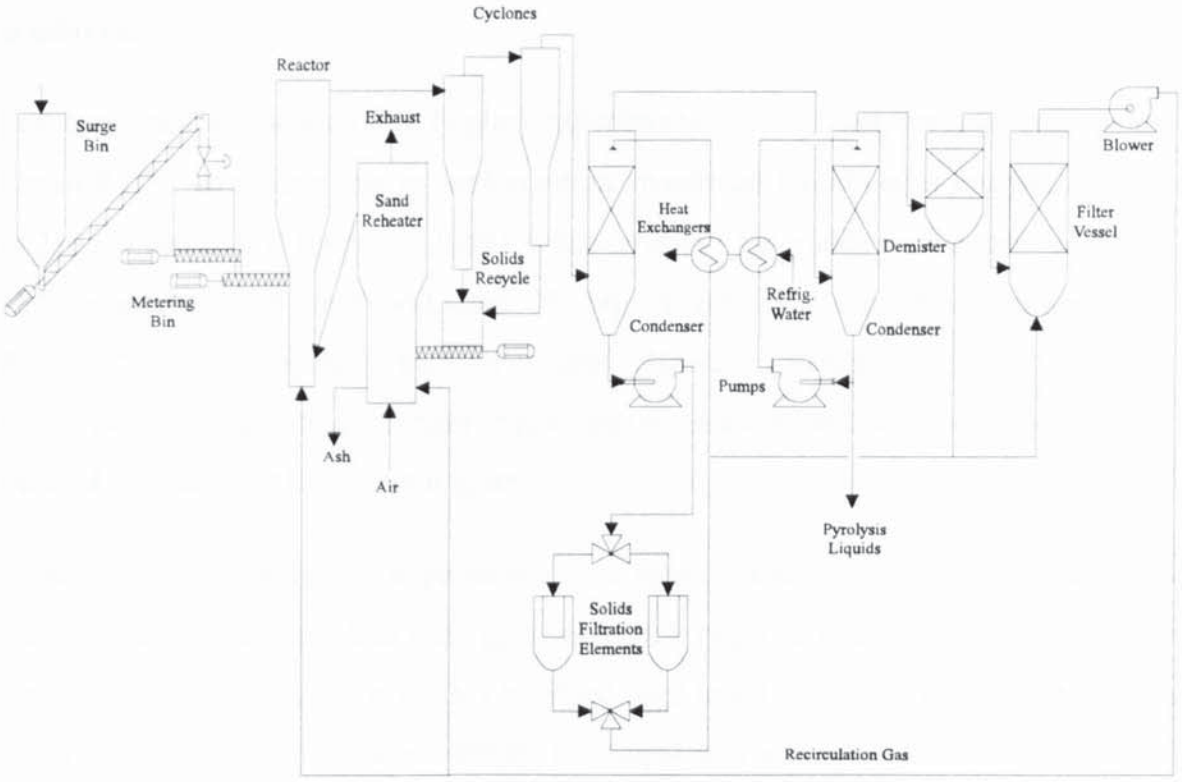

Figure 3-9: ENEL's Ensyn RTP 15 tonnes/day plant

3.6.3 Scale-up considerations

One clear indication of successful scale-up is whether product yields are reproducible as the equipment gets larger. In the Ultrapyrolysis equipment, more than 400 fast pyrolysis experiments using wood (IEA poplar) and cellulose feedstocks were carried out in the temperature range of 600 to 900°C and at residence times between 60 and 1500 ms. In these

experiments very small biomass particles were used (i.e. 100 μm), and gaseous nitrogen was used as the Thermofor assuming that for small particles, the fast pyrolysis product yields would be independent of the type of the Thermofor, gas or solid, as long as it was chemically inert. The overall yields of total gas, char and liquid were measured and were found to fit very well with a first order model (Bergougnou *et al.*, 1983). These experiments have provided a thorough data base for comparison with subsequent experiments in other fast pyrolysis equipment.

For Avicel cellulose trials, maximum liquid yields approached 90 % wt at 109 ms and 650°C (Graham, 1993), while gas yields were about 10 % wt, the char yields being negligible at these conditions. Maximum total gas yields from cellulose exceeded 90 % wt at 900°C and residence times in the range of 300 to 700 ms, while maximum ethylene, total olefinic gas, and total hydrocarbon gas yields were 7, 11 and 18 % respectively, at these reactor conditions.

For hardwood feedstock (IEA Poplar) experiments in the Ultrapyrolysis system and the Ensyn RTP-1 downflow reactor configuration, maximum liquid yields approached 70 % wt at 210 ms and 650°C (Graham, 1988), while char and gas yields were approximately 7 and 18 %, respectively, at these conditions. No experiments were conducted at temperatures less than 650°C in the originally built UP system. However, trends in the data suggested that liquid yields would increase further at reduced temperatures and residence times, which was verified later in the RTP-1 reactor system.

More than 300 fast pyrolysis experiments have been carried out in the RTP-1 reactor system using hardwood and cellulose over the temperature range of 450 to 900°C and at residence times between 90 and 1500 ms. This provided for a broad overlap of experiments conducted in the two systems at similar conditions of temperature and residence time. Data from the RTP-1 experiments were also fitted to a first order model and exhibited good agreement with the UP data (Freel *et al.*, 1988; Graham, 1993). For hardwood feedstock experiments conducted using the RTP-1 reactor, maximum liquid yields approached 77 % wt at 250 ms and 525°C, while char and gas yields were approximately 11 and 12 % wt, respectively, at these conditions. Maximum total gas yields from hardwood approached 80 % wt at 900°C and residence times in the range of 250 to 400 ms, while maximum ethylene, total olefinic gas, and total hydrocarbon gas yields were 5, 8 and 15 %, respectively.

The two RTP-2 reactor systems were not flexible research tools, but dedicated to operate over a very small range of temperatures and residence times. As a result, the data from the 30 kg/h RTP-2a unit were largely gleaned from a steady-state run conducted at 500°C and 1400 ms. Data from the operation of the 100 kg/h RTP-2b unit were recorded during a steady-state experiment carried out at 525°C and 800 ms. Table 3-8 illustrates the effectiveness of the scale-up from 0.3 to 100 kg/h and summarizes the good agreement of the overall liquid product yields in different fast pyrolysis equipment at similar reactor temperatures and residence times.

3.6.4 Special features and problems

The RTP process developed by Ensyn, Inc., seems to be one of the more suitable ones for biomass fast pyrolysis, since it overcomes the limitations posed by heat transfer, scalability and residence time controllability. However, the assessment of this process cannot be thorough due to the fact that since being a commercial process, little about the basic features has ever been published in the open literature.

The basic configuration of the RTP reactor concept is that of a Circulating Fluidised Bed reactor type, with rapid heat transfer occurring in a transport section in the pyrolysis reactor just above the biomass-solid heat carrier mixer. This section provides, besides rapid heat transfer, also for the pneumatic transport of solids and vapors to the solids disengagement section and subsequent solids recirculation back to the mixing section. The provision of heat to meet the process energy requirements has also been dealt with. More specifically, a fluidised bed char combustor has been incorporated at ENEL's plant, Figure 3-9, adjacent to

the pyrolysis reactor, where the byproduct char is combusted and the heat carrier (sand) reheated (Trebbi and Rossi, 1993).

In the RTP process, recirculating hot solids (sand) are used to heat biomass instead of gas. This leads to a more compact design since the heat capacity of solids per unit volume is higher than for gas. Solids, moreover, facilitate the separation from the product gas stream thus avoiding dilution and providing a higher energy density.

Graham (1993) suggests that in RTP reactor configurations, ablation of the reacting particles play a dominant role in overcoming heat transfer limitations and attaining high yields of pyrolysis liquids (Graham *et al.*, 1984). According to the discussion in Section 2.7.2, ablation was defined as a physical-mechanical mechanism that removes the primary depolymerization liquids at a surface reaction rate that is of the same order of magnitude as the thermal penetration rate. That simply means that the surface found below the external biomass surface undergoing pyrolysis is kept at a far lower temperature and is not exposed to temperatures high enough to enhance charring or undesired depolymerisation/cracking reactions.

Problems include:

- sand separation and recycling
- materials of construction at high temperatures with abrasive solids (extended wear and corrosion problems)
- process complexity given the existence of a twin fluidised bed system.

3.7 Ablative pyrolysis for liquids (NREL - USA and Aston University - United Kingdom)

3.7.1 Introduction

As discussed above, ablative pyrolysis may be defined as the meeting or thermal "erosion" of biomass in intimate contact with a hot solid or surface under such conditions that rapid thermal degradation of the biomass particles occurs (Peacocke and Bridgwater, 1994).

Key work in this area has been carried out in a number of research institutes, universities and industries. An excellent review on ablative fast pyrolysis systems has been presented by Peacocke (1994). In this context the work carried out by NREL and Aston University are

reviewed, since it both represents the state-of-the-art in biomass ablative pyrolysis research and conforms with the basic requirements of fast pyrolysis for maximisation of liquids.

The work developed by NREL was a continuation of exploratory research at the Naval Weapons Research Centre at China Lake initiated in 1975 to evaluate the production of automotive fuel from organic wastes (Diebold and Benham, 1984). From this work, the research moved from a bench scale reactor with a throughput of 5 kg/h to a 50 kg/h entrained flow ablative pyrolyser, which is described and discussed below. This is one of the first developed ablative reactor technologies and research has been ongoing for 16 years into ablative pyrolysis in NREL.

The work at Aston University initiated in 1991 in the framework of the European XII JOULE programme to carry out fundamental research on the ablative fast pyrolysis of biomass in order to develop a new reactor technology and obtain detailed information on the operation of a 3-5 kg/h prototype reactor.

3.7.2 The NREL biomass ablative pyrolyser

The NREL biomass ablative pyrolyser operates as follows:

The woodchips, with a size of approximately ~5 mm, are metered into the system by a screw feeder, entrained by a recycle stream of inert gas, unreacted feed and pyrolysis products into a supersonic jet of hot carrier gas (steam or nitrogen). A long entrainment tube is used to allow the particles to accelerate to the high entering velocities of over 400 m/s. The particles enter the vortex reactor tangentially generating high centrifugal forces, up to 2.5×10^5 "g's", which press the particles against the wall. In this way, the reactor functions like a horizontal cyclone in that the gas is ejected and the woodchips are retained in continuous contact with the hot walls in a spiral movement.

The stainless steel reactor has an internal diameter of 13.4 cm, a length of 70 cm, and is heated by three wall heaters. The gases, vapors and char fines leave the reactor though the axial exit, which extends part way into the reactor. The typical carrier gas to biomass mass ratio is in the range of 0.7 - 1.5. Relevant updates on the initial reactor performance, commissioning and experimentation are to be found elsewhere (Diebold and Scahill, 1983; Diebold and Scahill, 1984). After extensive experimentation and development, the current configuration of the NREL ablative pyrolysis is that shown in Figure 3-10 below (Diebold and Power, 1988).

Figure 3-10: NREL ablative pyrolysis system (Diebold and Power, 1988)

Cold flow studies confirmed that approximately only 20 % of the available heat transfer surface in the smooth walled reactor was covered by wood chips in the first and second reactor configurations (Diebold and Scahill, 1981). A fabricated helix was placed inside the reactor to force the biomass to flow over the entire reactor heat transfer area. This was partially effective but a proportion of the biomass passed below the helix due to non-ideal sealing of the helix against the reactor wall. It was noted that at lower temperatures (<625°C), 30% of the feedstock remained partially pyrolysed on a once through basis despite the helix increasing the contact area of the wood particles with the reactor wall (Diebold and Scahill, 1984). In order to reduce the char yield, a solids recycle loop was added and a new reactor built with an integral helix having a pitch of 25 mm, width 6 mm and height 3 mm. Addition of the solids recycled loop reduced, in conjunction with the ribbed reactor, the char yield to 7-10 %, compared with the previous values of 30 % at a wall temperature of 625°C.

With the present ribbed reactor configuration, a 5 mm particle was calculated to be recycled 23 times to achieve a final thickness of 50 μm, at which point it would be entrained out of the reactor with the gas and vapor products. Assuming only ablative pyrolysis to be significant a particle would ideally be ablatively pyrolysed in 0.7 s (Diebold and Power, 1988). In practice, the particle pyrolysis time is much longer as the particle tangential velocity and thickness decrease along the length of the reactor to 100 m/s and then the particle is recycled (Diebold and Power, 1988). Unlike other entrained flow reactors (GTRI, Section 3.2; EGEMIN, Section 3.3), recycle of the partially pyrolysed biomass is not difficult and the solids residence time is decoupled from the gas/vapor product residence time. A proportion of the product vapors and gases must, however, be recycled. The recycle loop functions by

ejection of the steam or nitrogen entering the reactor via a venturi which causes a suction effect on the recycle stream.

Using the experimental set-up shown in Figure 3-10, the highest published total liquid yield for the NREL ablative pyrolysis system is 67 % wt (including moisture) or 55 % wt (dry oil/maf feed basis) based on direct measurement (Diebold and Power, 1988). The yields are comparable with those produced by fluid bed fast pyrolysis technologies (Scott *et al.*, 1991). The design throughput, i.e. 50 kg/h, has, however, not been achieved: the maximum throughput achieved is 36 kg/h maf wood. Overall mass balances are given in Table 3-9. Experiments have been carried out with thermal cracking of the vapor products, but the exact conditions of thermal cracking temperature and product yields and compositions are not given (Czernik *et al.*, 1993).

3.7.3 The Aston University biomass ablative pyrolysis system

The reactor and product collection system for the ablative pyrolyser developed by Aston University is shown in Figure 3-11 below (Peacocke, 1994). The biomass inlet slot from the feeder is fitted with a nitrogen line for purging. Ablation is achieved by means of four asymmetric blades rotating at 160 rpm which press and move biomass particles relative to the heated surface. Preheated nitrogen is used to control the gas/vapor product temperature and residence time and assist in product removal from the reactor. During operation, biomass is rapidly ablated by the rotational action of the blades on the heated base. Fine char particles and vapor products exit through the reactor base where the char is removed in the trace heated cyclone and are collected in the char pot. The hot gas and vapor products enter the ice-cooled condensers - the first one containing ice and the second one a dry ice/acetone mixture. The remaining cooled and stabilised aerosols and non-condensable gases pass into the pre-dried cotton wool filter which removes any residual aerosols and water vapor. The non-condensable gases pass through a gas meter and are then vented to atmosphere. Batch gas samples are taken to the gas meter for analysis by GC.

Figure 3-11: Aston University ablative pyrolysis system (Peacocke, 1994)

Results for four runs from 450 to 600°C with mass balances and product analyses for the Aston University ablative pyrolysis system are summarised in Table 3-10, with a maximum organic liquid yield of 62.1 % wt at 502°C (Run CR25). The residence time increases at lower temperatures due to the lower gas/vapor phase exit temperature, although the effects of gas/vapor on product yields at 400-450°C is small.

3.7.4 Special features and problems

On a small scale, ablative pyrolysis reactor configurations meet most of the requirements for effective fast pyrolysis. As seen from the results presented above, liquid yields are very high comparing to the highest yields achieved by the most successful fluidised bed systems, such as the WFPP in Section 3.4.

However, the potential for commercial application is minimal, because of the inherent limitation of heat transfer rate through a reactor wall, complexity associated with scale-up and the general absence of other commercial application of these reactors in the chemical process industry.

None of the two processes reviewed above, i.e. the NREL ablative pyrolyser - Section 3.7.1 and the Aston University ablative pyrolysis system, Section 3.7.2 - reached their design value as far as biomass throughput is concerned, typical capacity values corresponding to a maximum of 60-70 % of the design value for these two systems.

The main reason for this phenomenon in the NREL system is believed (Peacocke, 1994) to be heat transfer limitations, since ablative pyrolysis systems typically have a fixed heat transfer area. Therefore the heat flux, which is dependent upon the reactor wall temperature, biomass density and the ablation rate, must be maximised to achieve high specific throughputs.

As far as the Aston University ablative pyrolysis system is concerned, it is believed that the main reason for lower than design value thoughput is the incomplete use of contact area below the rotating blades and low biomass density as evaluated and described in detail by Peacocke (1994).

3.8 Vacuum pyrolysis for liquids (University of Laval - Canada)

3.8.1 Introduction

Vacuum pyrolysis is a particularly unique technology which has been under development at the Universities of Laval and Sherbrooke since the early 1980's (Bridgwater and Double, 1989). As Graham (1993) points out it is not strictly fast pyrolysis in terms of heat transfer requirements, but the relatively low heating rate of the solid biomass is not restrictive, since primary products are drawn quickly from the reacting surface and out of the reactor as soon as they are formed, thereby precluding secondary reactions.

Bench scale batch units at Sherbrooke and Laval Universities resulted in a 25 kg/h Process Development Unit (PDU) being tested at Laval (Roy *et al.*, 1983; Roy *et al.*, 1988). A 200 kg/h continuous demonstration project was initiated but stopped in progress because of the licensee's financial difficulties (Roy *et al.*, 1989).

A new reactor design has been developed at Institut Pyrovac, Inc., which is claimed to address the heat transfer limitations usually encountered in vacuum pyrolysis technologies, and a demonstration unit with a capacity of 100-400 kg/h has been built and is undergoing extensive testing (Roy *et al.*, 1996).

3.8.2 Description and operation

A schematic view of the Process Development Unit (PDU) used at Laval University is shown in Figure 3-12 (Roy *et al.*, 1988). The reactor was a multiple hearth furnace 2 m high and 0.7 m in diameter, with six hearths. Multiple hearths have been extensively used for the thermal disposal of sludge or other waste materials (Kavarov, 1985) and are consisted of rabble arms and teeth attached to a vertical shaft, rotating to spiral wastes across the hearth and through the furnace. The wastes drop from hearth to hearth through passages alternately located either along the periphery of the hearth or adjacent to the central shaft.

In the PDU heat was provided by heating elements, the heating plates temperatures increasing from top to bottom of the reactor. A typical temperature profile was 200 to 450°C, the radial temperature for any heating plate being lower than 5°C during a typical run. At the onset of an experiment woodchips were poured batchwise into a hopper, equipped with an hermetically sealed feeding device. A mechanical vacuum pump removed the organic vapors and gas products from the reactor through a series of outlet manifolds set along the reactor cylinder. Each outlet was connected to a heat exchanger where the vapors were condensed and recovered as liquid in individual glass receivers. The vapors from the heat exchangers were collected in a train of receivers that served as a secondary condensing unit.

Pressure in the system was lower than 11 kPa (absolute) under steady-state conditions. The non-condensable gas was continuously pumped into a 500 l vessel that was set under vacuum at the beginning of the run. The solid residue (char) was directed towards the bottom of the reactor and was collected in a metallic vessel installed on a load cell.

Figure 3-12: Schematic of the vacuum pyrolysis Process Development Unit at University Laval (Roy *et al.*, 1988)

3.8.3 Results

Results for the operation of the multiple hearth furnace at varying final thermal decomposition temperatures and reactor pressures are presented in Table 3-11 (Roy *et al.*, 1988).

The results of Table 3-11 indicate that the largest amount of liquids was produced at the lower pressure conditions. The liquid yield drops rapidly with even a slight increase in pressure. A reactor temperature in the range of 425 to 450°C is optimum for maximum yield production.

3.8.4 Special features and problems

In general, vacuum processes tend to be expensive to operate on a commercial scale. For this reason and given the complexity of the reactor system developed, Pyrovac has chosen (Roy, 1996) to move away from low value resources and products (biomass and pyrolysis liquids) to exploit environmental "niche" markets where high tipping-fee wastes can be converted in a vacuum processes to value-added chemicals (Roy, 1996).

Besides the complexity and the high cost of the vacuum pyrolysis process, the most serious problem is heat transfer limitations. An overall heat transfer coefficient of 25 W/m^2 K has been reported (Roy *et al.*, 1988), which is at least an order of magnitude below those reported in the literature on fluidised bed and entrained/transported bed reactors, as discussed in Section 2.7. Heat is primarily transferred by radiation, since heat transfer by convection is negligible due to low pressure conditions in the reactor and heat transfer by conduction is limited by the continuous occurrence of phase changes during the thermal decomposition of wood in the different compartments (hearths) of the reactor system.

These problems will be dealt with during the development of a novel, semi-continuous horizontal pilot plant, currently being developed by Pyrovac (Roy *et al.*, 1996). This moving bed vacuum pyrolysis reactor uses a novel transport and agitation device which produces a forced exchange between the particles heated at the surface of the heating plate and the colder particles located at the core of the packed bed of particles. This novel reactor configuration is claimed to achieve total heat transfer coefficients in the range 70 to 250 W/m^2 K, i.e. comparable to those achieved in other pneumatically operated fast pyrolysis system described in previous sections.

3.9 Char energy exploitation schemes and the proposed reactor configuration

As seen from the extensive review of biomass fast pyrolysis reactor configurations, the energy exploitation of byproduct char has been given little attention, the only exceptions being the OFPP, Section 3.5 and RTP - Configuration 2B, Section 3.6, processes. However,

in a commercial application of biomass fast pyrolysis, the energy content of char has to be utilised internally in order to reduce imported energy and, hence, minimise production costs. In this section, the following important aspects are discussed:

- conceptual char energy exploitation schemes to supply the heat for pyrolysis, Section 3.9.1
- classification of reactor configuration according to the desired gas-solids contacting patterns, Section 3.9.2
- conception of a new integral biomass fast pyrolysis/char combustion reactor concept, Section 3.9.3.

3.9.1 Schemes to utilise biomass derived char energy content

During the biomass fast pyrolysis processes reviewed in Chapter 3, the organic vapors are produced in a high heat transfer environment and subsequently transported in an inert gaseous atmosphere, to avoid further degradation to non-condensable gases, to the downstream equipment for further recovery and collection. In these cases, the gases are either used as heat transfer media or simply to transport pyrolysis vapors to downstream processing equipment, adjusting accordingly the vapor residence time.

In a commercial process, however, the char and the pyrolysis gas produced during pyrolysis will have to be combusted to provide the heat for both the pyrolysis reactions and biomass pre-treatment (drying). The heat required for the pyrolysis reactions may then be supplied to biomass particles by conduction with an inert heat carrier which passes, relatively cold, through a combustion system, where it is heated up by char combustion and returned, relatively hot, to the pyrolyser, where the energy requirements of biomass devolatilization are satisfied.

Two ways to utilise the char energy content may be examined, i.e. the indirect way, which uses two physically separate reactors like the systems utilising twin fluidised bed configurations and the direct one, which utilises an oxidation medium in a single fluidised bed system.

These two reactor systems configurations to utilise char energy content are shown below in simplified form in Figure 3-13.

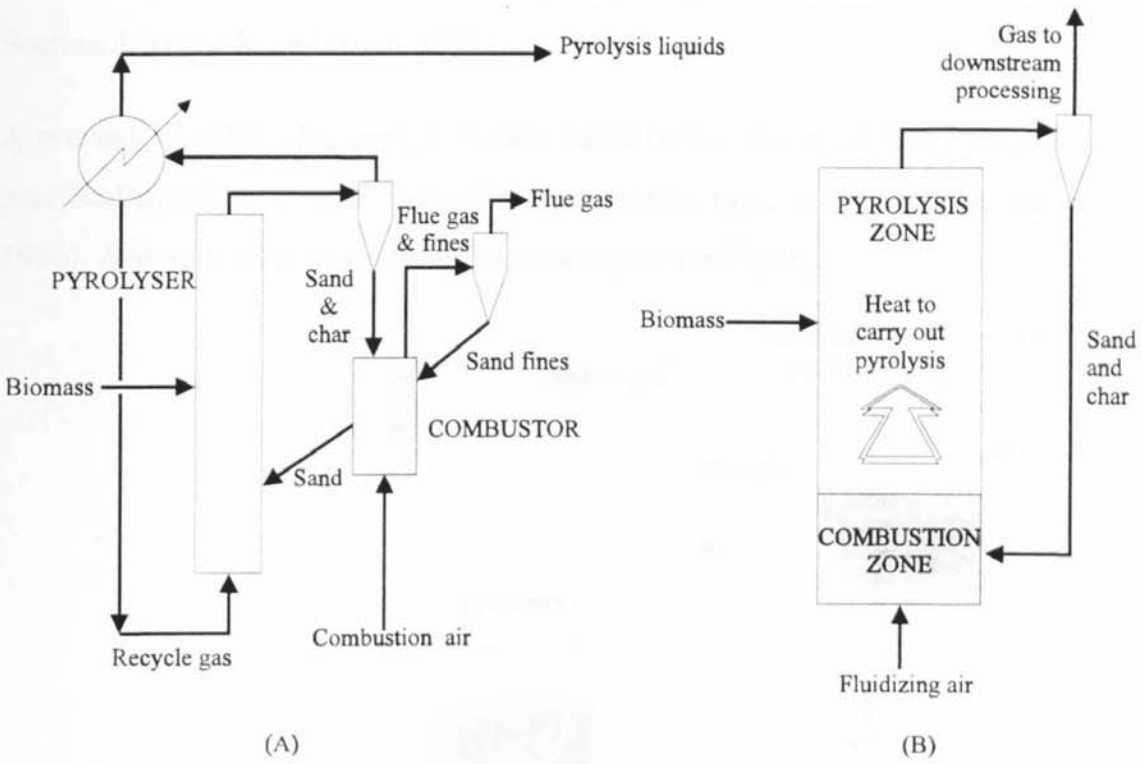

Figure 3-13: Twin (A) and single (B) fluidised bed system configurations

In the twin reactor configuration, Figure 3-13(A), the heat is provided indirectly by using two physically separate reactors. The twin fluidised bed system has long been practised in the petroleum industry (Fluid Catalytic Cracking-FCC) to crack catalytically heavy petroleum fractions (Venuto and Habib, 1979; Avidan, 1993). In FCC units, the endothermic cracking (pyrolysis) of the heavy oils to gasoline occurs in a transported bed type reactor (riser) and results in the formation of coke and its deposition on the catalyst/heat carrier surface. The coke-laden catalyst is continuously removed from the pyrolytic bed and sent to a regenerator, virtually a fluidised bed combustor, where the coke deposited during the cracking process of the crude feedstock is burned off. The exothermic oxidation of coke in the regenerator reheats the catalyst, which is circulated back to the pyrolysis reactor to both meet the energy requirements of the cracking process and provide the selectivity required to maximise the desired products yield. In the FCC process, the energy transfer is actually a physical transport of the heat carrier, i.e. the catalyst carrier, from the combustion to the pyrolysis zone.

The concepts of the twin bed system configuration for biomass fast pyrolysis were also practised by Occidental Research Corporation (OFPP), as discussed in Section 3.5, in the late 1970's to produce liquid fuels from biomass and other low grade fuels, such as Refused-Derived-Fuel (Bogley *et al.*, 1977). The same concept has also been exploited by Ensyn, Inc.,

for the implementation of a twin-bed pyrolysis system for the ENEL plant, discussed in Section 3.6 (Trebbi and Rossi, 1993).

A process to utilise char energy content based in the twin fluid bed configuration was also practised by Alten, a consortium of KTI and Italenergie, no longer in partnership (Cogliati, 1986). A simplified scheme of this process is given in Figure 3-14.

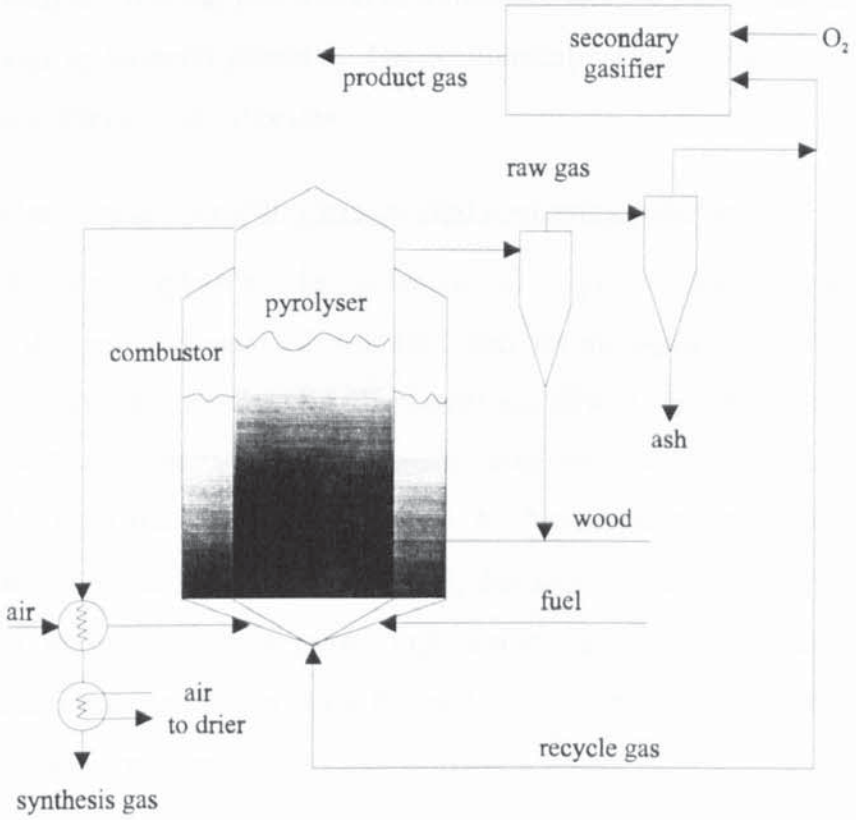

Figure 3-14: The Italenergie/AGIP S.p.a. process

A simpler solution to meet the biomass pyrolysis energy requirements would be the combustion of char in the same reactor vessel, i.e. the pyrolysis reactor, to directly provide the heat to pyrolysing particles. This could be achieved by supplying the char to the bottom of a bubbling fluidised bed, configuration (B) in Figure 3-13, where it is burnt by addition of an oxidation medium (air), the quantity of which should be restricted to the amount necessary to carry out stoichiometric char combustion, and hence depletion of oxidant so that undesired combustion of volatiles could be avoided. The simplicity of the single fluidised bed system, in terms of complexity and related equipment cost, led International Energy Agency (IEA) experts to characterise such a system as the "potential" case for fast pyrolysis reactor configurations (McKeough *et al.*, 1988). In this way, an overall higher economy and performance compared to systems based on conventional (present case), fluidised bed design,

as that proposed by the University of Waterloo (WFPP) and practised by Union Fenosa, Section 3.4, may be achieved.

The reactor configurations employed in either options discussed above present entirely different contacting patterns for gas and solids. These patterns are considered of major importance to adequate mixing, promotion of turbulence and, hence, the development of high heat transfer rates to biomass particles. The relationship of gas-solids contact and reactor configuration is further discussed below.

3.9.2 Reactor classification according to gas-solid contacting patterns

In order to further emphasize the potential of higher velocity gas-solids reactor configurations, the major classes of fluidised bed technologies classified by degree of fluidisation are presented in Figure 3-15. This chart is a plot of superficial gas velocity versus bed expansion with a comparison made between mean gas velocity (gas passing unhindered through the solids bed) and mean solids velocity. As the differential velocity, also called slip velocity, decreases between these two velocities, the degree of solids carryover increases to the point where the solid particle passes unhindered through the process. Increased slip velocity indicates severe turbulence in the bed and hence increased heat transfer and possibly domination of ablation mechanism.

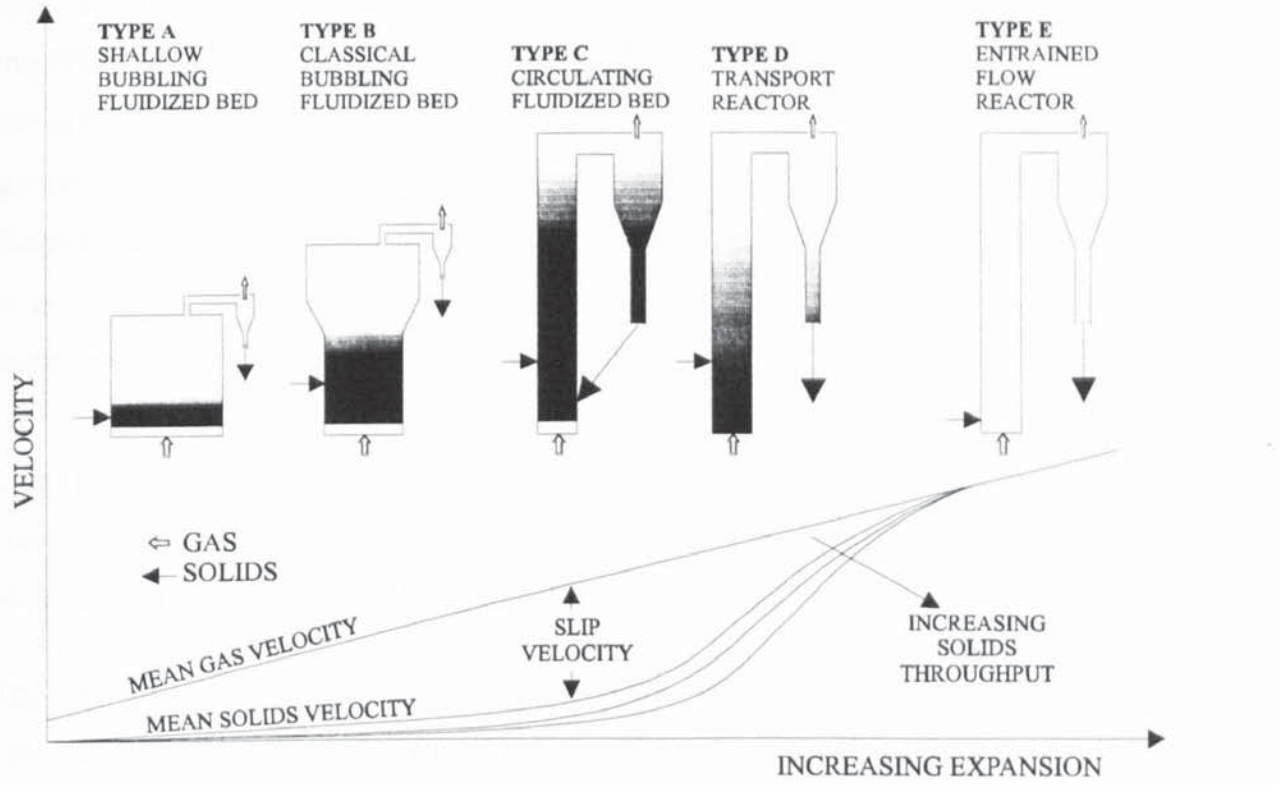

Figure 3-15: Major classes of gas-solids reactors according to slip velocity

Over the range of this expansion there is Type A, shallow fluidised bed (WFPP, Section 3.4), Type B, classical bubbling fluidised bed (probably ERCO, Section 3.4) and Type D, transport reactor, (OFPP, Section 3.5 and Ensyn, Section 3.6). Although there has been little agreement about what constitutes a Circulating Fluidised Bed (CFB) and how it might be characterized, it appears that a recirculating system with the maximum slip velocity best represents a CFB definition, Type C. Finally, for comparison purpose, an upflow entrained bed reactor system Type E (GTRI, Section 3.2), exhibiting virtually no slip, is included in the upper limit of gas velocities. As depicted, there are four basic types of beds in these categories, with two being circulating beds.

At low gas velocities, the Type A-WFPP bed has a defined fluidised-solids/freeboard interface that is readily visible. This type of bed, operating in the "blow-through" mode, has a very low entrainment of the bed material, achieving a selective and gradual removal of the lighter char particles, practically depleted of the great majority of volatile matter.

Higher gas velocity creates a higher rate of particle elutriation (carryover). Also the fluidised-solids/freeboard interface becomes less defined. This is a Type B bed, which is the bed closest to the ERCO approach. This bed typically elutriates a much larger portion of char together with sand, so that some recycling would be necessary.

The Type C circulating bed differs in that much higher gas velocities are used, than those employed in Types A and B. Extensive product recycling creates a condition known as particle "clustering". These clusters have much higher transport velocities which explains the greater slip velocities at increasing solids throughput. An extensive description of the CFB characteristics and gas-solids contacting patterns is beyond the scope of this thesis and some recent excellent reviews on CFBs' characteristics and operation may be found in the relevant literature (Yerushalmi and Avidan, 1985; Yerushalmi, 1986a, 1986b; Grace, 1990; Dry and La Nauze, 1990). It is worthwhile mentioning that the inherent beneficial characteristics of CFB reactors are best exploited in fast, non-catalytic gas-solids reactions such as coal combustion, coal and biomass gasification, alumina calcination and reduction of ores (Reimert and Mehrling, 1986; Reh, 1988).

The type D transport reactor system differs from the CFB type in the sense that the gas velocities are high enough to blow all bed material without the phenomenon of clustering and hence the observed slip is greatly reduced.

Due to their greater solids elutriation and subsequent extensive recycling via cyclones when compared to Types A and B beds, these two reactor types, Types C and D, can exploit the energy content of char by circulating it around the suitable reactor loop and utilize it for fueling the pyrolysis process. It is important to remember, however, that both "B" and "C" still retain a dense lower bed relative to the lower density upper zone. In some respects this dense lower bed is similar to a bubbling bed but with much greater gas-solids heat and mass transfer.

3.9.3 Conception of a new integral biomass fast pyrolysis/char combustion reactor

From the description above, it may be concluded that the single fluidised bed system configuration, Figure 3-13(B), constitutes a suitable reactor configuration for biomass fast pyrolysis and integral byproduct char energy utilisation. In such a configuration, the combustion chamber basically constitutes the lower part of the fluidisation column with a solids carry over into the riser. The temperature in the combustion chamber will be likely between 800 and 1000°C subsequently cooled to approximately 500°C by the section where biomass is fed and pyrolysis reactions occur. Biomass is introduced to the hot sand stream, where it decomposes into char, pyrolysis vapors and gases. The entrained char-and-sand mixture is separated from the gas and recirculated to the combustion chamber, where char is combusted and sand is reheated directly and blown up the riser to fuel the pyrolysis reactions.

The above can be easily achieved in an entrainment type reactor, operating at relatively high gas velocities. The solids, forming a lower dense bed in the reactor, are entrained by the gas flow to the top of the reactor, where they are collected by the solids capture device (recycling cyclone) and returned through the proper recycle device, to the base of the reactor.

A CFB reactor appears to consist of many strands of refluxing particles, continuously coalescing and reforming. The very existence of these strands or clusters of particles, dispersed uniformly over the reactor cross-section, has led to the development of a number of theories for CFBs. According to one of them (Yerushalmi and Cancurt, 1978), each cluster is assumed to behave like a single larger particle, in a mean time sense, evidently being in a continuous state of formation and destruction. These larger "effective agglomerates" give the CFBs their high slip velocities, Figure 3-15, which may exceed individual particle mean velocity by an order of magnitude. A number of potential advantages can be attributed to these high velocity gas-solids reactors:

- the ability to maintain relatively dense beds of fine particles at high velocities, allowing high specific throughput
- intense backmixing of solids promoting temperature uniformity
- substantial conductive heat transfer, due to the fact that the surface area of each individual particle remains active, since the agglomerates are in no sense close packed
- flexible control features, associated with the ability to change the external solids circulation rate and, hence, vary heat transfer.

The external solids circulation in a CFB is accompanied by an internal circulation of material due to the constantly changing densely packed strands and clusters. This leads to an intensive mixing of gas and solids, characterised by the increase in slip velocity, Figure 3-15. The slip velocity is further increased by increasing the solids throughput, which is accomplished by adjusting the rate of solids recirculation.

Thus, such a reactor configuration seems to be very suitable for biomass fast pyrolysis combined with integral combustion of byproduct char. The integrated CFB reactor configuration proposed, according to the discussions so far, should consist of:

- an upflow, elongated transport conduit (riser)
- a solids capture device (usually a cyclone system)
- a downflow standpipe to convey heat carrier solids, along with char, from the cyclone to the combustion chamber
- an appropriate solids circulation system to both ensure solids recirculation and provide for control of solids circulation rates
- a dense-phase, bubbling fluidised bed, where char is combusted with the addition of incoming air and sand is recycled and reheated.

The single-bed reactor system, Figure 3-13(B), to achieve the proper char recirculation, should be based on a Circulating Fluidised Bed (CFB) design, Type C reactor configuration in Figure 3-15, where inert solids (silica sand), acting as the heat carrier, and biomass are entrained in a vertical tubular reactor (riser) to carry out the pyrolysis reactions. The pyrolyser is then followed by a solids recovery device, where the entrained solids (i.e. sand and char) are separated, recycled down a standpipe and returned to the base of the CFB reactor, where char is burned in a stoichiometric flow of air to reheat the sand and provide a hot gas flow to entrain the reheated sand up the riser and carry out the pyrolysis process.

In the proposed new reactor configuration, the following can be accomplished :

- rapid heat transfer from the solid heat carrier to biomass particles by both convective and conductive mechanisms
- precise control of uniform, very short vapor residence time
- controlled elevated temperature and minimisation of temperature gradients along the riser length
- effective recycling of the cold heat carrier to a "thermal regenerator" (char combustor), hence avoiding the need for complicated indirect energy recovery systems
- a reactor configuration amenable to quick solids-vapor removal and hence to rapid product quench.

The basic components of the proposed CFB reactor configuration for biomass fast pyrolysis are shown in Figure 3-16.

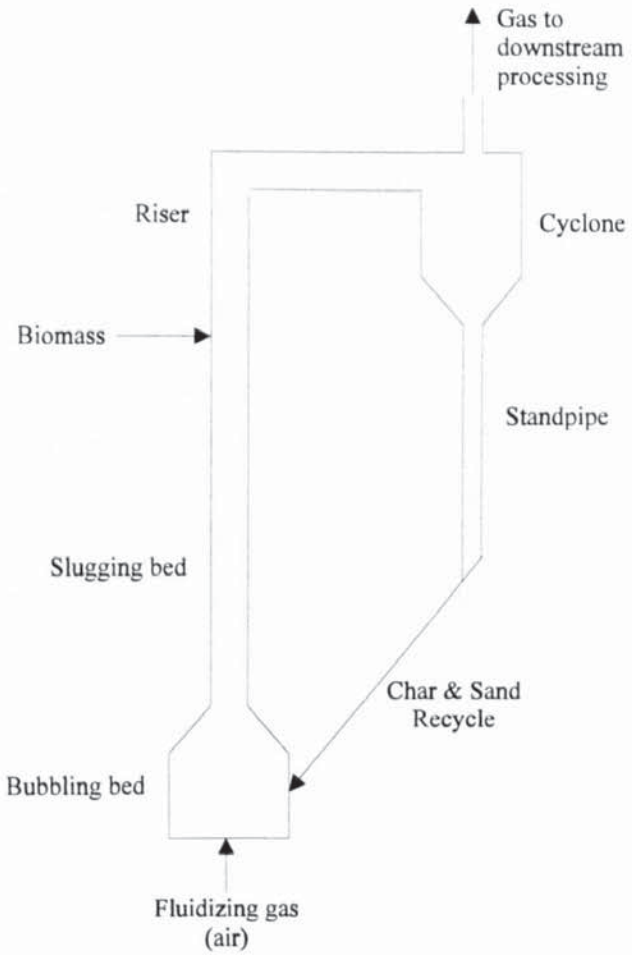

Figure 3-16: Proposed CFB biomass fast pyrolysis reactor main components

In designing such a circulating system, it should be born in mind that one should account for the kinetics of two different reactions: one carried out to stoichiometric equilibrium (char combustion), while the other one aimed to maximise the yield of non-equilibrium products

(pyrolysis vapors), derived by suitably exposing biomass feedstock to unusual process conditions (extremely high heat transfer rates). As a consequence, these considerations should be taken into account for the proper sizing of the different reactor system components. As a general guideline it should be mentioned that longer residence times should be strived for in the char combustor, while minimum residence time should be accomplished in the pyrolysis section (riser).

The sizing methodology for the proposed CFB different reactor components is further discussed in detail in Chapter 4.

3.10 Summary and Conclusions

A review of the different atmospheric reactor systems that have been utilized to maximise liquid products from biomass has been carried out and the limitations as well as the advantages of each approach has been analysed and critically reviewed.

The main limitations of the systems examined in this Chapter include:

- inadequate heat transfer to biomass particles (GTRI, EGEMIN, Pyrovac)
- extensive gas/vapor residence times (ERCO)
- potential difficulties for scale-up (WFPP, Union Fenosa, NREL)
- conceptual complexity (OFPP, Ensyn, Pyrovac)
- incorporation of moving parts (Aston University)

The ideal reactor candidate should also provide adequate heat transfer to biomass particles incorporating some form of ablation, good scale-up potential and short gas/vapor residence times. Furthermore, in an industrial process the opportunities for integral char combustion to provide the biomass pyrolysis heat requirements will have to be considered.

The above design aspects have been pointed out and a single Circulating Fluidised Bed reactor incorporating integral char combustion has been selected as one of the most appropriate reactor configurations for biomass fast pyrolysis.

In the following chapter, a methodology for the proposed CFB reactor components sizing procedure will be developed and analysed in detail, including the derivation of necessary correlations between critical process parameters (temperature, gas/vapor residence time, heat transfer), reactor dimensions and operating variables (biomass throughput).

CHAPTER 4: THE CIRCULATING FLUIDISED BED AIR-BLOWN PYROLYSER PRINCIPLES AND DESIGN METHODOLOGY

4.1 Introduction

In Chapter 3 the most important processes developed on a pilot or demonstration scale for biomass fast pyrolysis in order to maximise liquids production have been discussed and their features critically reviewed. A Circulating Fluidised Bed (CFB) with integral char combustion has been selected as a suitable reactor configuration to overcome most of these biomass fast pyrolysis processes drawbacks incorporating autothermal operation by utilising byproduct char energy content.

The objective of this chapter is to further specify the CFB reactor operating principles and design methodology in order to size properly the different reactor components.

The design methodology for the proposed CFB reactor for biomass fast pyrolysis has to take into consideration three important aspects, namely:

1. to operate so as to achieve high heat transfer rates to biomass pyrolysing particles
2. to account for relatively short (<2 s) gas/vapor residence time
3. to exploit the energy content of byproduct char to provide the heat for pyrolysis.

General equipment design considerations for the CFB reactor configuration as well as a general map of the reactor design methodology is given in Section 4.2, while a quantitative definition of fast fluidisation as an operating regime of velocities and particle sizes is presented in Section 4.3.

Heat transfer issues and the favourable influence of the proposed CFB reactor system in order to achieve high heat transfer rates to biomass pyrolysing particles is further discussed in Section 4.4.

Finally, a design methodology for the sizing of the biomass fast pyrolysis is given in Section 4.5. Relationships correlating the reactor basic dimensions to both operating variables (air and biomass flowrates) and process variables (temperature and gas/vapor residence time) are derived and evaluated.

4.2 Equipment design considerations

The necessity of satisfying the specific process conditions for biomass fast pyrolysis, namely moderate temperature, short vapor residence time (VRT) and high heat transfer rates, has been thoroughly discussed in Chapter 2, while the different system configurations adopted to overcome the various limitations imposed on biomass pyrolysis reactor design have been reviewed in Chapter 3.

Moreover, a potential reactor candidate to overcome the restrictions imposed by short gas/vapor residence times (VRTs) and high heat transfer rates incorporating integral char combustion operating on the CFB principle has been conceived and proposed in Section 3.9.3. Besides the basic components shown in Figure 4-1, the proposed CFB reactor must also incorporate a proper solids circulation device so that a stable and continuous circulation of solids between biomass pyrolysis and char combustion section is ensured.

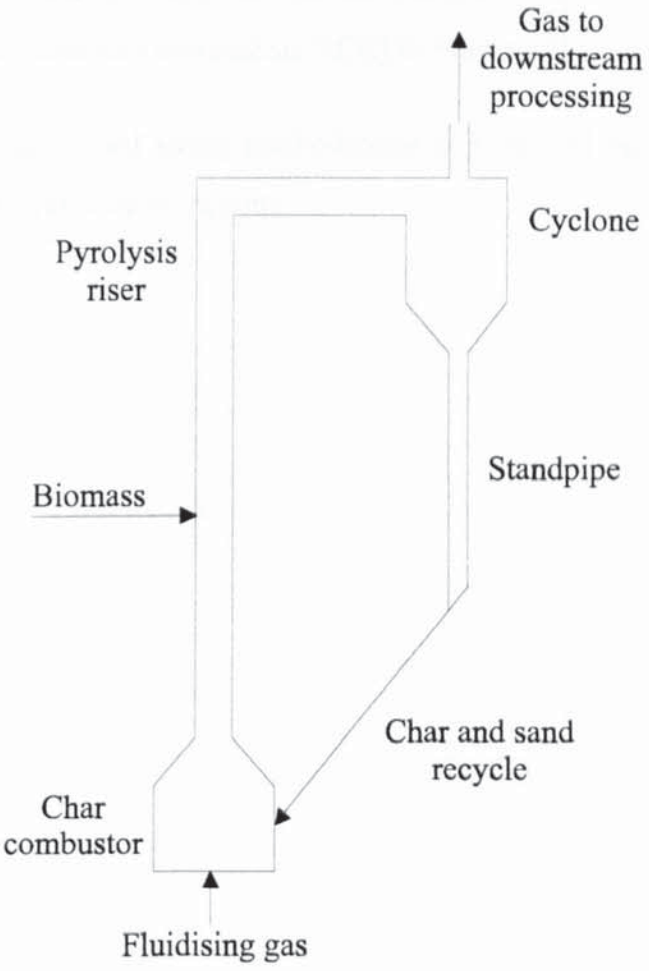

Figure 4-1: CFB biomass fast pyrolysis reactor main components

In order to match the different components (biomass pyrolyser/riser and char combustor) dimensions of the CFB reactor to the specific biomass fast pyrolysis conditions, the basic process requirements must be properly defined and related to operating parameters.

First, in order to correlate process conditions with reactor sizing, the choice of a realistic kinetic model of biomass fast pyrolysis is required. The kinetic model predictions will associate product yield distribution with the most important process parameters, namely pyrolysis (riser) temperature and VRT. Second, the reactor operating regimes will be established taking into considerations the remarks provided by gas-solids flow regimes, see below in Section 4.3, as far as the operation in the fast fluidisation mode in the pyrolysis (riser) section is concerned. As a consequence, the sizing of the CFB system pyrolysis section (riser) and the char combustion section (combustor) will be made possible.

Finally, in order to satisfy the high heat transfer requirements and avoid undesirable low-heat transfer favoured char-forming reactions, the calculation of solid heat carrier-to-biomass ratio, or the solids circulation rate correlation (SCR) to biomass throughput, is necessary.

A general map of the developed sizing methodology is presented below in Figure 4-2, the details to be given in the respective sections.

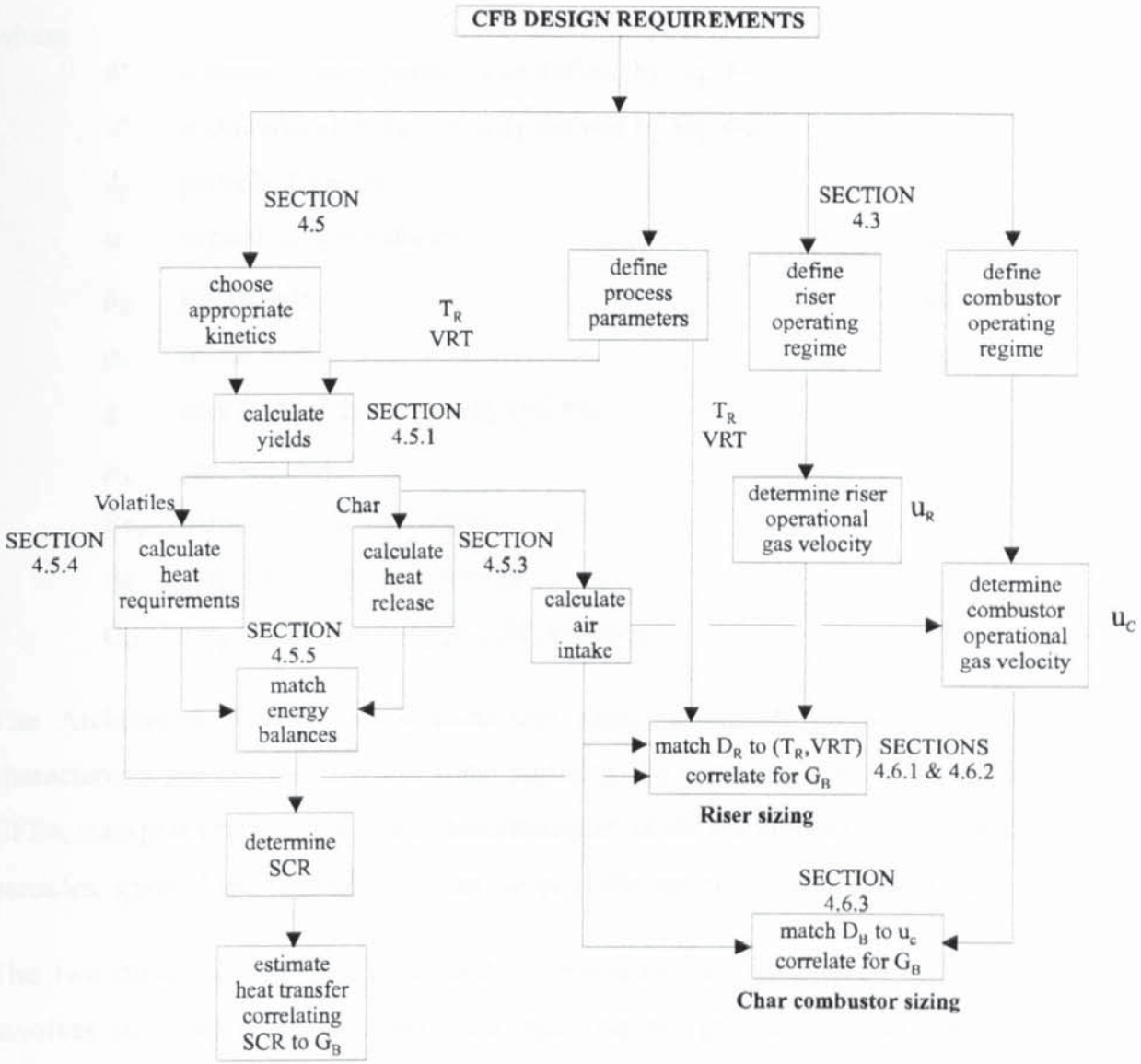

Figure 4-2: Flowsheet of the CFB biomass fast pyrolysis reactor sizing methodology

4.3 CFB reactors and operating regimes

After the qualitative description of fast fluidisation, discussed in Sections 3.9.2 and 3.9.3, a more quantitatively view of it can be derived from the appropriate gas-solids flow regime diagrams such as the one proposed by Grace (1986), based on diagrams by Reh (1971) and shown in Figure 4-3. This diagram identifies flow regimes for combinations of gas velocity and particle properties, introducing a dimensionless particle size d^* and a dimensionless gas velocity u^*. These useful measures are defined as follows:

$$d^* = d_p[\rho_g(\rho_s - \rho_g)g/\mu^2]^{1/3} = Ar^{1/3} = (3C_D\,\mathrm{Re}_p^2/4)^{1/3} \qquad \text{(Eq. 4-1)}$$

$$u^* = u\,[\rho_g^2/(\rho_s - \rho_g)g\mu]^{1/3} = \mathrm{Re}_p/Ar^{1/3} = (3\,\mathrm{Re}_p/4C_D)^{1/3} \qquad \text{(Eq. 4-2)}$$

where

d^*	a dimensionless particle size defined by Eq. 4-1	[-]
u^*	a dimensionless gas velocity defined by Eq. 4-2	[-]
d_p	particle diameter	[m]
u	superficial gas velocity	[m/s]
ρ_g	gas density	[kg/m^3]
ρ_s	solids density	[kg/m^3]
g	acceleration due to gravity (=9.81)	[m/s^2]
μ_g	gas viscosity	[Pa s]
Re_p	particle Reynolds number	[-]
Ar	particle Archimedes number	[-]
C_D	drag coefficient ($=4g(\rho_s-\rho_g)d_p/(3\rho_g u^2)$)	[-]

The Archimedes number, Ar, characterizes basic gas-particle properties, while Re_p/C_D characterizes the gas velocity. For small particles, the operating options are fluidised beds, CFBs, transport reactors and dilute phase transport as the gas velocity is increased. For large particles, spouted and fluidised beds are the available options with increasing gas velocity.

The two dimensionless groups, u^* and d^*, introduced are particularly useful, since each involves only two process characteristic units, namely gas velocity and particle diameter, raised to the first power and properties which are generally invariant for any other process variable. Hence, these dimensionless groups can characterise the hydrodynamics of any given gas-solid system in a simple and unified approach.

According to Grace's diagram, fast fluidisation occupies a region of limited velocities and particle sizes. The velocity limits are imposed by lack of transport at the lower end, and by dilute suspensions at the upper end, where the slip velocity approaches particle terminal velocity (u_t) and where the CFB behaves as an entrained bed flow reactor, as already depicted in Figure 3-15, Section 3.9.2.

Figure 4-3: Regime diagram for gas-solids contacting according to Grace (1986)

From the above discussion, it may be concluded that the proposed CFB reactor configuration must operate with optimum effect in the range of maximum possible slip velocity within a strictly defined gas velocity regime. Within these gas velocity limits very good heat and mass transfer with negligible axial temperature gradients are provided. It should thus be kept in mind that the results of the CFB reactor sizing procedure should lie within the operating regimes specified by the diagram for gas-solids contacting shown in Figure 4-3 above.

4.4 Heat transfer and reactor hydrodynamics

As already stated in Chapter 2, Section 2.7, a high heat transfer rate to the pyrolysing biomass particles is one of the critical elements for successful fast pyrolysis.

Heat transfer in a fluidised bed reactor configuration combines the characteristics of various mechanisms. These mechanisms include gaseous convection heating, which is a difficult approach to attain high heat fluxes and heat transfer from the inert bed particles, where some form of solid conductive heat transfer, such as ablation, is incorporated. Ablation is

especially dominant when relative motion between particles and inert heat carrier (Graham, 1993) or heated surfaces (Diebold, 1986) is encountered.

In general, the ability to control and design CFB reactors is a direct function of the ability to be able to predict heat transfer and fluid mechanics. This last issue is essential since in all heat transfer processes there is also a necessary associated momentum transfer, which is high with gases and can be very high with solids. High rates of momentum transfer are very important to remove quickly and effectively the products of pyrolysis (the product organic vapor and the byproduct char that are formed) and thus to minimize the effects of slow heat up which enhances charring reactions, and extended vapor residence times which promote secondary reactions.

The parameter for evaluating the high heat fluxes to incoming biomass feedstock is the total heat transfer coefficient between biomass particles and the reactor environment. As reviewed by Lidén (1985) the total heat transfer coefficient, h_t, to biomass particles in a bubbling fluidised bed of silica sand with a mean particle size of 450 μm (with a voidage ε=0.40), lies between 300 and 510 W/m^{2}K, figures which were derived by extrapolating from correlations applied to immersed surfaces assuming 1 mm wood particles (Lidén, 1985). Temperature profiles for spherical and cylindrical particles have showed that, even in the worst case, i.e. h_t = 300 W/m^{2}K, the wood particle centre attains a temperature of 400^{o}C within 2 seconds. Thus, the heat transfer criterion for biomass fast pyrolysis, referred to in Section 2.7, is satisfied. Concluding, it may be claimed that the heat transfer rates in a bubbling bed of small particles are considered to be sufficient for the fast pyrolysis of 1 mm wood particles.

A Circulating Fluidised Bed (CFB) reactor is, as discussed extensively in Section 3.9.2, a lean phase reactor operating at high velocities and high voidages, i.e. much lower solids densities than those encountered in a dense, bubbling fluidised bed. In spite, however, of the significantly lower gas-solids suspension densities, Kobro and Brereton (1986) correlated h_t with the density of the suspension flowing past heat exchange surfaces and found it lay between 100 and 300 W/m^{2}K depending on the particle size. Figure 4-4 shows that there is an approximately linear function between measured heat transfer coefficients and suspended solids density in circulating bed boilers (Stromberg 1981, 1982; Kobro and Brereton, 1986; Zheng *et al.*, 1990).

The significance of suspension density, an alternative expression of gas-solids suspension voidage, is demonstrated in Figure 4-4, where data from Kobro and Brereton (1986) are presented.

Figure 4-4: Heat transfer coefficient versus suspension density in a CFB (Kobro and Brereton, 1986)

The above discussion indicates that, considering the suitability of circulating versus bubbling fluidised bed pyrolysers in terms of heat transfer, comparable heat transfer characteristics are obtained although a much lower voidage in the case of circulating fluidised bed reactor systems is obtained.

The answer lies in the fact that the unique features, such as the high slip velocities and the clustering phenomenon of the CFB reactor systems, discussed in Section 3.9.2, promote substantial conductive heat transfer (ablation) between the pyrolysing biomass particles and the surrounding hot heat carrier particles (clusters). The phenomenon of ablation was also discussed in a transport reactor system by Graham (1993), who defined ablation as a physical/mechanical mechanism that removes the primary depolymerised liquids from biomass reacting surface at a surface regression rate that is comparable with the thermal penetration rate, Section 3.6.4. The pyrolysis regime for a single particle is then approaching the ablative pyrolysis regime, Section 2.7.2, where the temperature at an infinitesimal distance below the retreating particle reaction surface remains far below the reaction temperature.

As a result, the intensive mixing and high turbulence characteristics of the CFB reactor systems provide nearly the same heat transfer characteristics in them as those encountered in much denser reactor systems, such as the bubbling fluidised bed systems, which however, lack in flexibility and ways to utilise char energy content in an integral reactor configuration concept.

The flexibility of the CFB systems in terms of heat transfer is further seen from the data of Kobro and Brereton (1986) discussed above. Figure 4-4 presents a reasonably consistent pattern, showing that heat transfer increases with suspension density and decreasing sand particle size in the ranges covered by the data. If the above published results are extended qualitatively from suspension-to-surface to suspension-to-immersed particles (biomass) heat transfer, an extrapolation also followed by Lidén (1985) in his derivation of the heat transfer coefficients for a bubbling fluidised bed system, it can be claimed that a higher suspension density (lower voidage), resulting in a denser riser, will promote higher ablation and hence a higher overall heat transfer coefficient, enhancing the extent of pyrolysis reaction even for larger biomass particles, as reported by Graham (1993).

The ability to be able to control heat transfer rates is accomplished by manipulating the density in the riser by adjusting the Solids Circulation Rate (SCR) around the CFB reactor system. Thus, SCR is a critical parameter and has to be calculated carefully, so that the desired heat transfer rate to biomass particles is achieved in order to meet the fast pyrolysis high heat flux requirements and bypass the low heat transfer region, where the undesired charring reactions prevail.

4.5 Sizing the CFB reactor for biomass fast pyrolysis

In the following sections, the CFB sizing methodology both for biomass pyrolysis and char combustion sections is fully developed and thoroughly examined. This examination incorporates pyrolysis kinetics, solids circulation rate correlation to biomass throughput, mass and energy balances in the riser and char combustor and concludes with CFB reactor system performance for biomass fast pyrolysis.

4.5.1 Biomass fast pyrolysis kinetics and predicted product yields

Experiments performed by different researchers have clearly shown that the maximum yield for liquid products from biomass fast pyrolysis is obtained at temperatures around 500°C and

occurs over a limited temperature range, the yield dropping off sharply on both sides. These results are summarised in Figure 4-5, where the liquid yields (excluding water) versus temperature is correlated by two independent research groups for a variety of experimental conditions, feedstocks and equipment used.

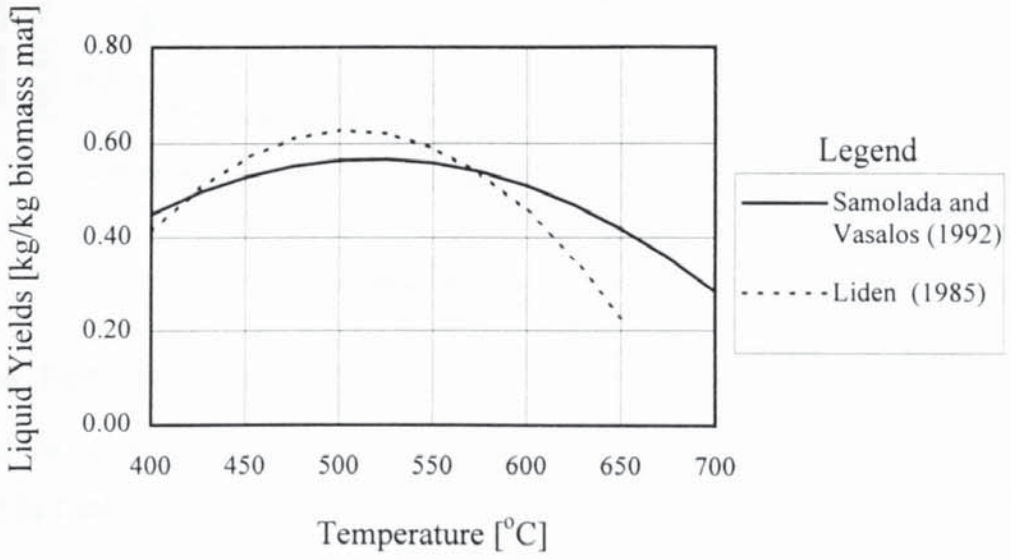

Figure 4-5: Prediction of liquid yields versus reactor temperature

To account for the liquid yield dropping at elevated temperatures, a reliable kinetic model of biomass fast pyrolysis should incorporate both primary and secondary pyrolysis reactions, as discussed earlier (Section 2.6.3). Such a model realistically predicts pyrolysis vapors yield at elevated temperatures.

Very few kinetic models incorporating secondary reactions have been proposed in the literature and even fewer tested and verified. Of the models proposed, Section 2.6.4, that of Lidén (1985, 1988), also tested by Scott *et al.*, (1987) has been established as one of the most successful models in predicting pyrolysis liquids yields over a wide range of conditions. Moreover, this model tends to be validated by the fact that the total liquid and organic liquid (i.e. excluding moisture and reaction water) yields have been successfully predicted. Figure 4-6 shows the variation of total liquid, char and gas yield as function of temperature for a hardwood (eastern maple) and a feedstock particle size between 250 and 600 μm (Scott *et al.*, 1988).

Figure 4-6: Prediction of pyrolysis products yield from maple (Scott *et al.*, 1988)

Based on the above predictions (for T= 500°C and VRT= 0.5 s) the product distribution presented in Table 4-1 below will be adopted for the derivation of reactor sizing.

4.5.2 Correlation between SCR and biomass throughput

After selecting the appropriate fast pyrolysis kinetic model, the next step in the design methodology of the biomass air-blown pyrolyser is to match the energy balances for the main reactor components, i.e. char combustor and biomass pyrolysis riser.

The heat requirements for the pyrolysis of biomass must be met by combustion of pyrolysis byproduct char. This heat may then be transferred by gases and, mainly, by solids through a

continuous circulation of solids between the main CFB reactor components, namely char combustor (or simply combustor) and biomass pyrolyser (riser).

The capacity of the CFB reactor system to perform as a biomass pyrolyser depends on heat transfer. Since heat transfer is proportional to the solids circulation rate (SCR), according to the discussion held in Section 4.4, the circulation system between the CFB reactor sections, i.e. biomass pyrolyser (riser) and char combustor, must be properly designed. In the following, the calculation procedure involved to correlate the required SCR to biomass throughput will be derived.

First, the complete CFB system, including both systems, as well as the involved streams and their respective temperature is considered, Figure 4-7. In this system, an exothermic ($-\Delta H_C$) reaction occurs in the char combustor and the circulating solids (G_s) are entrained from the char combustor and transfer this heat to the riser, where the heat requirements imposed by the biomass devolatilisation process (Q_{pyr}) are met. Figure 4-7 shows the situation with the pertinent symbols and temperatures of the various streams:

- assuming that the temperature of the solids leaving the combustor, T_2, is the same as that of the gas leaving that unit (which, as shown by experimental evidence (Kunii and Levenspiel, 1991), is a very good approximation), and
- using mass rather than molar units for enthalpies, heats of reaction (- for exothermic, + for endothermic) and flowrates of gases and solids.

The optimum combination of temperature (for the maximisation of pyrolysis liquids, as determined by fast pyrolysis kinetics) and SCR (for the provision of the adequate heat transfer to biomass pyrolysisng particles), is required in order to derive the appropriate operating conditions for any biomass throughput. This problem can be solved by setting up the overall and the individual balances for the two reactors and combining them, considering the SCR as an independent variable.

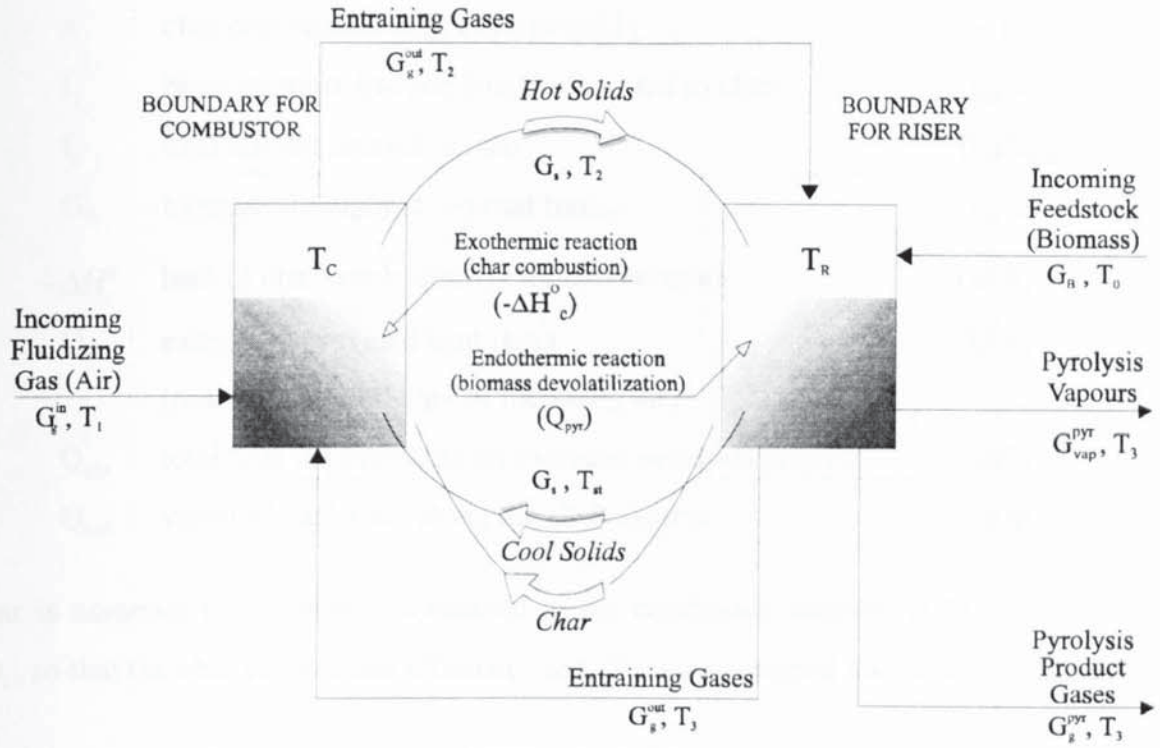

Figure 4-7: Mass and energy balances in the CFB reactor sections (the symbols and their significance are denoted in the text)

The overall energy balance, derived over the boundary for the entire CFB system as shown in Figure 4-7, gives:

$$\left\{\begin{array}{c}\text{Heat released}\\ \text{by char combustion}\end{array}\right\}+\left\{\begin{array}{c}\text{Heat in}\\ \text{incoming stream}\end{array}\right\}=$$

$$\left\{\begin{array}{c}\text{Heat required for biomass}\\ \text{devolatilisation}\\ \text{(Pyrolysis-to-Organics/PTO)}\end{array}\right\}+\left\{\begin{array}{c}\text{Various heat}\\ \text{losses}\end{array}\right\}$$

(Eq. 4-3)

Assuming that char is stoichiometrically burnt by the fluidising air, Eq. 4-3 may be written as follows:

$$xf_1 f_c G_B(-\Delta H_c^o) + Q_{ext} = Q_{pyr} + Q_{loss}$$

(Eq. 4-4)

where

x	char combustion efficiency ($0<x\leq1$)	[-]
f_1	biomass mass fraction (maf) converted to char	[kg/kg]
f_c	total carbon content in char	[kg/kg]
G_B	biomass throughput (on maf basis)	[kg/h]
$-\Delta H_c^o$	heat of char combustion (- for exothermic)	[kJ/h]
Q_{ext}	externally provided heat input (measured as enthalpy of incoming air)	[kJ/h]
Q_{pyr}	total heat requirements for biomass pyrolysis process	[kJ/h]
Q_{loss}	various heat losses along the CFB system	[kJ/h]

Char is assumed to be entirely consumed in the combustor, entirely (100 %) converted to CO_2, so that the char combustion efficiency to CO_2 , x, is assigned the value 1 in Eq. 4-4.

For the char combustor, the energy balance is given by:

$$\left\{\begin{matrix}\text{Heat released}\\ \text{by char Combustion}\end{matrix}\right\}+\left\{\begin{matrix}\text{Heat in}\\ \text{incoming stream}\end{matrix}\right\}=$$

$$=\left\{\begin{matrix}\text{Heat gained by}\\ \text{entraining gas}\end{matrix}\right\}+\left\{\begin{matrix}\text{Heat gained}\\ \text{by solids}\end{matrix}\right\}+\left\{\begin{matrix}\text{Heat losses in}\\ \text{the combustor}\end{matrix}\right\}$$

(Eq. 4-5)

or (see Section 4.5.3 for details),

$$f_1 f_c G_B(-\Delta H_c^o)+Q_{ext}=\sum G_{g,i}^{out}\Delta H_{i,T_c\to T_o}^0+G_s c_{p,s}(T_C-T_{st})+Q_{loss,C}$$

(Eq. 4-6)

where

$G_{g,i}^{out}$	mass flowrate of component i in entraining gas stream	[kg/h]
ΔH_i^0	enthalpy of the component i in entraining gas stream	[kJ/h]
T_C	temperature in the combustor	[K]
T_o	datum temperature (=298 K)	[K]
T_2	temperature of the entraining gas stream	[K]
G_s	solids circulation rate(=SCR)	[kg/h]
$c_{p,s}$	solids specific heat capacity	[kJ/kg K]
T_{st}	temperature of the return solids	[K]
$Q_{loss,C}$	heat losses in the combustor	[kJ/h]

Similarly, the energy balance for the biomass pyrolysis riser may be written as:

$$\left\{\begin{array}{c}\text{Heat lost by}\\ \text{entraining Gas}\end{array}\right\} + \left\{\begin{array}{c}\text{Heat lost by}\\ \text{entrained Solids}\end{array}\right\} =$$

$$= \left\{\begin{array}{c}\text{Heat required for Biomass}\\ \text{Devolatilisation}\\ \text{(Pyrolysis-to-Organics/ PTO)}\end{array}\right\} + \left\{\begin{array}{c}\text{Heat losses}\\ \text{in the riser}\end{array}\right\} \qquad \text{(Eq. 4-7)}$$

or (see Section 4.5.4 for details),

$$\sum \mathrm{G}_{\mathrm{g,i}}^{\mathrm{out}} \Delta H_{i,T_c \to T_o}^{0} + G_s c_{p,s}(T_2 - T_R) = \mathrm{Q}_{\mathrm{pyr}} + \mathrm{Q}_{\mathrm{loss,R}} \qquad \text{(Eq. 4-8)}$$

where

$\mathrm{Q}_{\mathrm{loss,R}}$ heat losses in the riser [kJ/h]

The heat losses, are assumed to be a fraction (10 %, Maniatis, 1986) of the incoming energy in the riser, i.e. the energy carried by entraining gases and the entrained solids, or:

$$Q_{loss,R} = 0.1[\sum \mathrm{G}_{\mathrm{g,i}}^{\mathrm{out}} \Delta H_{i,T_c \to T_o}^{0} + G_s c_{p,s}(T_2 - T_{st})] \qquad \text{(Eq. 4-9)}$$

The three energy balances, described by Eq. 4-4, Eq. 4-6 and Eq. 4-8, represent two independent equations, so that any of the three balances can be obtained from the other two. Either of the individual energy balances, Eq. 4-6 and Eq. 4-8, gives the necessary solids circulation rate. Thus:

$$G_s = \frac{f_1 f_c G_B(-\Delta H_c^o) + \mathrm{Q}_{\mathrm{ext}} - \sum \mathrm{G}_{\mathrm{g,i}}^{\mathrm{out}} \Delta H_{i,T_c \to T_o}^{0}}{c_{p,s}(T_2 - T_{st})} =$$

$$= \frac{\mathrm{Q}_{\mathrm{pyr}} + Q_{loss,R} - \sum \mathrm{G}_{\mathrm{g,i}}^{\mathrm{out}} \Delta H_{i,T_c \to T_o}^{0}}{c_{p,s}(T_2 - T_R)} \qquad \text{(Eq. 4-10)}$$

The above equations provide the correlation between biomass throughput, $\mathrm{G_B}$, and Solids Circulation Rate (SCR), $\mathrm{G_s}$. In order to quantify this correlation, and hence determine the necessary heat carrier-to-biomass ratio, the mass and energy balances of the two CFB components have to be fully analysed and correlated to biomass throughput, $\mathrm{G_B}$. This will be achieved by considering the combustor and riser independently and analysing the different

terms in detail, correlating input and outlet streams to biomass throughput, which is varied accordingly.

The mass and energy balances of these two reactor components are described in the following sections in detail.

4.5.3 Mass and energy balance in the combustor

The char combustor is further shown in Figure 4-8.

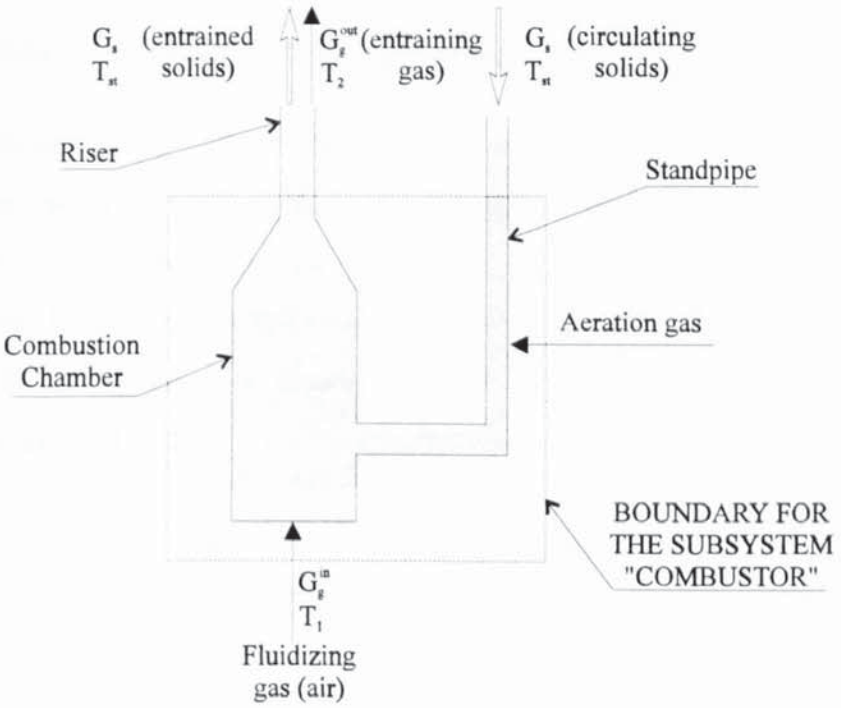

Figure. 4-8: The char combustor of the CFB reactor

In order to formulate the appropriate energy equation, a mass balance for the char combustor must be written. The mass balance for the combustor is based upon the char combustion stoichiometry, described by the following, simple equation:

$$C_{(s)} + O_2 + N_2 \xrightarrow{(1)} CO_2 + N_2$$

	$C_{(s)}$	O_2	N_2	CO_2	N_2
	1 mole	1 mole	3.77 moles	1 mole	3.77 moles
	12.01 g	1 x 32 g	3.77 x 28.02 g	1 x 44.01 g	3.77 x 28.02 g
In	$f_1 f_c G_B$ (2)	2.66 $f_1 f_c G_B$	8.80$f_1 f_c G_B$	-	-
Prod.	-	-	-	3.66 $f_1 f_c G_B$	-
Out	-(3)	-(4)	-	3.66 $f_1 f_c G_B$	8.80 $f_1 f_c G_B$

(1) $-\Delta H_c^0$ =393.8 [kJ/mol] (or 32816 kJ/kg) at 20°C (Buekens *et al.*, 1985)

(2) where f_1 denotes char yield for a given conversion temperature, f_c denotes fixed carbon content in char and G_B is biomass flowrate [kg maf/h]

(3) all char is assumed to be consumed stoichiometrically in the combustor1)

(4) oxygen is assumed to be consumed entirely during the combustion process

A further analysis of the energy balancefor the char combustor, Eq. 4-6, can now be written as follows:

$$\left\{\begin{matrix}\text{External}\\ \text{energy input}\end{matrix}\right\}+\left\{\begin{matrix}\text{Energy in}\\ \text{incoming solids}\end{matrix}\right\}+\left\{\begin{matrix}\text{Energy provided}\\ \text{by char combustion}\end{matrix}\right\}=$$

$$=\left\{\begin{matrix}\text{Energy in}\\ \text{entraining gas}\end{matrix}\right\}+\left\{\begin{matrix}\text{Energy in}\\ \text{entrained solids}\end{matrix}\right\}+\left\{\begin{matrix}\text{Various}\\ \text{heat losses}\end{matrix}\right\} \qquad \text{(Eq. 4-11)}$$

The different terms in the energy balance equation are analyzed in detail below.

First, the "External Energy Input" denoted as TERM IN-C1 is a generic term, that incorporates the energy supplied directly or indirectly to the char combustor chamber, in order to compensate for insufficient heat supply to the overall energy requirements of the pyrolysis process. In the case of the CFB air-blown pyrolyser, this energy is provided by preheating the fluidising gas to a certain degree, denoted by a temperature rise from T_o (datum temperature) to T_1. Thus:

$$TERM\ \text{IN-C1}:\left\{\begin{matrix}\text{External}\\ \text{energy input}(=Q_1)\end{matrix}\right\}=\left\{\begin{matrix}\text{Energy in}\\ \text{fluidizing gas}\end{matrix}\right\}=\sum G_{g,i}^{in}\int_{T_o}^{T_1} c_{p,i}\,dT \qquad \text{(Eq. 4-12)}$$

Similarly:

$$TERM\ \text{IN-C2}:\left\{\begin{matrix}\text{Energy provided}\\ \text{by char combustion}\end{matrix}\right\}=f_1 f_c G_B \Delta H_c^0 \qquad \text{(Eq. 4-13)}$$

$$TERM\ \text{IN-C3}:\left\{\begin{matrix}\text{Energy in}\\ \text{incoming solids}\end{matrix}\right\}=G_s c_{p,s}(T_{st}-T_o) \qquad \text{(Eq. 4-14)}$$

$$TERM\ \text{OUT-C1}:\left\{\begin{matrix}\text{Energy in}\\ \text{entraining gas}\end{matrix}\right\}+\left\{\begin{matrix}\text{Various}\\ \text{heat losses}\end{matrix}\right\}=\sum G_{g,i}^{out}\int_{T_o}^{T_2} c_{p,i}\,dT \qquad \text{(Eq. 4-15)}$$

$$TERM\ \text{OUT-C2}:\left\{\begin{matrix}\text{Energy in}\\ \text{entrained solids}\end{matrix}\right\}=G_s c_{p,s}(T_2-T_o) \qquad \text{(Eq. 4-16)}$$

The specific heat capacity, $c_{p,i}$, for each gaseous component i is given, as a function of T, by the following equation:

$$c_{p,i} = A_i + B_i T + C_i T^2 + D_i T^3 \qquad \text{(Eq. 4-17)}$$

where

A_i, B_i, C_i, D_i,	constants given in Table 4-2	[-]
T,	temperature	[K]

Table 4-2: Constants for $c_{p,i}$ calculation (c_p in kJ/kmol K and T in K)

Component \ Constant	A	B	C	D
O_2	28.11	-3.680×10^{-2}	1.746×10^{-5}	-1.065×10^{-8}
N_2	31.15	-1.357×10^{-2}	2.680×10^{-5}	-1.168×10^{-8}
CO_2	19.80	7.344×10^{-2}	-5.602×10^{-5}	1.715×10^{-8}

Gas in- and out-let streams flowrates can be correlated to G_B by means of char combustion reaction stoichiometry. These correlations are given in Table 4-3.

Table 4-3: In-and outl-et gaseous streams mass flowrates

$G_{g,i}$ (kg/h)	As a function of G_B
$G^{in}_{g,O2}$	$2.66\, f_c f_1 G_B$
$G^{in}_{g,N2}$	$8.80 f_c f_1 G_B$
$G^{out}_{g,CO2}$	$3.66\, f_c f_1 G_B$
$G^{out}_{g,N2} = (G^{in}_{g,N2})$	$8.80 f_c f_1 G_B$

Substituting the above values of in and out energy terms in Eq. 4-11, the energy equation for char combustor can finally be written as:

$$f_1 f_c G_B [\frac{2.66}{32} \int_{T_o}^{T_1} c_{p,O2} dT + (-\Delta H_c^\circ)] =$$

$$= f_1 f_c G_B [\frac{3.66}{44.01} \int_{T_o}^{T_2} c_{p,CO2} dT + \frac{8.80}{28.02} \int_{T_1}^{T_2} c_{p,N2} dT] + G_s c_{p,s} (T_2 - T_o)$$

(Eq. 4-18)

In deriving the above equation, the following assumptions are further made:

i) char particles entering the combustion chamber instantaneously attain the fluidised bed temperature (i.e. from T_{st} to T_c)

ii) the heat requirements to reach char ignition temperature are very limited in comparison to those for the solids heat carrier

iii) $G_{char} << G_s$, so that $G_{char} + G_s$ may be approximated by G_s

iv) the reaction products in the exit of the combustor are solely CO_2 and N_2 (thus the presence of CO, which is a product of incomplete conversion of carbon char to CO_2, i.e. $x<1$, as well as of unreacted O_2 is neglected).

4.5.4 Mass and energy balance in the riser

The riser is further shown in Figure 4-9.

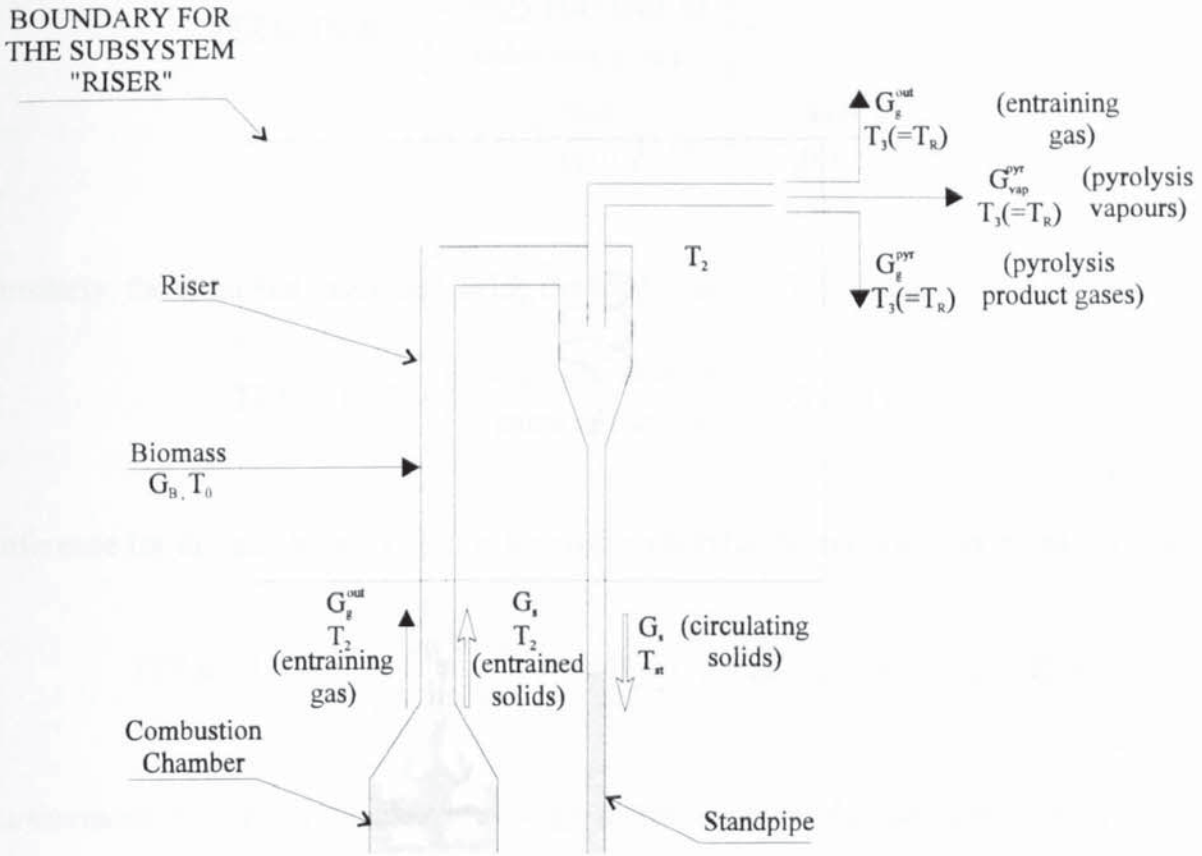

Figure 4-9: The riser of the CFB reactor

An energy balance for the riser section may be written as follows:

$$\left\{\begin{matrix}\text{External}\\ \text{energy input}\end{matrix}\right\}+\left\{\begin{matrix}\text{Energy provided by}\\ \text{entraining gases}\end{matrix}\right\}+\left\{\begin{matrix}\text{Energy provided by}\\ \text{entrained solids}\end{matrix}\right\}=$$

$$=\left\{\begin{matrix}\text{Heat losses}\\ \text{in the riser}\end{matrix}\right\}+\left\{\begin{matrix}\text{Heat required for the}\\ \text{Pyrolysis-to-Organics}\end{matrix}\right\} \qquad \text{(Eq. 4-19)}$$

The different terms appearing in Eq. 4-19 will now be examined in more detail. First, since no external energy is provided in the riser section the first term equals 0. Thus:

$$TERM\ \text{IN-R1:} \left\{ \begin{matrix} \text{External} \\ \text{energy input} \end{matrix} \right\} = 0$$

(Eq. 4-20)

Then, the combustor flue gases (entraining gases) are not undergoing any chemical reaction, i.e. the combustion and aeration gases, which are solely N_2 and CO_2, are considered inert in the temperature interval considered, leaving the riser at $T_3 (=T_R)$, so that it may be written:

$$TERM\ \text{IN-R2:} \left\{ \begin{matrix} \text{Energy provided by} \\ \text{entraining gases} \end{matrix} \right\} =$$

$$= f_1 f_c G_B \left[\frac{3.66}{44.01} \int_{T_R}^{T_3} c_{p,CO2} dT + \frac{8.80}{28.02} \int_{T_R}^{T_3} c_{p,N2} dT \right]$$

(Eq. 4-21)

Similarly, the entrained gases are leaving the reactor at $T_3 (=T_R)$, so that:

$$TERM\ \text{IN-R3:} \left\{ \begin{matrix} \text{Energy provided by} \\ \text{entrained solids} \end{matrix} \right\} = G_s c_{p,s} (T_2 - T_R)$$

(Eq. 4-22)

Reference for the heat losses, $Q_{loss,R}$, in the riser section has been previously given, so that:

$$TERM\ \text{OUT-R4:} \left\{ \begin{matrix} \text{Heat losses} \\ \text{in the riser} \end{matrix} \right\} = 0.1 \left[\sum G_{g,i}^{out} \Delta H_{i,T_c \to T_o}^{0} + G_s c_{p,s} (T_2 - T_{st}) \right]$$

(Eq. 4-23)

Furthermore, in order to calculate the energy requirements for the transformation of biomass to organics (simply, Pyrolysis-to-Organics/PTO) a detailed analysis of biomass thermal decomposition, that is a mass balance for the pyrolysis reaction, is required. Unfortunately, this is not possible directly, due to the lack of defined and clear mechanisms, exact temperatures of decomposition and suitable model compounds. However, the total heat requirements for the pyrolysis of biomass feedstock may be approximated by considering it composed of different parts, namely:

- sensible heat requirements for the dry biomass feed
- the heat of vaporisation of the primary products
- the heat of reaction
- the sensible and latent heat requirements of the moisture content.

At this stage it should be noted that a considerable effort has been dedicated to determine the heat of reaction for primary pyrolysis, with a wide range of values existing in the literature (Lidén, 1985; Graham, 1993; Peacocke, 1994). This range can be attributed to variations in the biomass feedstock, experimental equipment, reaction conditions, and the extent to which the reactions are permitted to occur in each case (Graham, 1993). There is, however, general agreement that primary fast pyrolysis is moderately endothermic (NREL/SERI 1980; Antal, 1981; Scott *et al.*, 1991). A few authors speculate that fast pyrolysis is athermic (i.e. the heat of reaction equals zero, as also discussed in Section 2.7.1) at approximately 700°C and increases in endothermicity with increasing temperature (Lédé *et al.*, 1980; Deglise and Lédé, 1982). For engineering applications, the heat of reaction of primary pyrolysis is often assumed to be negligible when compared to other heating effects referred to above. Thus, the energy requirements are limited to heat for raising the temperature of biomass to reaction temperature (sensible heat) and heat of vaporisation of raw material and/or products.

The heat of vaporisation is estimated from the distribution of the vaporised products out of the pyrolysis reactor. The reaction occurring in the riser is simply biomass thermal decomposition to vapors/organic products, char, water and non-condensible gases. Given the product distribution presented in Table 4-1, the mass balance for the riser section may be depicted schematically from Figure 4-10, incorporating data derived by Lidén (1985) and McKeough (1988) . It should be clearly emphasized that the above product distribution is valid only for the process variables maximising pyrolysis liquids yields, i.e. 500°C and 0.5 s. For a moisture and ash free (maf) as well as a representative (7.5 % wt moisture-0.5 % wt ash content) biomass feedstock, the riser outlet streams correlated to G_B are listed below in Table 4-4.

Table 4-4: Distribution of biomass pyrolysis products as a function of maf biomass (G_B) and a "typical" (7.5 % wt moisture-0.5 % wt ash) biomass feedstock (G_{BWA})

Outlet Stream	$f(G_B)$ [kg/h]	$f(G_{BWA})$ [kg/h]
Organic liquids		
- Light organics	0.107 G_B	0.107 x RF[1)]xG_B =0.0984 G_{BWA}
- Heavy organics	0.493 G_B	0.493 x RFxG_B =0.4536 G_{BWA}
Solids (char)	0.15 G_B	0.15 x RFxG_B =0.138 G_{BWA}
Gas (CO, CO_2 and CH_4)	0.145 G_B	0.145 x RFxG_B =0.1334 G_{BWA}
Reaction water	0.105 G_B	0.105 x RFxG_B =0.0966 G_{BWA}
Feedstock water	-	=0.075 G_{BWA}
Feedstock ash	-	=0.005 G_{BWA}

[1)]where RF=[100-(7.5+0.5)]/100=0.92 [kg maf biomass/kg total feedstock]

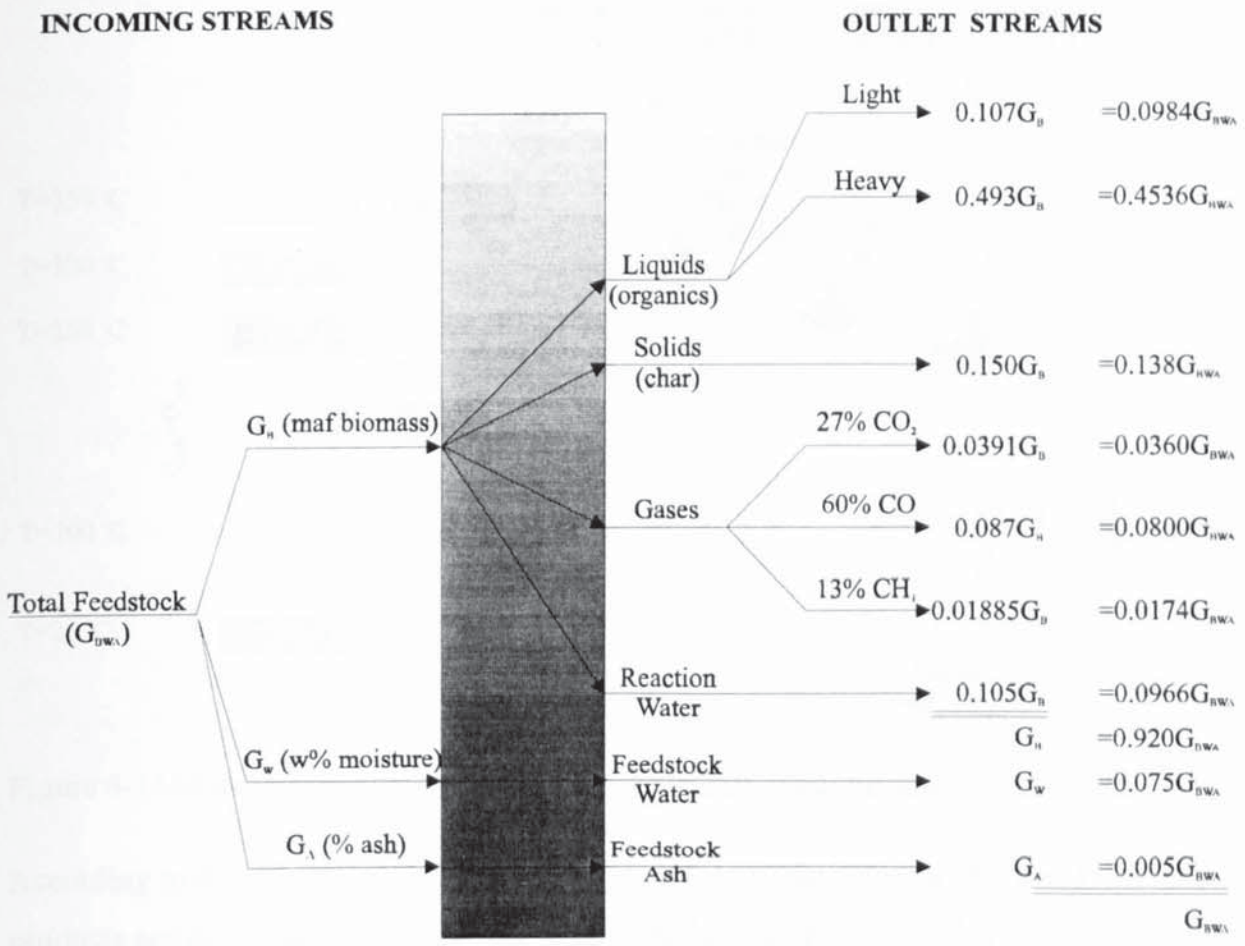

Figure 4-10: The product distribution of the biomass fast pyrolysis reaction (riser mass balance for the biomass feedstock in the riser)

The energy to vaporise these products as well as sensible heat to bring biomass and pyrolysis products to reaction temperature is required. The problem is that the temperature at which the

pyrolysis products are vaporised is uncertain, which strongly influences the required heat. As this temperature is unknown two cases have been studied in the past (McKeough *et al.*, 1988), described in detail below.

A) In the first case, referred to as direct products evolution - also characterised as case A and schematically shown in Figure 4-11, biomass remains intact up to a temperature of about 250°C. It is assumed that at this temperature, a breakdown starts releasing light organics (methanol, acetone, acetic acid and so on) and gas. At about 300°C water is produced from the rupture of biomass. Heavy organics ("oil product" or "primary tar") are vaporized at 350°C. The non-condensible gases are being formed over the entire range of temperatures and they originate (evolve) directly from biomass.

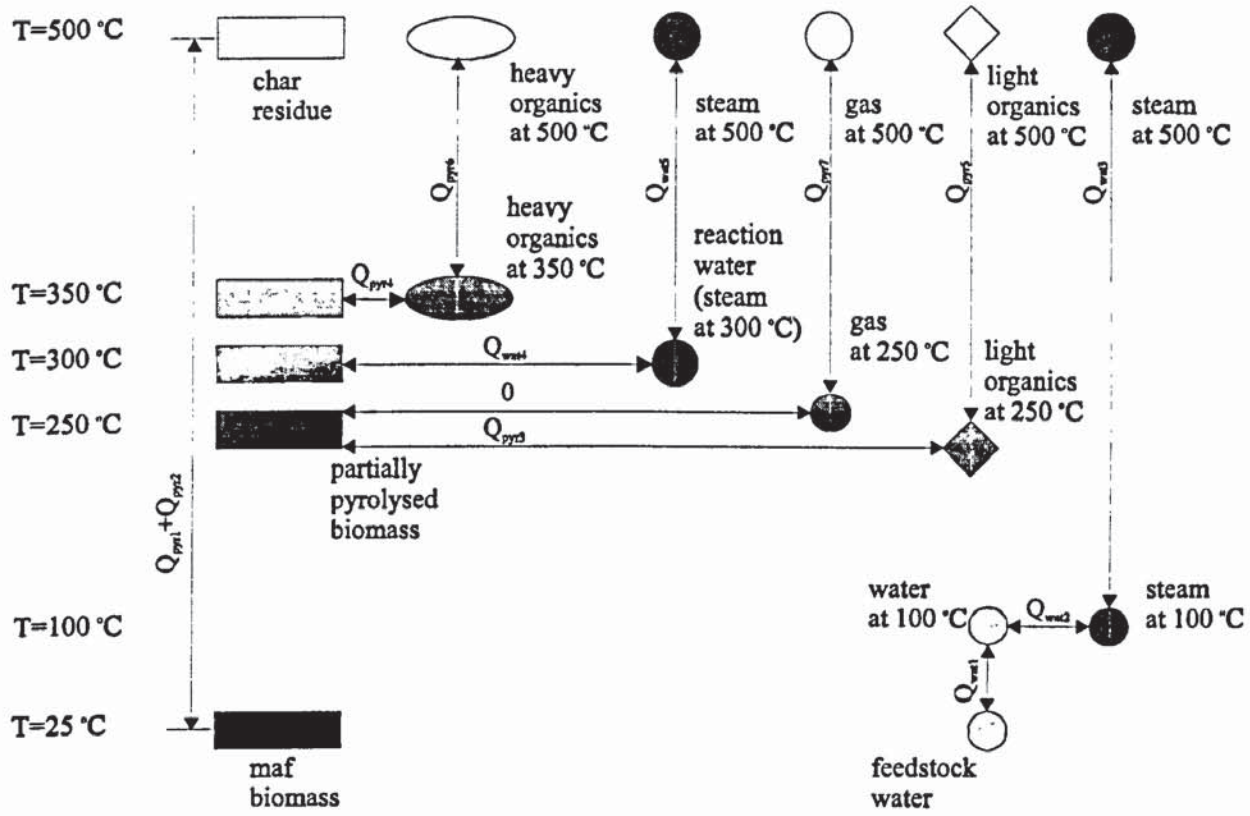

Figure 4-11: Biomass thermal decomposition, Case A (CA)-direct products evolution

According to this case (CA), biomass pyrolysis would occur between 250 and 350°C and all products are generated directly from biomass. The heat for PTO is, in this case, comprised of the following terms:

CA1: Energy to heat up biomass from datum temperature (T_o) to reaction temperature $T_3=T_R=500°C$ is comprised of two terms, namely:

$$Q_{pyr1} = G_B[1.11(T_1 - T_o) + \frac{0.00486}{2}(T_1^2 - T_0^2)] \quad \text{(according to Dunlap, 1992)}$$

$$Q_{pyr2} = \frac{(G_B + f_1 G_B)}{2} * [1.11(T_3 - T_1) + \frac{0.0037}{2}(T_3^2 - T_1^2)] \quad \text{(according to Parker, 1988)}$$

with T_o=20°C, T_1=100°C and $T_3(=T_R)$=500°C.

The term $[(G_B+f_1G_B)/2]$ accounts for the linear decomposition of biomass from the initial (G_B) to the final value (f_1G_B) for the temperature interval considered.

CA2: Energy to vaporise light organics directly from biomass:

$$Q_{pyr3} = G_B * (Yield - to - light - organics) * 165 \quad \text{(according to McKeough } et\ al.\text{, 1988)}$$

where $\Delta H_{vap(l)}$=165 [kJ/kg] at average T=25°C.

CA3: Energy to vaporise heavy organics directly from biomass:

$$Q_{pyr4} = G_B * (Yield - to - heavy - organics) * 600 \quad \text{(according to McKeough } et\ al.\text{, 1988)}$$

where $\Delta H_{vap(h)}$=600 [kJ/kg] at average 350°C.

The mean heats of vaporisation for light (l) and heavy (h) organics respectively have been approximated by Nilsson (1982).

CA4: Energy to bring light organics and heavy organic vapors from $T_{2(l)}$, $T_{2(h)}$ respectively, to reaction temperature $T_3(=T_R)$:

$$Q_{pyr5} = G_B * (Yield - to - light - organics) * c_{p(l)} * (T_R - T_{2(l)}) \quad \text{(according to Nilsson, 1988)}$$

$$Q_{pyr6} = G_B * (Yield - to - heavy - organics) * c_{p(h)} * (T_R - T_{2(h)}) \quad \text{(according to Nilsson, 1988)}$$

where $c_{p(l)}$=2.05[kJ/kg K], $c_{p(h)}$=2.45 [kJ/kg K] and $T_{2(l)}(=273+250)=523$ K, $T_{2(h)}(=273+350)=623$ K for light (l) and heavy (h) organics respectively.

CA5: Energy to bring gaseous products from $T_g(=273+250)=523$ K to reaction temperature:

$$Q_{pyr7} = G_B * (Yield - to - gaseous - products) * c_{p,g(m)} * (T_R - T_g)$$

where

$$c_{p,g(m)} = \sum y_i c_{p,m(i)} \text{ and } c_{p,m(i)} = \frac{\int_{T_g}^{T_R} c_{p,i}\,dT}{T_R - T_g}$$

the mean specific heat of the pyrolysis gas mixture for the temperature interval T_g to T_R.

CA6: Energy to bring feedstock moisture to T_1(=273+100)=373 K and vaporise it at T_1:

$$Q_{wat1} = G_B * (\frac{w}{1-w-a}) * c_{pH2O} * (T_1 - T_0) \qquad \text{where } c_{pH2O}=4.2 \text{ [kJ/kg K]}$$

$$Q_{wat2} = G_B * (\frac{w}{1-w-a}) * \Delta H_{vap,w1}(T_1 = 373\ K) \quad \Delta H_{vap,w1}=2260 \text{ [kJ/kg] at } T_1=373 \text{ K}$$

CA7: Energy to bring feedstock steam from T_1(=273+100)=373 K to reaction temperature T(=T_R=273+500)=773 K:

$$Q_{wat3} = G_B * (\frac{w}{1-w-a}) * [\Delta H_{vap,wR}(T_R = 773\ K) - \Delta H_{vap,w1}(T_1 = 373\ K)]$$

CA8: Energy to vaporise reaction water at T=(273+300)=573 K:

$$Q_{wat4} = 0.0966 G_B * \Delta H_{vap,w2}(T = 573K) \qquad \Delta H_{vap,w2}=1400 \text{ [kJ/kg] at T=573 K}$$

CA9: Energy to bring reaction steam to reactor temperature T_3(=T_R)=773 K:

$$Q_{wat5} = 0.0966 G_B * [\Delta H_{vap,wR}(T_R = 773\ K) - \Delta H_{vap,w2}(T = 573\ K)]$$

Inserting the values given above and summing up the different terms, CA1 to CA9, the total heat requirements for fast pyrolysis for Case A are given as a function of G_B, w and a as:

$$Q_{pyr} = \sum Q_{pyr,i(A)} + \sum Q_{wat,i(A)} \Rightarrow$$

$$\Rightarrow \frac{Q_{pyr}}{G_B} = [991.5 + 3392(\frac{w}{1-(w+a)})]$$

(Eq. 4-24)

In this case, the mean heat of vaporisation will be (on a maf basis, i.e. w=a=0) 1166.5 kJ/kg of actually vaporised biomass (excluding the char).

B) In the second case, referred to as subsequent products evolution - characterised as case B and schematically shown in Figure 4-12, the different products are subsequently released from biomass. Steam is evolved at 135°C, light organics at 150°C and heavy organics ("oil product") at an average of 275°C. The gases are formed in a vapor phase cracking of the "oil product", which means that their heat of vaporization is the same as that of the 'heavy' organics, in accordance with Lidén's model, Section 2.6.3. The adaptation of this assumption considers the fact that at least some products are formed before others when the temperature is increased, an hypothesis also confirmed by Elliott (1985) and discussed at Section 2-5, see Figure 2-14.

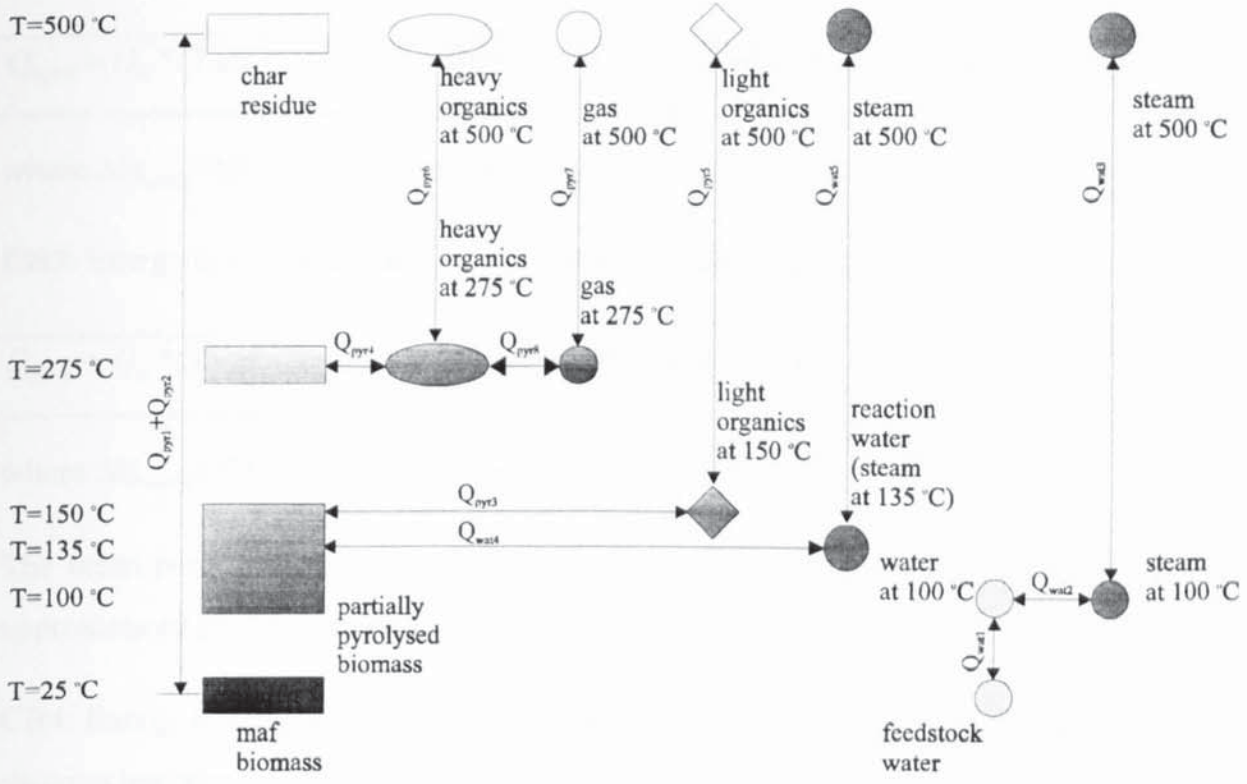

Figure 4-12: Biomass thermal decomposition, Case B (CB)-subsequent products evolution

According to this case, the pyrolysis would occur at approximately 275°C and the final products are either generated directly from biomass or evolved by heavy organics by vapor phase, secondary reactions. The heat for PTO is, in this case (CB), comprised of the following terms:

CB1: Energy to heat up biomass from datum temperature (T_o) to reaction temperature $T_3=T_R=500°C$ is comprised of two terms, namely:

$$Q_{pyr1} = G_B[1.11(T_1 - T_o) + \frac{0.00486}{2}(T_1^2 - T_0^2)] \quad \text{(according to Dunlap, 1992)}$$

$$Q_{pyr2} = \frac{(G_B + f_1 G_B)}{2} * [1.11(T_3 - T_1) + \frac{0.0037}{2}(T_3^2 - T_1^2)] \quad \text{(according to Parker, 1988)}$$

with T_o=20°C, T_1=100°C and $T_3(=T_R)$=500°C. The term $[(G_B+f_1G_B)/2]$ accounts for the linear rate of biomass decomposition from the initial (G_B) to the final value (f_1G_B) for the temperature interval considered.

CB2: Energy to vaporise light organics directly from biomass:

$$Q_{pyr3} = G_B * (Yield - to - light - organics) * 480 \quad \text{(according to McKeough } et\ al.\text{, 1988)}$$

where $\Delta H_{vap(l)}$=480 [kJ/kg] at average T=150°C.

CB3: Energy to vaporise heavy organics directly from biomass:

$$Q_{pyr4} = G_B * (Yield - to - heavy - organics) * 600 \quad \text{(according to McKeough } et\ al.\text{, 1988)}$$

where $\Delta H_{vap(h)}$=778 [kJ/kg] at average 275°C.

The mean heats of vaporisation for light (l) and heavy (h) organics respectively have been approximated by Nilsson (1982).

CB4: Energy to bring light organics and heavy organic vapors from $T_{2(l)}$, $T_{2(h)}$ respectively, to reaction temperature $T_3(=T_R)$:

$$Q_{pyr5} = G_B * (Yield - to - light - organics) * c_{p(l)} * (T_R - T_{2(l)}) \quad \text{(according to Nilsson, 1988)}$$

$$Q_{pyr6} = G_B * (Yield - to - heavy - organics) * c_{p(h)} * (T_R - T_{2(h)}) \quad \text{(according to Nilsson, 1988)}$$

where $c_{p(l)}$=2.05[kJ/kg K], $c_{p(h)}$=2.45 [kJ/kg K] and $T_{2(l)}$(=273+150)=423 K,$T_{2(h)}$(=273+275)= =548 K for light (l) and heavy (h) organics respectively.

CB5: Energy to vaporise gaseous products from heavy organics, occurring at the same temperature, i.e. $T_{2(h)}$(=273+275)=548 K:

$$Q_{pyr7} = G_B * (Yield - to - gases) * 778$$

where $\Delta H_{vap(g)} = \Delta H_{vap(h)} = 778$ (kJ/kg) at average 275°C, since the gases are formed (evolved) in a vapor phase cracking of the 'heavy' organics, hence their heat of vaporisation being the same as that of the organic vapors.

CB6: Energy to bring gaseous products from T_g(=273+275)=448 K to reaction temperature:

$$Q_{pyr8} = G_B * (Yield - to - gaseous - products) * c_{p,g(m)} * (T_R - T_g)$$

where

$$c_{p,g(m)} = \sum y_i c_{p,m(i)} \text{ and } c_{p,m(i)} = \frac{\int_{T_g}^{T_R} c_{p,i} dT}{T_R - T_g} = 1.49 \quad \text{[kJ/kg K]}$$

the mean specific heat of the pyrolysis gas mixture, consisting of CO, CO_2 and CH_4 as calculated by Lidén (1985) for the temperature interval T_g to T_R.

CB7: Energy to bring feedstock moisture to T_1(=273+100)=373 K and vaporise it to steam at temperature T_1:

$$Q_{wat1} = G_B * (\frac{w}{1-w-a}) * c_{pH2O} * (T_1 - T_0) \qquad \text{where } c_{pH2O}=4.2 \text{ (kJ/kg K)}$$

$$Q_{wat2} = G_B * (\frac{w}{1-w-a}) * \Delta H_{vap,w1}(T_1 = 373\ K) \quad \Delta H_{vap,w1}=2260 \text{ (kJ/kg) at } T_1=373 \text{ K}$$

CB8: Energy to bring feedstock steam from T_1(=273+100)=373 K to reaction temperature T(=T_R=273+500)=773 K:

$$Q_{wat3} = G_B * (\frac{w}{1-w-a}) * [\Delta H_{vap,wR}(T_R = 773\ K) - \Delta H_{vap,w1}(T_1 = 373\ K)]$$

CB9: Energy to vaporise reaction water released at T=(273+135)=408 K:

$$Q_{wat4} = 0.0966 G_B * \Delta H_{vap,w2}(T = 408K) \qquad \Delta H_{vap,w2}=2158 \text{ [kJ/kg] at T=408 K}$$

CB10: Energy to bring reaction generated steam to reactor temperature T_3(=T_R)=773 K:

$$Q_{wat5} = 0.0966 G_B * [\Delta H_{vap,wR}(T_R = 773\ K) - \Delta H_{vap,w2}(T = 408\ K)]$$

Inserting the values given above and summing up the different terms, CB1 to CB10, the total heat requirements for fast pyrolysis for case B are given as a function of G_B, w and a as:

$$Q_{pyr} = \sum Q_{pyr,j(A)} + \sum Q_{wat,j(A)} \Rightarrow$$
$$\Rightarrow \frac{Q_{pyr}}{G_B} = [1332.9 + 3702.7(\frac{w}{1-(w+a)})]$$

(Eq. 4-25)

In this case, the mean heat of vaporisation will be (on a maf basis, i.e. w=0) 1568.1 kJ/kg of actually vaporised biomass (excluding the char).

It is nowadays believed, see further discussion in Section 2.6.3, that secondary products are formed in the vapor phase from 'heavy organics' and not directly from biomass, which has also been confirmed by Elliott (1985). Thus, it is reasonable to assume that biomass organic vapors are formed according to the procedure described by the subsequent products evolution (Case B) model, shown in Figure 4-12.

As a consequence of the above analysis, the last term, Term OUT-R5, in Eq. 4-19, can now be estimated, given as a function of G_B, w and a below, considering an additional 15 % increase to account for unaccounted energy requirements:

$$TERM\,\text{OUT - R5: } \left\{ \begin{matrix} \text{Heat required for the} \\ \text{Pyrolysis - to - Organics} \end{matrix} \right\} =$$
$$= 1.15 G_B [1332.9 + 3702.7(\frac{w}{1-(w+a)})]$$

(Eq. 4-26)

Substituting the values of the different in- and out- energy terms derived above in Eq. 4-19, the energy balance equation for the riser is finally written as:

$$f_1 f_c G_B [\frac{3.66}{44.01} \int_{T_R}^{T_2} c_{p,CO2} dT + \frac{8.80}{28.02} \int_{T_R}^{T_2} c_{p,N2} dT] + G_s c_{p,s} (T_2 - T_R) =$$
$$= 0.1[\sum G_{g,i}^{out} \Delta H^0_{i,T_2 \to To} + G_s c_{p,s} (T_2 - T_{st})] + 1.15 G_B [1332.9 + 3702.7(\frac{w}{1-(w+a)})]$$

(Eq. 4-27)

At this point, the energy balances for both the CFB reactor configuration units have been derived and all the different energy terms have been correlated to biomass (maf) throughput (G_B) and feedstock moisture and ash content (w and a). This detailed analysis will permit in

the following the calculation of the required solids circulation rates (SCR), by means of Eq. 4-10, derived by combination of the char combustor and riser energy balance equations, for a wide range of biomass throughputs and feedstock moisture content.

4.5.5 CFB system performance for biomass fast pyrolysis

The energy balance equations for the CFB reactor sections, i.e. Eq. 4-18 for the combustor and Eq. 4-27 for the riser section, are now used to determine the overall process energy surplus/deficit, $E_{sur/def}$, of the process incorporating integral char combustion in the lower part of the CFB reactor, which is defined as:

$$E_{sur/def} = \frac{Energy\ provided\ by\ char\ combustion - Energy\ provided\ to\ fluidizing\ gas}{PTO\ energy\ requirements + Various\ energy\ losses} \qquad \text{(Eq. 4-28)}$$

The overall process energy surplus/deficit is shown in Figure 4-13 for feedstock moisture contents varying between 5 and 25 % wt (wet basis). Figure 4-13 demonstrates that for low-moisture content biomass feedstocks (<17.5 % wt moisture content) energy self sufficiency is achieved ($E_{sur/def}$>1), while for medium and high moisture content feedstocks (>17.5 % wt moisture content), where $E_{sur/def}$ is below unity (deficit), additional fuel must be imported. In deriving these correlations it should be born in mind that, for reasons of safety, PTO energy requirements were deliberately overestimated, by 15 % as in Eq. 4-26 in Section 4.5.4, and that the pyrolysis gas energy content utilisation has not been taken into account, which could further improve the proposed CFB reactor system energy self sufficiency.

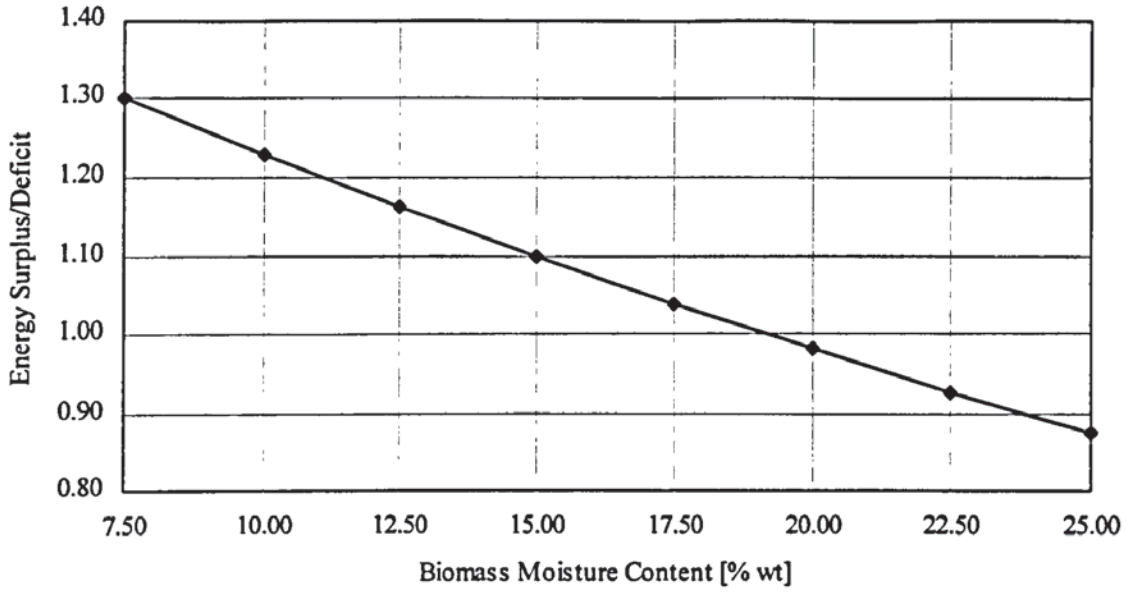

Figure 4-13: CFB reactor energy surplus/deficit for biomass feedstock moisture contents between 7.5-25 % wt (wet basis)

Secondly, the energy balance equations, (Eqs. 4-10), may be used to determine the value of SCR that thermally balances the two CFB reactor sections, i.e. gas combustor and riser. Combining Eqs. 4-10, Eq. 4-18 and Eq. 4-27, SCR is correlated to biomass throughput, G_B, and water content, w, as shown in Figure 4-14 below.

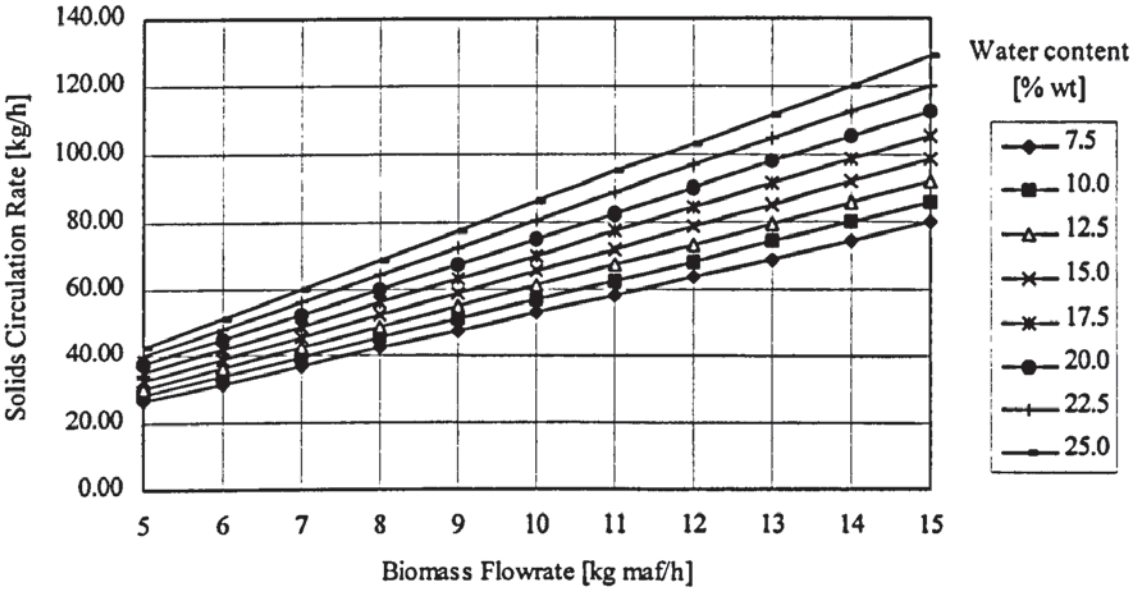

Figure 4-14: The effect of water content on SCR for biomass throughputs in the range 5-15 kg maf/h

As seen from Figure 4-14, a higher biomass throughput will require higher solids circulation rates to meet the energy requirements for the fast pyrolysis process. Moreover, Figure 4-14

shows that wet feedstocks would require higher SCRs than dry ones as expected combining Eq. 4-10 and Eq. 4-27.

In conclusion, it may be claimed that the proposed CFB reactor system meets both the objectives of energy self sufficiency by utilizing the energy content of byproduct char in an integral approach and high heat transfer rates by properly regulating SCR and, hence, adjusting heat carrier:biomass ratio. In this way, process costs as well as complexity (single systems are considered more simple than twin ones, Figure 3-13) are substantially reduced and heat losses greatly minimised.

4.6 CFB reactor sizing procedures

Now that the mass and energy balances for the CFB char combustor and riser have been derived and correlated to input variables, the reactor sizing procedures may be carried out.

This procedure is first carried out for the riser section of the CFB reactor, Section 4.6.1, where the gas/vapor residence time constraints as well as the requirements for the operation of the CFB system in the fast fluidisation regime set up a spectrum of specific reactor sizing requirements. From this follows the sizing of the char combustor, Section 4.6.2, where the special features of the desired hydrodynamics constitute the major factor for the determination of its dimensions.

4.6.1 Riser sizing

One of the most important requirements for the maximisation of pyrolysis liquids has been shown to be the gas/vapor products residence time (VRT). As discussed in Section 2.6.4, prolonged VRTs (>1.5-2 s) at temperatures greater than 500°C may lead to gas/vapor phase reactions and, hence, to reduced yields of organic liquids as depicted in Figures 4-5 and 4-6, Section 4.5.1, as well as from Figures 2-20 and 2-21, Section 2.6.5. Thus, control not only of the gas/vapor phase temperature but also of the gas/vapor residence time is considered essential for biomass fast pyrolysis.

Gas/vapor product residence time, sometimes also called apparent residence time (Graham, 1993), may be calculated using the reactor system operational volume and the total gas/vapor volumetric flowrate, or:

$$t_{res} = \frac{V_R}{\overline{F_g^{tot}}} \qquad \text{(Eq.4-29)}$$

where

t_{res}	gas/vapor product residence time	[s]
$\overline{F_g^{tot}}$	mean gas flowrate including entraining gas and mean pyrolysis product formation rate at actual conditions	[m^3/s]
V_R	reactor operational volume	[m^3]

The effect of the gas/vapor product residence time on the yields of products were studied by Scott and Piskorz (1984) and Peacocke (1994), who showed that the liquid yield rapidly decreased with increasing residence time as shown in Table 4-5. Based on these results, Scott and Piskorz specified residence times of the order of 0.5 s for optimal liquids production at 500°C (in conjuction with small particles <595 μm). This value of t_{res} will be adopted in the following as the reference residence time for optimal pyrolysis liquids production.

Table 4-5: Variation of organic liquid yield with t_{res} at 500°C (Scott and Piskorz, 1984)

Residence time (s)	0.38	0.44	0.54	0.64	0.68	1.07
Organic liquid yield (% wt)	57.5	57.5	53.1	51.7	50.0	45.2

As Peacocke (1994) points out, researchers do not usually describe their methods for calculating the residence time, neither what they consider to be the reactor operational volume, V_R, nor the assumed average molecular weight of the product vapors, which leads to incorrect conclusions or wrong assessment of results. In the following, the reactor operational volume is defined as the reactor volume the organic vapors apparently "see" from the very moment they are first evolved, i. e. from biomass feeding point, to the point where they start to condense, i.e. "first drop out". An estimation of this apparent operational volume is given below.

The term mean gas flowrate, the denominator in Eq. 4-29, accounts not only for the entraining gas but also for formation along the operational reactor volume of both pyrolysis gases and vapors as well as the evolution of steam. To incorporate the gas/vapor products in residence time estimations, their densities must first be calculated according to the following expressions:

$$\rho_v = \frac{M_v P}{RT_R} \quad \text{and} \quad \rho_g = \frac{M_g P}{RT_R}$$

(Eq. 4-30)

where

ρ_v,	pyrolysis vapors density at reactor conditions	[kg/m^3]
ρ_g,	pyrolysis gas density at reactor conditions	[kg/m^3]
M_v, M_g	vapors and gas molecular weights respectively	[kg/kmole]
P	reactor pressure	[N/m^2]
R	universal gas constant (=8314)	[Nm/kmole K]

The gas/vapor yields are then used in conjunction with gas/vapor temperature to calculate the volume of products exiting the reactor per second, i.e. the total gas flowrate. However, it is difficult to assign a molecular weight to different species, since as biomass pyrolysis continues throughout the reactor length, the gas/vapor products continue evolve reacting thermally degrading in the vapor phase, hence causing a gradual reduction in molecular weight over the reactor length (LeLan, 1984; Diebold, 1985; Chang, 1987; Graham,1993).

For the calculation of t_{res} in the present work, the following assumptions are made:

- the gas/vapor product temperature is the same as the reactor temperature (a reasonable assumption, since the CFB operates isothermally, see below)
- organics have an average molecular weight of 100 kg/kmole and obey the ideal gas law (Graham, 1993)
- all non-condensible gas products behave ideally at reactor conditions
- volatiles are evolved linearly over the entire reactor length
- solids recovery system volume, i.e. cyclone volume, including piping comprises 10-15 % of the reactor "operational" volume.

In the following, it should be noted that CFB reactors operate isothermally, since solids are transferred (blown) out of the reactor together with biomass particles. As a consequence, adiabatic quenching of the vapor products, a phenomenon denoting the cooling effect encountered at the freeboard of conventional bubbling fluidised bed systems, as a result of the endothermic gas-phase reactions prevailing (Scott and Piskorz, 1984), is not observed. Thus, the volume of the components downstream of the reactor and prior to the vapors entrance to the liquid recovery section must be taken into consideration when calculating the gas/vapor residence time, t_{res}, in Eq. 4-29. Hence, the residence time discussed in this context

is defined as the time the gas/vapor products reache the liquid recovery system where cooling is applied, without encountering the favourable effect of freeboard cooling occurring in the fluidised bed adiabatic mode of operation. On the other hand, the residence time in CFBs may be more easily adjusted due to the higher gas/vapor velocities that these reactor configurations operate in, compared to bubbling fluidised beds. Reduced residence times may, for example, be achieved by reducing the reactor length, by slightly increasing the entraining gas flowrate or by introducing inert or recycled gas at the upper points of the riser. The loss of the adiabatic quenching advantage, namely the suppression of the undesired secondary reactions, Section 2.4, may be justified by increased turndown flexibility and substantial cost savings as will be discussed below.

Based on the assumption that the volume of the cyclones and piping prior to the vapor condensation section comprises 15 % of the pyrolysis section (riser) volume, and the riser pyrolysis section is a cylindrical conduit, the reactor "operational" volume is given by:

$$V_R = L_R A_R + 0.15 L_R A_R = 1.15 L_R A_R = 1.15 L_R \pi D_R^2 \qquad \text{(Eq. 4-31)}$$

where

L_R	riser length above biomass feeding point	[m]
A_R	riser cross sectional area	[m^2]
D_R	riser diameter	[m]

Furthermore, the mean total gas flowrate is expressed as:

$$\overline{F_g^{tot}} = \overline{u_R} A_R \qquad \text{(Eq. 4-32)}$$

where

$\overline{u_R}$	mean gas/vapor velocity at reactor conditions	[m/s]

Substituting Eq. 4-31 and Eq. 4-32 in Eq. 4-29, an expression relating t_{res} with mean riser velocity is derived, namely:

$$t_{res} = 1.15 \frac{L_R}{\overline{u_R}} \qquad \text{(Eq. 4-33)}$$

Considering now Figure 4-15, i.e. linear evolution of vapor pyrolysis products, an expression for the mean gas/vapor velocity is given by:

$$\overline{u_R} = \frac{u_R(A)+u_R(B)}{2} \qquad \text{(Eq. 4-34)}$$

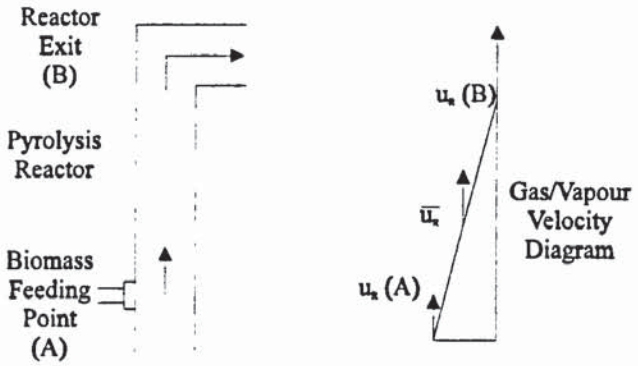

Figure 4-15: Gas/vapor velocities at reactor points A (biomass entrance) and B (pyrolyser exit) respectively

The gas/vapor velocities $u_R(A)$ and $u_R(B)$ at points A (just above biomass feeding point) and B (pyrolysis reactor exit) respectively, Figure 4-15, will be estimated in the following.

In order to estimate the velocities at points A and B, the volumetric flowrates for the various gas/vapor components are needed, shown in Table 4-6. The relative proportions are applicable to pyrolysis at 500°C and biomass moisture content 7.5 % wt (wet basis).

The expression for $u_R(A)$ is given below:

$$u_R(A) = \frac{\sum F_g^{tot}(A)}{A_R} = \frac{4 f_1 f_c G_B \left(\frac{8.80}{\rho_{N2}} + \frac{3.66}{\rho_{CO2}}\right)}{\pi D_R^2} \Rightarrow$$

$$\Rightarrow u_R(A) = \frac{4 f_1 f_c G_B (8.80\rho_{CO2} + 3.66\rho_{N2})}{\pi D_R^2 (\rho_{CO2}\rho_{N2})} \qquad \text{(Eq. 4-35)}$$

Table 4-6: Gas/vapor components volumetric flowrates at points A and B

Gaseous Component	N_2	CO_2	Organic Vapors	Pyrolysis Gas	Steam
Point A	$\frac{8.80 f_1 f_c G_B}{\rho_{N2}}$	$\frac{3.66 f_1 f_c G_B}{\rho_{CO2}}$	———	———	———
Point B	$\frac{8.80 f_1 f_c G_B}{\rho_{N2}}$	$\frac{3.66 f_1 f_c G_B}{\rho_{CO2}}$	$\frac{0.60 G_B}{\rho_v}$	$\frac{0.145 G_B}{\rho_g}$	$\frac{0.180 G_B}{\rho_{st}}$

Similarly and assuming the following values:

- ρ_v=2.3 kg/m^3 (based on a pyrolysis vapors molecular mass of 100 (Reed *et al.*, 1980) and calculated by Eq. (4-28) at T=500°C)
- ρ_g=0.48 kg/m^3 (based on a 27 % CO_2 - 60 % CO-13 % CH_4 gas mixture (Lidén, 1985) at T=500°C)
- ρ_{st}=0.284 kg/m^3 (steam density at 101300 N/m^2 and T=500°C)

for the densities of the various outlet stream components, the expression for $u_R(B)$ is given by:

$$u_R(B)=u_R(A)+\frac{4G_B}{\pi D_R^2}\left(\frac{0.60}{2.3}+\frac{0.145}{0.48}+\frac{0.180}{0.284}\right)\Rightarrow$$

$$\Rightarrow u_R(B)=u_R(A)+\frac{4G_B}{\pi D_R^2}*1.20\Rightarrow u_R(B)=u_R(A)+\frac{4.8G_B}{\pi D_R^2}$$

(Eq. 4-36)

Inserting the values of $u_R(A)$ and $u_R(B)$ from Eq. 4-35 and Eq. 4-36 in Eq. 4-34, an expression for mean gas/vapor velocity which takes into account the rate of formation of pyrolysis gas/vapor product evolution is derived, namely:

$$\overline{u_R}=\frac{u_R(A)+u_R(A)+\frac{4.8G_B}{\pi D_R^2}}{2}=\frac{2u_R(A)}{2}+\frac{4.8G_B}{2\pi D_R^2}\Rightarrow \overline{u_R}=u_R(A)+\frac{2.4G_B}{\pi D_R^2}$$

(Eq. 4-37)

Inserting Eq. 4-37 in Eq. 4-33 and expressing $u_R(A)$ as a function of G_B by means of Eq. 4-35, a simple expression correlating vapor residence time with biomass throughput and reactor dimensions (L_R, D_R) is derived. This expression, which will form the basis for pyrolysis reactor sizing, is given below:

$$t_{res}=\frac{1.15\pi L_R D_R^2}{11.33G_B+2.4G_B}=\frac{1.15\pi}{(11.33+2.4)}\frac{L_R D_R^2}{G_B}\Rightarrow$$

$$\Rightarrow t_{res}=0.263\frac{L_R D_R^2}{G_B}$$

(Eq. 4-38)

while the riser mean gas vapor velocity at reactor conditions is derived by inserting the value of t_{res} from Eq. 4-38 to Eq. 4-33:

$$0.263\frac{L_R D_R^2}{G_B} = 1.15\frac{L_R}{\overline{u_R}} \Rightarrow \overline{u_R} = 4.37\frac{G_B}{D_R^2}$$

(Eq. 4-39)

Eq. 4-38 and Eq. 4-39 constitute the performance equations on which the sizing of the reactor pyrolysis section (riser) will be based. Plotting residence times (t_{res}) versus biomass flowrate (G_B) for various diameters (D_R), considering a constant reactor length (L_R=2.0 m), a graph is obtained, showing the combined effect of reactor size and biomass (feedstock) throughput (G_B) on gas/vapor product residence time (t_{res}). Plotting gas velocity ($\overline{u_R}$) versus biomass throughput for various diameters (D_R) and the same reactor length (L_R=2.0 m) gives a similar graph, for the combined effect of reactor size and biomass throughput on mean gas/vapor velocity at reaction conditions. These two graphs are shown superimposed in Figure 4-16.

The combined graph in Figure 4-16 shows that, for example, in a 5 cm diameter riser (D_R=5 cm), the vapors formed by fast pyrolysis of 10 kg maf/h biomass throughput will have a total VRT of approximately 0.500 s, the mean gas velocity in the riser being approximately 4.7 m/s at actual reactor conditions, i.e. 500°C and atmospheric pressure.

The combined graph of Figure 4-16 provides another important conclusion, namely the fact that the biomass throughput increase has only a slight effect on gas/vapor residence times for narrow risers, while for larger diameter columns variations of up to 300 % may be encountered.

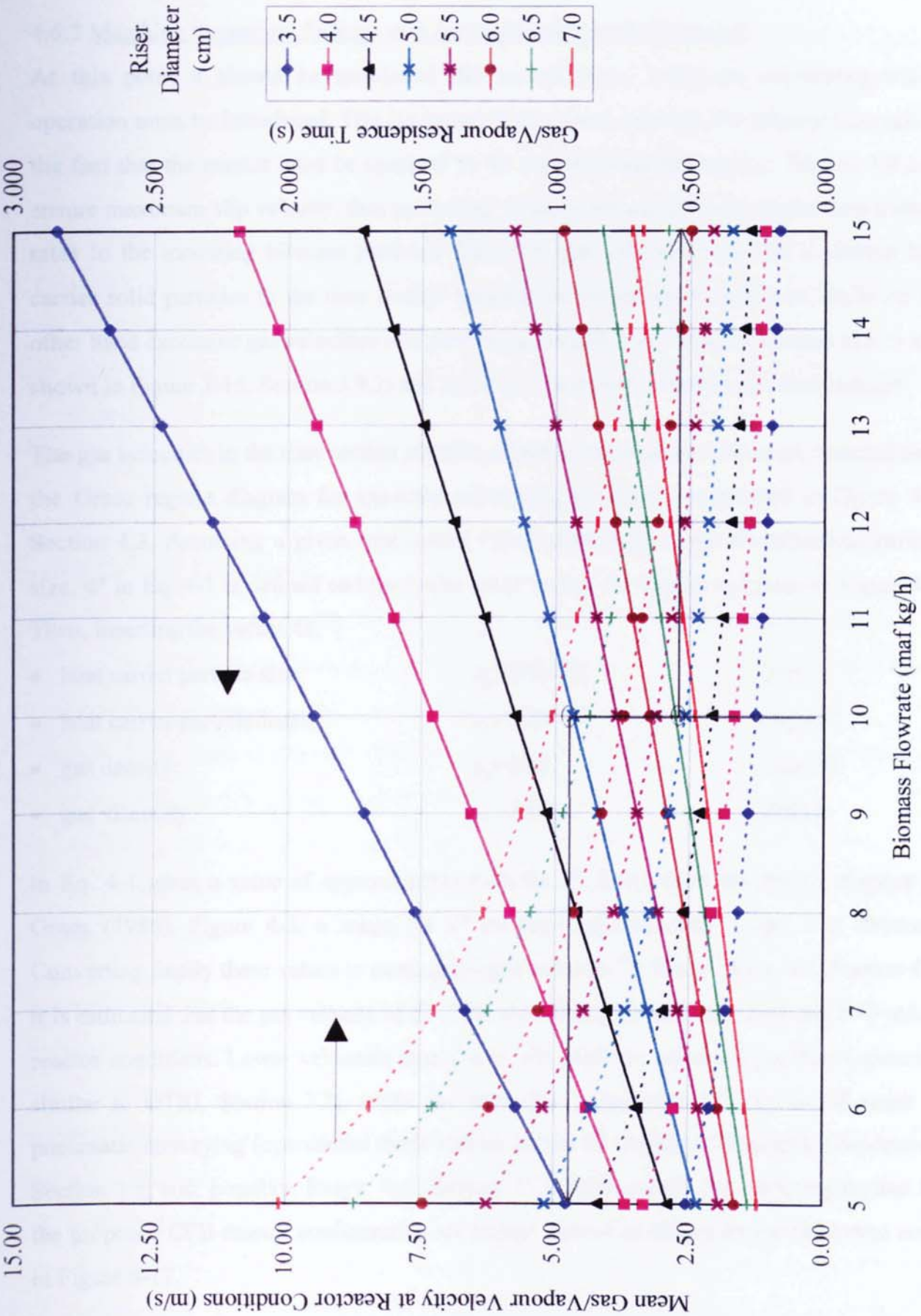

Figure 4-16: Gas velocity and gas/vapor residence time versus biomass throughput as a function of reactor diameter (T=500°C and fixed reactor length, L_R=2.0 m)

4.6.2 Matching theoretical findings with fast fluidisation hydrodynamics

At this point it should be mentioned that an additional constraint concerning reactor operation must be introduced. This limitation is associated with the requirement imposed by the fact that the reactor must be operated in the fast fluidised bed regime, Section 3.9.2, to ensure maximum slip velocity, thus promoting ablation and significantly higher heat transfer rates to the incoming biomass particles. Very low gas velocities will fail to entrain heat carrier solid particles to the riser section resulting in lean-phase suspensions, while on the other hand excessive gas velocities will promote pneumatic conveying (minimum slip as also shown in Figure 3-15, Section 3.9.2) and hence poor suspension-to-biomass heat transfer.

The gas velocities in the riser section must be at least in accordance with those depicted from the Grace regime diagram for gas-solid contacting, previously introduced in Figure 4-3, Section 4.3. Assuming a given heat carrier (sand) particle size, the dimensionless particle size, d^* in Eq. 4-1 is defined and the limits for u^* in Eq. 4-2 clearly specified in Figure 4-3. Thus, inserting the values of:

- heat carrier particle size: $d_p=200 \times 10^{-6}$ [m]
- heat carrier particle density: $\rho_s=2560$ [kg/m^3]
- gas density: $\rho_g=0.52$ [kg/m^3]
- gas viscosity: $\mu_g=3.45$ [Pa s]

in Eq. 4-1 gives a value of approximately 4.40 for d^*. Then, from the regime diagram of Grace (1986), Figure 4-3, a range for u^* between approximately 3 and 8 is obtained. Converting finally these values to mean gas/vapor velocity, by means of Eq. 4-2, Section 4.3, it is estimated that the gas velocity of the CFB reactor must be between 2.04 and 5.43 m/s at reactor conditions. Lower velocities than 2 m/s will result in entrained gas flow (operation similar to GTRI, Section 3.2), while gas velocities higher than 5.5 m/s would result in pneumatic conveying (operational mode similar to that of Occidental Research Corporation, Section 3.5, and, possibly, Ensyn, Inc., Section 3.6). Subsequently the operating regime for the proposed CFB reactor configuration are further limited as shown by the shadowed areas in Figure 4-17.

This means that, for example, in a 5 cm diameter riser (D_R=5 cm), biomass throughputs (G_B) between approximately 4 and 12 kg maf/h can be tolerated, i.e. a turndown ratio of 3:1, the mean gas velocity in the riser lying within the allowable range limits, i.e. between 2 and 5.5

m/s, where the higher slip and hence the higher heat transfer between gas-solids suspension is achieved according to the discussion held in Section 3.7. Varying biomass throughputs will need to be adjusted by an analogous variation of the SCR to match the heat as shown in Figure 4-14, Section 4.5.5.

The above discussion shows that the proposed CFB reactor configuration for biomass fast pyrolysis offers favourable features in terms of heat transfer and energy integration, and it also operates optimally in terms of:

- high turndown, expressed as low sensitivity on biomass throughput for a given reactor diameter, and thus increased operational flexibility, and
- high specific throughput (defined as the ratio of biomass throughput per unit reactor area), which leads in turn in maximum feedstock utilisation and substantial cost savings.

4.6.3 Char combustor sizing

The combustion chamber of the CFB reactor should satisfy the following requirements:

- provide sufficient residence time of char particles to ensure complete char conversion, i.e. complete oxidation of solids biomass char to inert CO_2
- provide complete combustion of oxygen to avoid breakthrough in the pyrolysis zone in the riser section and hence unnecessary volatile products cracking
- ensure operation of the bubbling bed in a mode which will ensure constant blowout of the solids heat carrier for the provision of a dense suspension to satisfy the high heat transfer rate requirement in the riser section.

In order to satisfy the two first requirements, a suitable kinetic model for the oxidation of char by means of atmospheric air is needed. Unfortunately, such a detailed model for woodchar combustion could not be found in the relevant literature and a theoretical approach had to be adopted instead. In the following discussion, the theory developed by Nilsson (1990) will be adopted. This theory is based on the following assumptions:

- char combustion is isothermal
- all oxygen is consumed forming carbon dioxide with char (Ross and Davidson, 1979)
- the temperature difference between particles and gas in the emulsion phase is neglected
- biomass char is much more reactive than carbon char (Rensfelt *et al.*, 1978).

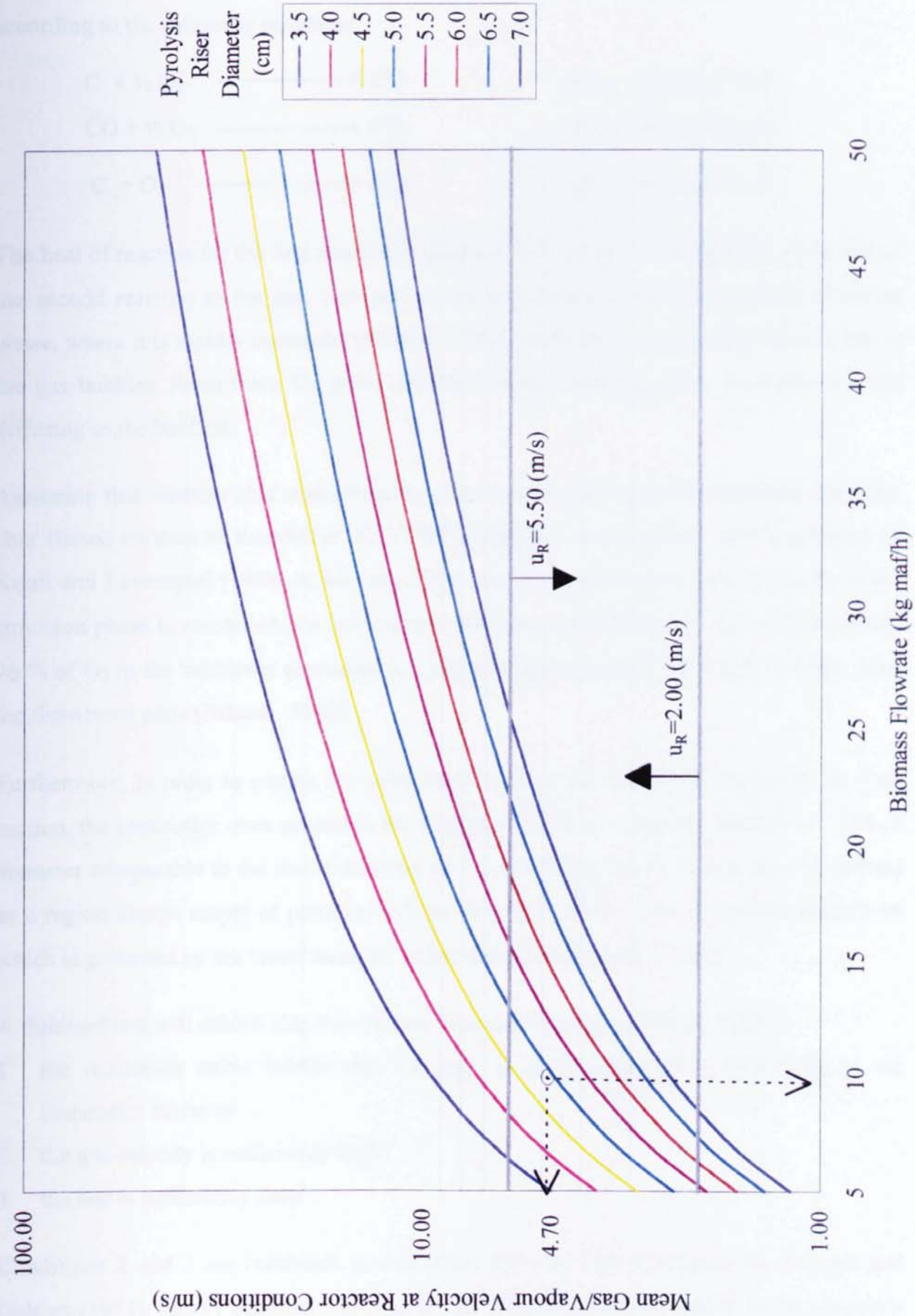

Figure 4-17: Reactor operability for various diameters (moisture content 7.5 % wt on a maf basis and L_R=2.0 m)

Furthermore, in Ross and Davidson's (1979) model, it is assumed that char is combusted according to the following equations:

$C + \frac{1}{2} O_2$	$\longrightarrow$ CO	$-\Delta H_{r1} = 110.68$ kJ/mole
$CO + \frac{1}{2} O_2$	$\longrightarrow$ CO_2	$-\Delta H_{r2} = 282.24$ kJ/mole
$C + O_2$	$\longrightarrow$ CO_2	$-\Delta H_c = 392.92$ kJ/mole

The heat of reaction for the first reaction is assumed to be given to the particles, while that of the second reaction to the gas. One part of the incoming O_2 flows through the emulsion phase, where it is rapidly consumed (Nilsson, 1990), while the rest passes through the bed in the gas bubbles. From there, O_2 partly diffuses into the emulsion phase or reacts with CO diffusing in the bubbles.

Assuming that biomass char reacts with O_2 at least two orders of magnitude faster than coal char (based on data of Rensfelt *et al.*, 1978) and using a three-phase model developed by Kunii and Levenspiel (1969), it was calculated that for stoichiometric conditions, O_2 in the emulsion phase is consumed in a very narrow zone over the distributor, while approximately 96 % of O_2 in the bubbles is consumed at a distance approximately 13 % of bed height from the distributor plate (Nilsson, 1990).

Furthermore, in order to entrain the solid particles from the combustor system to the riser section, the combustor must operate in the slugging bed mode. Slugs are bubbles or voids of diameter comparable to the inside diameter of the containing vessel. A slug may be defined as a region almost empty of particles and not densely packed, shape, the rising velocity of which is governed by the vessel diameter rather than by the bubble volume.

A fluidised bed will exhibit slug flow if three conditions are met (Geldart, 1986):

1. the maximum stable bubble size, $(d_{eq})_{max}$, is greater than $0.6D_B$ where D_B is the combustor diameter
2. the gas velocity is sufficiently high
3. the bed is sufficiently deep.

Conditions 2 and 3 are combined in a criterion for slug flow developed by Baeyens and Geldart (1974), simply claiming that in order for a fluidised bed to operate in the slug flow regime, the superficial gas velocity, u_o, must exceed the minimum slugging velocity, u_{ms}:

$$u_{ms} = u_{mf} + 1.6\text{x}10^{-3}(60D_B^{0.175} - H_{mf})^2 + 0.007\sqrt{(gD_B)}$$

(Eq. 4-40)

where

u_{ms}	the minimum slugging velocity	[cm/s]
u_{mf}	the minimum fluidisation velocity	[cm/s]
D_B	bed diameter	[cm]
H_{mf}	height of bed at minimum fluidisation	[cm]

(Note that the above equation is given in c.g.s. units.)

Given that u_{mf} = 3.5 cm/s (determined experimentally - Appendix 2) and assuming that D_B = 20 cm, H_{mf} = 30 cm, a value of u_{ms} higher than 14.5 cm/s Eq. 4-40, must be considered.

A simple relationship relating operational (slugging) bed velocity, u_C, to biomass input, G_B, and bed diameter, D_B, similar to that obtained for operational riser velocity, u_R in Eq. 4-39 may now be obtained :

$$u_C \geq u_{ms} = \frac{4G_{g,air}^{in}/\rho_{air(T_c)}}{\pi D_B^2}$$

(Eq. 4-41)

Substituting the mass air flowrate, given as a function of incoming biomass feed, from the stoichiometry of the char oxidation reaction, as derived from Section 4.5.3, the following expression is derived:

$$u_{ms} = \frac{4\text{x}11.46 f_1 f_c G_B}{\pi D_B^2 \rho_{air(T_c)}}$$

(Eq. 4-42)

The values for combustor operating velocities as a function of biomass throughput (G_B) for various combustor geometries (D_B) are further depicted from Figure 4-18. The Geldart (1986) criterion for slugging flow is fulfilled for all velocities exceeding u_{ms}, i.e. greater than approximately 0.145 m/s at actual conditions (T_c=500°C).

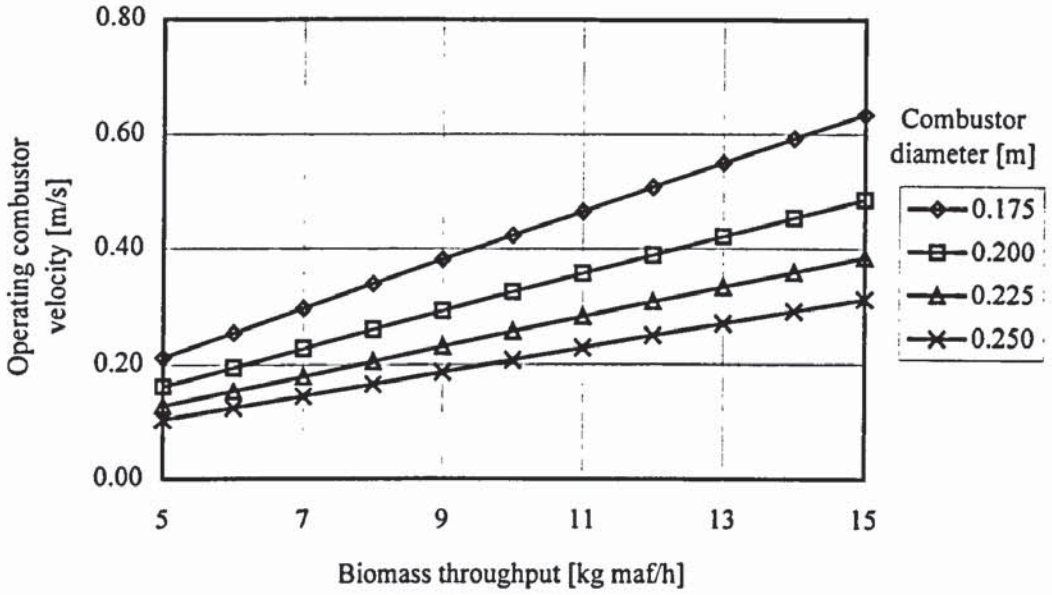

Figure 4-18: Combustor operating velocity versus biomass throughput for different combustor geometries (expressed as D_B variations)

In order to further assure a sufficiently deep bed, so that slugs have an opportunity to form, the third criterion for slug flow should be met, namely that the bed should be sufficiently deep. That is, the bed aspect ratio (height-to-diameter ratio), L_B/D_B, should be sufficiently high. An empirical correlation for L_B/D_B is given by Yagi and Muchi (1952):

$$\frac{L_B}{D_B} \geq 1.9 \frac{1}{(\rho_s d_p)^{0.3}} \qquad \text{(Eq. 4-43)}$$

where

d_p	sand particle diameter	[m]
ρ_s	sand density	[kg/m^3]

Inserting the above values in Eq. 4-43 the correlations, shown in Figure 4-19, between combustor height, L_B, and combustor diameter, D_B, as a function of char particle size, is obtained.

Concluding, it may be claimed that a bed of L_B =0.5 m and D_B =0.175 m would satisfy the hydrodynamic requirements of the proposed CFB reactor, i.e. operation in the slugging regime, for a biomass throughput of 10 kg/h on a maf basis.

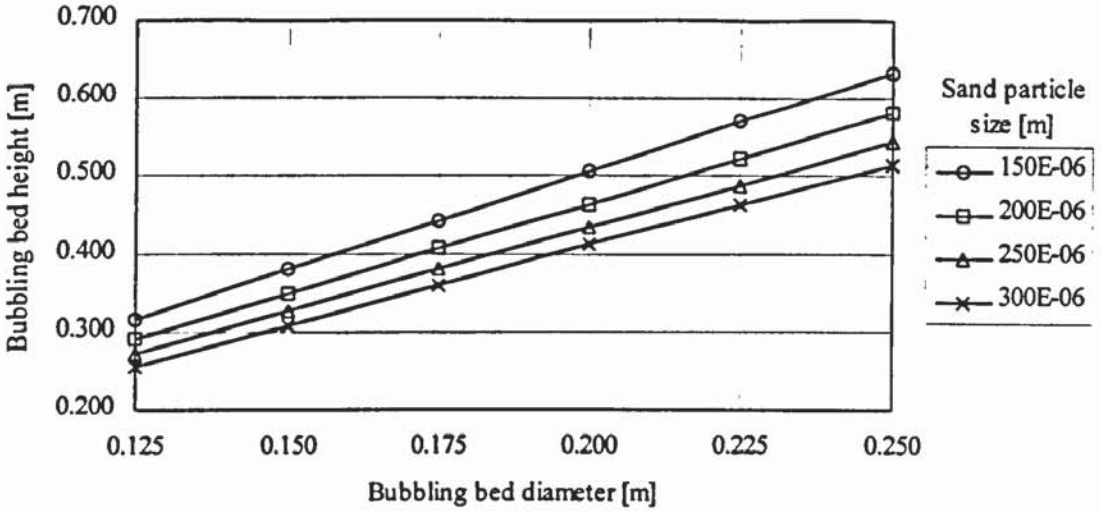

Figure 4-19: Correlation between bed height and diameter as a function of sand particle size to ensure slugging mode operation

Deriving the above relationships, it must be emphasized that reliable biomass char oxidation kinetic models do not exist in the literature, so that extrapolations should be made from charcoal combustion. Thus, the char combustor main dimensions are based on assumed empirical correlations, and it depends on an exhaustive experimental procedure to determine whether these dimensions would achieve a satisfying char conversion. Hence, char combustor dimensions may have to be modified to match actual biomass char oxidation kinetics. In the sizing procedure methodology developed in this thesis, char combustor dimensions were so selected as to satisfy known relationships of gas velocities and hydrodynamic requirements.

4.7 CFB reactor system peripheral components

After the determination of the basic dimensions of the CFB reactor have been set out, the peripheral systems design will be discussed. These systems include the distributor, the solids reinjection system and the solids recovery and separation system.

4.7.1 The gas distributor

The gas distributor to the CFB reactor serves two functions, namely to support the sand bed and distribute the gas (air) equally over the cross sectional area of the bed.

Most small-scale studies in fluidisation use ceramic or sintered metal porous plate distributors, because they have a sufficiently high flow resistance to give a very uniform

distribution of gas across the bed. Although gas-solids contacting is superior with such distributors, they have several drawbacks for larger scale operation:

- high pressure drop leads to increased compressor power requirements, often a major operating cost factor
- low construction strength, hence impractical for large-scale use
- high cost for some materials
- low resistivity against thermal stresses
- possible gradual clogging by fine char and sand particles.

Tuyere and cap designs are commonly used under severe operating conditions such as high temperature or a highly reactive environment. However, because of their complicated construction, such distributors are expensive and inappropriate for small-scale operation.

On the contrary, perforated plate distributors are cheap and easy to fabricate. These may be simple or staggered to prevent solids from raining through the orifices when the gas flow is stopped. Disadvantages of perforated plates distributors may also be listed such as their unpredictable deflection under heavy load and, hence, the required reinforcing for support or gas leaks at the bed perimeter during thermal expansion.

Taking into consideration the above advantages and drawbacks for the different gas distributor types it was concluded that for the even gas distribution in the CFB reactor a perforated gas distributor should be preferred over a sintered plate distributor. The procedure for the design of a perforated plate distributor for the bench scale CFB reactor is further given in Appendix 3.

4.7.2 The solids reinjection system

The requirement to maintain a stable and continuous circulation of solids between the major CFB reactor subsystems, i.e. combustor and riser, rests primarily on the proper design of a system for circulating solids in a reliable and predictable way.

In principle, there have been many approaches and classification of solids circulation loops, extensively reviewed by Kunii and Levenspiel (1991). These configurations range from complex arrangements of the catalyst circulation loops in the early use of Fluid Catalytic Cracking (FCC) reactors, similar to the twin fluid bed reactor configuration as in Figure 3-13(A), to simpler single loop systems, usually incorporated in conventional CFB boilers

extensively used in the power industry, as in the single bed reactor configuration, Figure 3-13(B). In order to keep the design of the proposed system as simple as possible, it was earlier proposed, Section 3.9.3, that a single loop system should be incorporated as a basis for the biomass fast pyrolysis reactor design.

The solids transfer configuration of the CFB reactor consists of a standpipe, to return solids entrained in the riser section to the char combustor, and a device to ensure reinjection and control of solids back to the combustion chamber. The purpose of the standpipe is to transfer solids from a region of low pressure (cyclone dip-leg) to a region of higher pressure (bubbling fluidised bed), while that of the reinjection device is to provide a seal against gas flow in an undesired direction, and regulate the solids circulation rate (SCR).

The reinjection device at the base of the standpipe may be either a mechanical valve (e.g. plug or slide valve) or a non-mechanical arrangement, such as a V-valve, J-valve or L-valve and its primary purpose is to provide a restriction so that the solid material above it forms a dense bed. Maintaining a dense bed in the standpipe keeps the voidage in the downcoming gas-solids suspension as low as possible and allows the maximum pressure build-up in the pipe. A comparison of the main features of the two valve options available for controlling the solids circulation rates as well as for maintaining the dense bed up the standpipe, is shown in Table 4-7, below.

Table 4-7: Comparison between mechanical and non-mechanical valves

Mechanical valves	Non-mechanical valves
1. Valve position regulates SCR	Aeration Gas Flowrate (AGF) regulates SCR
2. ΔP across valve is relatively high	ΔP across valve is relatively low
3. Expensive	Inexpensive
4. Needs careful specifications	Constructed of ordinary pipe and fittings
5. Difficult and costly maintenance	Practically no maintenance is needed
6. Long delivery times associated with purchase or replacement	May be quickly and easily fabricated as well as installed in-house
7. Moving mechanical parts are subject to wear and seizure	No moving mechanical parts

Moreover, a mechanical valve does require some aeration, since solids just above the valve are compacted to form moving beds, which then may unduly restrict the flow of solids. For

smooth and adjustable control of solids flow, adequate aeration should be incorporated into the design of mechanical valves.

As seen from the above, non-mechanical valves offer several advantages over traditional mechanical valves and therefore a non-mechanical valve was considered in order to control the flowrate of particulate solids through it. The three most commonly used types of non-mechanical valves are the L-valve, the J-valve and the reverse seal (Knowlton, 1986), as shown in Figure 4-20. These non-mechanical valves operate on the same principle, the difference between them being their shape, the direction in which they discharge solids, and the distance between the control aeration injection point and the solids discharge point (Zenz and Othmer, 1956).

Figure 4-20: Control of solids flow in non-mechanical valves (Knowlton, 1986)

Among the three different non-mechanical valves types, the L-valve (so named because it is shaped like the letter 'L') was selected as the solids flow control device because its shape is easiest to construct and is slightly more efficient than either the J-valve or the reverse seal in terms of mass flux of solids and pressure drop across the valve (Knowlton and Hirsan, 1977).

4.7.3 Solids recovery system

Gas-solids separation plays an important role in the performance of CFB reactors. Among the different devices used, cyclones are considered the most suitable ones because of the absence of moving parts, simple construction and high efficiency. Cyclones have proven themselves as the most economical, reliable and effective means of recovering suspended solids from process gas streams (Perry and Green, 1984).

However, the operating conditions of cyclones in CFB reactors are to some degree different from those usually encountered in the process industries. The CFB cyclones are subjected to much higher solids concentrations and temperatures. Higher temperatures increase the drag

on the particles due to higher gas viscosities, which in turn decreases the inertial separation of particles (Patterson and Munz, 1989).

The cyclone geometry adopted was that of the high efficiency, reverse flow Lapple-type cyclone design, shown in Figure 4-21. The main design data are expressed in dimensionless forms by dividing the cyclone dimensions by the cyclone diameter. Although a cyclone design procedure for small scale CFB applications could not be found, the cyclone diameter for a high efficiency cyclone can be determined by adopting the following rigorous procedure (Perry and Green, 1984):

- choose an acceptable inlet gas velocity (from relevant literature, e.g. Basu and Fraser, 1991), that will give acceptable gas-solids separation
- calculate gas flowrate, measured at actual conditions
- use the empirical equations, shown in Figure 4-21, to determine cyclone diameter (Swift, 1969).

For a base case of G_B= 10 kg maf biomass/h and w=7.5% wt moisture a= 0.5%wt ash, the total gas flowrate at the riser exit at actual (500°C and atmospheric pressure) conditions is:

$$F_g^{tot} = 42.25 \text{ m}^3/\text{h}$$

where

F_g^{tot} total gas flowrate including combustion gases, air N_2 and pyrolysis condensable vapors + non condensable gases [m^3/h]

To account for thermal expansion a value of 45 m^3/h is chosen.

The relative proportions of the cyclone dimensions are given above in Figure 4-21.

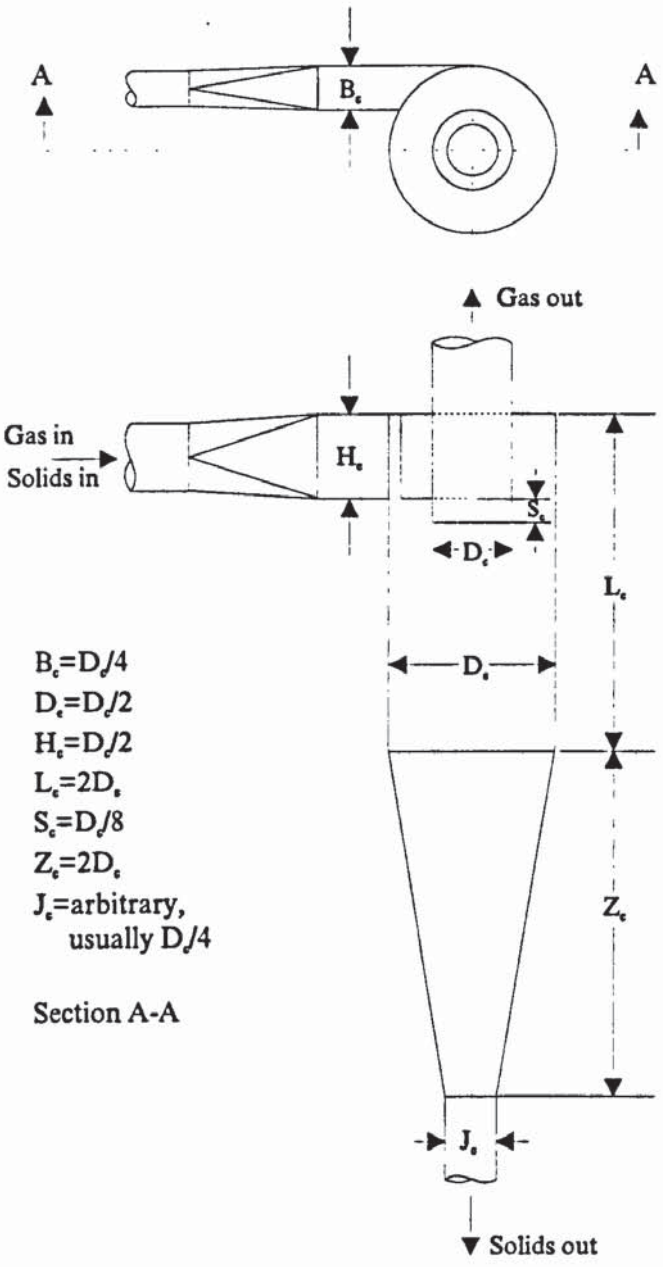

Figure 4-21: Lapple type reverse-flow cyclone proportions

Choosing an inlet gas velocity of 15 m/s (Basu and Fraser, 1991) the area of the rectangular duct (cyclone inlet) can be found as:

$$A_d = \frac{\textit{Total Gas Flowrate}}{\textit{Inlet Gas Velocity}} = \frac{45}{15}\left[\frac{m^3/h}{(3600h/s)\ \mathrm{x}\ (m/s)}\right] \Rightarrow A_d = 8.33\times10^{-4}\ m^2 \Bigg\} \Rightarrow$$

$$A_d = B_{C1}H_{C1} = 0.5D_{C1}\ \mathrm{x}\ 0.25D_{C1} = 0.125D_{C1}^2$$

$$\Rightarrow \quad D_{C1} = \sqrt{\frac{8.33\times10^{-4}}{0.125}} \Rightarrow D_{C1} = 0.082\ m \text{ or } D_C = 82\ \text{cm}$$

(Eq. 4-44)

where

A_d cyclone inlet area [m2]

A cyclone diameter of 84 cm was used. After the cyclone diameter was specified, the various cyclone dimensions are then adjusted accordingly.

Furthermore, it was decided to use a second cyclone in series with the first one, due to the problems listed below:

1. In CFB systems, the reentrainment of solids is a major source of particles escaping through the cyclone. The downward vortex often enters the collection pipe below the cyclone and entrains solids. Particles separated sometimes bounce back into the exiting stream. This phenomenon affects cyclone collection efficiency.
2. Char particles are considerably lighter than the sand, and may be difficult to separate in a single collection stage, being entrained with the gas stream leaving the first cyclone.

In such a configuration, the exhaust gas stream from the first cyclone is fed into the inlet of the second one, the effect of such a series being cumulative: if the first cyclone collects 90 % of, for example, the 20 μm particles from the gas stream, the second cyclone will also collect (at least theoretically) 90 % of the 20 μm particles remaining in the stream exhausted from the first cyclone. This will create a theoretical cumulative collection efficiency of 99 % at 20 μm for the two cyclones in series system.

Moreover, in order to further enhance collection efficiency, the second cyclone diameter was reduced by approximately 30 % (i.e. D_{C2}= 64 cm) and solids captured by second cyclone were directed to the standpipe.

Although this cyclone system configuration (two cyclones in series), with the second cyclone discharging feeding solids directly to the outlet of the first one, proved to be effective in the experiments performed during a cold flow model testing, Chapter 5, its performance proved poor in the actual hot CFB reactor operation as will be discussed in Section 8.4.3.

4.8 Scale of operation and detailed design of the CFB reactor

An important issue worthwhile of further consideration is the actual biomass throughput to the CFB reactor. Too small (<5 kg maf/h) biomass throughputs would require very narrow risers where wall friction phenomena would prevail obscuring the effect of inert heat carrier heat transfer, while higher (>15 kg maf/h) biomass throughputs would require extensive feedstock preparation procedures, which are considered extremely time consuming, as further

discussed in Chapter 6. A moderate value of approximately 10 kg maf/h biomass throughput constitutes an optimal solution for a reactor configuration operating on a realistic scale.

Once the biomass fast pyrolysis CFB reactor components have been specified, and the peripheral systems, i.e. the gas distributor, the solids transfer configuration and the solids separation system, are selected and designed for a 10 kg maf/h biomass throughput, the equipment components are dimensioned and are shown in Appendix 4.

The solids reinjection configuration comprised of a straight standpipe, connected to the first cyclone dipleg and a non-mechanical L-valve, as discussed in Section 4.7.2, while the solids separation system comprised of two high efficiency cyclones in series, as referred to in Section 4.8.

4.9 Conclusions

A novel Circulating Fluidised Bed reactor has been conceived and designed in order to satisfy the requirements of biomass fast pyrolysis. A key feature of the proposed CFB reactor configuration is the autothermal operation provided by char energy content utilisation in an integral char combustor at the base of the fast pyrolysis riser.

The main dimensions of the CFB reactor for biomass fast pyrolysis, based upon a biomass throughput of 10 kg maf/h, are given in Table 4-8.

Table 4-8: Main CFB fast pyrolysis reactor dimensions based on a 10 kg maf/h biomass throughput

Reactor type	CFB	Sections 4.1 to 4.5
Biomass throughput [kg maf/h]	10.0	selected, Section 4.5
Riser height-L_R [m]	2.0	assumed, Section 4.5.1
Riser diameter - D_R [m]	0.05	Eq. 4-38, Eq. 4-39
Combustor diameter - D_B [m]	0.175	assumed, see also Eq. 4-40
Combustor height - L_B [m]	0.50	Eq. 4-41
Solids circulation device	L-valve	Non-mechanical, Section 4.7.2
Solids separation system	2 cyclones	Section 4.7.3

Though the assumptions made and the simplifications introduced, a meaningful CFB sizing procedure was derived and developed. The main uncertainties of this procedure are associated with the proper operation of the char combustor and more specifically:

- the sizing of the char combustor, due to the lack of the proper kinetic model
- the operation of the CFB combustor in the slug flow regime
- the complete consumption of air oxygen in the char combustor.

Another major uncertainty derives from the ability of the proposed CFB reactor configuration to meet the high heat transfer requirements set by the biomass fast pyrolysis reaction.

The proposed CFB design procedure and the underlying assumptions remain to be verified in the subsequent series of experiments, discussed in the remainder of this thesis.

CHAPTER 5: CFB COLD MODEL PERFORMANCE

5.1 Introduction

In Chapter 4 a design methodology for a novel reactor system for biomass fast pyrolysis, comprising a Circulating Fluidised Bed (CFB) with internal char combustion, was presented and a sizing procedure proposed and applied. As a result, the major components of the proposed reactor were identified and their dimensions determined for a biomass throughput of 10 kg maf/h.

It has also been pointed out that the heat transfer between the different sections of the CFB reactor is accomplished by integral char combustion and transfer of hot inert solids by means of a proper solids circulation device, comprising a vertical standpipe and a non-mechanical aeration valve. The proposed heat transfer and the absence of moving parts has minimum impact on system complexity and operability.

Two important issues must be investigated when considering the operability of a CFB system, the first being the influence of hydrodynamics on the performance of the proposed reactor system in terms of the achieved heat transfer rates to the incoming biomass particles. This issue was extensively discussed in Sections 2.7 and 4.3. The second important issue associated with CFB reactor performance is the provision of smooth standpipe operation and controlled solid circulation around the different components of the reactor system. The principles of flow stability in standpipes is discussed in Section 5.2.

Since there was no previous experience on CFB reactor operation, it was decided that a full scale, cold model replica of the proposed CFB reactor should be built and operated, Section 5.3. The cold model construction and testing was justified in order to gain operational experience, examine the hydrodynamics and establish operating regimes and system limitations.

Two series of experiments were conducted in the CFB cold model. During these experiments the main operating variables crucial to the CFB operation and their effect on important operating parameters, associated with heat transfer and solids circulation stability were identified and discussed, Section 5.4.

5.2 Gas-solids flow stability in the standpipe

The poor understanding of the many and different aspects of two-phase gas-solids flow often leads to a variety of problems. In particular, standpipes with non-mechanical valves, despite their conceptual simplicity, usually suffer from instability problems, since the gas-solids suspensions may be transported in several flow-modes, each with its own inherent quirks and peculiarities. The problem is the proper coupling of the different flow modes to achieve a smooth, stable transfer of solids over a wide range of operating conditions.

Gas flowing upwards relative to the solids causes a frictional pressure drop to be generated. The relationship between pressure drop per unit length ($\Delta P/L$) and relative (slip) velocity is determined by the fluidization curve shown in Figure 5-1 and generated usually in a fluidization column when the solids are not flowing (Geldart, 1986). The curve shown is typical for Geldart Type B solids, i.e. solids that fluidise well with vigorous bubbling action and bubbles that grow large (Geldart, 1973).

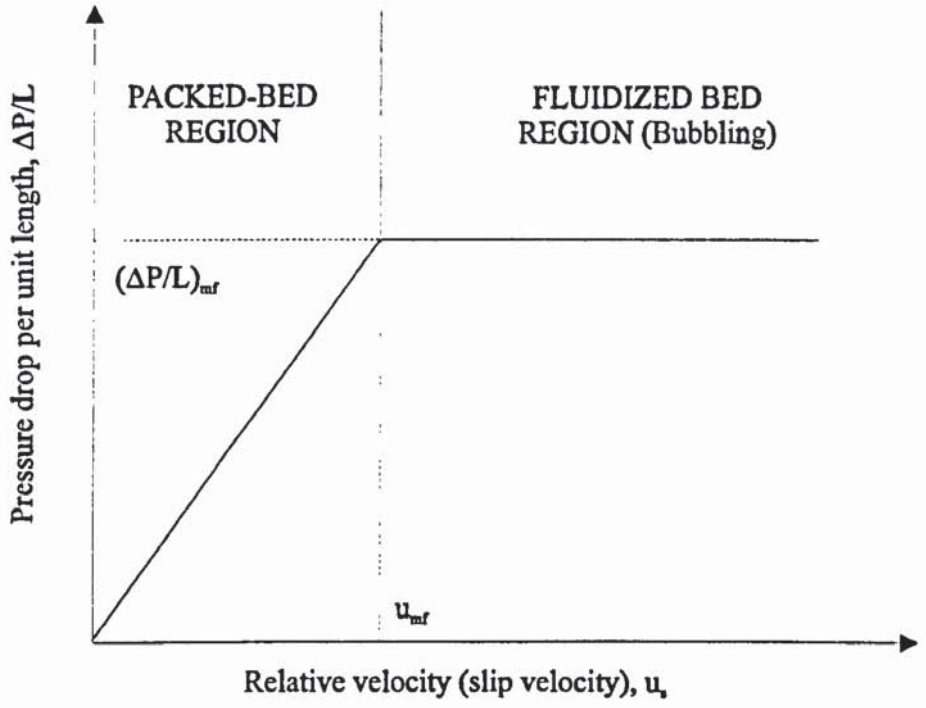

Figure 5-1: Typical fluidization curve for Geldart B solids

Two main modes of solids downflow in standpipes can then be identified, namely fluidised solids flow, in which particles are in suspension, and moving (mobile or packed) bed flow, with relative motion between particles. As seen from Figure 5-1, a moving bed leads to small pressure gradients, whereas a fluidised bed operates at or nearly at minimum fluidizing velocity, results in aerated flow and leads thus to higher pressure gradients. Moreover, in the case of the standpipe flow, the bulk flow of solids is accompanied by an interstitial gas flow.

The flow problems most commonly encountered in two-phase flow standpipes occur in the extremes of the above two modes of flow behaviour, recognized as that of defluidization in the former and poor pressure buildup in the latter case. This is recognised even in industrial standpipes (Matsen, 1986). To understand their occurrence a more detailed discussion follows.

Coarse particles like sand are usually made to move down vertical pipes slowly and in moving bed flow. In this type of flow the movement of gas relative to the solids, characterized by the slip velocity u_r, determines the pressure gradient ($\Delta P_{st}/L$) in the standpipe. While u_r, an interstitial velocity, is kept lower than u_{mf}, a superficial velocity, the gas-solids flow is held in the moving bed regime, thus keeping the voidage in the standpipe as low as possible allowing maximum pressure buildup along the pipe.

From pressure profiles obtained experimentally, it seems that there is a flow of gas up the standpipe (Knowlton and Hirsan, 1977; Knowlton and Hirsan, 1980). However, as shown by Knowlton (1986), a decrease in pressure drop from bottom to top of the standpipe will also be obtained if the velocity of the gas relative to the particles (slip velocity) is upwards, which means that the solids are transferred against a pressure gradient. This can be accomplished if gas flows upwards relative to solids flowing downwards. The definition of slip velocity, u_r, is schematically shown in Figure 5-2.

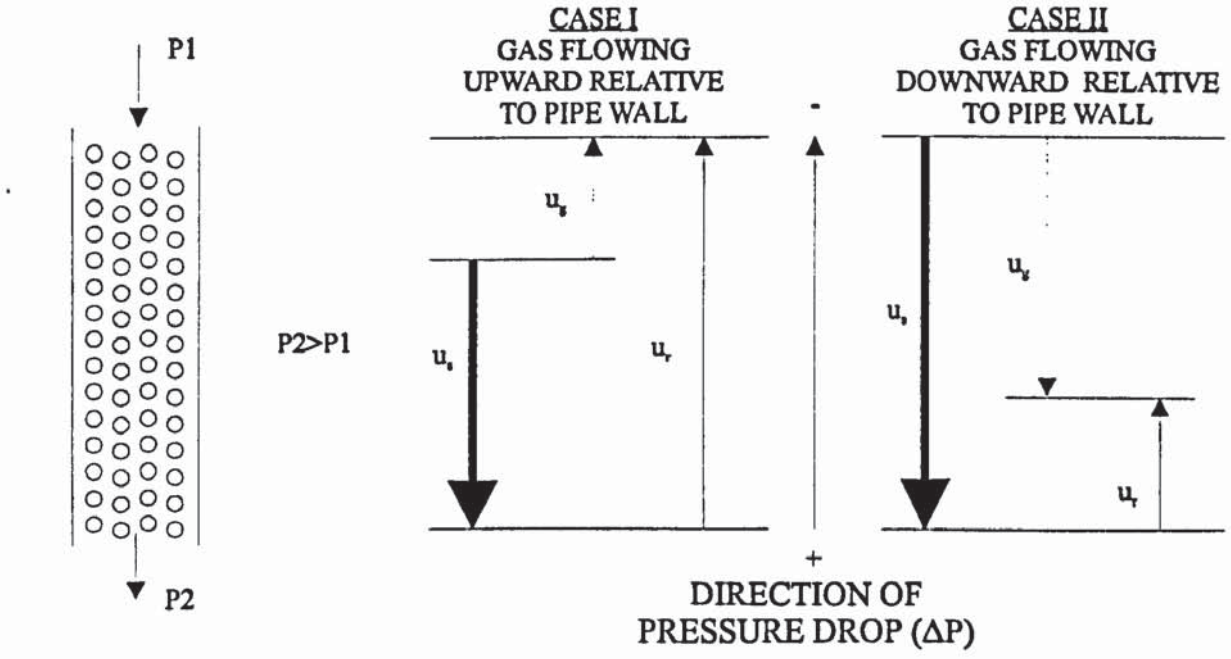

Figure 5-2: Schematic representation of gas flow down and up relative to standpipe wall

The relative gas-solids velocity (also called slip velocity, u_r) is furthermore defined mathematically as:

$$u_r = |u_s - u_g|$$

(Eq. 5-1)

where

u_r	numerical value of slip (relative) gas-solids velocity	[m/s]
u_s	solids velocity in the standpipe	[m/s]
u_g	interstitial gas velocity in the standpipe	[m/s]

Given that for standpipe flow the positive reference direction is downwards, i.e. the direction solids are flowing, the slip (relative) velocity in CASE I, Figure 5-2, is equal to the sum of the solids velocity and the gas velocity, according to Eq. 5-1:

$$|u_r| = u_s - (-u_g) \Rightarrow |u_r| = u_s + u_g$$

(Eq. 5-2)

whereas the slip velocity in CASE II, Figure 5-2, is equal to the difference between the solids and gas velocity, according to Eq. 5-1:

$$|u_r| = u_s - u_g$$

(Eq. 5-3)

In this case (CASE II) the gas carried down the standpipe with the solids is traveling downwards relative to the wall, i.e. in the same direction as the particles, at a velocity u_g, but upwards relative to an observer on the particles, since gas is moving more slowly than the particles. In both cases the solids are being transferred downwards in a standpipe from a pressure P_1 to a higher pressure P_2 regardless of the direction of gas flow as long as the relative gas solids velocity is directed upwards. The above analysis show the principles for standpipe flow, namely the transfer of solids from a region of lower to a region of higher pressure.

The slip velocity at which the ΔP generated is equal to the weight of solids per unit area is called the interstitial minimum fluidization velocity ($u_{r,mf}$) and is often referred to as the fluidised bed density, $(\Delta P/L)_{mf}$, Figure 5-1. Operation of the standpipe at the packed bed region, i.e. at u_r values below $u_{r,mf}$, would lead in a reduced pressure gradient in the standpipe and consequently by low circulation rates around the CFB reactor loop. The low SCRs may result in low heat transfer in the riser section and hence reduced heat transfer rates to biomass pyrolysing particles. Increases in u_r above $u_{r,mf}$ do not lead in turn to further

increase in pressure gradient in the standpipe ($\Delta P_{st}/L$), and hence to increased SCR and high heat transfer rates to the riser section, since any increase in gas flow in excess of that required going into formation of bubbles and hence leaner gas-solids suspension. This phenomenon would consequently lead to poor pressure build-up, decreased SCRs and subsequent flow instabilities in the standpipe.

The above discussion shows that as far as the operation of a non-mechanical L-valve in order to transfer and control solids circulation rates in the proposed CFB reactor configuration is concerned, it should be kept in mind that aeration should be kept at an optimum value in order to avoid instabilities deriving from poor pressure build-up on one hand (instabilities in the standpipe) and low SCR (poor heat transfer) on the other.

5.3 CFB cold flow model and experimental procedures

When operating a Circulating Fluidised Bed (CFB) reactor it is important to characterise riser density, solids circulation along the reactor loop and subsequent standpipe stability. More specifically:

- The importance of the CFB riser voidage, characterised by the riser suspension density along the riser section, and its impacts on reactor performance as a biomass fast pyrolyser in terms of increased heat transfer coefficients has already been pointed out in Section 4.4.
- The establishment of some key relationships between operating parameters and define the flow regimes for smooth reactor operation providing also for standpipe stability, as discussed in Section 5.2, is also of major concern to the operation of the CFB bimass fast pyrolysis reactor.

In order to satisfy the above needs and since there existed no practical experience in CFB operation, it was decided that a CFB cold model of similar dimensions to the original pyrolyser should be constructed and tested. In this way, experimental data on the interaction would be obtained in order to evaluate the influence of important operating parameters such as initial bed inventory and fluidizing gas flowrates on CFB riser density and standpipe stability. In the following sections the cold model design considerations, the methodology followed and the experimental results as well as the important conclusions drawn from CFB cold model operation are discussed in detail.

5.3.1 CFB cold model design considerations

The necessary measurements for determination of hydrodynamic characteristics were conducted on the cold model CFB unit, constructed specifically for this work. The construction of this unit and the accompanying instrumentation are described below.

The CFB cold flow model was built of similar dimensions to the hot unit and made transparent to permit observation of the flow phenomena. The CFB cold model, shown in Figure 5-3, comprised of four sections, namely:

- a dense bed of 172 mm internal diameter (i.d.) and 500 mm long (the combustion chamber), operating in the bubbling/slugging mode, according to the requirements discussed in Section 4.6.3. Solids are entrained through a conical section by the gas (air) into the riser section
- a high velocity riser, of 50 mm ID and 2500 mm long
- a solids separation system, consisting of a single cyclone
- a solids reinjection system, comprising of a long (3000 mm), narrow standpipe, of 25 mm i.d., and a non-mechanical valve (L-valve) serving to aerate the standpipe and return the separated solids to the dense bed.

Two series of experiments were held with the above CFB cold model configuration, the objectives being:

- to get acquainted with CFB operation
- to obtain preliminary data on the interaction of Initial Bed Inventory (IBI) and Fluidizing Gas Flowrate (FGF) on riser average voidage, which was investigated during the first series of experiments, and
- to derive detailed correlations for IBI and FGF, defining the desired operating regimes
- to evaluate the achieved Solids Circulation Rate (SCR) values along the CFB loop
- to determine the operating parameters for standpipe stability.

The last three issues were investigated during the second series of experiments in the CFB cold model configuration.

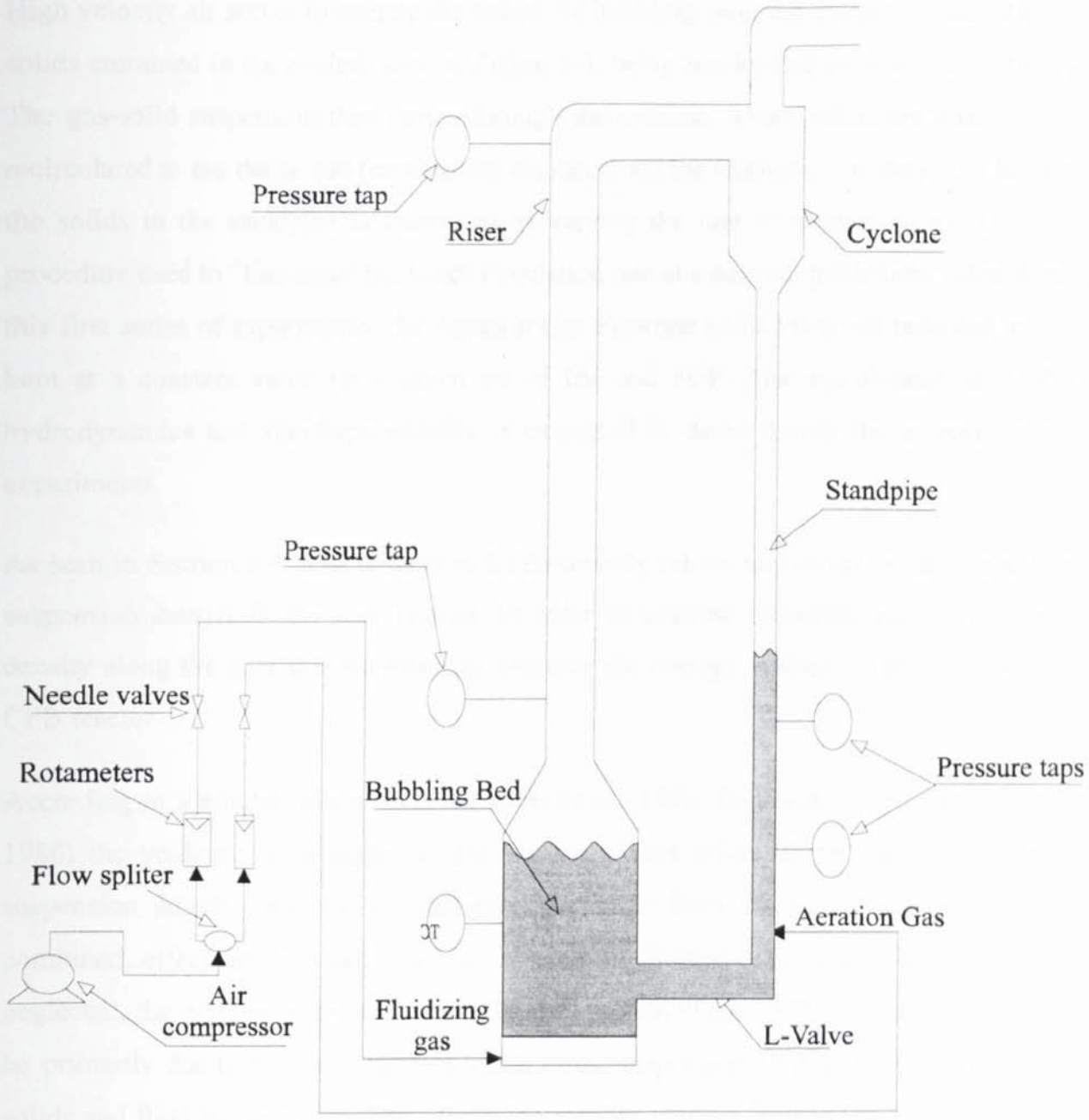

Figure 5-3: The CFB cold model (shown not in scale)

5.3.2 First series of experiments - Preliminary results

Under steady operating conditions, the CFB unit typically operates as follows:

Inert solids (silica sand) are placed in the bubbling bed. In this first series of experiments the amount of solids is measured by reaching a certain height in the bubbling bed. The amount of solids present is called thereafter the Initial Bed Inventory (IBI). These solids are then fluidised by a given amount of fluidizing air, called thereafter the Fluidizing Gas Flowrate (FGF). During operation, air is passed through the bed via the windbox and the gas distributor and the bed expands.

High velocity air serves to operate the bed at the bubbling/slugging mode of fluidization, the solids entrained in the conical section, Figure 5-3, being accelerated and carried up the riser. The gas-solid suspension then passes through the cyclone, where solids are recovered and recirculated to the dense bed (combustion chamber) via the reinjection system. The height of the solids in the standpipe is controlled by varying the rate of aeration to the L-valve, a procedure used to "fine-tune" the solids circulation rate at a desired, predefined value. During this first series of experiments, the Aeration Gas Flowrate (AGF) was not recorded and was kept at a constant value for a given set of IBI and FGF. The significance of AGF on hydrodynamics and standpipe stability is examined in detail during the second series of experiments.

As seen in Section 4.4, heat transfer in CFBs directly relates to average voidage and hence suspension density in the riser section. In order to evaluate quantitatively the suspension density along the riser it is necessary to estimate the average voidage in this section of the CFB reactor.

According to a number of researchers (Arena *et al.*, 1986; Han *et al.*, 1985; Kojima *et al.*, 1986) the voidage, i.e. average volume fraction of the solids in the riser and hence the suspension density, may be conveniently calculated from the pressure gradient. If the combined effect of gas-wall friction, solids-wall friction and solids acceleration are neglected, the pressure measured across the riser section of the CFB riser section is taken to be primarily due to the static head of solids in the suspension, that is, to the weight of the solids and fluid per unit area. This allows the average voidage between two pressure taps to be calculated. The assumption made is that:

$$\Delta P = (\rho_s - \rho_g) \times g \times (1 - \varepsilon) \times \Delta z \qquad \text{(Eq. 5-4)}$$

where

ΔP	pressure drop along the riser section	[N/m^2]
ρ_s	solids (sand) density	[kg/m^3]
ρ_g	gas density	[kg/Nm^3]
g	acceleration due to gravity (=9.81)	[m/s^2]
ε	voidage	[-]
Δz	distance between pressure measurements	[m]

The suspension density in the riser section, is then directly correlated to the voidage by the following relationship:

$$\rho_{susp} = (1 - \varepsilon_{avg}) \times (\rho_s - \rho_g) \qquad \text{(Eq. 5-5)}$$

where

ρ_{susp}	suspended solids density	[kg/m^3]

In order to measure static pressures at different points along the length of the riser and the standpipe, access ports/pressure taps, shown in Figure 5-5, were located at regular intervals along the system. Pressure taps are connected to U-tube water manometers and to the pressure monitoring system by flexible tubes. In order to keep the air passage clear of particles, a small amount of glass wool is inserted in the tubes. Each pressure tap is screwed on to a nut permanently fixed to the riser wall.

During this first series of experiments, riser pressure profiles were determined using the pressure taps located at 400 mm increments along the riser length. Any of these taps could be connected to the pressure monitoring system, which consists of a cyclic scanner, linked to a pressure transducer, subsequently converting the pneumatic to electrical signals shown as outputs (mm H_2O) on the transducer LCD screen. In this way, the gauge pressure of every point can be determined and the differential pressures (ΔP) between any two adjacent points can be measured to generate the riser pressure profile.

However, a number of problems was encountered during these measurements, the most important being:

- the pressure measurements, based on manometer observations, proved very difficult and uncertain, since severe pressure fluctuations in the riser section were noticed
- the transducer used had a slow response (of the order of 15-18 s), which resulted in longer than expected time intervals between two subsequent measurements, so that a pressure loop along the whole system for a given moment could not be generated
- another very important parameter, the solids circulation rate, could not be evaluated since the standpipe operation was very unstable, due to severe electrostatic effects and standpipe operational instabilities.

Despite these problems, experiments were carried out in order to obtain mean pressure drops in the CFB riser section, by varying the two most important process parameters, namely the

static height of solids in the bubbling bed, H_o (denoting changes in IBI) and the superficial gas velocity of air approaching empty riser, u_{or}, (denoting changes in FGF). Pressure drop measurements were estimated by evaluating the water manometer indications and correlating them with mean pressure transducer response. The variation of the operating parameters dring the second series of experiments is summarized in Table 5-1 below.

Table 5-1: Variation of the operating parameters (IBI, FGF and AGF) during the first series of experiments in the CFB cold model

IBI (H_o in m)	0.245	0.310	0.335
FGF (Nm^3/h)	21, 26, 28, 31	21, 26, 28	21, 26, 28
AGF (Nlit/min)	kept constant for a given set of IBI and FGF		

Inserting the experimentally derived pressure drop data, evaluated and correlated as above, in Eq. 5-4 and Eq. 5-5, voidage and suspension density correlations for different IBIs (H_o) and FGFs (u_{or}), are obtained. The average riser voidage is derived, from the riser pressure drop, Eq. 5-4. As shown in Figure 5-4, a lower voidage, i.e. a denser riser, can be achieved for a given FGF by varying IBI, adjusting the sand height to a higher level, H_o.

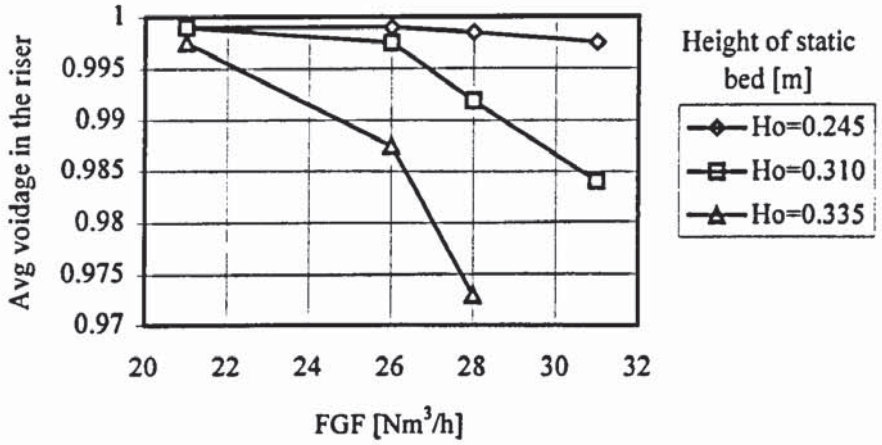

Figure 5-4: Average riser voidage versus FGF for different IBIs

Subsequently, the average suspension density in the riser is derived applying Eq. 5-5. The results are shown in Figure 5-5, clearly indicating that a denser suspension, and hence a higher heat transfer rate, as already discussed in Section 4.4, can be achieved for higher total solids charging (higher H_o) for the same fluidising gas flowrate (FGF).

It may further be expected that higher suspension densities would promote higher heat transfer rates to the pyrolysis section of the CFB reactor analogously with the experimental

findings of other researchers, as discussed in Section 4.4. Thus, it may be concluded that the performance of the CFB reactor as a biomass fast pyrolyser is greatly dependent on riser density profile, which in turn is mainly determined by IBI (H_0) and FGF (u_{or}).

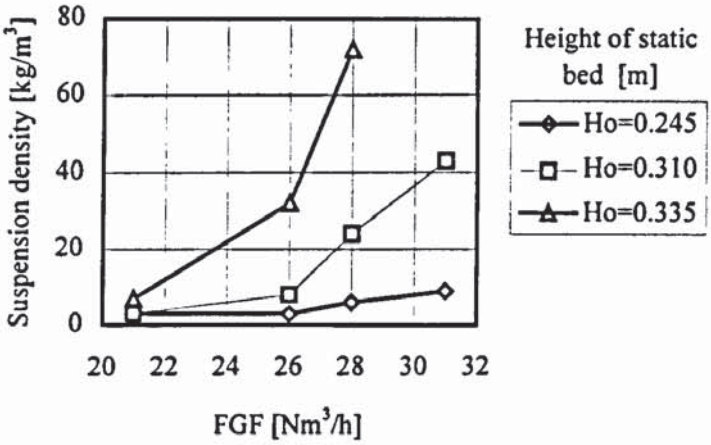

Figure 5-5: Suspension density versus FGF for different IBIs

From this first series of experiments in the cold model it can be concluded that IBI and FGF have a pronounced effect on the macroscopic structure of the gas-solids suspension, characterized by suspension density/voidage in the riser section of the CFB. More specifically, it was shown that higher riser suspension densities are obtained at higher solids inventories for a given gas velocity

Despite these initial findings, important issues like a more reliable riser density profile characterization, and the role of the non-mechanical valve operation in both standpipe stability and control of SCR required futrher experimental investigation, which was undertaken during the second series of experiments on the cold CFB model.

5.3.3 Second series of experiments

Literature data from similar circulating fluidised bed experimental studies (Arena *et al.*, 1986) indicate that more experimental points are required in order to derive a meaningful correlation between riser voidage and fluidization parameters, expressed as variations in IBI and FGF. However, the subjective estimation of pressure drop variation observations from both the U-tube water manometers and the slow response transducer during the first series of experiments in the CFB cold flow model could not provide a rigorous and accurate acquisition of experimental data.

Thus, it was decided to substitute the slow response pressure transducer, for fast response (0.5 s), differential pressure transmitters (Fischer-Rosemount Model 1151 DP) connected to a data acquisition system to obtain reliable data for the critical pressure drop measurements along the entire CFB loop. The outputs from the transmitters were sent to a Keithley 706 Scanner connected to a Keithley 6½ digits Multimeter. Plug-in modules were used in conjuction with the scanner to allow measurements of specific functions including the electrical signal (4-20 mA) from the pressure transmitters. The data acquisition system was controlled by a PC equipped with a General Purpose Interface Board (GPIB) card through an IEEE-388 protocol and a set of TurboPascal subroutines to simplify the communications and the processing of primary results.

In the first series of experiments, Section 5.3.2, the L-valve Aeration Gas Flowrate (AGF) was not varied, since the major objective was to identify the significance of the major operating parameters ensuring CFB stable operation by setting AGF to a preset value.

In order to characterize the riser solids fraction and standpipe stability in terms of the CFB operating parameters, namely FGF, IBI and AGF, a second series of experiments, discussed below, were conducted. During these experiments two given IBIs and three different values of FGFs were tested, which gave six (2 x 3) experiments. The variation of the operating parameters dring the second series of experiments is summarized in Table 5-2 below.

Table 5-2: Variation of the operating parameters (IBI, FGF and AGF) during the second series of experiments in the CFB cold model

	Low IBI			High IBI		
IBI (kg)	9.5	9.5	9.5	10.5	10.5	10.5
FGF (Nm^3/h)	27.95	32.86	37.33	24.96	28.78	32.86
AGF (Nlit/min)	Varied accordingly, covering the range from 2.5 to 11.5					

During each experiment, AGF is continuously varied, the starting point being that of the appearance of standpipe solids flow (moving packed bed flow mode) and the ending point being that of the appearance of severe flow instabilities (slugging flow mode) in the standpipe. During AGF variations, the pressure drop along the riser as well as the pressure drop in the standpipe are continuously monitored by the pressure transmitters, and sent via the data acquisition system to a PC-based station where they are properly processed.

During these experiments, special care was taken to ensure moving bed or near to minimum fluidization flow mode conditions along the standpipe by observation of the solids flow, as discussed in Section 5.2. The window for the standpipe stable operation proved quite narrow, being bounded by the need to avoid defluidization (moving packed bed flow) on one hand, adversely affecting solids flowrate and pressure head, and lean gas-solid mixture on the other, resulting in poor pressure buildup and inadequate solids circulation in the riser section.

The results from the second series of experiments in the CFB cold flow model are presented in the following section.

5.3.4 Results and discussion from the CFB cold flow model second series of experiments

The average voidage in the riser versus AGF for the low IBI (9.5 kg) and the high IBI (10.5 kg), Table 5-2, and the respective FGFs, are shown in Figures 5-6 and 5-7 respectively.

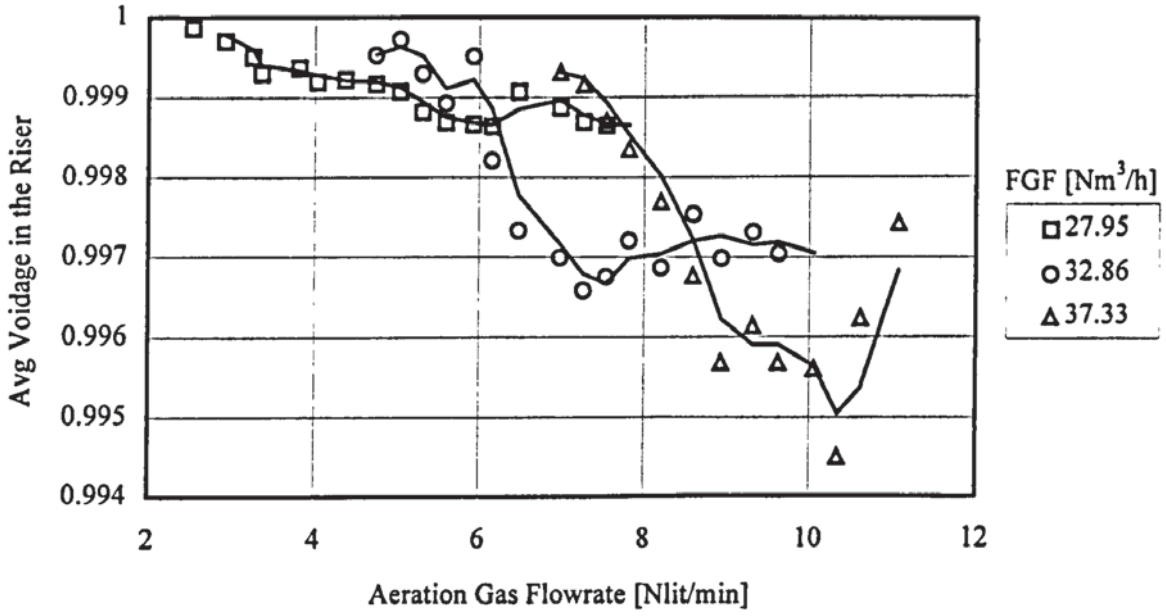

Figure 5-6: Riser average voidage versus AGF for different FGFs (IBI = 9.5 kg)

As seen from Figures 5-6 and 5-7, AGF variations affect the density profile in the riser, the minimum voidage values, i.e. higher suspension densities in the riser, being obtained for the higher FGF values, as expected from the results obtained during the first series of experiments. Thus, given a set of IBI and FGF, it is possible to vary the average voidage profile, and regulate the rate of heat transfer, by simply manipulating AGF.

By examining the family of curves in Figures 5-6 and 5-7 it may also be concluded that the lower voidage values, and hence the higher riser densities, are obtained at lower FGFs for the higher IBI, Table 5-2, which shows the positive effect of an increased IBI in the CFB reactor.

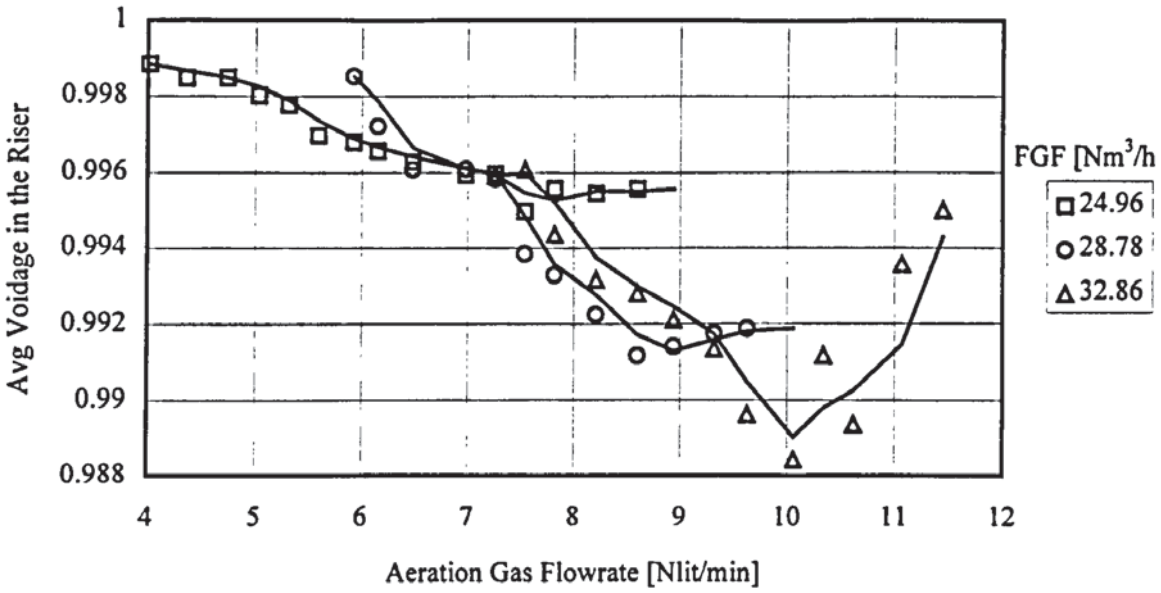

Figure 5-7: Riser average voidage versus AGF for different FGFs (IBI = 10.5 kg)

While AGF has a minor impact at low FGFs, its significance becomes increasingly important at higher FGFs for any given IBI.. The minimum voidage, and hence the denser riser, is obtained up to a certain value of AGF after which the voidage increases again resulting in a leaner riser and hence reduced heat transfer rates. This is attributed to standpipe instabilities at high AGFs as discussed below.

In the following diagram, Figure 5-8, the FGF is kept constant so that the effect of IBI on CFB suspension density is marked, recorded as the average voidage in the riser versus variations in the AGF.

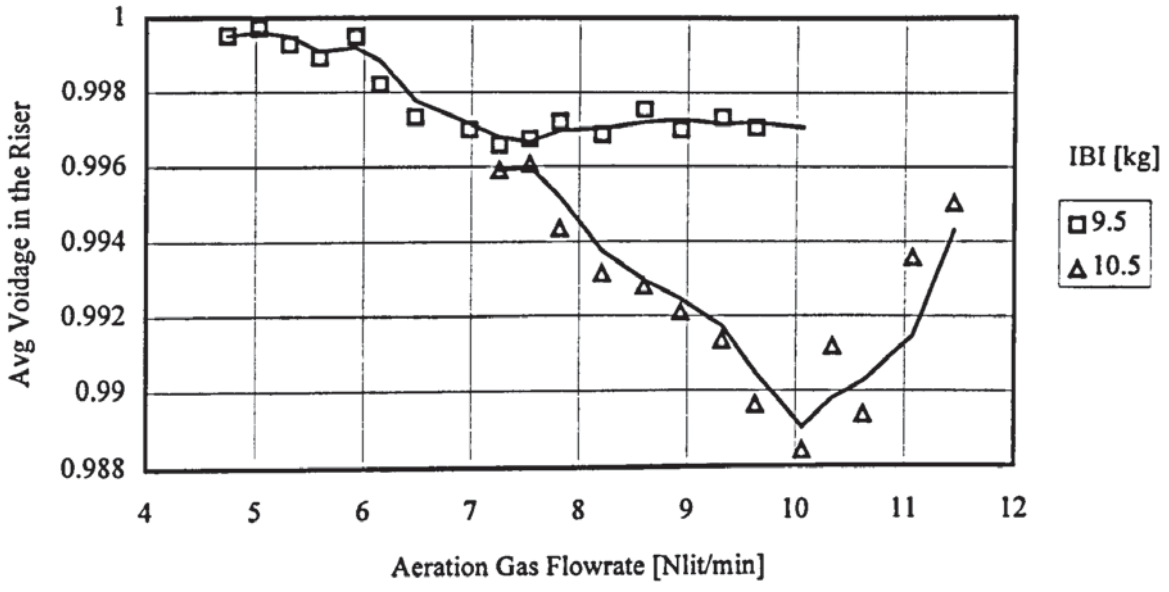

Figure 5-8: Riser average voidage versus AGF for the same FGF and different IBIs.

Comparing the data presented in Figure 5-8, it is clearly illustrated that for a given FGF a denser riser, reduced average riser voidage, is obtained at a higher IBI. It is also shown that at higher IBIs excess AGF is needed to initiate the flow of solids in the standpipe, since the aeration gas encounters a higher backpressure in its passage through the combustor chamber in the case of the higher IBI.

The conclusions drawn by the voidage versus AGF diagrams are summarised as follows:

- a denser riser, i.e. a lower voidage, is obtained for higher FGFs for a given set of IBI and AGF, which is attributed to the increased elutriation of solids from the bubbling bed to the riser section of the CFB reactor
- a denser riser is obtained at higher IBIs at a reduced FGF for a given AGF value
- a denser riser is obtained at increased AGF values for a given set of IBI and FGF up to a certain value of AGF after which the riser density decreases.

The standpipe pressure drop per unit length (standpipe pressure gradient) versus AGF for the low IBI (9.5 kg) and the high IBI (10.5 kg) and the respective FGFs, Table 5-2, are shown in Figures 5-9 and 5-10 respectively.

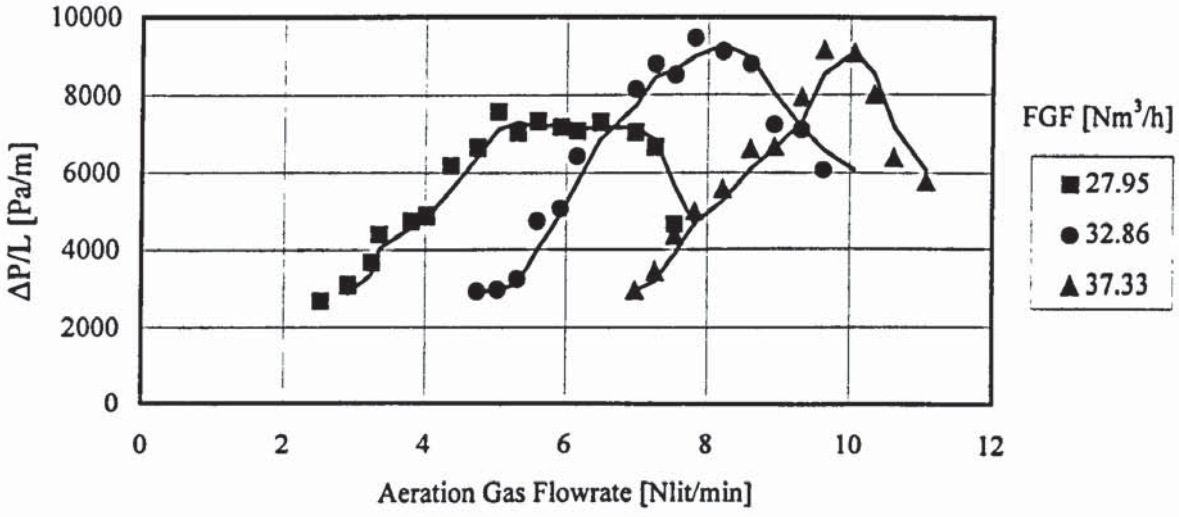

Figure 5-9: Standpipe pressure gradient versus AGF for different FGFs (IBI = 9.5 kg)

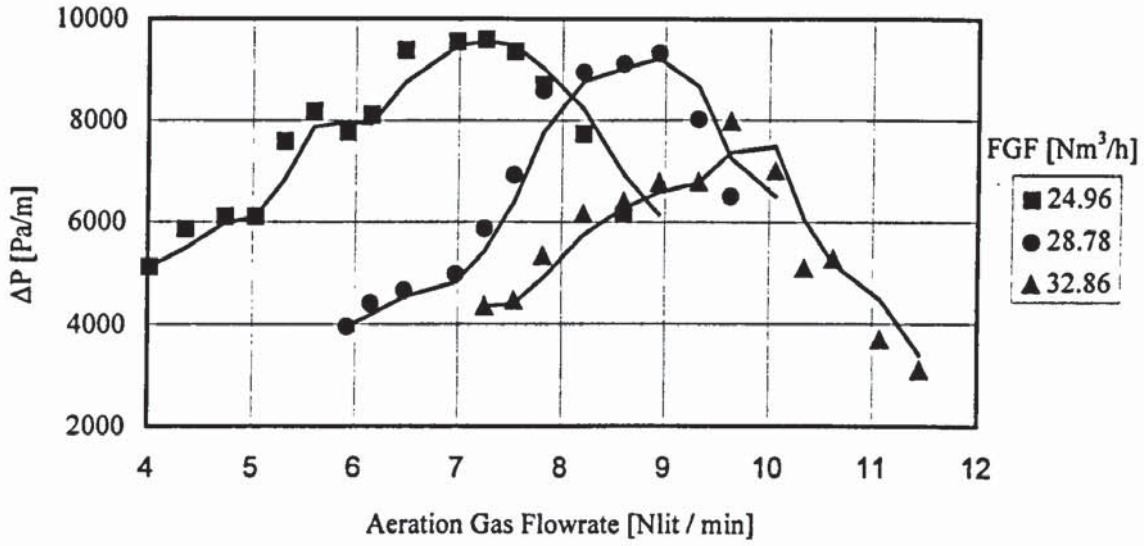

Figure 5-10: Standpipe pressure gradient versus AGF for different FGFs (IBI = 10.5 kg)

Referring now to standpipe stability, and carefully examining Figures 5-9 and 5-10, where the change in ΔP/L as a function of the amount of aeration gas added to the standpipe is plotted, it may be seen that the pressure drop per unit length, taken immediately above the standpipe aeration point, increases up to a certain value and then begins to decrease. The initial increase in ΔP/L causes the solids level in the standpipe to decrease since the total standpipe ΔP must remain constant. Therefore, aerating the standpipe near the bottom has a great effect on decreasing the solids seal height, maintaining the moving solids in the moving bed or near the fluidised bed flow mode, Section 5.2.

The reason for the pressure gradient increase in the standpipe is that the addition of aeration gas increases the relative gas velocity (slip velocity) until the solids become fluidised, as discussed in Section 5.2. After the minimum fluidization point is reached, $u_{r,mf}$ at Figure 5-1, bubbles begin to form causing a decrease in the average density of the standpipe gas-solids suspension. Hence, the ΔP/L in this section corresponds to the fluidised bed density, $(\Delta P/L)_{mf}$, which decreases when bubbles begin to form, as discussed in Section 5.2.

The maximum pressure gradients in all cases presented in Figures 5-9 and 5-10, remain approximately constant, at the range of 9000-10000 [Pa/m], since at these points the fluidised bed density of the sand bed, Section 5.2, has been reached and the highest pressure gradient for the particulate solids used (silica sand) has been attained, as depicted from Figure 5-1. Small increases of AGF beyond this point cause a rapid depletion of solids from the standpipe and result in lean suspensions in this part of the circulation loop. Deviations from

standpipe and result in lean suspensions in this part of the circulation loop. Deviations from this behaviour occur at low IBIs and FGFs on one hand (due to the slowly downmoving gas-solids suspension and, hence, insufficient pressure buildup in the standpipe, Figure 5-9 for low FGF) or high IBIs and FGFs on the other (pressure taps to be found in the freeboard of the rapidly depleted from solids fluidised bed solids column in the standpipe, Figure 5-10 for high FGF)

In the following diagram, Figure 5-11, the effect of IBI variation for the same FGF on the standpipe pressure drop per unit length versus AGF for the two different IBIs is shown.

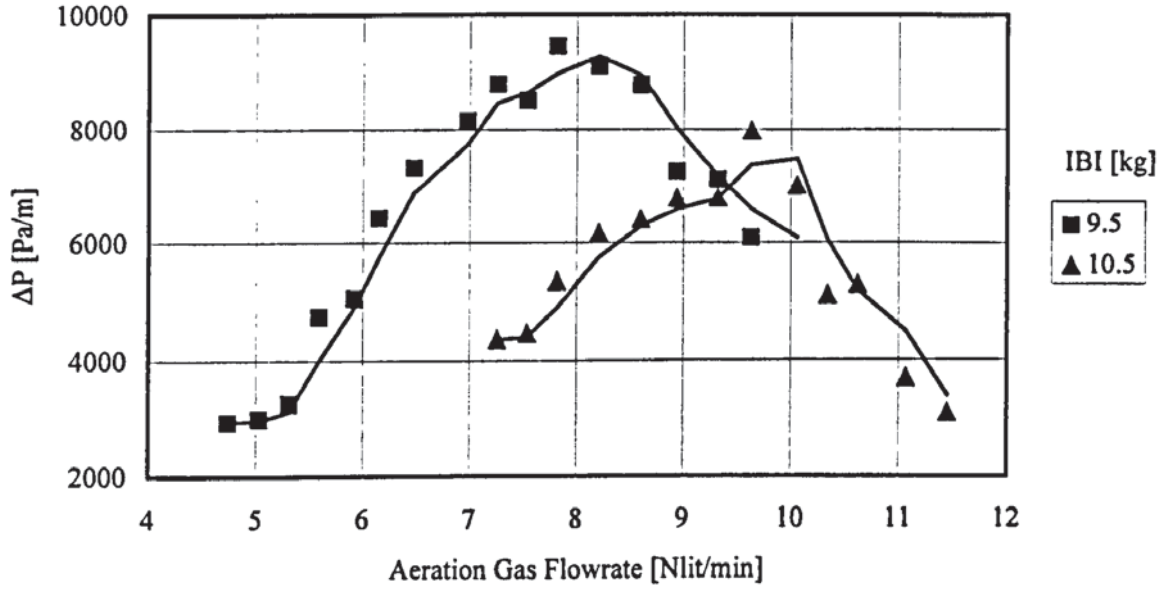

Figure 5-11: Standpipe pressure gradient versus AGF for different IBIs and the same FGF

Comparing the data presented in Figure 5-11 it is clearly illustrated that for a given FGF the standpipe operates in the lean phase once the fluidised bed density is obtained for the particulate solids involved.

The conclusions drawn by the standpipe pressure gradient versus AGF diagrams are summarised as follows:

- a gradual increase in the standpipe pressure gradient is obtained for a given set of IBI and FGF with increasing AGF, up to a certain value corresponding to the downmoving suspension fluidised bed density, after which slugging mode prevails in the standpipe leading to formation of bubbles, lean solids flow and decreased standpipe pressure gradient in the standpipe

- for the higher IBI involved, the fluidised bed density is obtained at higher AGF values, since in this case the aeration gas encounters a higher backpressure in its passage through the bubbling bed than that encountered in the lower IBI case.

The excess aeration in the standpipe results not only in unsteady flow in the standpipe (ΔP/L lower than the fluidised bed density at excess aeration, as shown in Figure 5-1) but also in an increase in riser voidage (and subsequent decrease in suspension density). This is due to the lower solids circulation rates obtained from poor pressure buildup in the standpipe, which is the result of leaner gas-solids suspensions. This phenomenon is illustrated in Figures 5-12 and 5-13 for two different sets of IBIs and FGFs.

These diagrams, Figure 5-12 and Figure 5-13, indicate that excessive aeration and operation of the standpipe in the lean, slugging flow mode of operation results in a leaner riser and hence a decreased suspension density and heat transfer rates in the riser section of the CFB reactor.

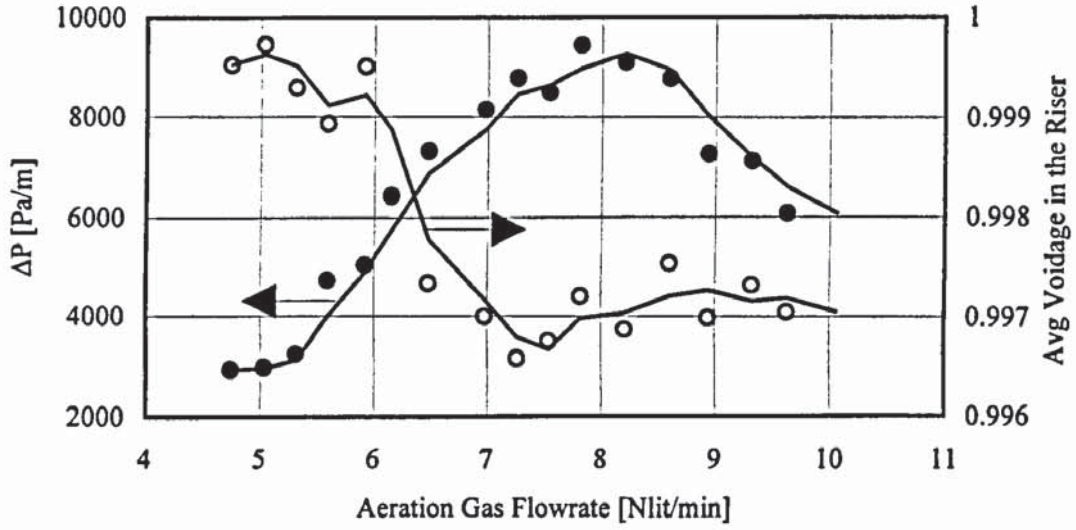

Figure 5-12: Standpipe pressure gradient and average riser voidage for IBI=9.5 kg and FGF=32.86 Nm³/h

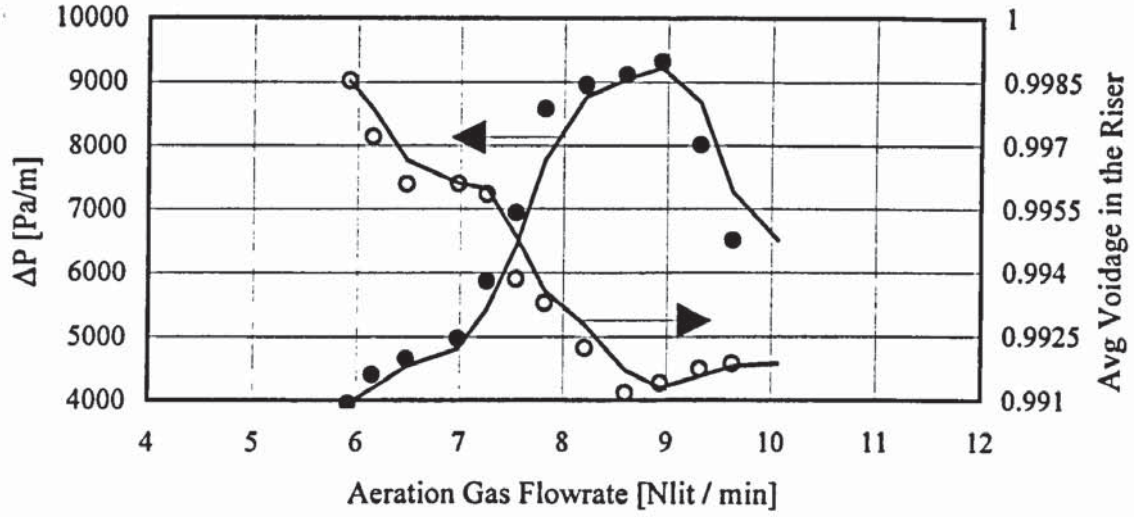

Figure 5-13: Standpipe pressure gradient and average riser voidage for IBI=10.5 kg and FGF=28.78 Nm^3/h

Concluding, it may be claimed that for the optimal operation of the CFB reactor, in terms of suspension density in the riser section and smooth solids circulation, standpipe operation in moving bed or near fluidised bed mode should be ensured for the various combinations of IBIs and FGFs.

5.3.5 Solids circulation rate measurements in the CFB cold model

The solids circulation rates (SCR) were also estimated during this second series of experiments in the CFB cold model, since they constitute an important process variable for the effective utilisation of the CFB reactor as a high heat transfer reactor configuration, Section 4.4. There are a number of different experimental techniques for estimating SCRs (Burkell *et al.*, 1988; Patience and Chaouki, 1990). According to experimental findings discussed in the relevant literature, an ideal measuring technique for SCR measurement should be: on-line, sensitive, non-interfering, capable of operation at elevated temperatures, scale-up possible, reliable, covering a large range of operation and not necessary to calibrate, criteria which is very difficult to satisfy together.

The technique chosen for reasons of simplicity was the flow diversion technique, according to which solids are diverted while descending the standpipe for a measured time interval. At the same time, solids are transferred from the standpipe to the fluidised bed via the L-valve, so that the bubbling bed inventory (IBI) is kept constant. The measurement is interrupted

when the standpipe is depleted of solids. The collected solids are reinjected to the system and a new experiment for SCR determination begins.

An additional sequence of experiments were conducted in order to determine the effects of the operating variables on SCR. More specifically, for a set of two different IBIs and two different FGFs, the SCR is determined as a function of AGF. The variation of the operating parameters is summarized in Table 5-3 below. The SCR is determined by the two-valves technique, described above.

Table 5-3: Second experimental sequence in the CFB-cold model (SCR variations)

IBI (kg)	10	11
FGF (Nm^3/h)	35	25
AGF (Nlit/min)	Varied accordingly	

The SCR versus AGF for the two different sets of IBI and FGF, Table 5-3, is presented in Figure 5-14, denoting that a higher SCR and hence a denser riser may be obtained at much lower FGFs provided there is a high initial bed inventory in the system.

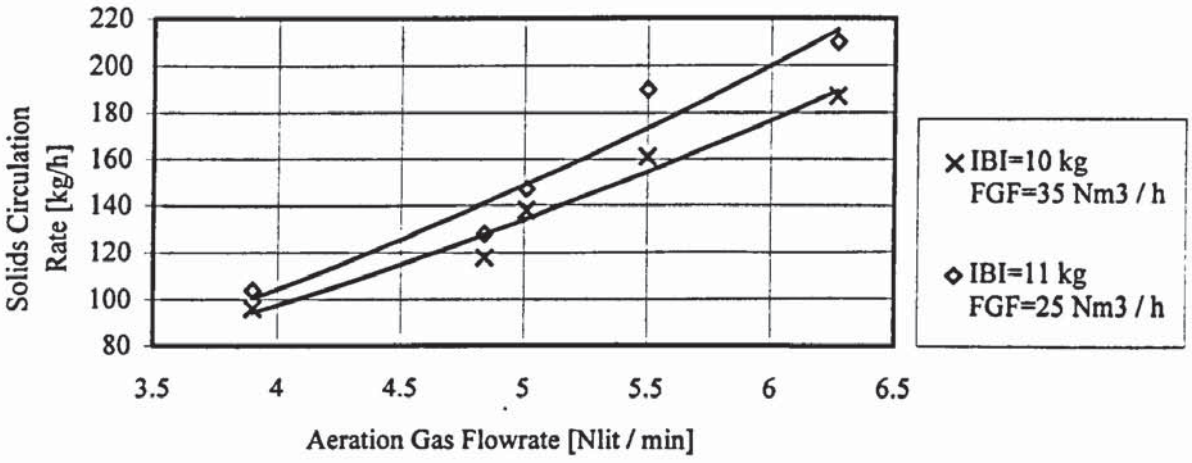

Figure 5-14: SCR versus AGF for two different pairs of IBIs and FGFs

As seen from the SCR measurement data obtained in Figure 5-14, values higher than 100 kg/h are obtained for the two sets of IBI and FGF investigated. These SCR values are considerably higher than those theoretically calculated to transfer the required energy, Figure 4-14 in Section 4.5.5, even to wet biomass feedstocks. However, the calculations procedure illustrated in Figure 4-14 is related to the satisfaction of energy requirements to biomass pyrolysing feedstocks rather than heat transfer rates to biomass particles.

illustrated in Figure 4-14 is related to the satisfaction of energy requirements to biomass pyrolysing feedstocks rather than heat transfer rates to biomass particles.

Nevertheless, heat transfer rates are considered sufficient according to the data derived from the CFB cold model experimentsgiven the fact for a biomass fast pyrolysis process a sand:biomass ratio of approximately 10:1 to 20:1 is practically required (Graham, 1993). The data shown in Figure 5-14 indicate that the proposed CFB reactor operating conditions successfully satisfy both the energy and the imposed heat transfer rate requirements even at the most extreme conditions (low values for IBI, FGF and AGF).

5.4 Summary

In this chapter, a cold model CFB reactor was constructed and tested.

The macroscopic phenomena of CFB reactor hydrodynamics, in particular riser voidage, were investigated in a cold model of similar dimensions to the proposed hot CFB bench scale biomass pyrolyser. The cold model was constructed and operated in order to gain experience on CFB operation as well as to study the effects of the main operating parameters on reactor performance, i.e. riser density and standpipe stability.

The major findings obtained from a series of experiments conducted on the cold CFB model are as follows:

- the proposed CFB reactor hydrodynamics theoretically should meet the high heat transfer rate requirements to the incoming biomass particles providing the appropriate suspension density to the riser section of the CFB reactor
- the proposed CFB reactor is quite flexible in operation since the high heat fluxes required, expressed as Solids Circulation Rates (SCR), may be obtained for a variety of operating parameters, namely the initial solids inventory of the system (IBI) and the fluidizing gas flowrate (FGF)
- control of the SCRs, riser voidage and heat transfer, is obtained by varying the Aeration Gas Flowrate (AGF) for a given set of IBI and FGF
- the operation of the standpipe in the moving packed bed or at near fluidizing bed conditions should be ensured in order to avoid defluidization or lean phase flow which would adversely influence suspension density and CFB reactor stability.

CHAPTER 6: CFB BENCH SCALE PLANT FEEDING AND LIQUID RECOVERY SYSTEMS

6.1 Introduction

This chapter deals with the conceptual design of two of the most important elements of a biomass fast pyrolysis system, namely the biomass feed and the liquid recovery systems.

A discussion on biomass feed issues may be found in Section 6.2, while the actual design and testing of the proposed feeder for the CFB reactor operation is described in Section 6.3, where the efforts to overcome the problems of keeping biomass moving and being accurately fed into the Circulating Fluidised Bed reactor are presented. The testing procedure and performance of the designed feed system as well as statistical analysis of the results obtained are discussed in Section 6.4.

Heat exchange is discussed in Section 6.5, where the applicability and the design concepts of an indirectly cooled heat exchanger is considered. A procedure to design and size the proposed heat exchanger for the liquid recovery from pyrolysis vapors, produced during operation of the CFB fast pyrolysis reactor, is presented in Section 6.6.

Finally, the conclusions concerning the design of these two items are summarised in Section 6.7.

6.2 Basic requirements for biomass feeding

The storage and movement of solids is usually more expensive and complicated than the movement of liquids and gases, which can usually be easily pumped through a pipeline. Solids are stored in a bin or a hopper and are usually transported to a reactor either mechanically (by being pushed along or dragged along or carried) or pneumatically. Excellent reviews for solids feeders can be find elsewhere (Levelton, 1982; Perry and Green, 1984). In the following some alternative solutions for feeder design are given in Section 6.2.1 while the material analysis and characteristics are given in Section 6.2.2.

6.2.1 Alternative solutions for feeder design

A feeder for the CFB reactor should incorporate the following components:

- a biomass storage container (bin, silo, hopper) which exhibits the right flow pattern for the material involved
- a conveying system which delivers biomass from the storage container, meters and delivers it unhindered to the CFB reactor riser.

Moreover, a number of important aspects should be considered when selecting a biomass feeder for the positive pressure CFB reactor riser, namely:

1. Good sealing in the feeder system, which is required to ensure combustion or pyrolysis gases do not leak from the reactor to the feed system.
2. Uniformity of biomass distribution across and within the riser diameter. In the case of the CFB reactor, the small reactor diameter (50 mm) does not impose any significant problems in feed distribution across the reactor diameter.
3. The feed system would provide storage, metering and transport of biomass to the CFB reactor riser.

Concerning the proper design of the biomass hopper it should be kept in mind that the undesired, funnel-flow pattern should be avoided at all costs. The funnel-flow pattern is characterised by a condition in which the walls of the hopper section at the bottom of the container are too shallow or rough for the bulk material to slide along them. As a result, material flows preferentially through a funnel-shaped channel located directly above the outlet, while material outside this flow channel is stagnant, leading to particle segregation, Figure 6-1(A). Ratholing is a common occurrence which can lead to flooding of fine powders or reduced usable capability of the biomass hopper. If the bulk material being handled is not coarse (<6.35 mm), free flowing, non-degrading and not segregating, a funnel flow pattern is no longer suitable (Marinelli and Carson, 1992a).

For the material in question (biomass saw dust, typically less than 2 mm) a mass-flow design, that is, one in which all of the material is in motion whenever any is withdrawn, as shown in Figure 6-1(B), must be considered. This design eliminates ratholing and the associated problems of flooding of the fine biomass feedstock as well as reduced usable bin capacity, while segregation is often minimised (Marinelli and Carson, 1992a). Mass flow hoppers are

suitable for fine powders, cohesive (non-free flowing) bulk materials, materials that tend to degrade when stored for extended periods of time and when segregation is important.

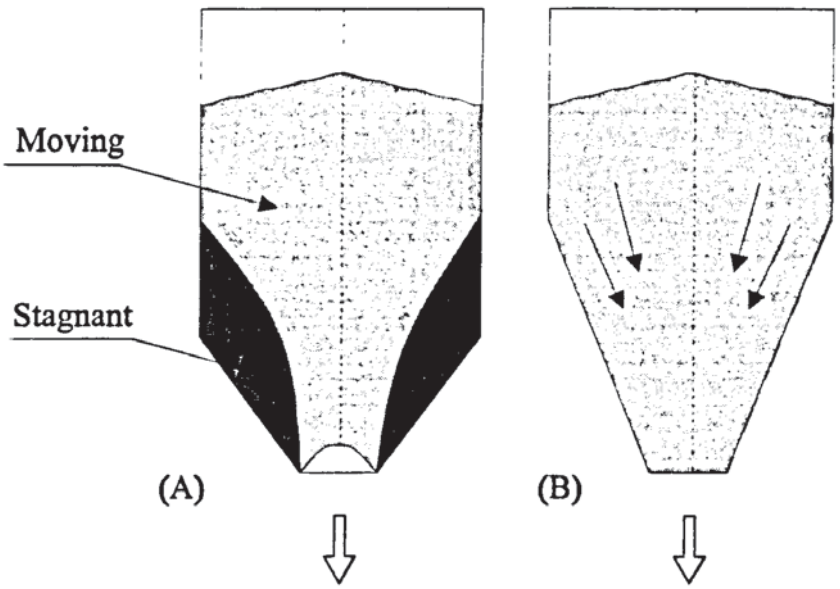

Figure 6-1: Ratholing (A) and free (B) material flow in bins and hoppers

As far as the choice of feeders for discharging material from biomass storage containers several types of feeders have been applied to fluidised bed systems operating under positive pressures, the most important being rotary valves (Maniatis, 1986), pneumatic feeders (Union Fenosa, Section 3.4.2) and screw feeders (Levelton, 1982). Rotary valves are expensive, not customised for small scale equipment and tend to leak when attached to systems operated at positive pressures, while pneumatic feeders are complex in design and require additional equipment such as blowers, rotary feeders (to feed the material to the stream of conveying gas), pipelines and include the use of a feedstock transport (conveying) gas. Screw conveyors on the other hand are very adaptable to volumetric control of material flow from the bottoms of bins or hoppers, their enclosing trough can be made tight enough to contain dusts and vapors and, hence, can be used effectively as an air vapor lock and generally they serve as transporting devices for a great variety of materials.

A list of feeders including their most important characteristics as far as their ability to feed the CFB reactor is concerned are listed in Table 6-1 below. These feeders were included on the basis of the requirements of operating under low positive pressures and with feedstocks ranging in size from 1 to 6 mm.

It may be concluded that that the most appropriate type of screw feeder is the constant section screw feeder, since it combines simple design and construction features and has been successfully used in similar applications.

The metering and transport portions of the screw feeder may or may not be combined in one piece of equipment. However, given the complexity associated with the design of a screw feeder that will accomplish both functions, because of the low capacity of the feeding system and the need for increased flexibility it was decided to incorporate a twin-screw system, the first screw to adjust accurately the biomass flowrate to the desired level (the metering screw), while also providing a gas seal. The second screw allows for rapid and unhindered propulsion of the metered material to the CFB reactor (the feeding screw).

In considering a dual-screw feeding system, it is important to have in mind that it is the metering screw that actually regulates the feedstock flowrate, and the feeding screw only transports the metered feedstock to the reactor. This requirement must be checked when calibrating the feeding system.

6.2.2 Material analysis

The initial step in engineering a biomass feeding system is to analyze the physical characteristics of the material and the rate at which this is to be handled. The material in question is known to vary not only in density but also in other properties (e.g. moisture, particle size, etc.), which affect metering and transport.

The feed materials that are planned to be used in the feeder are:

- cotton stalks
- sawdust
- wood chips
- wood flour
- wood shavings.

The properties of the above materials are summarised in Table 6-2. It should be noted that these materials are considered non-abrasive. Table 6-2 shows general flowability characteristics. As seen from the data presented, the materials of interest in this work (d_p<2 mm) are sluggish and prone to hangups, bridging and consolidation (Levelton, 1982). Consolidation occurs not only with depth in piles and bins but also during extrusion, i.e. screw-type, conveying, and results from mechanical interwining of the fibrous residues. Consolidation leads to worsened problems with bridging and reduces flowability.

Table 6-2: Properties of the materials considered for feeding

Material	Bulk density (kg/m^3)	Size (d_p in mm)	Flowability	Miscellaneous properties
Cotton stalks	250-440	d_p <5	Free flowing	Light, fluffy. Forms fibrous interlocks. Packs under pressure.
Sawdust dry	200-350	1< d_p <6	Sluggish	Hygroscopic. Packs under pressure
Wood flour	250-580	d_p <1	Very sluggish	Consolidates under pressure. Explosiveness.
Wood shavings	100-150	Irregular stringy fibers, cylindrical slabs, etc.	Very sluggish	Very light-fluffy. Interlocks, mats or agglomerates.
Wood chips (compacted)	160-400	d_p <5	Free flowing	Very light -f luffy Interlocks, agglom.
Wood chips (uncompacted)	160-350	d_p <5	Free flowing	Very light -f luffy Interlocks, agglom.

6.3 The design of the feeding system

The biomass feeding system must be effective in:

- continuously withdrawing material from the storage vessel
- accurately regulating the flow of material
- providing a high level of reliability and accuracy

- discharging and distributing the material inside the riser.

The specific components of the feeding system, namely

1. the feeder hopper
2. the metering screw
3. the transport screw

generally referred to in Section 6.2.1, will now be examined in detail.

6.3.1 The feeder hopper

In order to avoid the undesired funnel-flow, linked to most conical biomass storage vessels the shape of the feeder vessel was designed as a cylinder instead of a cone (Levelton, 1982),. The biomass storage vessel (feed hopper) had a capacity of 0.62 m^3 to provide up to 15 hours of continuous operation and was made of standard mild steel. The possibility of slight pressurization of the vessel with an inert purging gas (nitrogen), so as to avoid explosion hazards due to the concentration of air borne dust, and the installation of a manometer to check for inadequate gas sealing and pressurisation of the vessel had also to be considered.

In order to conform with the mass-flow design discussed in Section 6.2.1, and ensure that the feed material always flows, some form of agitation is required. Vibrators are typically used for biomass hoppers to eliminate the problems of ratholing and bridging. However, vibration may result in fatigue on the equipment and compaction of the material, which is then prone to flow cessation. Vibration may also cause segregation of the different-sized materials being fed, which will create a new problem in that the heavier, denser materials, will settle first, followed by the lighter material. Vibration also tends to compact most materials, creating in this way the very problem that it is meant to eliminate. By varying the length of the vibration cycle, compaction can be improved but varied densities may still prevail. Vibrators are also known to cause excessive noise problems. An alternative solution to ensure material flow would be the continuous agitation of the material by means of an internal stirring device in the hopper.

A device for the low-speed axial circulation of the feed material was therefore installed at the base of the hopper. This internal stirring device consisted of two curved s-shaped blades. These are kept around one cm above the bottom of the vessel, so that compacted material from the initially deposited feed plays the role of the bottom (stationary layer). Curved blades

have a lower starting torque than straight ones, which is important when starting up settled materials, the particles of which tend to bond together giving rise to flow obstructions. The stirring device continuously moves the material around, directing it towards an opening/gate in the bottom of the vessel, where the feedstock is pushed steadily to the metering device located vertically below. The hopper was designed to be gas-tight by providing O-rings around the stirrer shaft. A schematic of the hopper shown in Figure 7-3. Section 7.3.

This design permitted the material to flow uniformly over the entire area of the bottom hopper opening, thus avoiding localized flow that would lead to funnel flow, ratholing and bridging within the hopper.

6.3.2 The metering device

The modulation of biomass flow once discharged from the conical hopper is regulated by the metering device. This device is a vertical below the hopper, which imparts a smooth positive motion to the material as it rotates within its trough. Cold rolling of special analysis strip steel into a continuous helix produces a work-hardened smoothly finished flight surface. A helicoid flight is of superior strength with its diameter, pitch and thickness closely controlled. The flight was fastened to the pipe by intermittent welds and welded steel and lugs, Figure 6-2.

The screw and the containing trough has seamless internal collars and O-rings inserted in one end to accommodate the shaft. The flight pattern has a lead slightly longer than the pitch of the pattern. This assures a tight gripping action when mounted within the trough.

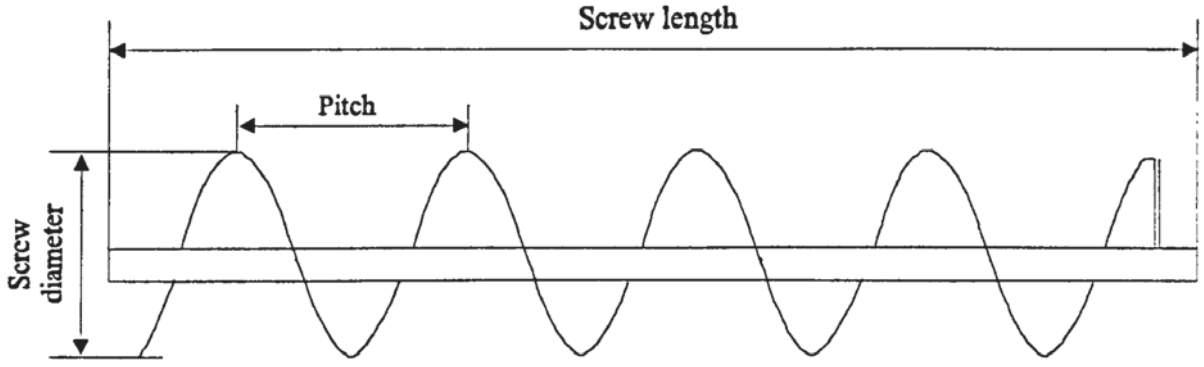

Figure 6-2:The metering screw with the helicoid flight (shown horizontally)

A screw conveyor manufactured according to the above described procedure, with a length of 0.5 m amd an i.d. of 0.15 m, was mounted vertically, on the opening in the bottom of the biomass hopper.

The metering device was used to regulate the flowrate to the CFB reactor volumetrically. It is known that gravimetric feeders, which regulate the rate of material transport according to weight (±2 % of the desired flowrate), are more accurate than volumetric ones, which regulate the volume of material conveyed (±10 % of the desired flowrate). However, volumetric feeding was practised because of the reduced cost and the simpler design than for gravimetric feeding.

6.3.3 The feed device

The device consists of a horizontal screw, set below the discharge point of the vertical (metering) screw. The horizontal screw had the same dimensions as the vertical one, while the spout went from 0.15 m to 0.07 m at the entrance to the CFB riser. The flight stops beyond the midpoint of the last discharge opening to affect complete discharge and reduce the possibility of material carryover. The feeding screw is shown in Figure 6-3.

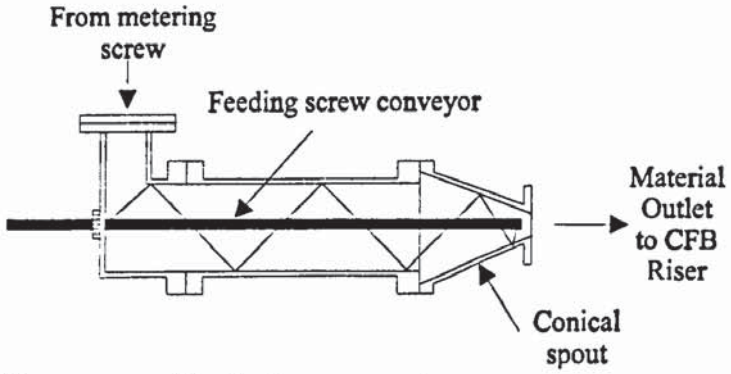

Figure 6-3: The feeding screw with discharge spout

6.3.4 Troughs, covers and control devices

The troughs, covers as well as control devices enclose completely the material being conveyed and the rotating parts. The troughs are of cylindrical type incorporated in the feeder to baffle the flow of material. The covers are of circular type equipped with O-ring flange and 4 bolts each to ensure gas-tightness and are used over the cylindrical vessel as required.

Regulation of material flowrate is accomplished by three motors coupled with each one of the separate devices, namely the stirring device (30-280 rpm), metering (17-225 rpm) and conveying screw (25-240 rpm). All three motors were deliberately oversized having a nominal power rating of one hp each. Steel roller chains are used as power transmission chains.

6.4 Testing of the feed system - Results and analysis

To feed relatively dry material accurately from a volumetric screw feeder one must ensure two things, namely:

1. The flights of the metering screw must be completely filled with uniform density material, which means that no compaction or segregation of material may take place, since either of these would result in some flights being filled with a more dense material and some with lighter density material thus causing an erratic feed rate. Screw feeders typically run between 95 and 100 % full and, by adjusting their speed, the rate of discharge may be modulated.
2. The metering screw speed should be kept between 2 and 40 rpm. Below 2 rpm the discharge from the end of the screw is very nonuniform and the cost of the reducer would become excessive. Above 40 rpm, screw efficiency decreases, while at the same time the power required to operate the screw, abrasive wear on the screw flights and particle attrition would all become greater.

Wood shavings of 4 to 10 mm mixed with sawdust (<2 mm) were used to test the system, in order to obtain calibration curves and to test the reliable performance of the biomass feeder. In these calibration tests, the influence of the separate feeder components on biomass flowrates was individually examined.

6.4.1 Effect of the internal stirring device speed on biomass flowrate

The speed of the metering screw was kept constant at 17 rpm, while the speed of the feeding screw was varied from 24 to 143 rpm. The rotational velocity of the internal stirring device was varied between a low (9 rpm) and a high speed (15 rpm). The results are plotted in Figure 6-4.

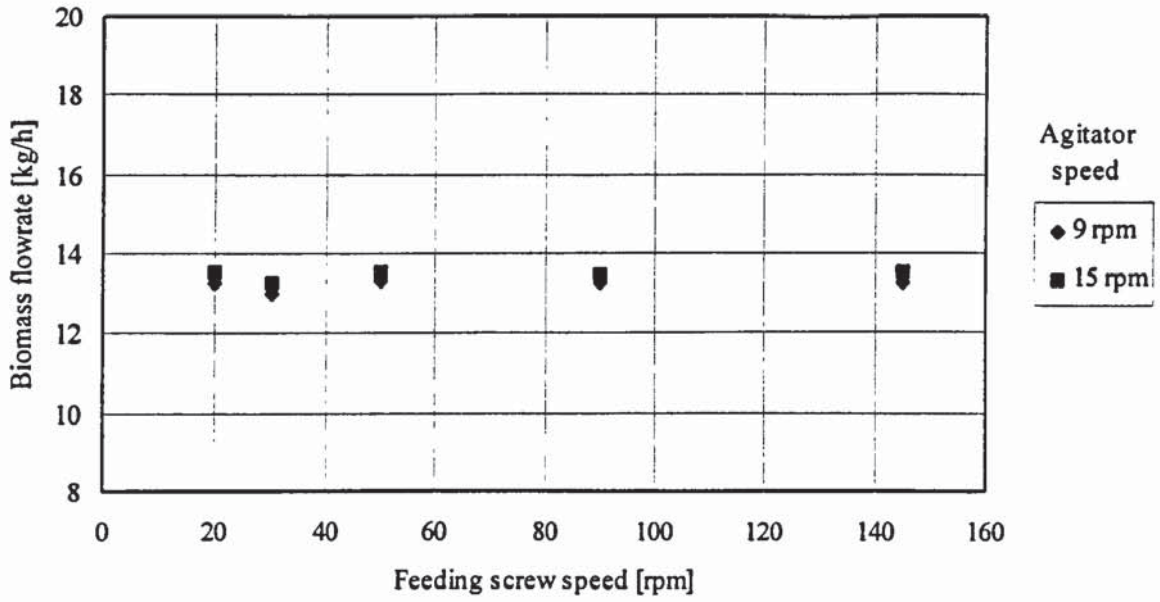

Figure 6-4: Effect of the internal stirring device speed on biomass flowrate (metering screw speed constant at 17 rpm)

These results indicate that the influence of the internal stirring device speed does not affect the biomass flowrate out from the discharge spout. An increase in the internal stirring device speed of more than 300 % results in an insignificant increase on biomass flowrate.

6.4.2 Effect of the metering screw speed on biomass flowrate

The speed of the first motor (internal stirring device) was kept constant at 28 rpm, while the speed of the feeding screw was varied from 24 to 143 rpm. The rotation speed of the shaft of the motor of the metering screw varied between the lowest possible (17 rpm) and a higher speed (21 rpm). The results are plotted in Figure 6-5.

These results indicate that the influence of the metering screw speed is very essential for the performance of the feeding system, since biomass flowrate out from the spout is proportional to the metering screw speed. Similar results, presented in Figure 7-5, Section 7.3, are obtained using feedstock of different sizes.

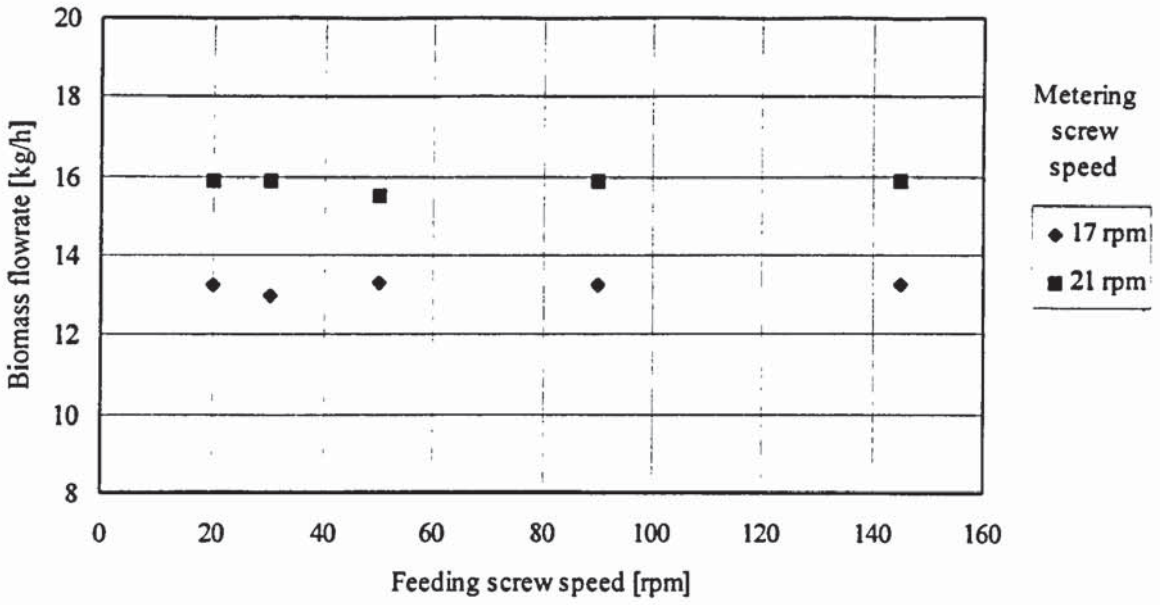

Figure 6-5: Effect of the metering screw speed on biomass flowrate (agitator speed constant at 9 rpm)

At this point it should be noted that the largest gear on the metering screw shaft had already been installed (space limitation did not allow the installation of a bigger size gear) and the smallest size gear available (8-teeth gear) was installed on the shaft of the metering screw driving motor. This indicates that the metering screw speed should be kept as low as possible, since the sizing of the CFB unit was carried out for a nominal biomass flowrate of 10 kg/h, see discussion in Chapter 4. Another solution was to replace the existing drive motor with a new one operating in the range of 4 - 45 rpm. This replacement was carried out and proved even more important because after testing it was shown that the motor of the feeding screw gave many operational problems in order to adjust the desired speed. Hence, repeated material build-up in the conical spout was encountered. The motor replaced was then used in the place of the third, problematic one, providing thus a practical solution.

6.4.3 Effect of the feeding screw speed on biomass flowrate

In order to ensure that the feeding screw should play a minor role as far as modulation of biomass flowrate is concerned, delivering the same amount of biomass at a wide range of rpm, once both the internal stirring device and metering screw motors are set at constant speeds, five tests with as sole variable the feeding screw speed were performed, the results are shown in Figure 6-6.

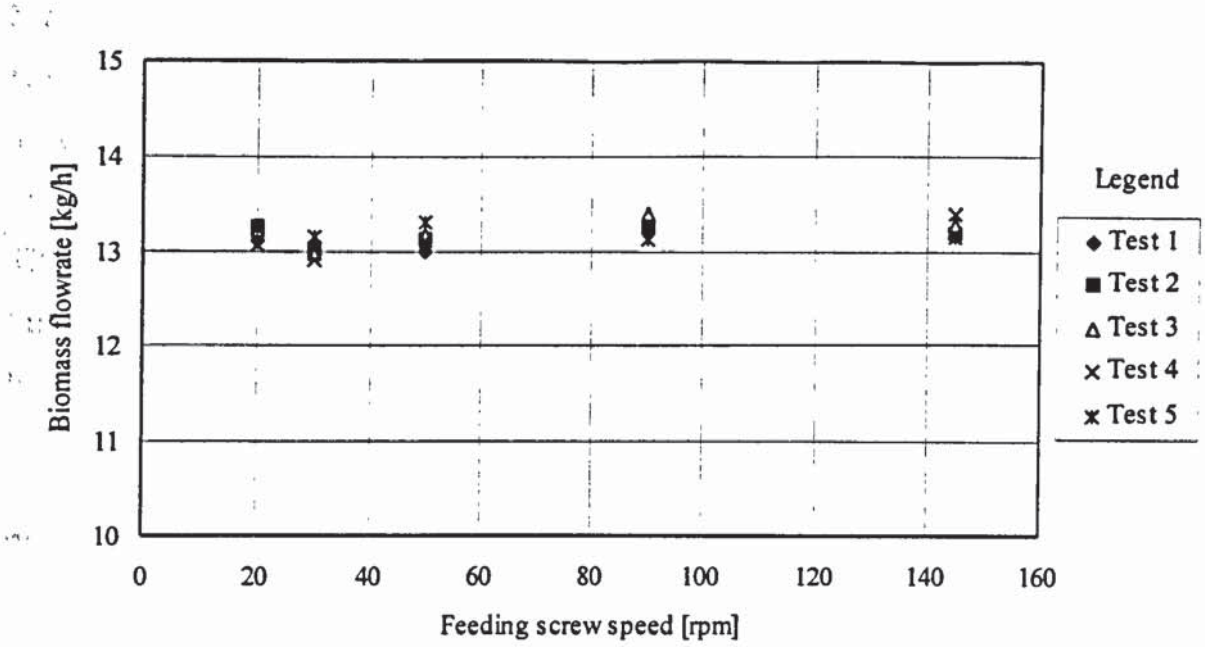

Figure 6-6: Effect of the third screw speed on biomass flowrate.

These results indicate that the requirement set in Section 6.2.1 for the performance of the feeding system, i.e. insensitivity of the feeding screw speed on biomass flowrate, is fulfilled, since the feeding screw speed variation does not show any significant effect on the output flowrate, which was fluctuating slightly around 13.2 kg/h. A further statistical analysis on the results obtained is discussed in Section 6.4.5 below.

6.4.4 Modifications in the feeding system-Observations-Conclusions

In the initial tests, it was found that material was steadily being built up in the flights of the conical spout, Figure 6-3. As a remedy, the flights of the third screw in the conical part had to be reduced in diameter, following the existing angle of the spout and leaving enough space between the inside surface of the spout and the spout flights. This modification made it possible to eliminate totally the build-up of material and the erratic operation of the feeding screw, even at higher biomass flowrates, i.e. above 15 kg/h.

In order to reach a minimum rpm from the metering, vertical screw shaft (under 10 rpm), and attain the relatively low specific biomass throughputs required, while maintaining the metering screw rpm above 2, as discussed in Section 6.4, new gears were constructed for both the shafts of the motor and screw, so the reduction ratio was changed from 1 to 3, to 1 to 6.

Moreover, it was found that when the metering screw operated at speeds over 10-12 rpm, the feeding screw must operate at much higher speeds, so that the incoming material does not accumulate in the feeding screw trough. Thus, another remedy employing the replacement of the gear of the horizontal feed screw shaft to a larger coupling gear had to be undertaken. This modification, from a 28- to a 38-tooth gear, made it possible to operate this screw at higher speeds, thus avoiding the build-up of the material, especially in the conical spout, at higher metering screw speeds of rotation.

The importance of the change of the second motor as well as the replacement of the problematic third has already been discussed in Section 6.4.2.

A chain slack for the driving chain between the gear of the first motor and the gear of the internal stirring device was installed, since the path between these two gears was long and the chain heavy, which resulted in an out-of-level curve causing problems in the internal stirring device operation. This problem was overcome by using a single temporary holding mechanism during the tests.

The horizontal, feeding screw should run at a constant moderate/low speed while the vertical, metering screw speed should be kept low, thus avoiding the build-up effects at the exit of the conical spout due to the increased friction and strain with the casing. After some hours of continuous operation (more than 6 h) the spout of the third screw was quite warm (40-50 °C) indicating the results of the internal friction. Since the direct contact of the conical spout with the high temperature environment of the CFB-riser would cause additional heat-up problems, probably resulting in premature biomass pyrolysis inside the horizontal screw conveyor, it was decided that a cooling medium should be provided. This would constitute a fan or a water mantle for more effective cooling. The latter solution was finally adopted.

The flexibility of the designed feeding system allowed changes in the field. The drive mechanisms of the three motion devices, namely internal stirring device, metering and feed screws, could be changed relatively quickly to adapt to a new material that must be fed or for changes in the feed rate of the material already used. The feeding system developed is also capable of being equipped with an extension hopper, if there is need for one, for storage of additional material or with a number of options such as dust elbows, special hoppers, nozzle extensions, and more.

6.4.5 Statistical analysis

A statistical analysis on the results obtained on the feeding system performance is further discussed. The statistical analysis, which was performed during five discrete tests, is important to prove whether the requirement for biomass flowrate dependency solely on the variation of the metering screw speed, as discussed in Section 6.2.1, is met. In these tests, the internal stirring device as well as the metering screw speed was kept constant, while the feeding screw speed was varied over a wide range. Table 6-3 shows the experimental results obtained.

Table 6-3: Experimental results for biomass flowrate measurements (kg/h) for five tests with varying feeding screw speed (rpm)

rpm	Test 1	Test 2	Test 3	Test 4	Test 5
20	13.11	13.27	13.22	13.05	13.24
30	13.08	12.99	12.96	12.91	13.14
50	12.98	13.13	13.17	13.10	13.30
90	13.30	13.25	13.39	13.26	13.13
145	13.22	13.20	13.28	13.40	13.15

Figure 6-7 illustrates one standard deviation error bars for Tests 1-5.

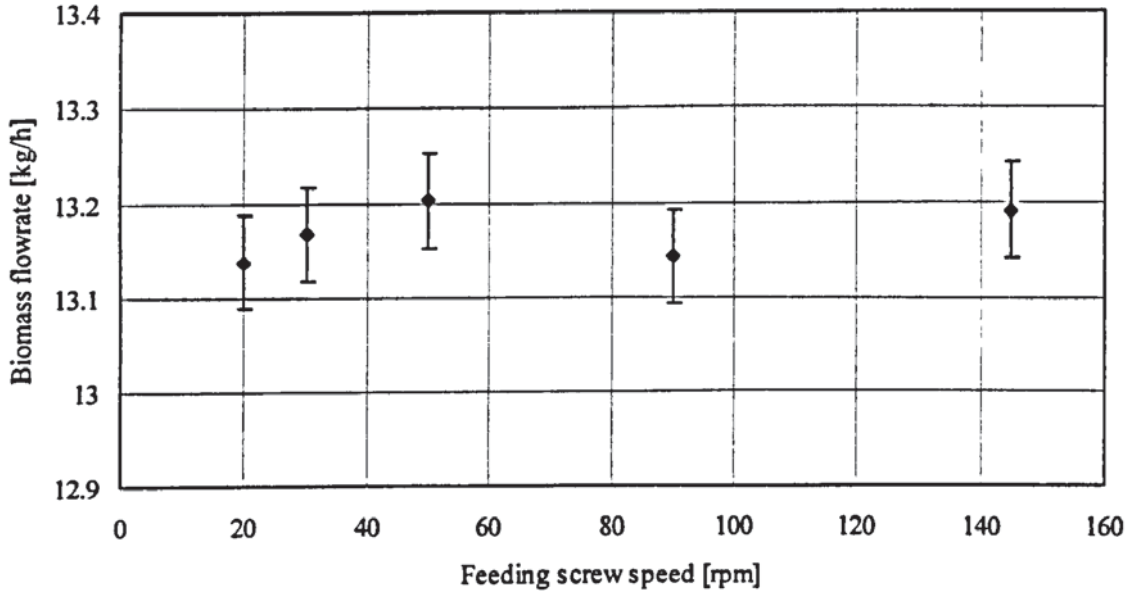

Figure 6-7: Y-error bars for mean values of the five tests undertaken

The above results indicate that there is no biomass flowrate dependency on the speed of the feeding screw, so that its variation was solely determined by regulating the speed of the metering screw, the internal stirring device and feeding screw speed being set at predetermined, constant values for each run performed.

6.5 Liquid recovery system

The condensable, pyrolysis vapors constitute a percentage of the total gaseous stream to be handled in the liquid recovery system, estimated to be 30 % wt of the total gas/vapor product volume. Comparing to other fast pyrolysis system, i.e. conventional fluidised bed reactors where excessive inert gas quantities are used to effectively transfer heat to pyrolysing biomass particle (see discussion in Section 3.4.4), this figure is approximately double (see also Peacocke, 1994) denoting the advantageous effect of the CFB reactor system for biomass fast pyrolysis as far as the gas-to-feed ratios are concerned.

To collect the liquid products (organics as well as reaction and feedstock water), processes such as the rapid cooling (quenching) of gases and condensation of organics and water in the appropriate liquid recovery system are required.

Although the development of high collection efficiency systems is considered very essential for the successful implementation of biomass fast pyrolysis processes, the fundamental design of these systems fundamental design has been given little attention and information. On the other hand information on the few successful demonstration plants that exist, is very limited due to proprietary information (Ensyn, Inc., Section 3.5). The systems generally used for liquid product recovery are summarised elsewhere (Peacocke, 1994), the main two categories being those of :

1. direct liquid-contact to quench the vapors with a liquid (pyrolysis liquids or water) to fulfill the requirements of cooling and collection
2. indirect heat exchange, which is preferable in smaller scale systems due to the problems of liquids handling and mass balance closure.

For the purpose of this work, it was decided that an indirect heat exchange system should be used to cool down and recover the product pyrolysis vapors. This was because of time and budget limitations and took into account the relatively high quantities of pyrolysis liquids that would be necessary to move around to quench the pyrolysis vapors.

Process data of importance for the thermal design and rating of shell-and-tube heat exchangers must be carefully considered. Density, viscosity, specific heat and thermal conductivity of the process streams undergoing heat transfer have the most profound effect on the size and type of heat exchanger, because such data enter directly into the calculations for heat transfer film coefficients and pressure drop. Hence, it is important that physical property data be as accurate as possible. Many exchangers have been known to fail due to errors in computing an effective temperature difference because of insufficient information in computing heat transfer film coefficients.

However, since most of the data for both gas/pyrolysis vapors as well as liquid properties are not known with great confidence, the thermal design of the heat exchanger, given the thermal loads estimated below in Section 6.6, was based on proven, commercial software, indirectly calculating heat transfer film coefficients and related issues. These issues are further discussed below in Section 6.6.5.

A general discussion on heat exchanger design follows, while the detailed calculations for the determination of the heat removal from the product gas/vapor stream follows in Section 6.6.

6.5.1 Heat exchanger design

The most common type for indirect heat exchange is the shell-and-tube heat exchanger, where the cold stream effectively removes heat from the hot one, the two streams moving across each other in separate circuits, the shell and the tubes.

Various shell designs are available for heat-transfer applications. These can be broadly classified as:

- single-pass
- two-pass
- split-flow
- divided-flow shells.

The single pass shell is the most common design. Two-pass is used for services where temperature cross is unavoidable due to process considerations, and where space limitations exclude the use of two, or more, shells in series. Split-flow and divided-flow shells are used in services where shellside heat transfer is not controlling, and low shellside pressure drop is

desired. Tie rods and spacers are used to retain all transverse baffles and tube-support plates securely in position.

International standard specifications are used for designating tube materials. Tube sizes used in the chemical process industries are 1.9, 2.5, 3.8 and 5 cm internal diameter. Thermal efficiency and economic considerations require as small a diameter as possible. However, the practical limit is the requirement for mechanical cleaning of tubes, which requires a minimum diameter of 1.9 cm for straight tubes.

Tubes are arranged in triangular, square or rotated-square pitch, Figure 6-8. Triangular tube layouts result in better shellside coefficients and provide more surface area in a given smaller diameter, where square or rotated square pitch are used when mechanical cleaning of the outside of the tubes is required.

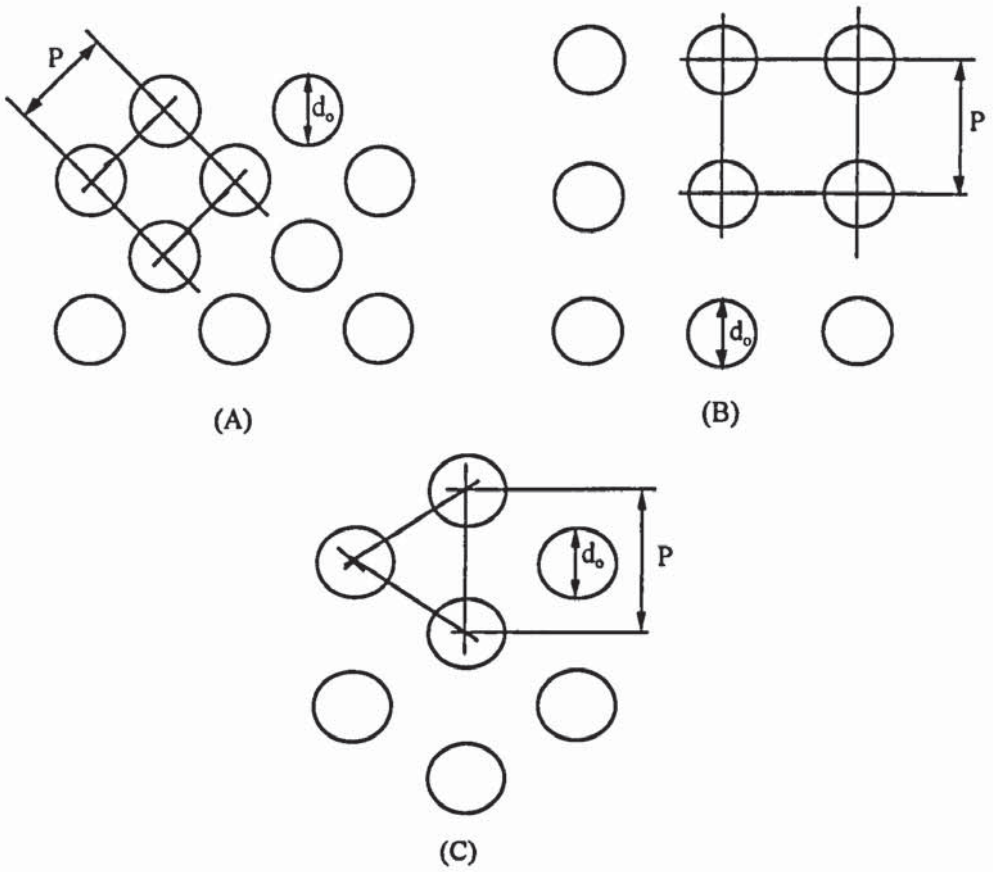

Figure 6-8: Tube pitch arrangements- (A) Rotated square pitch, (B) Square pitch, and (C) Triangular pitch.

The tubesheets perform the important function of separating the shellside and tubeside fluids, and provide the anchor point for tube ends. Tubesheets are usually machined from material similar to that specified for tubes.

Baffles are frequently used in shell-and-tube heat exchangers. The purposes of the baffles are to deflect the shellside fluid over the tubes in its passage through the exchanger, and act as tube supports to maintain tube pitch, prevent sagging of tubes and prevent flow induced vibrations.

The baffles establish the flow path of the shellside fluid, which depends on the type and arrangement of the baffles. The baffle cut is specified as a percentage of the shell diameter and the minimum baffle spacing is 0.2 of the shellside diameter.

Materials of construction are usually the same as for the shell. The common baffle and support plate types are: single segmental (horizontal or vertical cut), double segmental (horizontal or vertical cut), complete and longitudinal.

6.5.2 Guidelines for fluid allocation

Many factors must be taken into consideration in order to determine which fluid should be on the shellside and which on the tubeside of an exchanger. These are:

- Viscosity: Higher heat transfer rates are usually obtained by placing a viscous fluid on the shellside.
- Toxic and lethal fluids: Generally, the toxic fluid should be placed on the tubeside, using a double tubesheet to minimize the possibility of leakage.
- Flowrate: Placing the fluid having the lower flowrate on the shellside usually results in a more economical design. Turbulence exists on the shellside at much lower Reynolds numbers than on the tubeside.
- Corrosion: Fewer costly alloy or clad components are needed if the corrosive fluid is placed inside the tubes.
- Fouling: Placing the fouling fluid inside the tubes minimizes fouling by permitting better fluid-velocity control. Increased velocities tend to reduce fouling.
- Temperature: For high temperatures services requiring expensive materials, fewer components are needed when the hot fluid is placed on the tubeside.
- Pressure: Placing a higher pressure stream in the tubes will require fewer (though more costly) high pressure components.

- Pressure drop: For the same pressure drop, higher heat-transfer coefficients are obtained on the tubeside. A fluid having a low allowable pressure drop should be placed there as well.

In an exchanger having one shell pass and one tube pass, the two fluids transfer heat in either countercurrent or concurrent flow. This affects the value of the log mean temperature difference. There is a distinct thermal advantage in counterflow, except when one fluid is isothermal, which, however, is not the case here, since in concurrent flow, the hot fluid cannot be cooled below the cold-fluid outlet temperature.

Fouling is the deposition of undesirable materials on the heat exchanger surfaces, which increases resistance to heat transmission. Fouling is a complex phenomenon caused by many mechanisms, which may operate independently of each other or in parallel. The operating variables that have important effects on fouling processes are:

- Flow velocity: Very strong to moderate effect on a majority of fouling processes.
- Surface temperature: Affects most fouling processes, and in particular crystallization and chemical reaction.
- Surface: Roughness, size and density of cavities will affect crystalline nucleation, sedimentation, and the adherence tendency of deposits.
- Bulk fluid temperature: Affects rate of reaction and crystallization.
- Materials of construction: Possible catalytic action and corrosion.

The materials of construction and the nature of the surface have the greatest effect in initiating fouling rather than in continuing and sustaining it.

6.5.3 Conclusions for an effective heat exchanger design for pyrolysis liquids recovery

Concerning all the above information, problems, and guidelines, it was decided to design and construct a vertical shell-and-tube heat exchanger. The tubeside fluid would be the gas/pyrolysis vapors from the CFB-unit, while the shellside fluid would be the cooling medium, water. Tubeside and shellside material would be of stainless steel (AISI 304).

A vertical configuration for tubeside condensation is considered the best in relation to heat transfer and fluid dynamics, the process-vapor flowing down the tubes (downflow arrangement). In this arrangement vapors enter at the top, and the condensate plus non-condensibles will be removed from the bottom channel. A Dewar vessel arrangement would

be used to isolate the non-condensibles from the condensates remaining in the gaseous stream after cooling. The vertical arrangement has the following advantages:

- effective and stable operation
- inerts accumulation is not a problem
- true countercurrent flow enables use with a temperature cross
- condensate subcooling can be easily handled

while the disadvantage is that support structures may be expensive, and maintenance difficult, especially after-experiment cleaning of the tubes from tarry deposits.

6.6 Detailed calculations of downstream processing heat load

6.6.1 Total liquids sensible heat

The total liquids (condensibles), i.e. organics, pyrolysis/reaction water and moisture, sensible heat (Q_l) may be calculated by:

$$Q_l = G_{liq} c_{p,v} (T_{in} - T_{cond}) \qquad \text{(Eq. 6-1)}$$

where

Q_l	total liquids sensible heat	[kJ/h]
G_{liq}	total liquids mass flowrate	[kg/h]

The following assumptions are also made made:

- $c_{p,v}$ =2.75 kJ/kg°C is the total liquids specific heat capacity (Nilsson, 1990)
- T_{in} = 500°C is the gas/vapor inlet temperature to heat exchanger
- T_{cond} = 100°C temperature at which vapor condensation begins

A composition of the liquids produced, according to the discussions held at Sections 4.2.1 and 4.2.4 is illustrated in Table 6-4.

Table 6-4: Condensable organic compounds (Mc Keough *et al.*, 1988)

Eq. 6-1 becomes then:

$Q_1 = 7.76 \times 2.75 \times (500\text{-}100) \Rightarrow Q_1 = 8426$ kJ/h — Term (I)

6.6.2 Total liquids latent heat

The total liquids latent heat (Q_2) may be calculated by

$$Q_2 = G_{liq} * L_{liq} \qquad \text{(Eq. 6-2)}$$

Taking L_{liq} = 300 kJ/kg as the liquids heat of condensation (Nilsson, 1990), Eq. 6-2, becomes:

$Q_2 = 7.76 \times 300 \Rightarrow Q_2 = 2298$ kJ/h — Term (II)

6.6.3 Water vapor (Q_3)

The water vapor sensible heat (Q_{3A}) is calculated by:

$$Q_{3A} = G_w (c_{p,m(in)} T_{in} - c_{p,m(out)} T_{out}) \qquad \text{(Eq. 6-3)}$$

where

G_w water/steam mass flowrate [kg/h]

Assuming that:

- c_p,m(in) = 2.12 kJ/kg K, the mean steam heat capacity at T_{in}
- $c_{p,m(out)}$= 1.89 kJ/kg K, the mean steam heat capacity at T_{out}
- T_{in} = 773 K steam inlet temperature
- T_{out}= 373 K steam condensation temperature

Eq .6-3 becomes:

$$Q_{3A} = 1.86 \times \{(2.12 \times 773) - (1.89 \times 373)\} \Rightarrow Q_{3A} = 1737 \text{ kJ/h}$$

The water vapor latent heat (Q_{3A}) is calculated by:

$$Q_{3B} = G_{H2O} * L_{H2O} \qquad \text{(Eq. 6-4)}$$

Given that L_{H2O} = 2260 kJ/kg is the water latent heat, Eq. 6-4 becomes:

$$Q_{3B} = 1.86 \times 2260 \Rightarrow Q_{3B} = 4304 \text{ kJ/h}$$

The total heat that must be removed from the water vapor (Q_3) stream is calculated by:

$Q_3 = Q_{3A} + Q_{3B} \Rightarrow Q_3 = 6041$ kJ/h	Term (III)

6.6.4 Non - condensable gas (Q_4)

It is assumed that the non-condensable gases are consisted of pyrolysis gas (a mixture of CO, CO_2 and CH_4 with the proportions 27 %, 60 % and 13 % wt of maf feedstock respectively, Figure 4-13), char combustion produced CO_2 and inert N_2 from fluidizing air. Table 6-5 shows the non-condensable gas composition.

Table 6-5: Non-condensable gaseous components

Gaseous component	% wt	Flowrate (kg/h)
CO	5.29	0.87
CO_2	29.1	4.79
CH_4	1.15	0.19
N_2	64.46	10.61
Total gas flowrate	100	16.46

The heat removal from this stream, Q_4, must equal:

$$Q_4 = \sum_{i=1} \left(\frac{G_i \Delta H_i}{MW_i}\right)$$

(Eq. 6-5)

where

G_i	mass flowrate of gaseous component i	[kg/h]
MW_i	molecular weight of component i	[kg/kmol]
ΔH_i	enthalpy change from T_1 to T_2 for i	[kJ/kmol]

and

$$\Delta H_i = \int_{T_1}^{T_2} c_{p,i}\, dT$$

(Eq. 6-6)

It is further known that for each gas component, i, the specific heat is given by:

$$c_{p,i} = A_i + B_i T + C_i T^2 + D_i T^3$$

(Eq.6-7)

where

$c_{p,i}$	specific heat for component in gas steam	[kJ/kmol K]
A, B, C, D	constants found in literature.	
T	temperature	[K]

The heat load is calculated according to the data found in Table 6-6:

Table 6-6: Data for non-condensable gas components calculation

Component i	A	B	C	D	G_i (kg/h)	ΔH_i (kJ/kg)
CO	30.87	-1.285×10^{-2}	2.789×10^{-5}	-1.272×10^{-8}	0.87	433.59
CO_2	19.80	7.344×10^{-2}	-5.602×10^{-5}	1.715×10^{-8}	4.79	421.46
CH_4	19.25	5.213×10^{-2}	1.197×10^{-5}	-1.132×10^{-8}	0.19	1270.3
N_2	31.15	-1.357×10^{-2}	2.680×10^{-5}	-1.168×10^{-8}	10.61	429.5
Total gas flowrate (kg/h)					16.46	

Inserting the above data in Eq. 6-5, Q_4 is calculated:

$Q_4 = 7200$ kJ/h	Term (IV)

Thus the thermal load to be removed in the heat exchanger is found by adding the individual terms calculated by Terms (I) to (IV):

$$Q_{tot} = \text{Term (I)+Term (II)+Term(III)+Term(IV)} = Q_1 + Q_2 + Q_3 + Q_4 =$$
$$=8426 + 2298+ 6041 + 7200 \Rightarrow Q_{tot} = 23965 \Rightarrow Q_{tot} \approx 24000 \text{ kJ/h}$$

(Eq. 6-8)

Oversizing the heat exchanger by 25%, the thermal load to be removed is obtained as:

$$Q_5 = 1.25 * Q_{tot} \Rightarrow Q_5 = 1.25 \times 24000 \Rightarrow Q_5 = 30000 \text{ kJ/h}$$

(Eq. 6-9)

Heat taken out by cold stream (water), is given by:

$$Q_5 = G_{cH2O} * c_{pH2O} * \Delta T$$

(Eq. 6-10)

where

G_{cH2O}	cold water flow	[kg/h]
c_{pH2O}	specific heat capacity for water(=4.19)	[kJ/kg K]
ΔT	$T_{in} - T_{out}$ allowable water temperature rise	[K]

while the cold medium (water) flowrate is given by rearranging Eq. 6-7, given that $Q_5 = Q_{tot}$ and considering $T_{in} = 15^{\circ}C$ and $T_{out} = 85^{\circ}C \Rightarrow \Delta T = 70^{\circ}C$:

$$30000 = G_{cH2O} \times 4.19 \times 70 \Rightarrow G_{cH2O} = 100 \text{ kg/h}$$

(Eq. 6-11)

6.6.5 Heat exchanger design data

Taken the above derived data into consideration, a shell-and-tube heat exchanger was designed with the assistance of a exchanger dimensioning software: "Engineer's Aide"-Process Engineering Software, Version 3.01. This software utilises empirical equations for heat transfer coefficients, combined with heat balance equations and equations defining mechanical characteristics. The number of tubes in the heat exchanger is then increased until the combination of equations represents a valid heat exchanger design based on the available temperature driving force. This method allows the user to determine heat exchanger sizing all that is required being the incoming flows and fluid physical characteristics. However, it must be emphasized that the above software package sizes coolers and not condensers, i.e. does not take into consideration any phase changes.

The design data of the designed heat exchanger, utilising the derived data and the sizing procedure discussed above, are shown in Table 6-7 below.

Table 6-7: Shell-and-tube heat exchanger design data

Number of Tubes / Shell	40
Tube i.d. (mm)	18.05
Tube o.d. (mm)	21.35
Tube Length (m)	1.3
Tube Pitch	Triangular
Number of Shells / unit	1
Baffle Cut	25%
Baffle spacing (mm)	100
Shell i.d. (mm)	220
Shell thickness (mm)	4

6.7 Summary

In this chapter, two essential components of the biomass fast pyrolysis bench scale plant, namely the feeding and the liquid recovery systems, were conceived and properly designed and constructed. Moreover, the performance of the feeding system was extensively tested while that of the heat exchanger will be proved in the course of the experimental section.

Troubleshooting of the feeding system resulted in smooth and reliable operation, while the incorporation of individually controlled feeder components, namely the stirring device, as well as metering and feeding screws resulted in:

- easy control by means of one component (metering screw) speed variation
- reliable operation over a wide range of feedstock different sizes.

On the other hand, an indirect heat exchanger was chosen as the liquid recovery system. The heat exchanger comprises a shell-and-tube vertical condenser, where the hot gases/pyrolysis vapors enter the tubeside and are cooled with countercurrent moving water in the shellside. Thermal design of the heat exchanger was performed by the detailed calculation of the heat load to be removed from the product gaseous stream, as well as the incorporating of a commercial software application. However, the suitability of the heat exchanger constructed remains to be verified in practice, both in terms of heat exchange and process suitability.

CHAPTER 7: DESCRIPTION OF REACTOR SYSTEM

7.1 Introduction

In this chapter, the CFB bench scale biomass fast pyrolysis plant as first built is described, with all the peripheral pieces of equipment. A general schematic of the plant is given in Figure 7-1 and a picture is given in Figure 7-2.

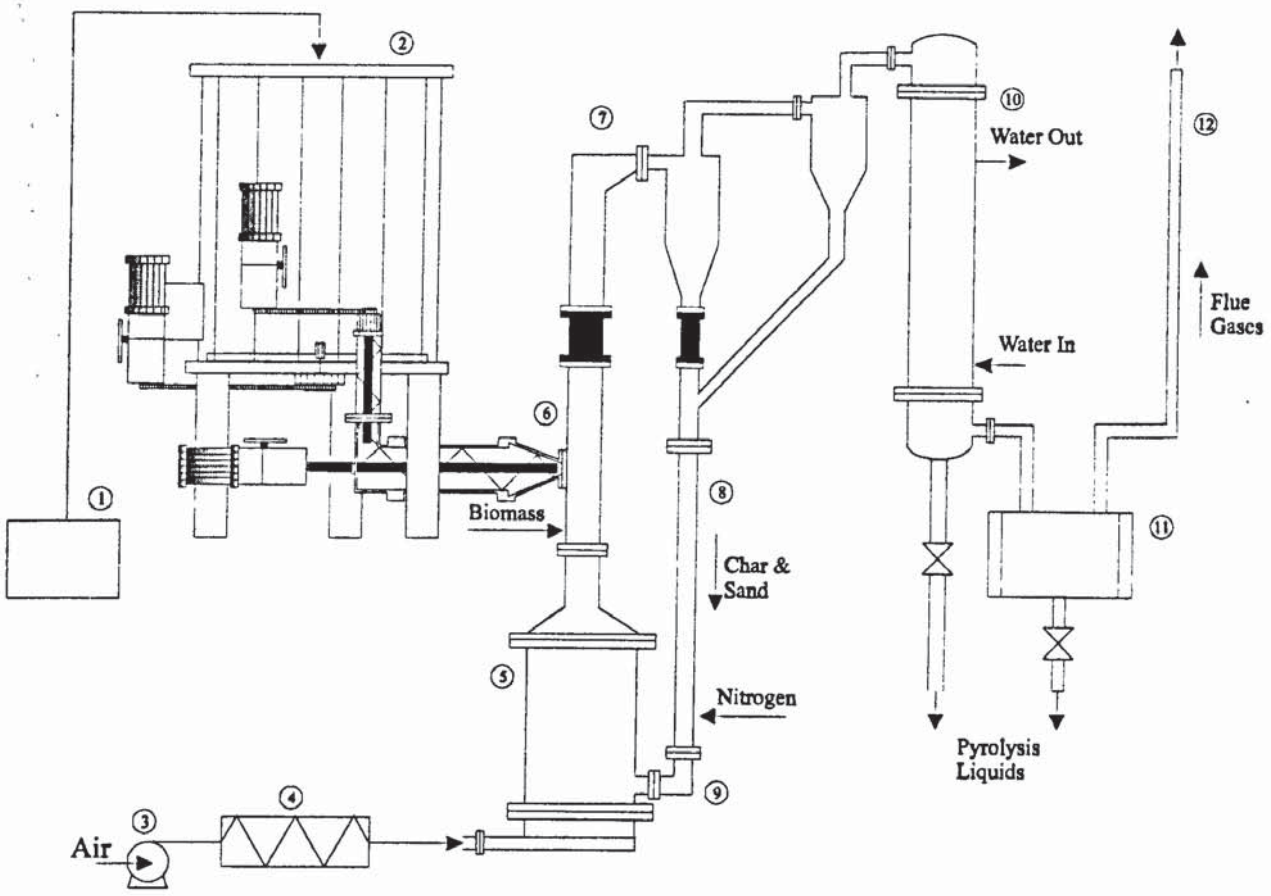

Figure 7-1: Biomass fast pyrolysis bench scale plant (not to scale)
(1-feedstock preparation, 2-biomass feeder, 3-air compressor, 4-air preheater, 5-char combustor, 6-biomass pyrolysis riser, 7-solids (sand and char) recovery system, 8-standpipe, 9-L-valve, 10-Shell-and-tube heat exchanger, 11-dewar vessel, 12-gas to vent)

The bench scale plant, its ancillary equipment and apparatus had to be designed, procured constructed and tested within a strict time limitation. The author supervised the construction of all equipment, which was almost entirely fabricated in the workshop of the Agricultural University of Athens, which also provided the space for the plant.

Figure 7-2: General view of the CFB biomass fast pyrolyser

The various pieces of equipment (except for the CFB reactor itself, the detailed description of which was already given in Chapter 4 as well as the feeder and liquid recovery systems discussed in Chapter 6) are described in the following sections, as summarised in Table 7-1.

Table 7-1: Subsidiary components of the fast pyrolysis unit

- Feedstock preparation system	Section 7.2
- Feeding system	Section 7.3
- Air-Nitrogen supply and reactor preheating system	Section 7.4
- Solids recovery system	Section 7.5
- Heat exchanger	Section 7.6
- Data acquisition and gas analysis	Section 7.7

7.2 Feedstock preparation system

The size of biomass feedstock is a major parameter for the fast pyrolysis process, as the particle size is restricted by limitations imposed by heat transfer, as discussed in Section 2.7. Some researchers suggested feedstock sizes in the order of a few hundreds μm (Scott and Piskorz, 1982), while others (e.g. Lidén, 1985) based on both theoretical findings and experimental work, suggested that biomass particles may be successfully pyrolysed in high heat transfer environments, provided they are smaller than 2 mm. More recently Graham (1995) claimed that particle sizes of up to 6 mm have been utilized in the Ensyn transported bed system (see Section 3.6).

Biomass was initially purchased from wood finishing stores, wood processing workshops, carpenters shops and furniture warehouses and was sieved by hand, a procedure which proved very dusty and time consuming. In view of the requirements for batches of uniformly sized feed of up to 50-100 kg per run, a more automated and reliable feed preparation system was required. The system developed consisted of a continuous feeder coupled to a set of vibro screen separators, as summarised in Figure 7-3. The technical characteristics of the sieving system (vibro screen separators) are listed in Appendix 5.

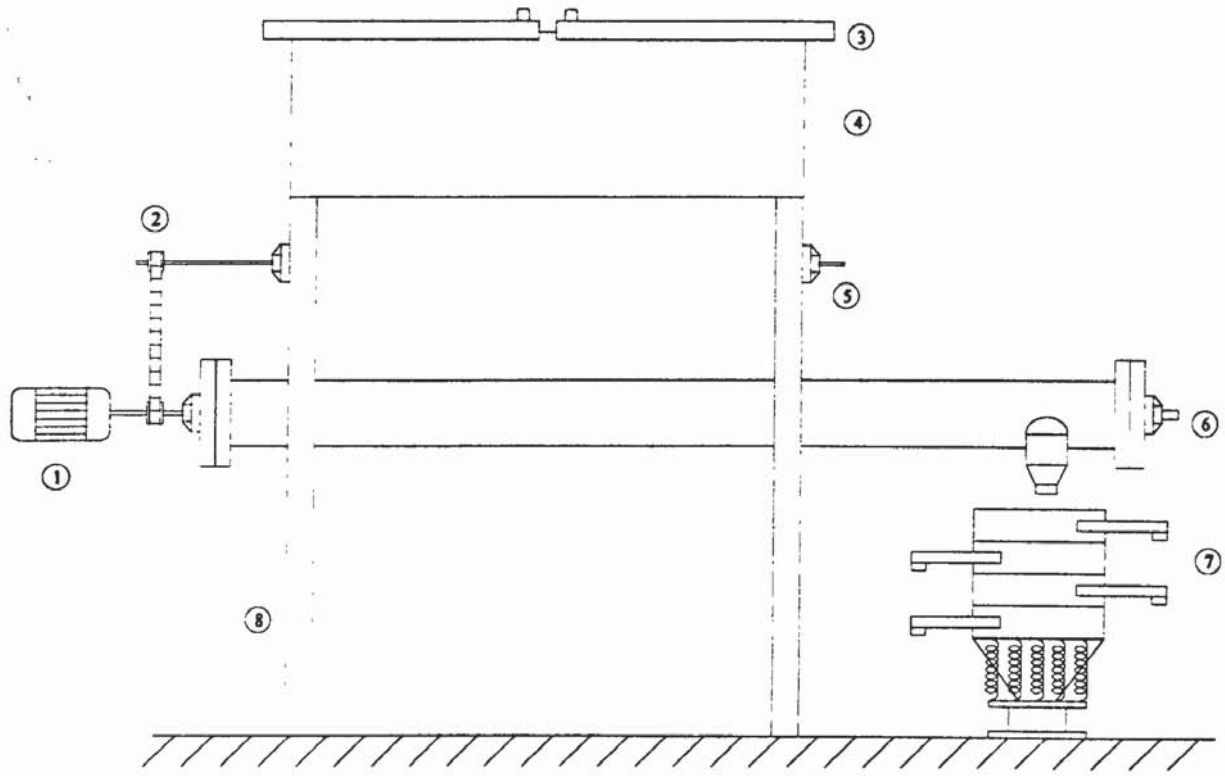

Figure 7-3: The raw biomass feeding/sieving pretreatment system

(1-motor, 2-drive chain, 3-raw biomass feeder lid, 4-raw biomass silo, 5-stirring shaft, 6-screw conveyor to shaft, 7- sieve separators, 8-raw biomass silo supporting legs)

The raw biomass feeding silo was constructed taking into consideration the following aspects:

- specific capacity (approximately 150 kg per batch)
- space availability (limited)
- climatological conditions (humidity, temperature)
- construction cost (low budget)
- construction simplicity and easy maintenance (minimum)
- feeding demands of the sieves (on/off feeding should be practiced).

Another factor that was taken into consideration during the raw biomass feeder design and construction, was the fact that the special physical properties of biomass, resulting in development of internal shear stresses leading to compaction in the feeding screw, makes its handling difficult. Given the large angle of repose of the feedstock (approximately 90° according to Maniatis, 1986) and hence its tendency to form regularly persistent bridges in the conical part of the angled silo (1), an internal stirring mechanism (2) keeping the material always agitated was installed, the rotating shaft of which was coupled to that of the screw

conveyor (3). This screw fed the raw material directly into the sieving device through the silo discharge (4). Taking all these considerations into account, a rectangular silo was designed and constructed, its large sides forming an edge after a certain point, Figure 7-4.

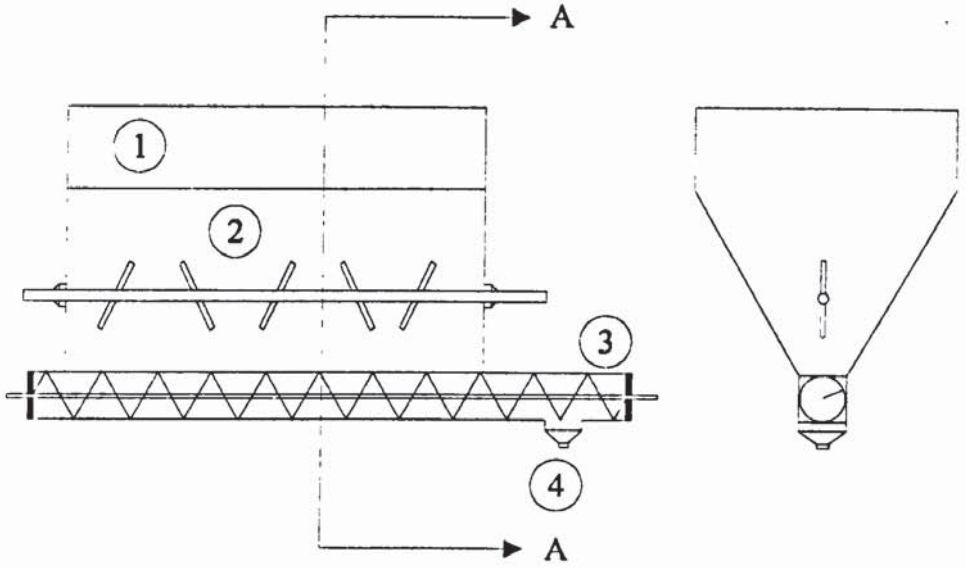

Figure 7-4: Side view and cross section of biomass feeding silo
(1-raw biomass feeder silo, 2-stirring mechanism, 3-screw conveyor, 4-raw feedstock discharge to sieving equipment)

The right dosing, and hence full exploitation of the sieving system capacity, of raw biomass to the sieves was controlled through an electric motor (1) with variable rotating speed. This motor, Figure 7-3, drives, as discussed above, both the raw biomass feeder discharging screw as well as the stirring device shaft through an appropriate chain coupling.

The combined raw biomass feeding/sieving system proved very reliable, since no bridging of the material in the raw biomass silo has been encountered, and much less time consuming than the manual operation practiced in the initial stages of biomass preparation. For example, using the above biomass preparation system about 100 kg of biomass were classified in one day, whereas it would have required at least 8-10 days to perform this task manually.

7.3 Biomass feeding system to the CFB reactor

In order to ensure smooth, reliable and relatively accurate feeding of the material, screened as above, into the pyrolysis reactor, a proper feeding system had to be designed and tested. The feeding system had three main objectives:

- free movement of dry biomass feedstock to avoid problems such as bridging and non uniform flow
- accurate metering
- rapid transfer to the reactor to avoid premature pyrolysis.

The objectives were met by the feeding system design shown in Figure 7-5.

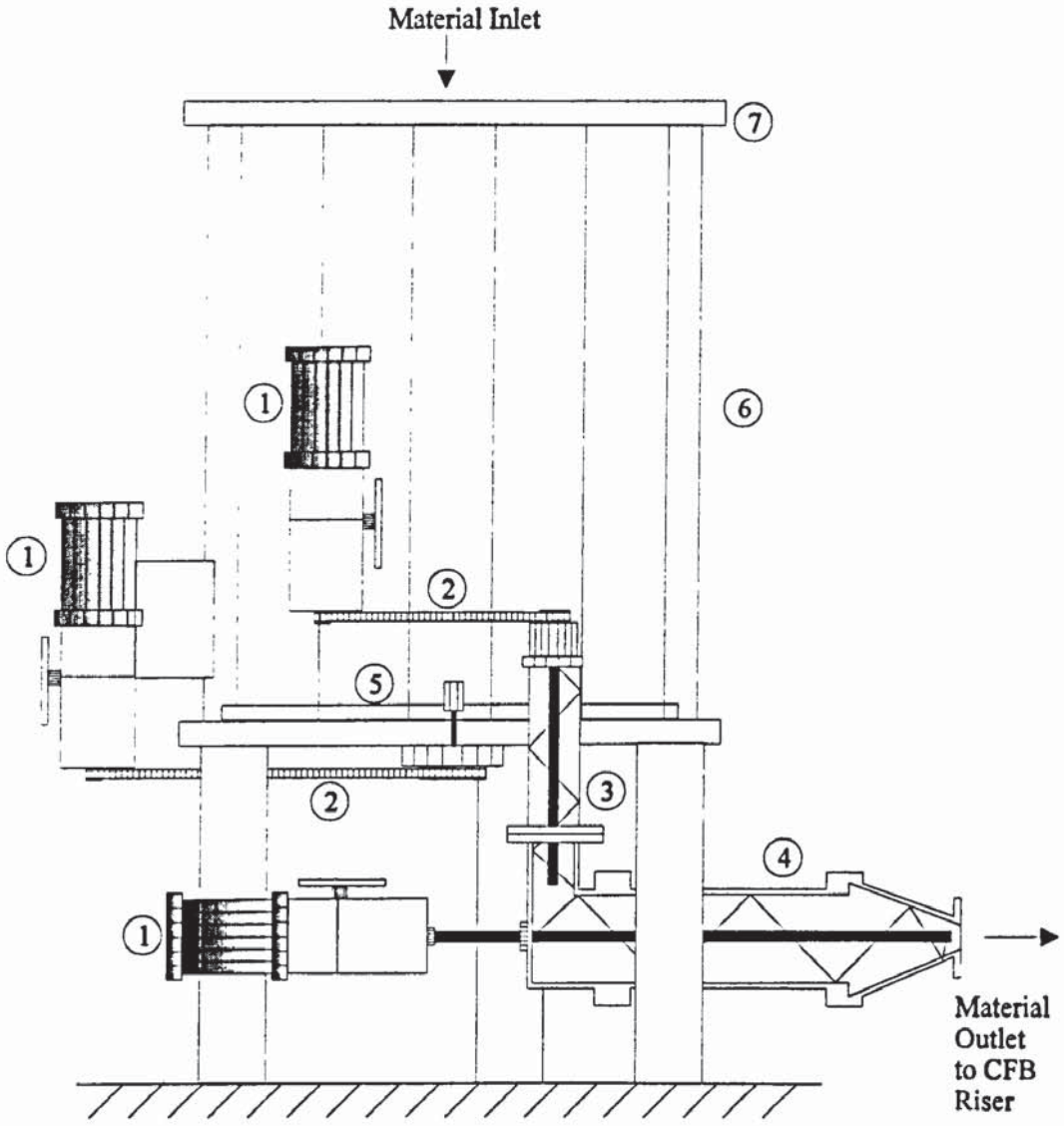

Figure 7-5: Layout of the biomass feeding system (not to scale)
(1-control devices, 2-driving chains, 3-metering screw, 4-transport screw, 5-stirring device, 6-buffer hopper, 7-hopper lid)

A detailed analysis of feeding system troubleshooting, commissioning and calibration procedures are given in Chapter 6. The main conclusions were:

- variations in the agitator speed result in slight changes in biomass flowrates (provided constant speed of metering and transport screws)

- the metering screw speed is the key determinant of biomass flowrates to the CFB reactor
- for a given metering screw speed, the transport screw delivers almost identical biomass flowrates over a wide speed range, when both the agitator and transport screw operate at constant speed.

The procedure adopted for feeding biomass to the CFB reactor was to run the internal stirring device at a moderate speed (held at approximately 60 rpm), while maintaining a high speed (above 120 rpm) on the transport screw and varying the speed of the metering screw, to achieve the desired biomass flowrate. Two typical calibration curves versus metering screw speed for two different feedstock sizes are presented in Figure 7-6.

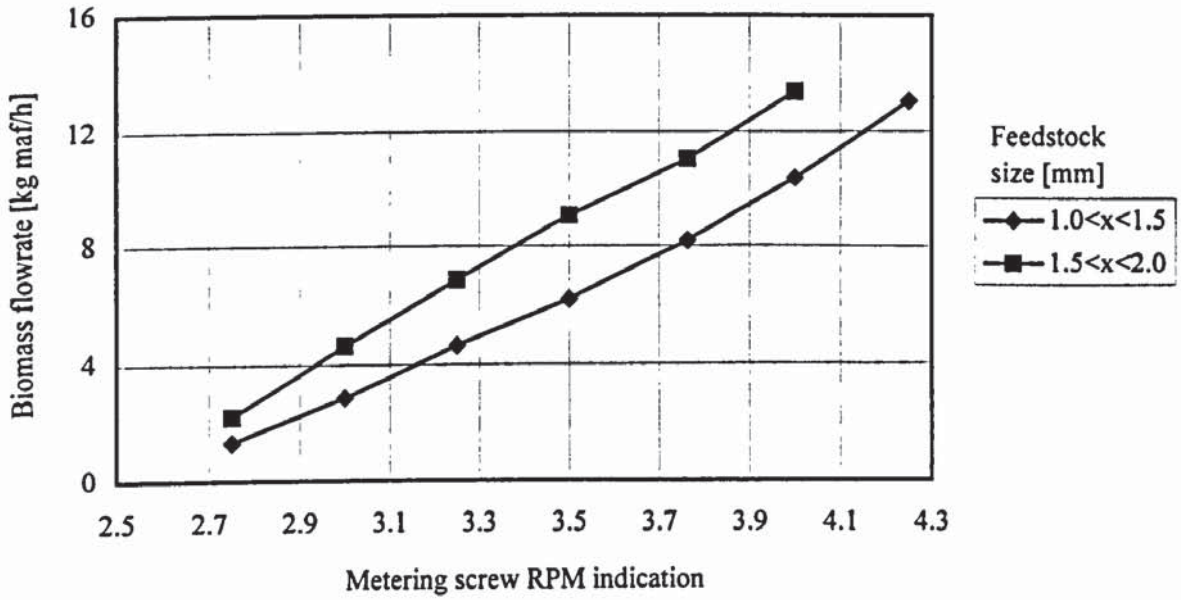

Figure 7-6: Feeding system calibration for two different feedstock sizes

7.4 Air-Nitrogen supply and reactor preheating

7.4.1 Air and nitrogen supply to the CFB reactor

Fluidising air was provided to the CFB combustor by an air-compressor, located outside the main building. Aeration gas (nitrogen) to the standpipe (L-valve) was provided by a high pressure nitrogen cylinder. In order to control nitrogen usage during start-up and reactor preheating, air was used at these times to aerate the standpipe by introducing an air flow-splitter to the air line and inserting a three-way valve between the air and nitrogen gas lines.

The air to the combustor was preheated in a Carbolite electrically heated ceramic oven. A separate air line, bypassing the air preheater, was also incorporated for steady-state operation,

when air could be safely fed cold to the hot char combustor. However, this operation was never exercised for fear of temporary loss of fluidisation conditions for sand recirculation due to the sudden change of air flow. Reduction of preheating oven temperature was practiced instead. The whole arrangement of the gas supply and preheat system is shown in Figure 7-7.

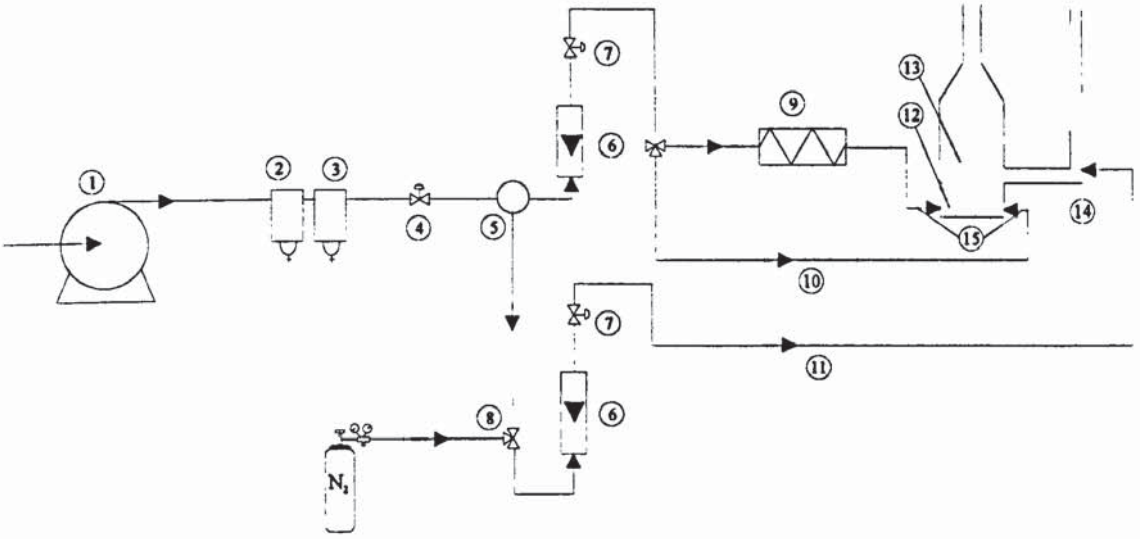

Figure 7-7: Arrangement of the gas supply/preheat system
(1-air compressor, 2-water filter, 3-oil filter, 4-pressure regulator, 5-flow splitter, 6-rotameter, 7-control valve, 8-3way ball valve, 9-preheating furnace, 10-heated line, 11-windbox, 12-combustion chamber, 13-L-valve, 14-fluidising gas inlet, 15-aeration gas inlet)

Air flowrate was measured by a rotameter (6), which was corrected for pressure and temperature. Flowrate was controlled by a high precision needle valve (7) located downstream of the rotameter.

However, the rotameter gave erroneous results, seriously underestimating air-flow to the combustor (by a factor of approximately 30 %), which in turn resulted in excess air being fed to the CFB reactor and promoting gasification. Moreover, the high air flowrates had as a result higher than designed gas velocities and operation in the lower end of pneumatic conveying regime of gas-solids two-phase flow, as depicted from Figure 4-3 (Grace, 1986) referred to in Section 4-3. This was remedied by the installation of a thermal mass flowmeter (Type FCI AF 8088) before the air rotameter, which was provided with a certified calibration curve, substantially improving air flowrate measurement accuracy.

Aeration gas (nitrogen) was not preheated, since its mass is insignificant to the mass flow of solids (G_s) through the L-valve to the combustion chamber, as indicated by the cold flow experiments, discussed in Chapter 5.

7.4.2 CFB reactor preheating

The gas preheating system proved inadequate to provide sufficient temperature (approximately 400-450°C) rise in the combustor prior to biomass feeding The temperature in the bubbling bed of sand never exceeded 300°C, even though the gas preheater was set to about 1000°C. Although the air feeding pipe was a multi passage arrangement to increase the residence time of gases in the hot furnace, this resulted in poor performance due to the high velocities of incoming air in the narrow (1/4") pipe. Thus, additional heat had to be provided by means of electrical resistances wrapped around the combustion chamber. Two (2) such coils were installed, capable of providing 6 kW and increasing the sand temperature to about 600°C at low fluidising gas flowrates.

Once the temperature in the combustor reached approximately 600°C, heat was transferred to the rest of the CFB unit by gradually increasing the fluidising gas flowrate (FGF), until the maximum FGF had been reached. This forces the solids to circulate along the entire reactor loop, effectively transferring the heat. The temperature profile versus time of operation in the different parts of the CFB reactor (combustor- indicated by thermocouple No TC3 and riser - by TCs 6, 10 and 15 and standpipe by TCs 23 and 24) are presented in the diagrams in Figures 7-8 and 7-9, respectively. The location of the thermocouples in the CFB loop is described in Section 7.7.1 below.

The diagrams presented below exhibit very clearly one of the CFB's main features, namely its ability to transfer heat by circulating the heated solids around the entire reactor loop. The overall procedure for start-up comprises two stages, as follows:

1. Preheating the sand in the bubbling bed/combustor chamber by electrically heating the fluidising gas and the combustor reactor walls up to approximately 600°C at low gas flowrates.
2. Gradually increasing the fluidising gas velocity-FGF and adjusting properly the SCR (by gradual increase of the aeration gas flowrate-AGF) to transfer heat to the entire CFB reactor loop.

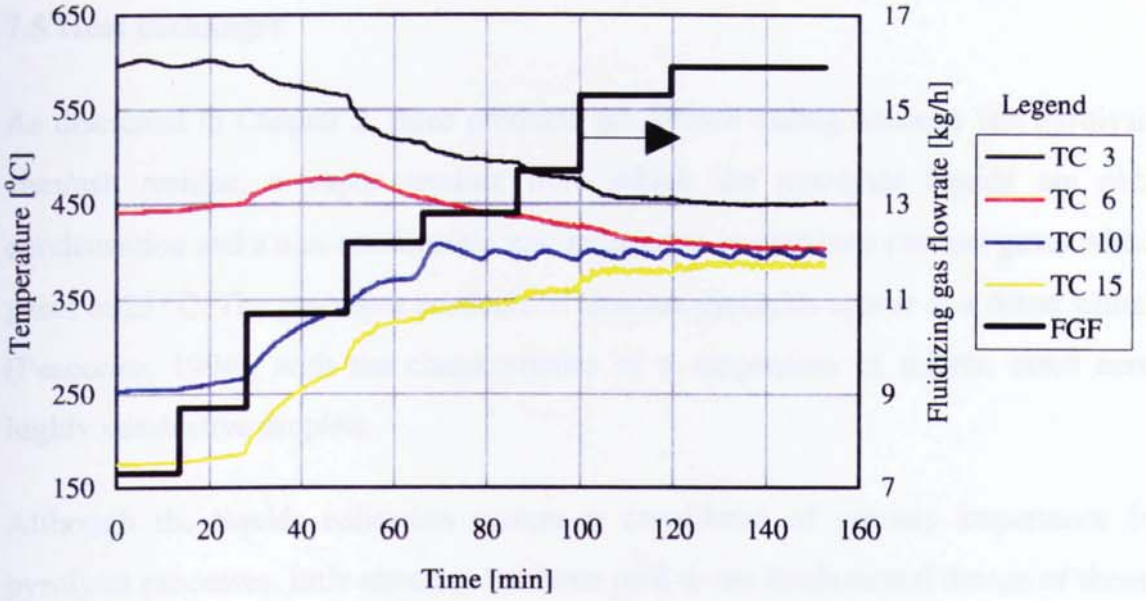

Figure 7-8: Temperature profile in the combustor and riser (TCs 3, 6, 10 & 15) versus FGF

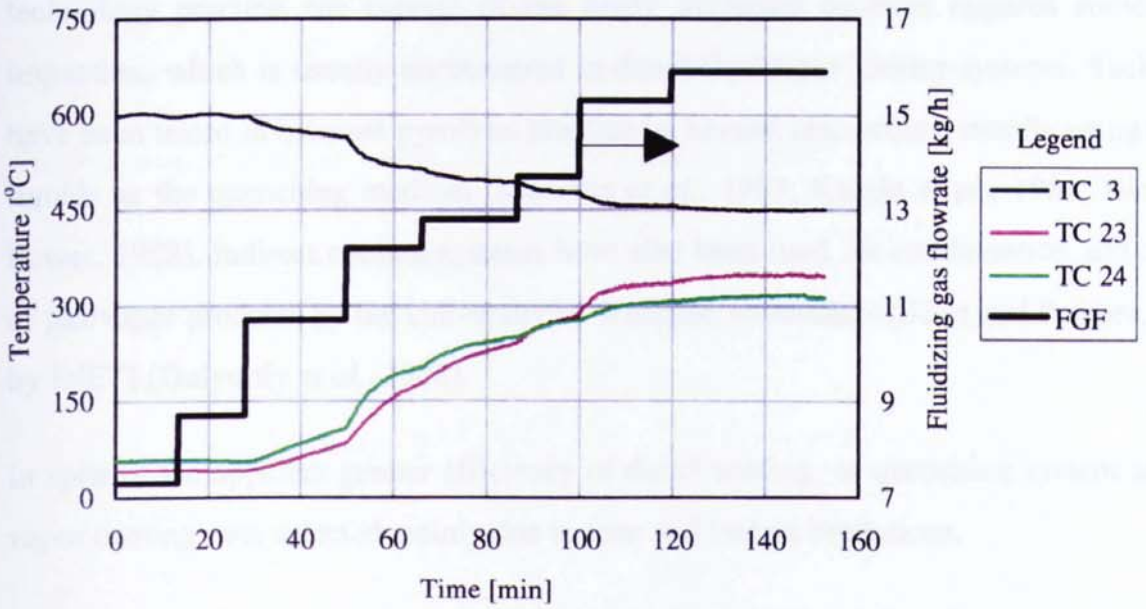

Figure 7-9: Temperature profile in the combustor and standpipe (TCs 23 & 24) versus FGF

As seen from the above diagrams, the overall heat-up period takes approximately 3.5-4.0 hours. This is distributed as approximately 1.5-2.0 hours for the first stage, i.e. the heat-up of the bubbling bed to 600°C, which is not shown in the above diagrams, and 2 hours for the second stage, i.e. the transfer of heat by solids circulation to the entire reactor loop. After the desired temperatures had been attained in the different parts of the CFB reactor, feeding of biomass could begin. Biomass feeding procedures are discussed in Section 8.8.2.

7.5 Heat exchanger

As discussed in Chapter 2, three products are formed during biomass fast pyrolysis: a solid char/ash residue, a vapor product from which the pyrolysis liquids are obtained by condensation and a non-condensible gas, referred to as pyrolysis product gases which exist as gases at 25°C. The gas/vapor products of biomass pyrolysis appear as a dense white "smoke" (Peacocke, 1994), with the characteristics of a suspension of micron sized aerosols and highly conductive droplets.

Although the liquids collection system is considered of primary importance in all fast pyrolysis processes, little attention has been paid to the fundamental design of these systems, which in turn results in poor collection efficiencies. Although gas/vapor products can be adequately cooled at sufficiently high rates by techniques readily available in chemical technology practice, the capture of the finely dispersed aerosols requires some form of impaction, which is usually encountered in direct liquid-gas contact systems. Such systems have been tested in biomass pyrolysis practice by several researchers, usually using pyrolysis liquids as the quenching medium (Maniatis *et al.*, 1993; Knight *et al.*, 1981; Diebold and Power, 1988). Indirect cooling systems have also been used for condensation and collection of gas/vapor products by the University of Waterloo researchers (Scott and Piskorz, 1984) or by INETI (Gulyurtly *et al.*, 1988).

In spite of the apparent greater efficiency of direct cooling or quenching system an indirect vapor cooling was selected mainly due to time and budget limitations.

A vertical, shell and tube heat exchanger (condenser) was designed and constructed, in a configuration similar to that used initially in the University of Waterloo bench scale fast pyrolysis plant (Scott and Piskorz, 1984, Section 3.4.2) or INETI (Gulyurtlu *et al.*, 1988). Information concerning the thermal load to be removed by the shell-and-tube heat exchanger may be found in Section 6.5. The heat exchanger, which was installed vertically is depicted in Figure 7-10.

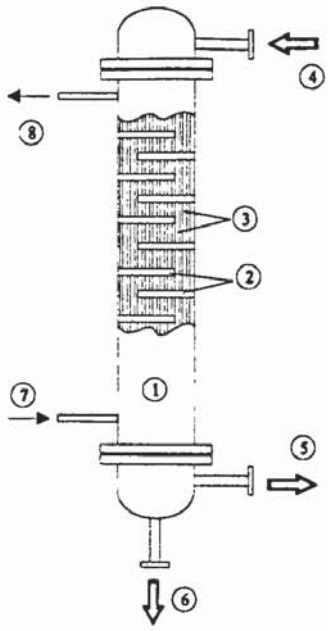

Figure 7-10: Shell-and-tube heat exchanger

(1-shell, 2-baffles, 3-tubes, 4-hot gas inlet, 5-cooled gas outlet, 6-pyrolysis liquids, 7-cooling water inlet, 8-cooling water outlet)

The heat exchanger main design data are presented in Table 7-2.

Table 7-2: Heat exchanger design data

Heat exchanger shell i.d.	[mm]	220
Heat exchanger hell o.d.	[mm]	228
Number of tubes/shell		140
Tube i.d.	[mm]	18.05
Tube o.d.	[mm]	21.35
Tube length	[m]	1.3
Tube pitch		Triangular
Number of baffles		12
Baffle cut		25 %
Baffle spacing	[mm]	100

7.6 Instrumentation and data acquisition system

In order to obtain information about temperatures, pressure drops, flows, etc., both the CFB cold model and the hot reactor were equipped with the appropriate instrumentation. More specifically, the following items were included:

(a) flow meters for measuring gas and water flow rates

(b) thermocouples throughout the system to allow measurement of temperature profiles

(c) pressure transmitters measuring both absolute pressures at various points and pressure drops overall at different intervals of the CFB reactor system.

(d) on-line gas analysers as well as a Gas Chromatography (GC) system.

The data acquisition system consisted of a Data Logger, namely a Keithley 706 Scanner with 10 plug-in modules (cards) for mV-mA measurements, a Digital Multimeter (DMM), namely a high precision Keithley 6½ digits Multimeter, and an IBM-compatible PC with a 50 MHz Intel processor, all instruments communicating through a General Purpose Interface Board (GPIB) based on IEEE protocols. The operational software was developed in Turbo Pascal. The data acquisition block diagram is presented in Figure 7-11.

The output from the thermocouples, the pressure transmitters, the thermal mass flowmeter and the gas analyzers are scanned by the data acquisition system every 25 seconds and converted to a form ready to be transferred to a spreadsheet for further processing and analysis.

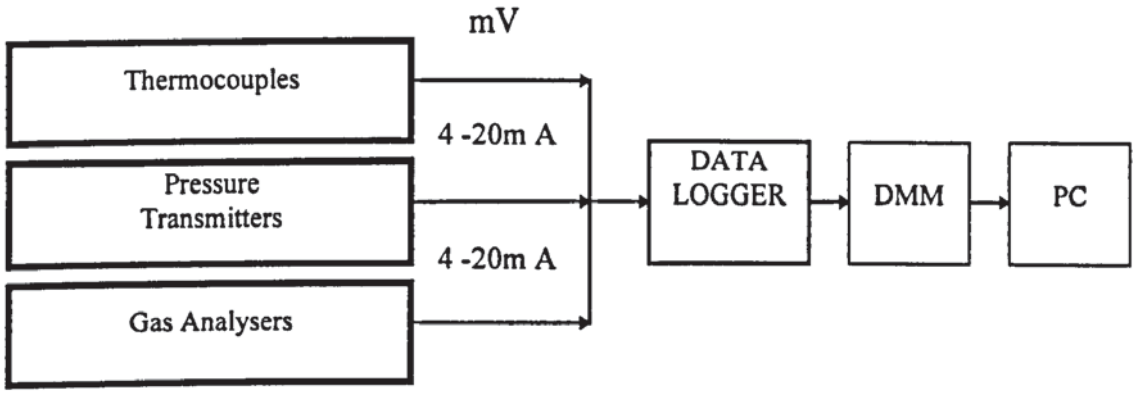

Figure 7-11: The data acquisition block diagram

7.6.1 Temperature measurements

The initial positions of the thermocouples along the CFB reactor loop are presented below in Figure 7-12.

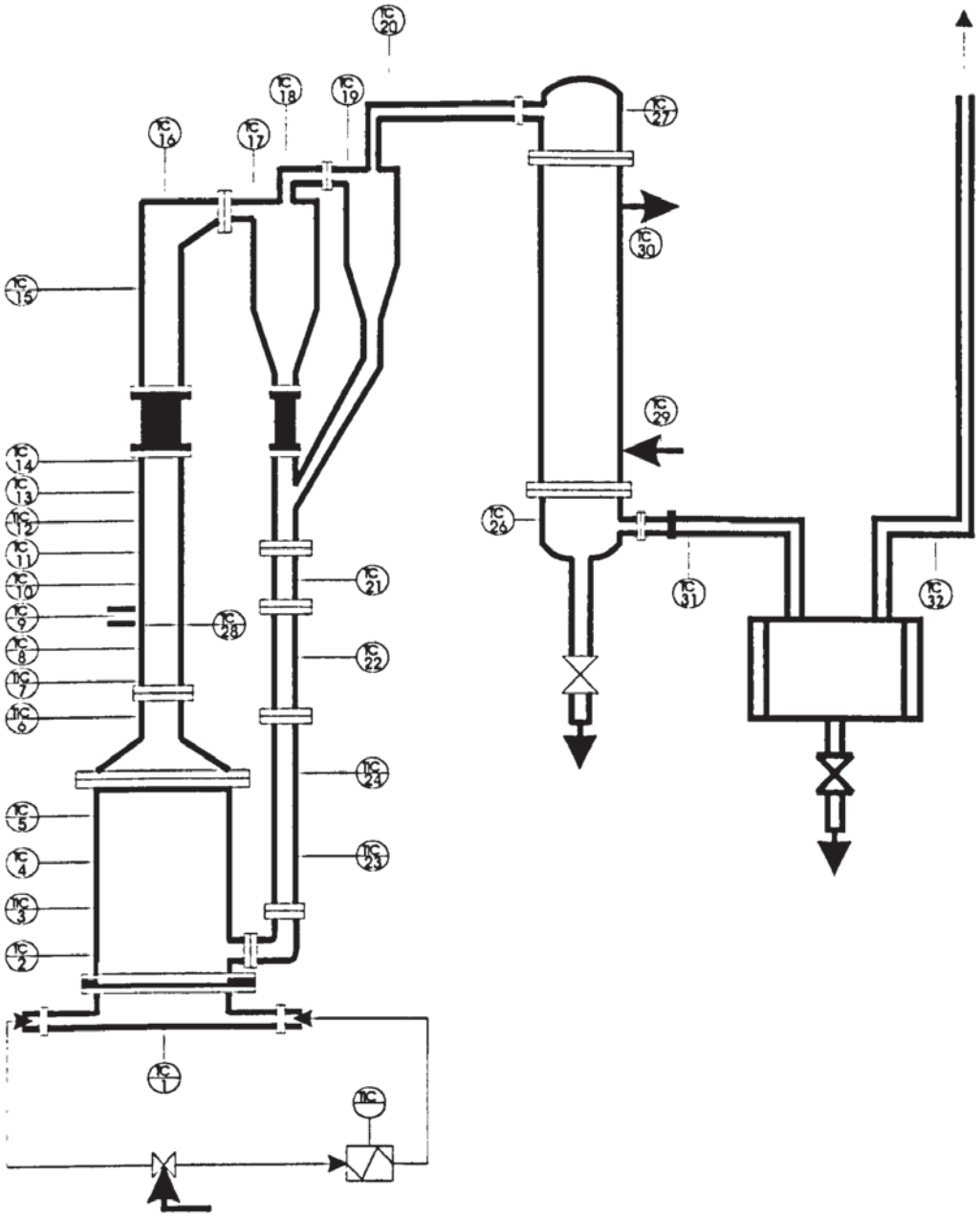

Figure 7-12: Thermocouples (TCs) location around the CFB pyrolysis pilot plant (the symbols and their significance have been denoted in Figure 7-1)

Temperatures are measured by 27 Type-K thermocouples and 4 Type-T thermocouples (TCs). The temperature measurement outputs are provided in millivolts (mVs) and are converted to degrees C through the software and communication protocol.

7.6.2 Pressure measurements

Eight pressure transmitters (PTs), Type Fischer-Rosemount 1151 DP, of different ranges for both pressure drops and absolute pressure measurements have been installed around the CFB reactor loop. The pressure measurement outputs are given in milli-amp (mA) and are converted to mmWG through the software and communication protocol. The positions of the pressure transmitters is shown in Figure 7-13.

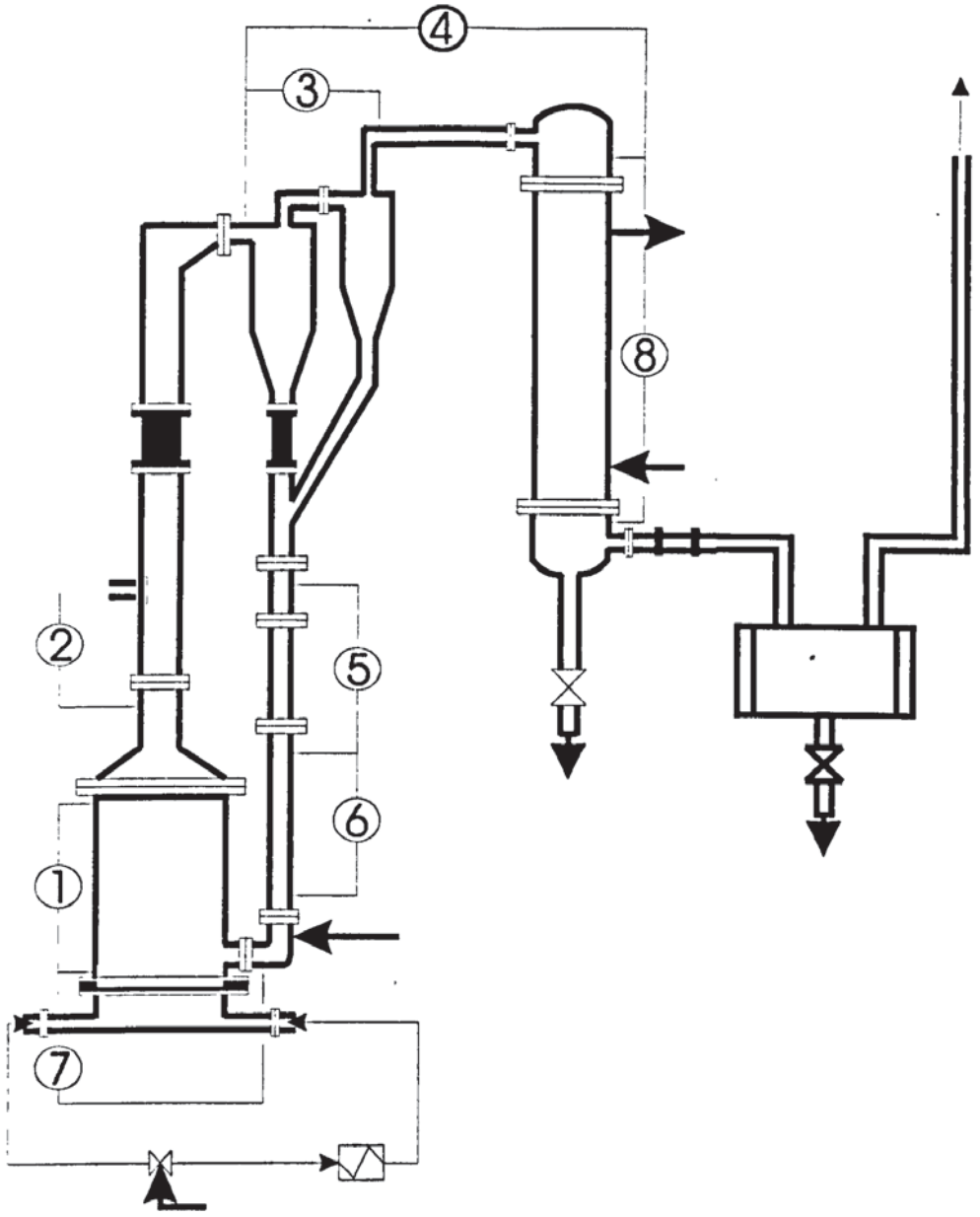

Figure 7-13: Pressure transmitters (PT) location around the CFB pyrolysis pilot plant (the symbols and their significance have been denoted in Figure 7-1)

7.6.3 Heat tracing elements

In order to minimise the start-up times, additional heat was provided to the different parts of the CFB loop by means of electrical resistances, as discussed above in Section 7.4.2, wrapped around the combustion chamber, riser and standpipe length as shown in Figure 7-14.

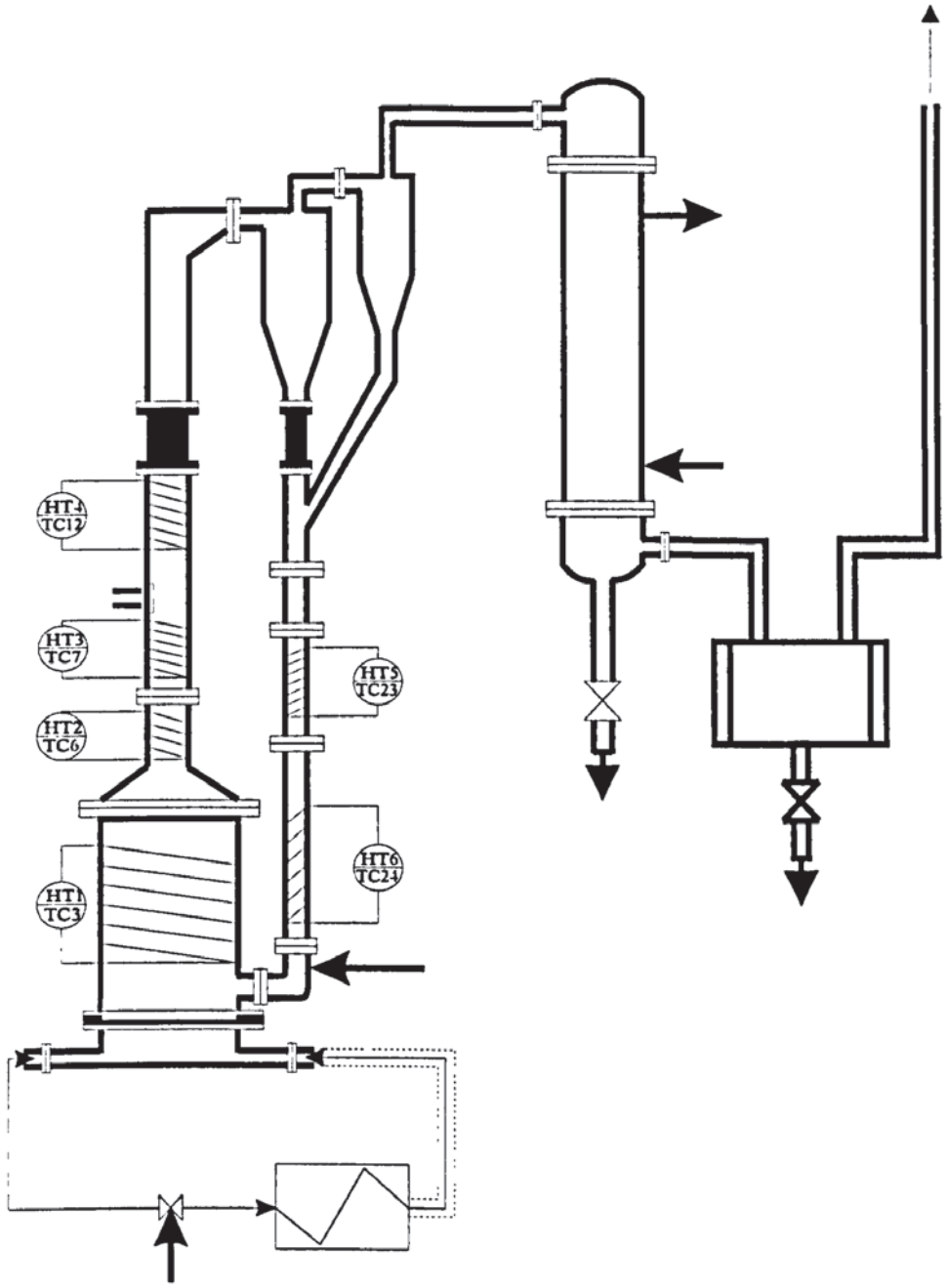

Figure 7-14: Heat resistances location around the CFB pyrolysis pilot plant (the controlling TCs are also shown, while the symbols and their significance have been denoted in Figure 7-1)

In addition, fluidising and aeration gas flowrates as well as water flowrates are measured via gas rotameters. The fluidising gas flowrate (FGF) was measured by a Thermal mass flowmeter, described in Section 7.4.1, the output of which (mA) was converted to kg air/h through the software and communication protocol.

7.6.4 Gas analysis

The dry pyrolysis gases were analysed by two methods: continuously (by on-line gas analysers) and batch-wise sampling (GC analysis). The on-line analysis allowed variation in the gas composition with time to be monitored. The gas analysers, purchased from Rosemount Analytical, were installed in the last series of experiments, Chapter 9. These analysers detected CO, CO_2 and ethylene (infrared), O_2 (paramagnetic) and H_2 (thermal conductivity). The analyser signals (mA) were converted to volumetric concentrations (% v/v) through the software and communication protocols.

In order to compare the on-line analyses during steady state operation batch sampling on a Gas Chromatography system, type Perkin Elmer 8700, was periodically carried out. The GC was equipped with a Thermal Conductivity Detector (TCD) and the column configuration selected for the analysis consisted of:

- a 2 m long, copper Molecular sieve 13X packed column, and
- a 4 m long, stainless steel Chromosorb 106 packed bed column.

The Chromosorb 106 column was used to analyse light hydrocarbons and CO_2, eluting the rest of the gases as a single peak. After passing the Chromosorb 106 column the gas mixture was diverted to the Molecular sieve 13X column, where the determination of CO, O_2, N_2 and H_2 could be performed.

7.7 Summary

The equipment and the analytical procedures during the biomass fast pyrolysis plant start-up and operation were presented and their function in the entire plant operation analysed. The performance of the different pilot plant components described in this chapter, is further discussed during the actual experimentation programme, presented in Chapters 8 and 9.

CHAPTER 8: IDENTIFICATION AND REMEDIATION OF OPERATIONAL PROBLEMS

8.1 Introduction

In Chapters 6 and 7 a detailed description of the fast pyrolysis bench scale plant components was given. During the bench scale plant commissioning experiments described in this chapter, a number of problems were encountered, the most important being those of solids separation from the gas/vapor stream and liquid recovery. This chapter is structured as follows:

- experimental programme, Section 8.2
- identification of problems, Section 8.3
- problems associated with solids recovery and separation system and measures taken, Section 8.4
- discussion on the char and ash problem, Section 8.5
- problems associated with liquid recovery and measures taken, Section 8.6
- other minor problems in peripheral equipment, Section 8.7
- summary of the commissioning and steady-state experiments as well as the development of the start-up procedure for reliable CFB operation, Section 8.8.

8.2 Experimental programme

During the actual experimental programme, two distinct series of experiments were carried out each with different objectives:

- The first series of experiments were commissioning experiments. The first four experiments in this series were conducted in order to establish operational experience and identify problems. Two additional commissioning experiments were held to take account of operational aspects concerning standpipe stability as well as adopt a proper start-up procedure for the CFB experiments. Table 8.1 summarises this programme.
- The second series of experiments, which were the main body of experiments, followed small but essential modifications in order to carry out prolonged runs at steady-state, conduct gas analyses and derive good mass balances. This series comprised of five experiments, reported in Chapter 9.

Table 8-1: Summary of experimental programme (first series of experiments)

Run No	Biomass feeding procedure	Run objectives
R1, R2	Continuous biomass feeding at design value. Intermittent biomass feeding was exercised with flowrate set at design value	Problems associated with gas-solids separation, standpipe stability, liquid recovery and data acquisition.
R3, R4	As above (R2)	Single temperature recordings.
R5, R6	Continuous biomass feeding gradually increasing to design value	Standpipe stability & establishment of the proper start-up procedure.

8.3 Problems identification

The initial system configuration was as described in Chapter 7, and is shown in Figure 8-1.

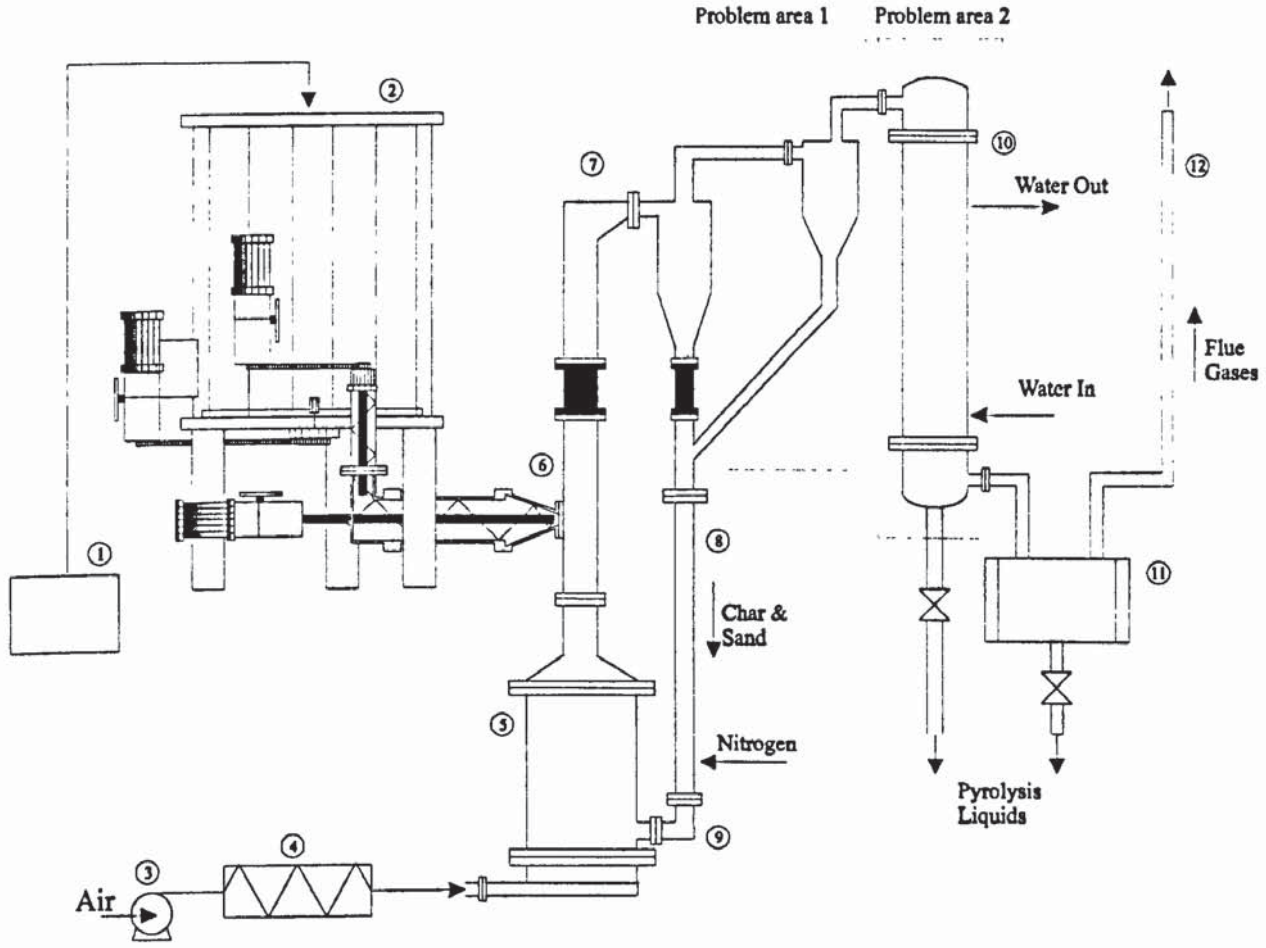

Figure 8-1: Biomass fast pyrolysis bench scale plant and problem areas

(1-feedstock preparation, 2-biomass feeder, 3-air compressor, 4-air preheater, 5-char combustor, 6-biomass pyrolysis riser, 7-solids recovery system, 8-standpipe, 9-L-valve, 10-heat exchanger, 11-dewar vessel, 12-gas to vent)

The major problem associated with the biomass fast pyrolysis system, at least in its early stages of development, was that its evaluation was mostly based on short-term, non steady-state, reduced capacity runs. Hence, most of the equipment was not at full design load conditions during these experiments, which did not permit the evaluation of system performance or the derivation of mass balances. Instead, valuable information was obtained and problems were identified and removed. The commissioning runs identified a number of significant problems that are described in the following sections. The most problematic areas, Figure 8-2, proved to be the solids separation, discussed in Section 8.4, and the liquid product recovery, discussed in Section 8.6. These and other minor problems encountered during the commissioning experiments are summarised in Table 8-2.

Table 8-2: Problems identification and solutions during the commissioning experiments

Problem	Solution	Run No	Section
Poor gas solids separation (1)	Addition of a third cyclone (from run R4 onwards)	R1, R2, R3	Section 8.4
Heat exchanger (HE) plugging	Replacement of HE with water-cooled pipes (from run R4 onwards)	R1, R2, R3	Section 8.6
Standpipe instability	Tests in the cold flow model	R1, R2, R3, R4	Section 5.5
Poor gas-solids separation (2)	Addition of an inertia impinger separator	R4	Section 8.4
Loss of condensibles	Installation of HE & two cyclonic condensers after HE	R4	Section 8.6
Lack of proper start-up procedures	Adoption of the proper feeding procedure	R1, R2, R3, R4	Section 8.7
Problems with data acquisition	Change of communication protocols and software- hardware	R1, R2, R3, R4	Section 8.8
Problems with gas analysis	Replacement of gas sampling pump. Modifications in the GC	R5, R6	Section 8.8
Unreliable mass balance closures	Installation of a gas by-pass line prior to steady-state	R5, R6	Section 8.6
Loss of light organics	Replacement of glass condensers with cotton-wool filter	R5, R6	Section 8.6

8.4 Solids recovery and separation system

This section describes the development of a successful solids recovery and separation system. The principal role of this part of the unit was to capture the char and sand escaping the riser (pyrolysis zone) and recycle them through the standpipe to the L-valve and back to the bubbling fluidised bed combustor, where the sand is reheated.

CFB cyclones are subjected to much higher solid concentrations and temperatures from those often prevailing in most chemical processes. In systems employing high solids circulation, such as circulating beds and pneumatic reactors, the entrainment of fines (char and sand in this case) may be a serious problem. Hence, the solids capture device adopted must have a fairly high collection efficiency to avoid loss of sand from the system and contamination of the product liquids.

According to the discussion held in Section 5.3 on solids recovery configuration for the CFB reactor, a system comprising two cyclones in series, shown in Figure 5-8, which proved effective in cold flow experiments, was selected, designed, constructed and installed. Although this system performed well during cold model experiments, its performance proved poor during hot reactor operation, as further discussed in the following.

8.4.1 The two cyclones in series solids recovery and separation system

To account for the fines losses in the CFB reactor, a two-stage cyclone system, as reported in Section 5-3, was initially adopted. This first version of the solids recovery system, consisted of two cyclones in series (denoted in the following as $2C_{ser}$) with the second cyclone discharge feeding directly into the standpipe, as shown in Figure 8-2, as practiced by Lurgi GmbH (Mehrling and Reimert, 1986).

This $2C_{ser}$ configuration was used in the commissioning runs R1, R2 and R3 respectively, see Tables 8-1 and 8-2. Its performance during the testing phase, i.e. CFB reactor operation in the hot mode but without biomass feeding, proved satisfactory, in the sense that only very small amounts of sand particles were carried over to the heat exchanger, as verified after dismantling and checking the heat exchanger tubesheet.

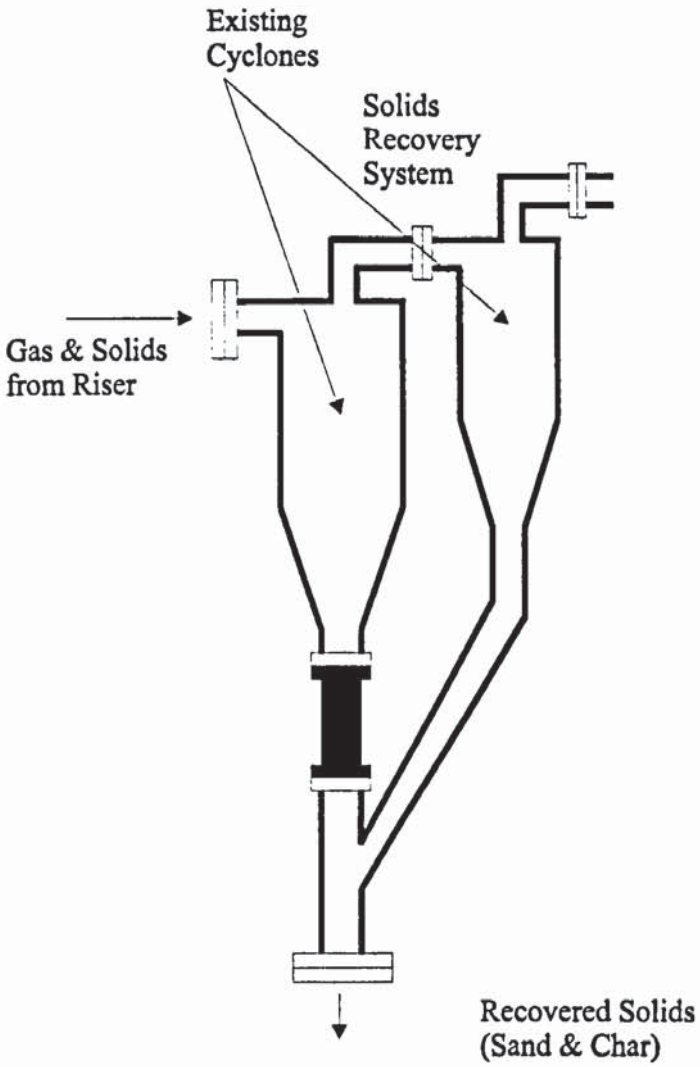

Figure 8-2: The first version of the CFB solids recovery and separation system (consisting of two cyclones in series, configuration $2C_{ser}$)

In the first series of experiments (Runs R1, R2 and R3) during biomass feeding to the CFB reactor, loss of solids circulation in the CFB reactor was encountered, resulting in necessary system shutdowns.

At the time this problem was attributed to the poor performance of the $2C_{ser}$ configuration to capture the fine char particles, combined with the inadequate performance of the shell-and-tube heat exchanger. Thus, it was concluded that the material escaping the solids recovery system was accumulating in the heat exchanger, causing a gradual pressure drop downstream of the $2C_{ser}$ configuration. This, in turn, affected standpipe pressure build-up, resulting in packed bed flow conditions in the standpipe and a subsequent loss of solids circulation in the CFB system (for further discussion of this effect see Section 5.5.5).

8.4.2 The three cyclones in series solids recovery and separation system

In order to further protect the heat exchanger and capture the fines (char and sand) escaping the $2C_{ser}$ configuration, a third high efficiency cyclone was added with an isolated solids receiver (char catchpot), where fine solids could be captured leaving the gaseous stream relatively free from particulates that could promote heat exchanger plugging. This resulted in the second version of the CFB solids recovery and separation system, which consisted of three cyclones in series. This is shown in Figure 8-3 and denoted as Configuration $3C_{ser}$.

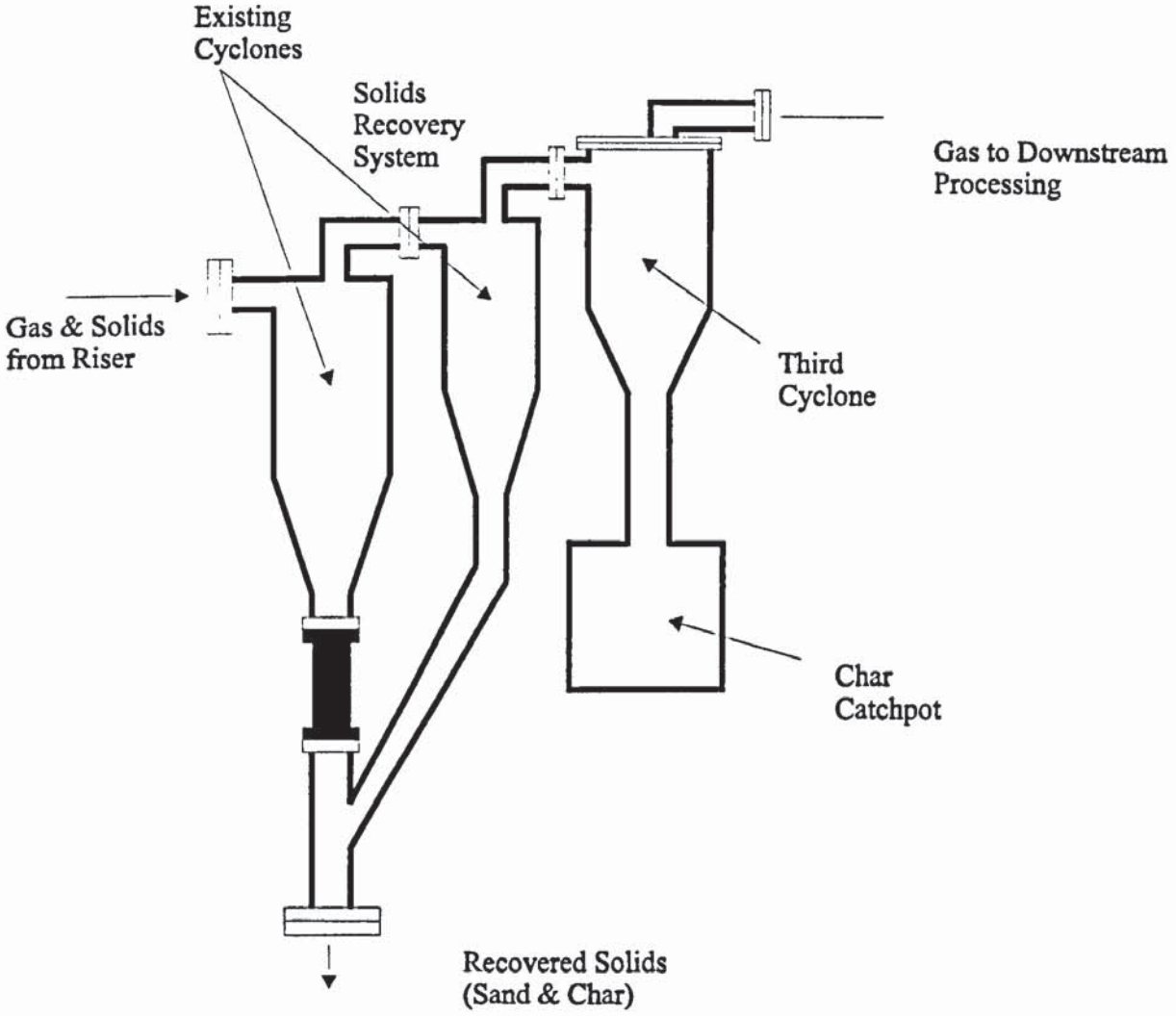

Figure 8-3: The second version of the CFB solids recovery and separation system (consisting of three cyclones in series, configuration $3C_{ser}$)

This $3C_{ser}$ solids recovery configuration was used in conjunction with a modified gas/vapor recovery system (discussed below in Section 8.6.2), consisting of three wide water-cooled pipes, which was used to replace the heat exchanger, in experiment R4. This run was also characterised by severe standpipe instabilities about 30 minutes after biomass feeding in the modified gas/vapor recovery system.

8.4.3 Reasons for standpipe plugging in the commissioning phase

In order to try to explain the observed standpipe instabilities and establish the cause for this phenomenon, which resulted in unsteady CFB reactor operation, runs R3 and R4 were closely examined as shown in Table 8-3.

Table 8-3: Examination of system failure and probable cause for standpipe instabilities

Run	Solids recovery	Liquid recovery	Possible cause	Identified cause
R1,R2, R3	Two-cyclones in series ($2C_{ser}$)	Shell-and-tube heat exchanger (HE)	1. $2C_{ser}$ plugging 2. HE plugging	Both components found plugged
R4	Three-cyclones in series ($3C_{ser}$)	Three water-cooled pipes	1. $3C_{ser}$ plugging 2. HE plugging	Only $3C_{ser}$ found plugged

This indicates that the problem lies between the different components of the solids recovery and separation system configuration, since upon inspection and dismantling of both this and the liquid recovery systems in run R4, it was only the solids configuration system, i.e. the $3C_{ser}$, that was found plugged.

It was concluded that the problem of both cyclone configurations ($2C_{ser}$ and $3C_{ser}$), was having a common outlet to the first two cyclones, which both discharged solids to the upper standpipe. This common outlet caused inadequate gas sealing, with some gas from the first cyclone flowing to the outlet duct of the second cyclone, in an opposite flow to that of the solids recovered from the second cyclone. This counterflow of gas and solids disturbed the formation of the vortex generated in the second cyclone thus reducing its collection efficiency (configuration $2C_{ser}$, Figure 8-2). Moreover, the fine char particles captured by the first cyclone tended to re-entrain in the second one, with the cumulative effect that the solids escaping the second cyclone blocked the entrance of the third one causing the plugging referred to above (configuration $3C_{ser}$, Figure 8-3).

8.4.4 Remedy to eliminate the solids recovery and separation system problems

One possibility to solve the problems referred to above was to revert to a single cyclone, but this is impractical because of the high solids loading. Another was to add a second and third cyclone in series but hydrodynamically separate from the first one to avoid interaction. A third solution was to add a different type of solids capture device and also isolate this from

the first cyclone with an independent solids collection system. This last course of action was adopted in the following.

Thus, the second and third cyclones were both replaced by an inertia separator (impinger) placed directly after the first cyclone. The impinger comprised a conical vessel with a steel plate positioned along the cylinder vertical axis, perpendicular to the incoming gas/vapor stream. The solids escaping the first cyclone are carried over with the gases, impacted the impinger steel plate losing their momentum and fall down to the solids catch pot. Final withdrawal of solids from the impinger was accomplished via a two-valve isolation system, Figure 8-4. The internal diameter of the discharge piping was double, i.e. 2" (0.0508 m) that of the standpipe, to avoid accumulation of material during sudden, pressure upsets in the standpipe.

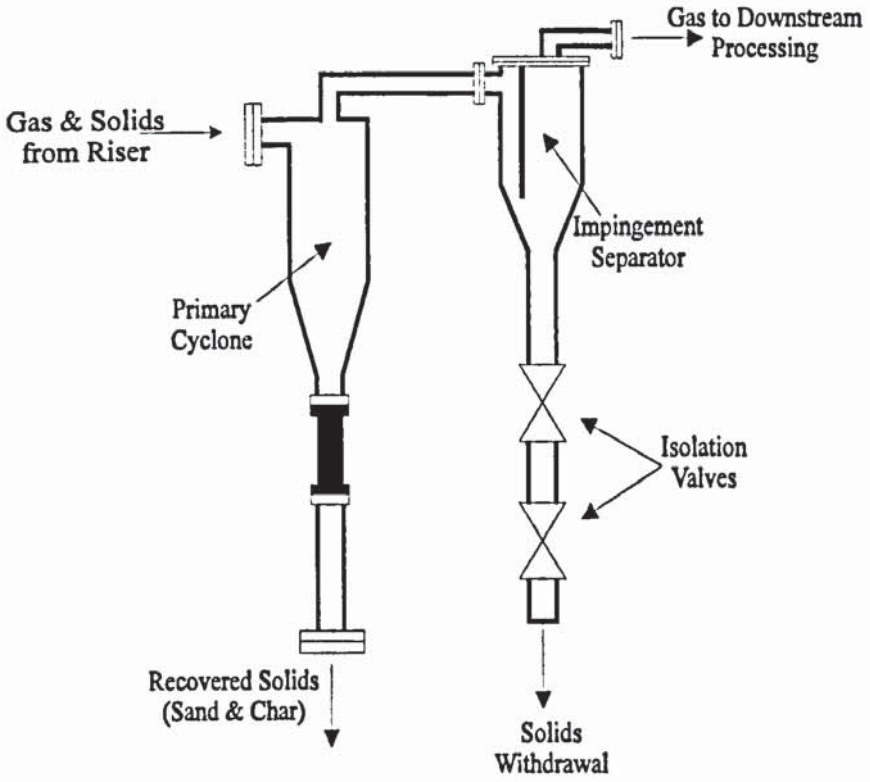

Figure 8-4: The third version of the CFB solids recovery and separation system (consisting of a single cyclone and impinger in series, configuration CI_{ser})

This cyclone and impinger in series configuration (denoted as CI_{ser}) was used in all the subsequent operational runs, i.e. during the commissioning runs R5 and R6 as well as the second series of experiments, Table 8-1. There were no problems subsequently associated with the CFB solids separation system. Unsteady sand circulation, standpipe plugging or similar flow interruptions encountered in the first four commissioning runs were not observed.

The CI_{ser} configuration efficiency to remove solids was measured in a separate experiment, which was conducted for two hours in the hot mode, i.e. without biomass feeding, the results of which are presented in Table 8-4.

Table 8-4: Solids removal efficiency for the stand-alone cyclone and the cyclone-impinger in series (CI_{ser} configuration) solids recovery and separation system (kg silica sand)

Initial Bed Inventory (IBI_b)	Final Bed Inventory (IBI_e)	Solids recovered by impinger (SR_{imp})	Solids entrained downstream
11.0	9.38	0.912	0.708

The solids removal efficiency, calculated as sand recovery, for this separate run is then given by:

$$Sand\ \text{Recovery}_{cycl} = \left\{1 - \frac{IBI_b - IBI_e}{IBI_b}\right\} = ... = 0.8527\ or \approx 85.3\%$$

$$Sand\ \text{Recovery}_{cycl+imp} = \left\{1 - \frac{IBI_b - \{IBI_e + SR_{imp}\}}{IBI_b}\right\} = ... = 0.9356\ or \approx 93.5\%$$

The conclusions drawn are that, with the solids recovery system consisting of a primary cyclone and inertia impinger in series three important improvements were achieved, namely:

- a 10% increase in solids capture efficiency (compared to a single cyclone configuration)
- a prolonged reactor operation
- less complexity (compared to the three cyclones configuration) and improved operability (CI_{ser} configuration less prone to plugging than the $2C_{ser}$ and $3C_{ser}$ ones).

Periodic losses of solids from the CFB were normally captured in the impinger and removed via the impinger withdrawal section. An alarm thermocouple in this part of the system warned for these unaccounted solids losses (the temperature rises quickly) and the solids recovered were removed manually via the two-valve isolation mechanism, Figure 8-4.

After the final solids recovery and separation arrangement was adopted, the section of the standpipe, where the outlets of the two cyclones (in the $2C_{ser}$ configuration, Figure 8-2) were connected, was substituted by a straight pipe. The standpipe then consisted of four flanged sections, which provided very simple during assembly and dismantling.

It was concluded that a simple system comprising of a cyclone and an impinger in series but hydrodynamically separated gave higher solids removal (by 10 % more than a single cyclone) and prolonged reactor operation.

8.5 The problem of char and ash removal

At this point an essential problem, common to all biomass thermochemical conversion processes, namely that of solids, such as char and ash, removal from the final product, i.e. pyrolysis liquids, will be discussed. The systems discussed below were not constructed or tested, but are suggested solutions to the problems identified.

The ash composition of biomass varies from approximately 0.5 % wt for most woods, including those tested in this thesis, to over 20 % wt for materials like rice hulls (Reed and Das, 1988). Ash has a two-fold effect on the process of fast pyrolysis as far as liquid product yields and composition are concerned:

1. Work carried out by Scott *et al.*, (1985) has shown that organic liquid yields dropped from 65 % wt (moisture free feed) in wood feedstocks at 0.6 % wt ash to 27.3 % wt at 11.0 % wt ash in corn stover for similar reactor parameters. These results are in accordance with those obtained by Gray *et al.*, (1984), where the ash is believed to catalyse the degradation of the primary vapors to char, water and gases with sodium (Na^+), present in the ash (approximately 13 % wt), thought to act as a gasification catalyst at fast pyrolysis temperatures.
2. Furthermore, sodium (Na^+) and potassium (K^+) compounds are particularly harmful in turbine applications, where they accelerate hot corrosion of the turbine blades and also contribute to deposition and cementing on the blades (Bain, 1991). Alkali, particularly sodium compounds, can also pose technical problems in long-term internal combustion (diesel engines) applications.

In addition to ash fine char also escapes the solids removal system, through entrainment in the gas/vapor stream in the downstream processing equipment.

Although the char has a high heating value per unit weight (about 50% more than the oxygenated organic liquids), char in the pyrolysis liquid severely lowers its value for the following reasons (Diebold *et al.*, 1994):

a) the solid char settles slowly over time, leading to sludge formation in the bottom of the storage vessel
b) the solid char increases the apparent viscosity of the liquids, which can lead to the fouling of condensers during the production of pyrolysis liquids (discussed in Section 8.6 below)
c) the solid char could plug the orifices of some burners and lead to difficulties in atomisation and smooth combustion
d) the burning characteristics of the solid char are different than those of pyrolysis liquids.

Moreover, the char has approximately seven times higher ash and alkali metal content than the original biomass feedstock, which could damage boilers and turbines, as well as require expensive flue gas clean-up equipment.

As a consequence of the above discussion it is apparent that there exists a need for improved char and ash removal from the pyrolysis vapor stream to reduce both the deleterious effects of ash, as far as pyrolysis liquids yields and quality are concerned, and to eliminate char from the product liquids to improve their characteristics for subsequent end-use applications.

In the following a series of measures is suggested to reduce char and ash content in the pyrolysis vapors and, hence, in the final product liquids.

8.5.1 Biomass pretreatment to reduce the ash content

As reported above, ash, in particular sodium (Na^+) and potassium (K^+) salts, has very significant effects on the chemical composition of pyrolysis liquids (Radlein, 1991) favouring the yields of levoglucosan by a factor of 10, reducing the yields of hydroxyacetaldehyde as well as amounts of low molecular weight species by a factor of 27. Moreover, these cations are concentrated in the liquids recovered causing problems in their subsequent utilisation.

Biomass pretreatment with acid washing (temperatures around 100°C and H_2SO_4 5 % wt for a period of 2 h) effectively removes the alkali metals and hence reduces the ash content, so that practically no cations of Ca^{2+}, Na^+ and K^+ are found in the pyrolysis liquids.

8.5.2 Hot gas filtration to remove char and ash in the vapor phase

Particulates, like fine char and sand as well as fly ash may also be removed by incorporating hot-gas filtration, i.e. gas cleaning at temperatures above 400°C. Particulates are removed in

barrier filters, which consist of a porous media (with distinct filter and cake surfaces) which intercepts dry, non-sticky, entrained solids from a gas stream. These filters may be further categorised as metallic, ceramic and baghouse filters.

Metallic filters have structural integrity but their commercial utility has historically been restricted by temperature and chemical resistance limitations (Simons *et al.,* 1983; Bain, 1991). Alkali concentrations of less than 0.024 mg/Nm^3 (20 ppb) have been reported, this level exceeding the typical 1.2 mg/Nm^3 (1 ppm) turbine constraint.

Ceramic filters are temperature- and chemical- resistant but can suffer structural failure, particularly at the seal/filter seams, during temperature cycling (Clift, 1983; Larson and Svenningsson, 1990; Bain, 1991). They are particularly effective for the removal of dry solids with particle sizes in the range of 0.5 to 100 μm. A 99 % removal rate has been given for plus 0.5 μm particle size (Brown *et al.*, 1988). The two most common configurations are the crossflow and candle ceramic filters.

Baghouse filters are technically feasible, but in practice are limited by temperature and the capital costs that are associated with relatively large surface area requirements. They also exhibit fouling when exposed to tars, and require special handling and disposal of the accumulated tar material.

Ongoing development at NREL has shown that a customised baghouse, using flexible, woven NEXTEL ceramic bags made by 3M or rigid stainless steel filters made by MEMTEC achieved very high char and alkali removal efficiencies, reducing ash concentration in the pyrolysis liquids from 6.0 % wt (60000 ppm) to 0.01 % wt (100 ppm). However, the liquids alkali reduction achieved by hot gas filtration is counteracted by lower liquid yields due to the long residence times and the heterogeneous secondary cracking reactions in the hot filter surface area (Diebold *et al.*, 1994).

8.5.3 Char and ash removal directly from the bed material

According to this approach a continuous removal of sand, along with a portion of the char and ash, from the bottom of the combustion chamber may be used, by means of a water-cooled screw conveyor, Figure 8-5. The continuous process shown below is a proposal and was not constructed or tested.

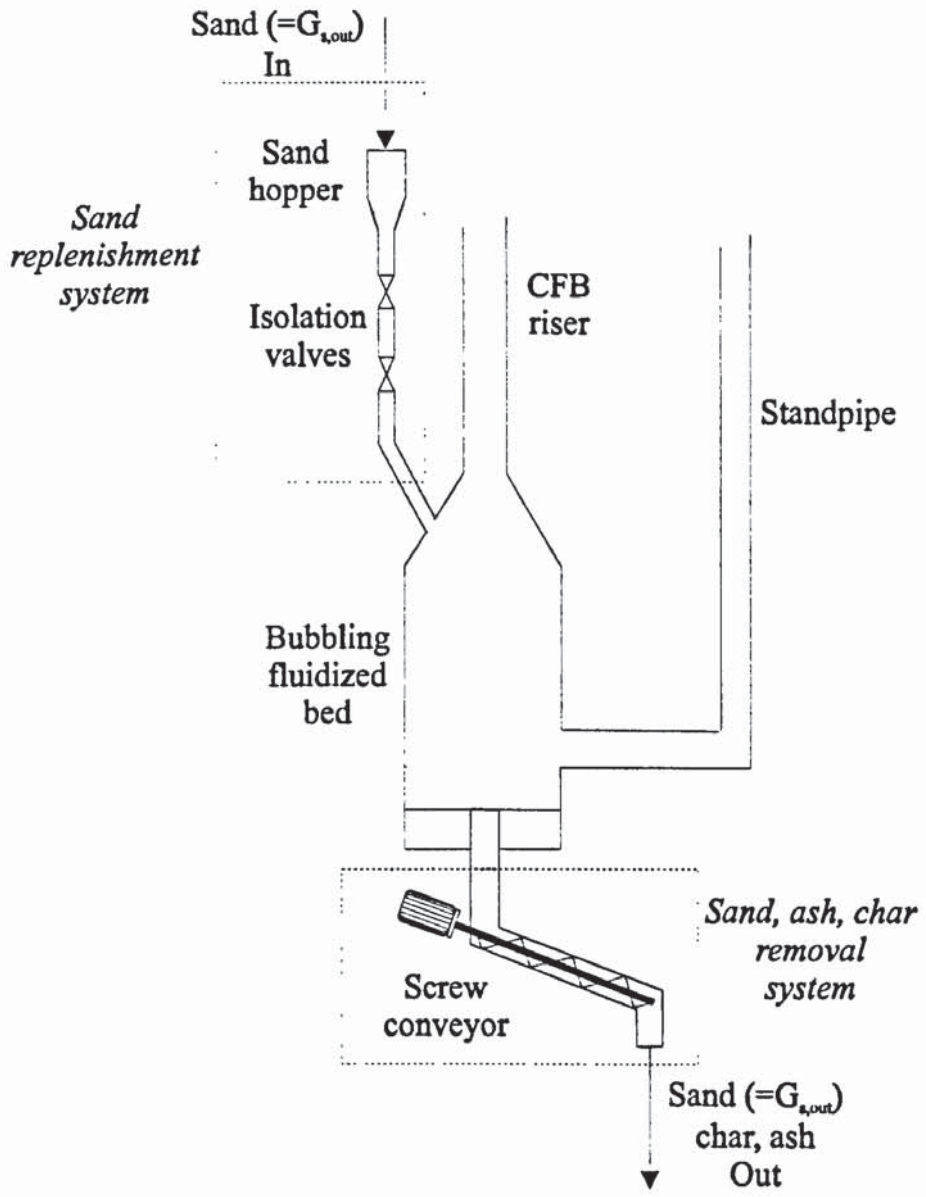

Figure 8-5: Proposal for a continuous process for the removal of char and ash from the CFB reactor (bubbling bed not in scale)

In the same time, the heat carrier subtracted from the bed is replenished regularly by means of a dosing sand hopper. In this way, there is a balance of sand in the CFB reactor, while the char and ash are continuously removed and, hence, do not accumulate in the bubbling bed material. Subsequently, char and ash are entrained with the inert solids and gases up the riser section at a much lower rate.

8.6 Gas/vapor product recovery system

Indirect cooling of pyrolysis vapors may serve as a solution to the problems of easy liquid handling and more direct mass balance closures, but it is hardly a rational way to achieve high collection efficiencies as already discussed in Sections 6.5 and 7.6 (Peacocke, 1994).

The recovery of the pyrolysis liquids is not a simple condensation process and rapid cooling of the product vapors leads to the formation of stable aerosols and micron-size droplets, possibly with polar molecules bonded onto the surface of water droplets. These aerosols readily escape collection in most of the indirectly used systems for heat exchange and may be captured effectively only in systems incorporating some form of impingement, such as a scrubber or a spray column.

The shell-and-tube heat exchanger and Dewar vessel configuration (denoted simply as HE) as designed, Section 6.6, proved quite efficient in removing the heat load from the gaseous stream, but did not succeed in actually collecting the liquids, which formed a fine mist entrained by the non-condensable gases and escaping collection.

In the following, the different configurations tested for liquid recovery as well as the problems associated with each of them are discussed in detail.

8.6.1 Shell-and-tube heat exchanger and Dewar vessel

The main problem for prolonged reactor operation in the commissioning phase (runs R1 to R4) was, besides those of solids recovery, see Section 8.4, that of tube plugging in the shell-and-tube heat exchanger. The occurrence of heat exchanger fouling is described below.

Since there was a significant temperature gradient through the heat exchanger tube walls (hot on the incoming gas/vapor mixture-tube side and cold on the circulating cooling water-shell side), the heavier molecular weight, high boiling point compounds are condensed on the inner, cold tube surfaces, and in slowly moving downwards, not only decrease the effective tube free area but also reduce heat removal from the gas/vapor flow. This undesirable effect of heavy tars has also been observed by Scott and Piskorz (1983) in their hot condenser, where the condensing liquids flew only with difficulty and apparently were fairly reactive. After this thin film of heavier organics along the tubes inner surface has been formed, solid fine char, feedstock ash and lighter sand particles escaping the solids recovery system adhere to it, forming sticky liquid-solids agglomerates and reducing further the area for free gas/vapor flow. The undesirable effects of these mechanical/physical processes were:

- the reduction of heat transfer coefficient between gas/vapors and cold tube surfaces
- the subsequent generation of a significant pressure drop along the heat exchanger
- a significant loss of heavy organics and hence a reduction in both liquids yield and quality (expressed as increased water content, lower density liquids).

The decrease of the gas/vapor stream heat removal could be observed in the gradual increase of the gaseous stream outlet temperature leaving the heat exchanger (temperatures increased gradually from 20-25°C in the beginning of a run towards to 40-45°C by the end of the run) and resulting in further loss of low molecular weight compounds, which escape collection and recovery in subsequent steps (Scott and Piscorz, 1983).

8.6.2 Water-cooled pipes

In order to prolong pyrolysis experiments as well as avoid premature downstream equipment plugging, the shell-and-tube heat exchanger was removed and a simple recovery system consisting of three 38.1 mm i.d., 1.5 m long, vertical, water-cooled, parallel pipes, followed by a Dewar vessel was installed. The gas entrance to this configuration (denoted as WC_{pip}) was heat traced in order to avoid premature vapor condensation of pyrolysis vapors. The modified liquid recovery system is shown in Figure 8-6 and was used in run R4.

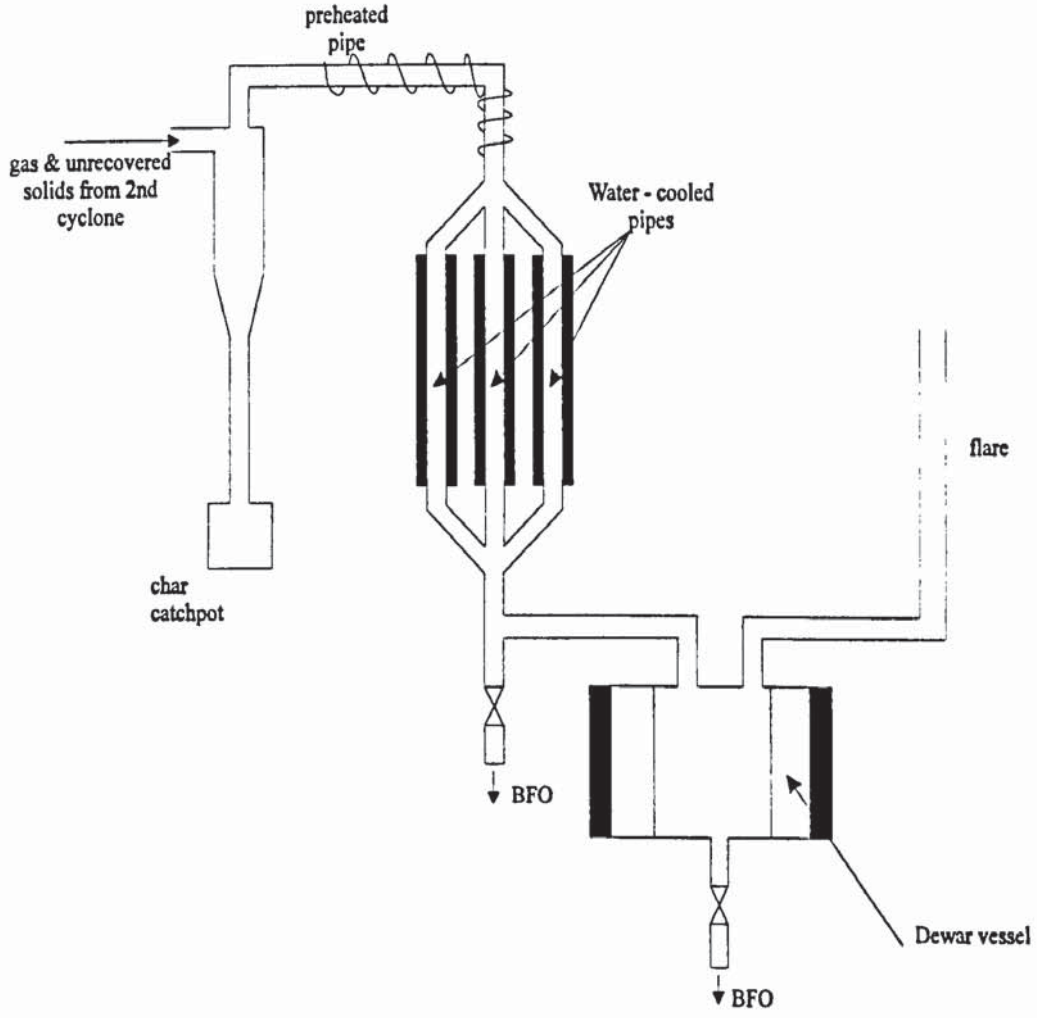

Figure 8-6: Modified gas/vapor recovery system (WC_{pip})

However, and despite the resistance of this wider diameter system to plugging, the WC_{pip} recovery configuration did not provide adequate cooling to the gaseous stream, proving in this sense much inferior to the shell-and-tube heat exchanger. This was due to the very short gas/vapor residence time within this system, and the passage of the bulk of the gas through the central tube, which was clearly insufficient to cool down the incoming gas/vapor stream (temperatures of about 130-150°C were recorded at the outlet of the water-cooled pipes).

Moreover, this system proved more troublesome in terms of assembly and cleaning than the previously installed shell-and-tube heat exchanger.

8.6.3 Shell-and-tube heat exchanger in conjuction with two cyclonic condensers

Due to the problems referred to above and considering the positive impacts of the solids recovery system modifications, provided by the CI_{ser} solids recovery configuration discussed in Section 8.3.4, would have on system operability and performance, the use of the shell-and-tube Heat Exchanger (HE) was once more justified. Thus, in the two last commissioning runs (R5 and R6) as well as all the steady-state runs (runs R7 to R11) the indirectly water-cooled HE was used as the main component for the collection of the pyrolysis liquids.

Furthermore, to improve the collection efficiency of the pyrolysis liquids in the last two commissioning runs (R5 and R6), two cyclonic-type ice-cooled glass condensers replaced the ineffective, in terms of liquid collection, Dewar vessel, providing a second stage of cooling. These two condensers were designed (Peacocke, 1994), manufactured and connected in series, after the HE. Cooled product vapors entered the first condenser at 35-45°C and then passed a U tube, connecting the two condensers, where they were collected as liquids. Remaining cooled and stabilised vapors and aerosols then entered the second condenser.

The pyrolysis droplets constituting a fine mist, were forced into a vortex movement (through a tangential gas inlet) as they entered the first condenser and condensed, while coming in contact with the chilled, glass walls. The condensate ran through the bottom of the first condenser, filling the condensers' interconnection tube. The vapors not fully recovered were then forced to coalesce through the liquid phase, which acted as a wet scrubber enhancing heat and mass transfer and improving the condensation of the unrecovered vapors. The other collection points for pyrolysis liquids were located each at the base of each condenser. After this second stage of cooling, the pyrolysis gas was vented to the atmosphere through the flare

pipe. This modified downstream equipment (denoted as HECC), is shown in Figure 8-7 and was used in runs R5 and R6.

Unfortunately, this system did not prove superior in performance to the first one, Section 8.6.1, using the heat exchanger and Dewar vessel configuration. Only small quantities of liquids could be recovered from the bottom of the cyclonic condensers. Moreover, HECC cleaning proved extremely difficult and occasional breaking, associated with the glass condensers, increased significantly this system's operating cost. Although the CI_{ser} solids recovery configuration provided much better protection of the HECC downstream configuration, fine solids were still being deposited on the tubesheets of the heat exchanger, so that the solids-liquids agglomerates discussed before were still a nuisance, even though to a lesser extent.

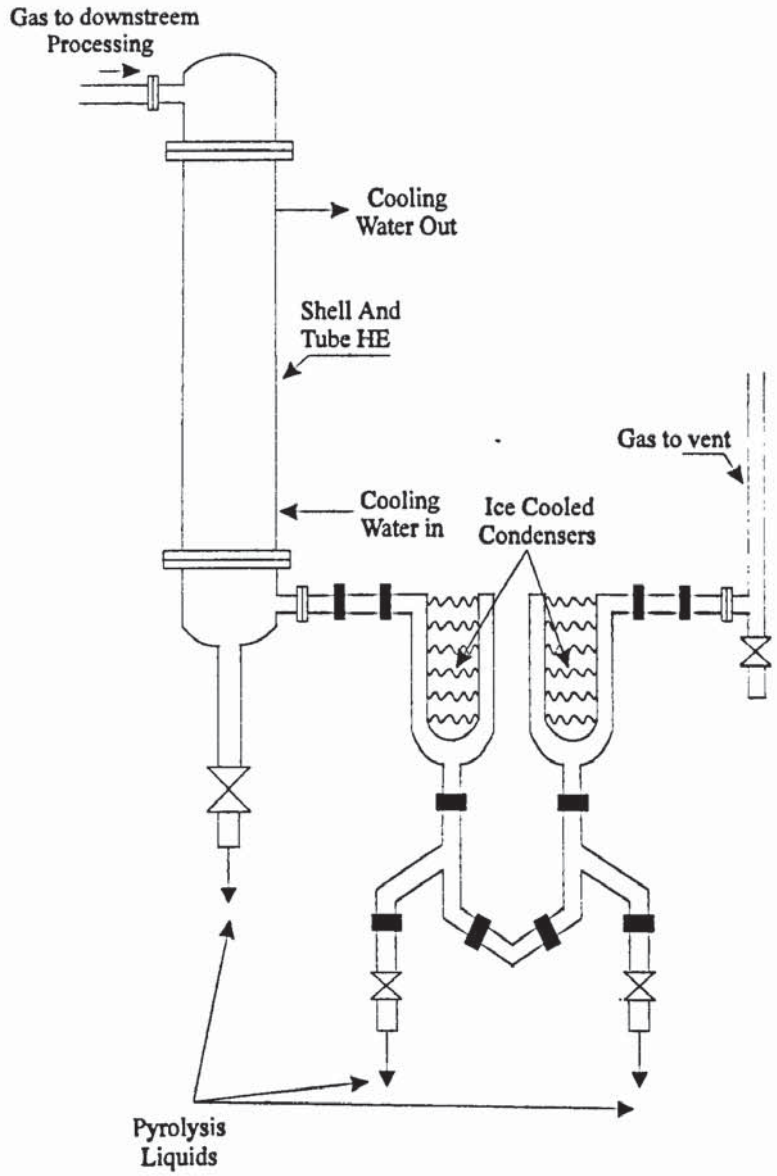

Figure 8-7: The modified downstream processing equipment incorporating the heat exchanger and two cyclonic condensers (HECC configuration)

8.6.4 Shell-and-tube heat exchanger in conjunction with a cotton-wool filter and a gas/vapor by-pass line

After a long period of commissioning and steady-state experiments, it was concluded that for proper start-up, the CFB reactor must undergo a gradual heat-up, the process passing through successive steps of combustion, gasification and pyrolysis (a procedure further discussed in Section 8.7). Adopting such a procedure would lead to measures in order to overcome a common disadvantage of all the liquid recovery configurations tested at that time, namely their inadequacy to collect the liquids generated during the pyrolysis mode of operation, excluding all other liquids generated during the gradual heat-up. Hence, reliable mass balances based on pyrolysis liquid yields as well as evaluation of reactor performance, as far as maximisation of pyrolysis liquids yields, could not be drawn up accurately.

In order to overcome this obstacle, it was finally decided to include a downstream equipment by-pass line, so that during reactor heat-up all gases and vapors were vented to the atmosphere. Once steady-state (or near steady-state) conditions prevailed in the CFB reactor (steady-state indicated by approximately constant temperature along the CFB loop and constant product gas composition) the gas/vapors stream would be diverted to the downstream equipment. Along with the installation of the gas/vapor by-pass line, the fragile ice-cooled glass condensers were substituted by a cotton wool filter, after which the gases were vented to the atmosphere.

This configuration of the gas/vapor recovery system used in the main series of experiments runs and denoted as ByPass-HE configuration, proved very efficient in terms of

- operational simplicity
- prolonged reactor operation (experiments could be performed without any significant pressure build up in the heat exchanger for longer time intervals than in the commissioning series of experiments)
- derivation of good mass balances for actual steady-state conditions

as will be discussed in detail in Chapter 9.

From the above discussion, it may be concluded that bypassing the gas/vapor products during system start-up proved very efficient in protecting downstream equipment and carrying out meaningful mass balance closures. Moreover, the installation of a cotton wool filter

downstream of the heat exchanger provided an additional device for capturing the majority of the persistent aerosols escaping recovery and collection.

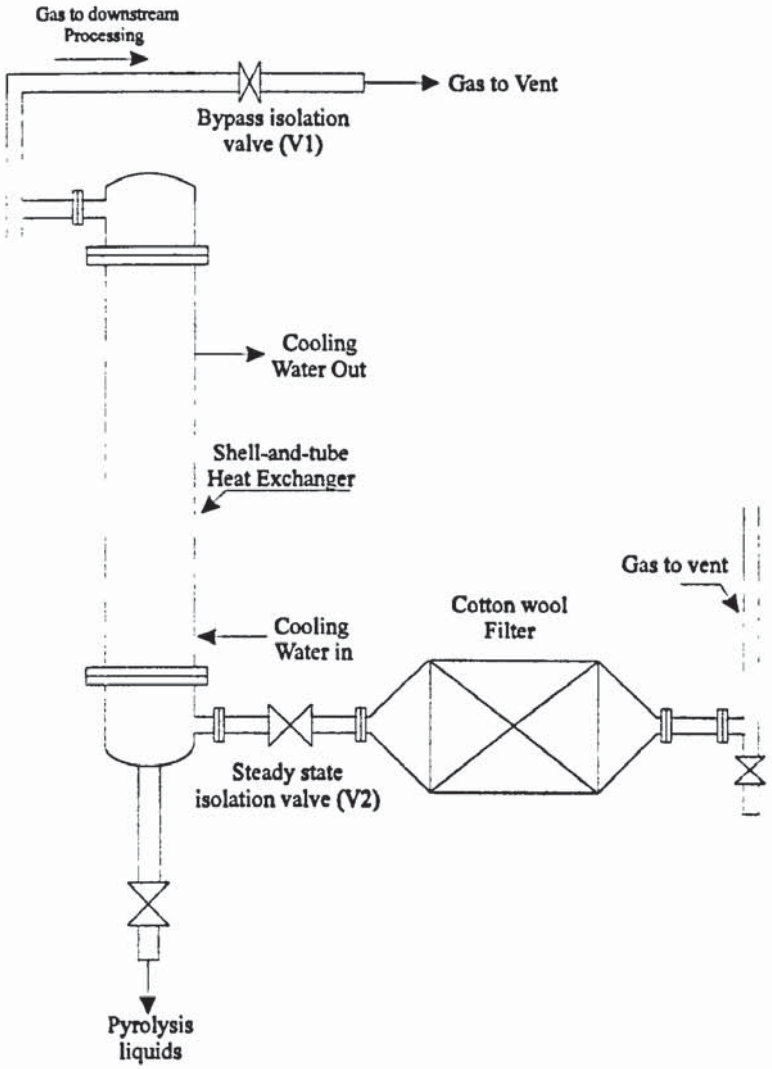

Figure 8-8: The modified bypass/HE gas/vapors products recovery system used in the main body of experiments (Bypass HE configuration)

8.7 Other problems associated with the operation of peripheral systems

The operation of the CFB reactor in a reliable and predictable way required that all other systems were functioning properly. This was true for the biomass feeding system, Section 7.3, and the air/nitrogen supply and preheating system, Section 7.4.

However, significant difficulties were encountered with the proper operation of the data acquisition system as well as the gas analysis systems.

8.7.1 Erroneous placing of thermocouples in the riser section

It was observed, from temperature measurements recorded periodically with a 12-point manually operated switch selector, that during the commissioning phase experiments,

thermocouple TC16 exhibited a quite higher temperature (in the range of 75-100°C) than the other TCs in the riser section. The same was observed when the continuous data acquisition system had been successfully installed for run R6, Figure 8-11 in Section 8.8.2, but also for the main-body experiment R7, Section 9-4. This temperature difference was initially attributed to exit effects, since TC16 is located near the riser exit. However, it was later concluded, i.e. after experiment R7, that it is the way the thermocouples are positioned rather than their placement along the riser section. In fact, TC16 is located in the middle of the gas-solid suspension, rather than adjacent to reactor wall as all the others TCs are in the riser section (TCs 11 to 16, Figure 7-12, Section 7.7.1). This problem is further discussed in Section 9.4.2.

8.7.2 Problems incorporating proper set-up of the data acquisition system

In the beginning of the commissioning runs, temperatures were recorded either from the outputs of temperature controllers, necessary to regulate CFB heating elements, or manually by means of a 12-input switch device. Absolute or differential pressures were estimated by the indication of U-tube water manometers, while flows of gases where estimated by means of variable area rotameters.

Gradually and due to the amount and complexity of data to be handled, manometers were replaced by pressure transmitters and the fluidising air (FGF) rotameter by a thermal mass flowmeter. Meantime, a continuous data acquisition system, discussed in Section 7.7, was set-up to allow continuous monitoring of all temperatures, pressures and flowrates. However, the set-up and tuning of this system presented many difficulties mainly due to poor understanding of software/hardware interaction and improper set-up. These problems were solved by continuous trial-and-error as well as the valuable help provided by an automation technician. After tuning and set-up the data acquisition proved to be very reliable, providing consistently high quality, low noise process data.

8.7.3 Problems associated with gas analysis

In the commissioning phase, no gas analysis equipment was employed. For the main body of experiments continuous on-line analysers as well as a Gas chromatography system were purchased.

The on-line analysers (paramagnetic for O_2, infrared for CO and CO_2, and thermal conductivity for H_2) referred to in Section 7.7.4, were calibrated by reference gases

(prepared specially for the case by Air Liquide Hellas S.A.) and gave reasonable results based on zero, span gas and air. The gas flow to the analysers was reduced to the manufacturer's recommended flows (of less than 1 l/min) by a mass flow controller and continuous gas flow was ensured by a gas sampling pump, which was positioned upstream of the gas analysis system, the sampled gases being pumped through the analysers. The gas sampling point was located at the exit of the ice-cooled condensers, Figure 8-7.

However, during operation the analysers did not perform as expected, due to inadequacies attributed to operational problems of the gas sampling pump. Thus, excessive amounts of air leaked through the gas pump giving erroneous results mainly to the O_2 analyser. Moreover, the CO analyser was out of range, so that its recalibration was necessary. Once these problems were faced the analysers performed satisfactorily and according to the specifications.

Besides the product gas composition analysis with the continuous on-line analysers, efforts were undertaken to achieve intermittent on-line measurements through the existing Gas Chromatography (GC) system, discussed in Section 7.7.4. This was secured through a two-packed column system, a gas sampling valve and a column switching valve. However, this system was not successfully set-up during the commissioning runs, due to a failure of an electronic board and the long replacement time encountered.

8.8 CFB reactor operation and start-up procedure

8.8.1 First four runs of the CFB reactor operation in the commissioning phase

A summary of the first four runs, carried out with a combination of solids removal and liquid recovery system basic configurations, was presented above in Table 8-2.

The main conclusions drawn from this first series of experiments were the identification of a series of problems, the most important of them referred to above and summarised as follows:

1. Solids recovery was problematic causing standpipe blockage and loss of solids circulation.
2. The liquid recovery system did not operate satisfactorily.
3. Minor problems such as the performance of the data acquisition and gas analysis systems were identified.

The above problems as well as remediation measures adopted for their removal have been discussed in Sections 8.4, 8.6 and 8.7.

Another significant problem proved to be the that of reactor preheating and start-up. Initially, continuous biomass feeding at the design value, i.e. approximately 10 kg maf/h, was practiced, Table 8-2. This procedure tended to overload the reactor, choking off the bed, and leading to quick, approximately 10 min of operation after biomass feeding commenced, loss of solids circulation and cyclone as well as liquid recovery systems plugging with unconverted feedstock (run R1). During the run R1 and prior to plugging, high temperatures were recorded in the solids recovery, cyclone-system, section (700-750°C) denoting combustion of volatile products released from the wood in the upper section of the riser. A very light liquid, probably combustion products and/or gasification water, was recovered ($\rho \approx 1$ g/ml) from the bottom of the heat exchanger during run R1. The liquid yields were very low, approximately 10-15 % wt on maf biomass fed. Upon dismantling the fouling material in the heat exchanger proved to be heavy tars, wood char and even unconverted biomass.

As a remedy to this start-up procedure, intermittent feeding of biomass at the biomass flowrate design value was decided to be practised in the subsequent runs. This approach was practised by Maniatis (1986), however for a much larger (approximately 400 kg/h) bubbling bed gasifier. At the time it was anticipated that the pyrolysis byproduct char would accumulate in the lower part of the system and burned at this point of the CFB system. In this way, heat would be gradually transferred, by means of sand circulation, to the riser section raising the temperature up to approximately 500°C. At this point, biomass could be added continuously at the design flowrate without any danger of choking off the bed. Thus, after this point had been reached high local heat transfer coefficients would be encountered, so as to fulfill biomass fast pyrolysis high heat transfer rate requirements, Section 2.7.

As seen from the temperature profile versus time diagram for experiment R2, shown in Figure 8-9 below, there was a direct response of the riser (TC14) and the combustor (TC2) temperature immediately after biomass was introduced to the system, mainly due to combustion and gasification reactions in the riser (direct contact of feedstock and oxidant-air), as well as to the recirculation of char and partially converted feedstock to the combustor. When biomass flow was interrupted, the temperatures drop, stabilising in a new, higher point and the cycle of intermittent biomass feeding was repeated.

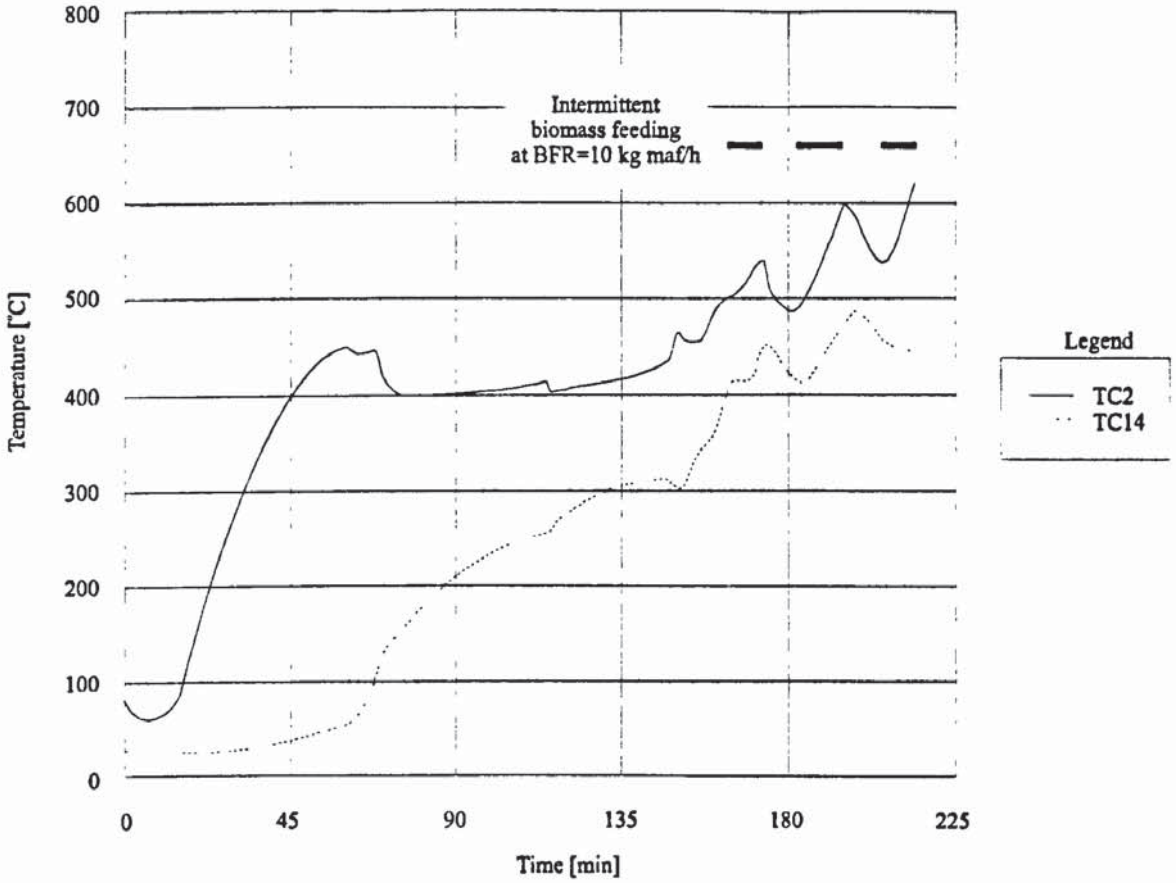

Figure 8-9: Temperature profile versus time for experiment R2

As depicted from Figure 8-9, the above described biomass feeding procedure was repeated three times for run R2. However, the intermittent loading of the CFB reactor with the maximum load at these low temperatures resulted in a series of problems, similar to those encountered in the continuous biomass feeding at design values (maximum load), although to a lesser extent.

The main reason for these problems encountered in the early commissioning runs was the feeding procedure as practised above. During this mode of feeding to the CFB reactor, the solids-gas suspension entrained in the riser section from the bubbling fluidised bed retained a relatively low temperature (≈ 450°C) and was quite lean (low riser velocities) at low (≈370°C) riser temperatures, Figure 8-9, so that there is limited heat transfer to the incoming biomass particles. This has as a result the partial conversion of feedstock and the thermal "choking" of the system (Maniatis, 1986), as already mentioned above. An additional reason for the quick choking of the CFB reactor is that the narrow piping incorporated in the standpipe cannot tolerate relatively large quantities of unconverted and/or partially pyrolysed wood being transferred to the combustor with the inert solids.

Finally, it was decided to feed biomass to the reactor gradually, in a stagewise mode, so that the small amount of char produced during the first stages was burnt to provide some additional heat that would "accommodate" the extra energy needs of the subsequent, higher biomass flowrates.

8.8.2 Commissioning runs under continuous gradual biomass feeding

In order to account for the problems encountered in the first four commissioning runs in the hot CFB fast pyrolysis pilot plant, the following corrective measures and procedures were adopted:

1. The solids recovery equipment consisted of a cyclone and an impinger in series, Section 8.4.4.
2. The downstream equipment was comprised of a shell-and-tube heat exchanger and two cyclonic condensers in series, Section 8.6.3.
3. The data acquisition was further improved and reliable, continuous on-line measurements could be carried out.
4. Biomass feeding procedure to the CFB reactor was given special consideration. It was found, Section 8.8.1, that biomass should not be fed to the CFB directly at the design value, neither continuously nor intermittently, since a high heat load was delivered to the system, while this still underwent slow heat-up.

These modifications were realised in the last two commissioning runs, which were focused on establishing best practice for pyrolyser start-up, improvement of the liquid products recovery system performance and possible identification of further problems. These runs, carried out with the system configuration shown in Figure 8-10, are denoted as R5 and R6 and are summarised below in Table 8-5.

The runs R5 and R6 were conducted without any severe problems associated with the reactor itself. Unsteady sand circulation, standpipe plugging or similar flow interruptions encountered in previous commissioning runs were not observed. The end of these two runs was marked by a sharp increase in pressure drop across the heat exchanger, indicating a gradual accumulation of the heavy tars and char-sand agglomerates, discussed in Section 8.6.1.

At this point it should be mentioned that due to an unexpected error in exiting the data acquisition system, the data collected during experiment R5 were not saved, so that this had to be repeated with the same operating parameters, the new experiment designated as R6.

Table 8-5 : Summary of the hot CFB reactor commissioning runs R5 and R6

Run No	Basic configuration	General comments
R5, R6	• Cyclone + Impinger in series • Heat exchanger followed by two ice-cooled cyclonic glass condensers Operating parameters: IBI=11 kg, FGF=14.6 kg/h, BFR=10 kg maf/h	*These two runs were characterised by :* * gradual increase in biomass flowrate * excellent reactor stability * prolonged operation * steady-state conditions * increased liquid yields * smooth char circulation * collection of valuable operational data *but still suffered from:* * lack of gas analysis * severe loss of organic vapors * other minor problems

Gradual biomass feeding resulted in entire different modes of CFB reactor operation during runs R5 and R6. First, when a low biomass flowrate was applied, the upper part of the riser operated in the combustion mode. At this time, the ratio of air-to-biomass fed to the CFB reactor was high, so that high temperatures in the cyclone and impinger were observed. Meantime, the char generated in the riser section as well as partially converted wood were circulating through the standpipe to the lower part of the CFB reactor combustion chamber, where char was burnt leading to:

- temperature increase at this point, i.e. char combustor, of the CFB loop
- consumption of the incoming oxygen in the char combustor due to the char oxidation
- entrainment of hot solids and inert gas in the riser section
- increased gas velocities, solids carry-over and enhanced heat transfer coefficients in the CFB riser section.

The gradual feeding of biomass in the CFB reactor caused a temperature shift. Initially, high temperatures in the riser and low temperatures in the combustor prevailed. In the course of the run, however, char circulation promoted oxygen consumption in the lower part of the CFB reactor (due to the exothermic char-oxygen reaction), so that there was a temperature shift with high temperatures in the char combustor and low temperatures in the CFB riser

(pyrolysis) section. This temperature shift is further discussed below and analysed in detail during the actual experimental programme, Section 9.6.

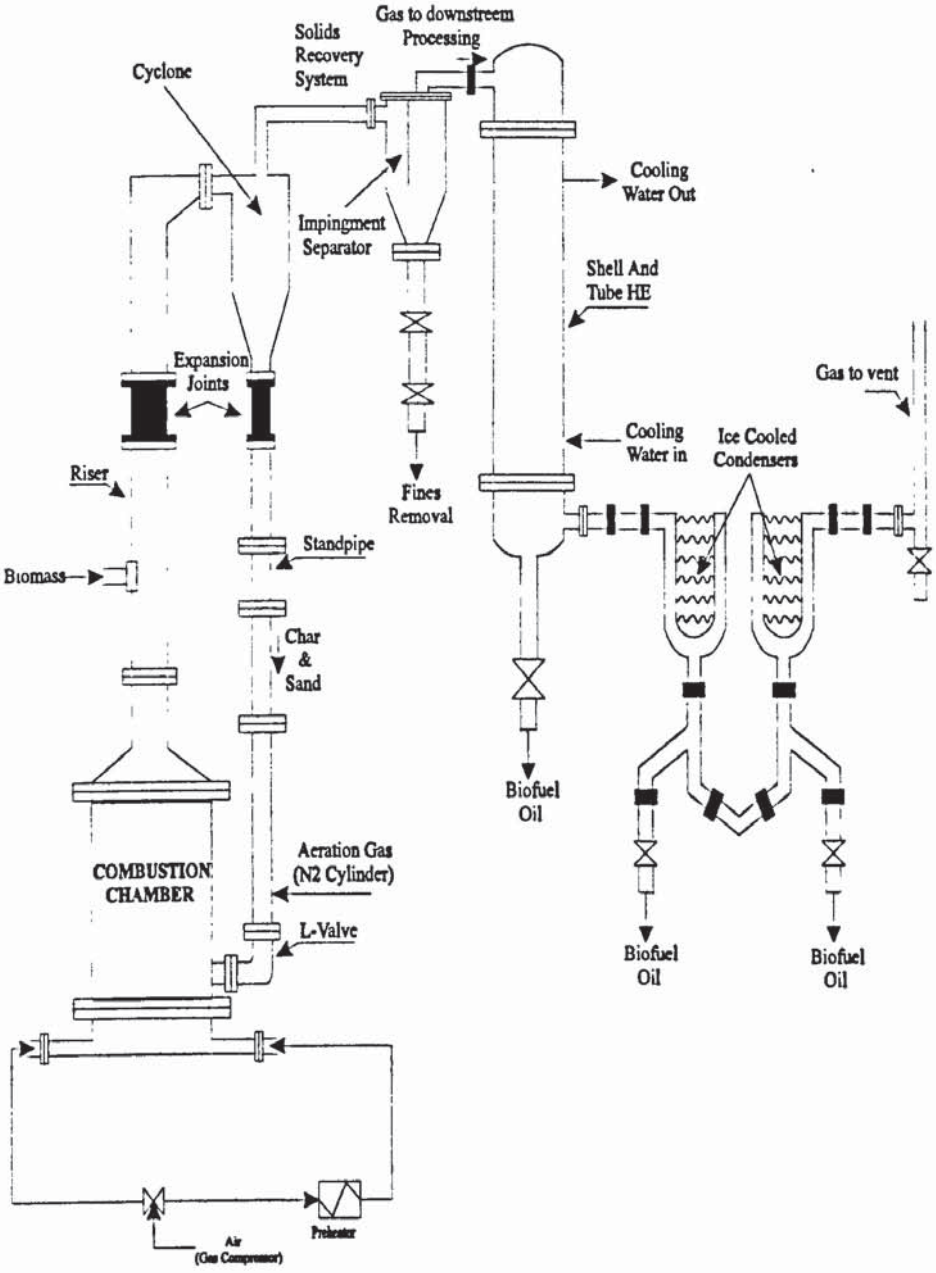

Figure 8-10: The biomass fast pyrolysis plant configuration adopted during the commissioning runs R5 and R6

a) Temperature measurements in the CFB reactor

As biomass flow rate was gradually increased, the reaction passed through the gasification mode, the air-to-biomass ratio decreasing steadily. The stagewise increase of biomass feeding resulted in the establishment of the desired thermal profile in the CFB reactor, that is, high temperatures (combustion) in the lower part (combustion chamber) and lower temperatures (pyrolysis) in the upper part (riser) of the CFB reactor.

This thermal shift in the temperature profile was an important issue for establishing the desired operating conditions, which favour both the exothermic char combustion (high temperatures in the combustion chamber) and the biomass devolatilization (moderate temperatures in the riser) maximising liquid yields.

The location of thermocouples in the CFB reactor was indicated in Figure 7-12, Section 7.7.1. The positions of the thermocouples referred to in the following graphs are indicated below, Table 8-6.

Table 8-6: Thermocouple location along the CFB loop

Thermocouple ID	Location in the CFB Fast Pyrolysis Reactor
TC 2	in the middle of the combustion chamber
TC 8	riser section, just before biomass feeding point
TC 9	riser section, in the height of biomass feeding point
TC 10	riser section, just above biomass feeding point
	riser section, at regular intervals (40 cm apart) along the riser
TCs 12 & 14	section, above biomass feeding point
TC 16	top of riser
TC 18	between cyclone and impinger

The gradual thermal shift described above is shown in Figures 8-10 and 8-11, where the temperature profile in different parts of the CFB reactor, char combustor and riser, is shown.

The conclusions based on the results shown in Figures 8-11 and 8-12 are as follows (a run interruption occurred between minutes 40-50 due to a sudden leakage in one valve, which however was rapidly repaired):

- The temperature increased steadily in the combustion chamber, Figure 8-11, and a temperature increase, of more than 300°C, i.e. from 460 to 770°C within a 3 hours from biomass feeding start-up, was recorded (TC2 indication). This temperature rise occurred without external heating, the heating elements being shut off as soon as biomass was introduced into the system, and was a clear indication that successful char circulation and combustion in the lower part of the CFB combustion chamber had been established.
- The temperature exhibited a sharp decrease at biomass feeding point, TC9, due to biomass inlet, while the temperature in the riser section was rapidly stabilised, TC10, as shown in Figure 8-12.

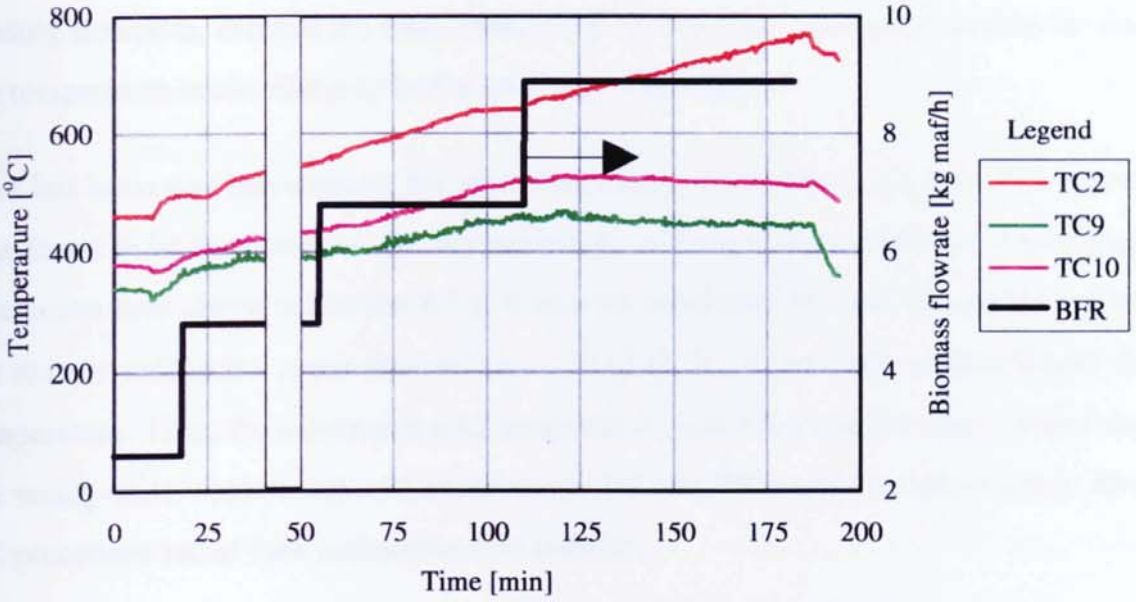

Figure 8-11: Temperature profile versus time in the combustor and around biomass feeding point (run R6)

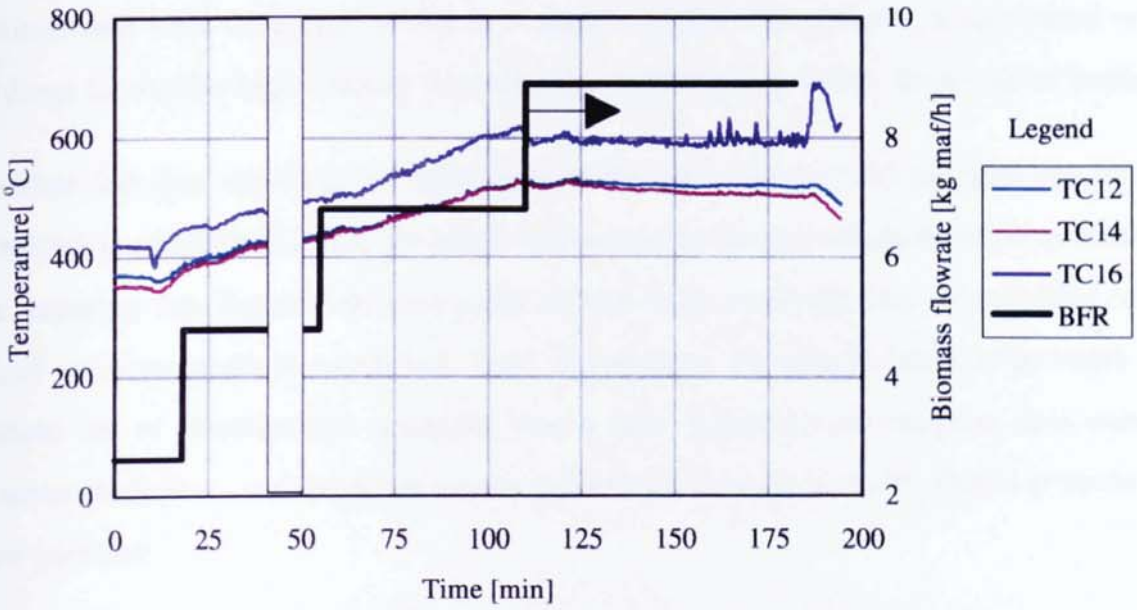

Figure 8-12: Temperature profile versus time in the upper riser section (run R6)

The data derived from Figure 8-12, show that there is a non-uniform temperature profile in the riser section, indicating inadequate heat transfer and lower than expected heat carrier (sand) circulation rates. The lower temperatures at thermocouples TCs 12 & 14 compared to those recorded by TC16, initially indicate some oxygen breakthrough in the pyrolysis zone or the existence of exothermic reactions in this (upper riser zone) part of the CFB reactor. However, the flat profile of these temperature profiles, especially at near-design biomass

feeding flowrates, exhibits the establishment of steady-state conditions, so that the cause for the temperature non-uniformity had to be sought elsewhere.

This last issue was investigated, the erroneous placement of the TC12 and 14 thermocouples was found to be the cause for the non-uniformity of temperature exhibited. According to the discussion held above in Section 8.7.1, it may be concluded that the TCs located adjacent to the reactor wall in the upper riser section, TCs12 & TC14, seriously underestimate the riser temperature. Thus, the substantial riser temperature gradient along the riser section shown in the steady-state, second series of experiments, R5 and R6, should be attributed to erroneous TC placement rather than inadequate heat transfer.

After relocation of the upper riser section thermocouples was accomplished, the results obtained from temperature measurements during the subsequent - main body - series of experiments, Chapter 9, verified that an isothermal profile and a high heat transfer environment were developed in the riser section of the CFB reactor, in agreement with the findings for similar high velocity risers (Kobro and Brereton, 1986), discussed in Section 4.4.

Another fact also verifying the fulfillment of the high heat transfer criterion (as far as fast pyrolysis is concerned) is that the solids withdrawn by the two isolation valves mechanism at the impinger leg, Figure 8-4, were more or less fully pyrolysed and no unburned or virgin wood particles could be identified. Thus, the absence of unburnt biomass particles at the bottom leg of impingement separator was a firm indication of adequate heat transfer to biomass particles, since the presence of unconverted biomass particles should precede that of char particles.

b) Liquid recovery in the commissioning experiments

As far as liquid recovery was concerned, an additional problem still to be faced during the steady-state series of experiments was that, as discussed above in Section 8.6.3, during the stagewise biomass feeding that had to be applied for a successful CFB reactor start-up procedure, undesirable liquid products, like combustion water and gasification liquids, were readily formed and collected. Thus, for good mass balances derivations these liquids had to be excluded. This was achieved once the entire gas/vapor stream by-passed the downstream equipment as discussed in Section 8.6.4. This remedy was, however, practised in the subsequent, main-body series of experiments, described in Chapter 9.

As a compromise measure to reduce the amount of water recovered from the initial CFB reactor start-up operation stages, a by-pass around the glass condensers was installed to divert the combustion gases by venting them to the atmosphere, thus removing product water and initially formed char from the condensers. At the same time, the liquids recovered from the bottom of the heat exchanger were not accounted for in the liquids mass balance. In spite of these measures, the start-up procedure was unnecessarily burdening the heat exchanger, so that it was partially blocked when steady-state had been reached and the actual liquid sampling began.

After some time of operation and whilst the system had achieved the pyrolysis mode of operation, there was sufficient liquid in the second condenser, Figure 8-9, to scrub the product gases and hence increase gas-to-liquid mass transfer and recovery of pyrolysis liquids, as described in Section 8.6.3. However, the clearance of the condensers was quite narrow (25.4 mm internal diameter piping was incorporated throughout), so that the excessive gas/vapor velocities caused very rapid passage of the gaseous stream through the entire condenser system, resulting to lower than expected mass transfer and to the entrainment of condensable gases out of the system. Significant pyrolysis liquid losses were indicated by a yellow smoke in the exhaust.

The heat exchanger behaved much better in terms of plugging during runs R5 and R6 comparing with the initial four commissioning runs. Upon dismantling 15 out of the possible 31 heat exchanger tube holes were blocked, mainly with fine char and fine sand. Liquids were recovered more as a thick and viscous paste rather than as a solid plug.

The overall liquid recovery for run R6 (excluding the combustion water, collected in the base of the heat exchanger and removed prior to steady-state conditions have been achieved, that is, below biomass flowrates of 8.9 kg maf/h, Figure 8-11) was approximately 35 % wt on a maf feedstock basis, which is considerably lower than findings from other biomass fast pyrolysis systems.

The above discussion indicates that, in spite of the various improvements and modifications that enabled the system to reach steady-state conditions, liquids collection still remained a very significant problem with the majority of the products escaping to atmosphere.

8.9 Summary

Significant operational experience of the CFB biomass fast pyrolysis reactor was gained through the identification and removal of a number of problems. The problems encountered during commissioning runs were of two types, hardware and procedure-like. The first type of problems were identified and solved in a series of four commissioning experiments as follows:

- Solids recovery and separation system. Through a sequential remediation procedure, Section 8.4, this problem was successfully solved by incorporating a high efficiency cyclone in series with an inertia separator (impinger) with separated solids outlets.
- Liquid recovery and separation system. Through similar trial-and-error experimentation procedure this problem has been partially removed but not entirely satisfactorily, so that further work to resolve this is required.

Other minor problems, including data acquisition and gas analysis systems set-up, have also been identified and successfully faced during the course of these four commissioning runs.

After the initial, hardware problems had been solved, two additional commissioning runs were carried out, to attempt extended reactor operation and achieve steady-state conditions. The biomass feeding procedure and careful start-up were identified as key issues, requiring the adoption of the appropriate procedures to achieve the proper temperature profiles in the different parts of the CFB reactor and to establish steady-state conditions.

It was found out that biomass should not be fed to the CFB reactor directly at the design value neither in a continuous or in an intermittent way, since a high heat load was delivered to the system, which was still undergoing a heat-up phase. Instead, biomass feeding should be exercised in a gradual manner, the system undergoing successively the combustion and gasification phases.

During the commissioning experiments, valuable experience was gained, reactor modifications and peripheral system improvements were accomplished and appropriate operational procedures were adopted in order to derive meaningful mass balances in the subsequent, main body of experiments, described in detail in Chapter 9.

CHAPTER 9: RESULTS AND DISCUSSION

9.1 Introduction

This chapter presents the results obtained from five operational runs, which constitute the main experiments in the CFB reactor, carried out to derive meaningful mass balance and additional operational data for the CFB pyrolyser. This chapter is structured as follows:

- summary of the operating parameters of the main experiments, Section 9.2
- CFB reactor configuration used in the main experiments, Section 9.3
- discussion of the operational behaviour of the reactor, Section 9.4
- product yields and mass balances, Section 9.5
- temperature profiles versus height in the reactor, Section 9.6
- pressure drop profiles versus time in the bubbling fluidised bed, Section 9.7
- summary of results, Section 9.8.

9.2 Summary of operating parameters of main experiments

In order to provide a quick reference and comparison of the results, the most important parameters, i.e. biomass flowrate (BFR), fluidising gas flowrate (FGF), air factor (S), initial bed inventory (IBI), temperature in the CFB riser (riser T) and vapor residence time (VRT) are summarised in Table 9-1. The nominal air factor (or equivalence ratio, S_b) is the ratio of oxidant (air) fed to the CFB reactor to that required for stoichiometric combustion of incoming biomass (Schoeters and Buekens, 1981; Maniatis, 1986). More specifically:

$$S_b = \frac{G_{air}}{\sum (y_i q_i^{air}) G_B} \qquad \text{(Eq. 9-1)}$$

where

G_{air}	mass flowrate of air (=FGF, Table 9-1)	[kg/h]
y_i	fraction of component i (C, H, O) in biomass	[-]
q_i^{air}	amount of air required for stoichiometric combustion of component i in biomass	[kg/kg feed]
G_B	biomass flowrate (=BFR, Table 9-1)	[kg maf/h]

The biomass used was a typical pine wood used by the furniture industry and received from a single wood finishing workshop. Moisture content was measured as 7.4 to 7.5 % wt, while the determination of biomass composition (Peacocke, 1994) for a similar feedstock was (% wt moisture-free): carbon 49.8; hydrogen, 6.1; nitrogen 0.05; oxygen [by difference] 43.5; sulphur trace and ash 0.5. Given this composition and taking into account Eq. 9-1. i.e. the calculation procedure adopted by Maniatis (1986), the nominal air factor is correlated to fluidising gas flowrate (FGF), using the typical analysis of biomass given above as follows:

$$S_b = 0.168\,\frac{G_{air}}{G_B} \Rightarrow S_b = 0.168\,\frac{FGF}{BFR}$$

Table 9-1: The operating parameters for runs R7, R8, R9, R10 and R11

Run No	IBI (kg sand)	FGF (kg air/h)	VRT (ms)	Riser T (°C)	BFR (kg maf/h)	Nominal air factor	Feedstock size d_p (mm)
R7	11.0	16.0	374	581	8.44	0.318	$1.5< d_p <2.0$
R8	11.0	14.7	388	605	10.45	0.236	$1.0< d_p <1.5$
R9	11.5	13.9	396	579	10.20	0.229	$1.0< d_p <1.5$
R10	11.75	12.1	458	496	8.96	0.226	$1.0< d_p <1,5$
R11	12.50	13.0	373	550	10.22	0.214	$1.5< d_p <2.0$

In all runs the biomass particle size was kept between 1.0 and 1.5 mm, except for runs R7 and R11, where it was kept between 1.5 and 2.0 mm. The selected feedstock sizes are considerably larger than those employed in most of the laboratory scale experiments conducted in the past, reviewed in Chapter 2, and constitute a reasonable compromise between desired dimensions and pretreatment costs at this scale of operation.

It should be pointed out that the nominal air factors shown in Table 9-1 are high for the pyrolysis of biomass and are more representative of air factors for biomass gasification (Maniatis, 1986). However, it should be remembered that in the proposed CFB reactor configuration, only byproduct char is combusted resulting in a hot gas and sand suspension to provide the thermal needs and the high heat transfer rates for biomass pyrolysis. Hence, these figures refer to an overall (nominal) air factor (incoming air to incoming biomass in the CFB reactor), the actual air factor to the point of biomass entrance being much lower since the oxygen is nearly all consumed in the char combustor chamber as will be discussed explicitly below. The air factor is, hence, specific to the point to which it is referred, i.e.

taking into consideration the actual flowrates of the fuel and the oxidant at the point of reference.

For example, for the case of the char combustor, the char air factor, S_c, is defined as:

$$S_c = \frac{G_{air}}{\sum (z_i p_i^{air}) G_{char}}$$

(Eq. 9-2)

where

G_{air}	mass flowrate of air (=FGF, Table 9-1)	[kg/h]
z_i	fraction of component i (C, H, O) in char	[-]
p_i^{air}	amount of air required for stoichiometric combustion of component i in char	[kg/kg feed]
G_{char}	char flowrate (=f(BFR) and temperature, Section 4.5.1)	[kg maf/h]

As discussed in Chapter 4, the char flowrate is a function of both pyrolysis temperature, Section 4.5.1, and biomass flowrate, Table 4-4 in Section 4.5.4. Thus, in order to determine the char air factor the char flowrate as well as its elemental composition is required. The determination of the char air factor is further discussed in Section 9.5.4.

9.3 CFB reactor configuration used in the main series of experiments

As discussed in detail in Chapter 8, the proper operation of the system is achieved through a gradual transition from combustion to gasification, and finally to pyrolysis, mode of operation in the riser section by fixing the FGF and gradually increasing the BFR to design (=10 kg maf biomass/h, Chapter 4), or near design, values. The establishment of the proper mode of operation, denoted by high temperatures in the combustion chamber (exothermic char combustion) and low temperatures in the riser section, followed by temperature and gas composition uniformity, is further defined as the steady-state and is characterised by uniformity of temperature in the different subsystems as well as constant gas composition in the reactor system outlet.

During these five runs (runs R7, R8, R9, R10 and R11 respectively), the CFB reactor configuration illustrated in Figure 9-1 was employed. The liquid recovery system configuration adopted during these experiments, described in Section 8.6.4, consisted of a shell-and-tube heat exchanger and a cotton-wool filter and was designed to both derive

meaningful mass balances and allow prolonged reactor operation. Thus, in order to carry out a mass balance during steady-state operation, all products were sent to the by-pass during reactor start-up.

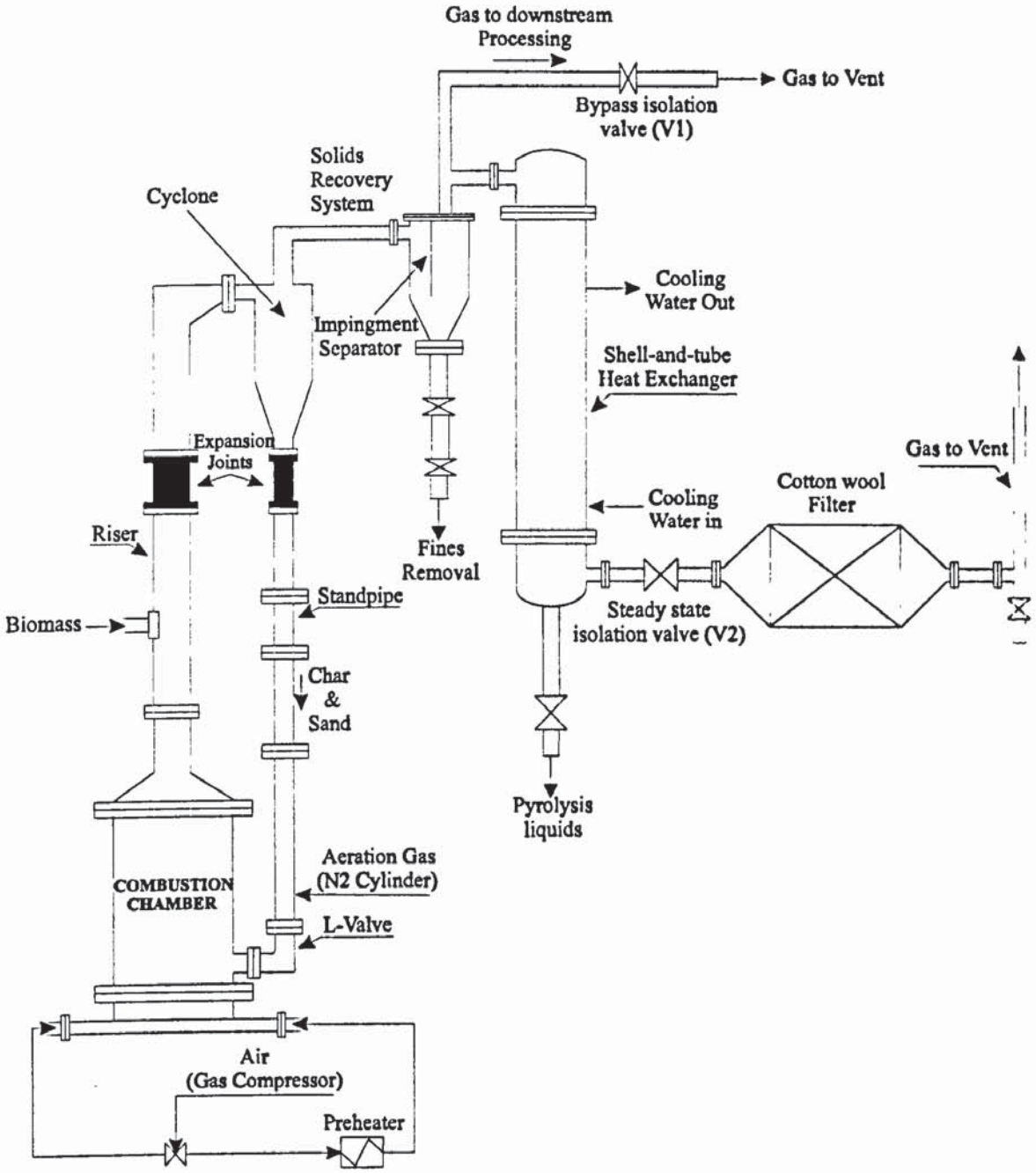

Figure 9-1: CFB pilot plant equipped with a gas/vapor by-pass line, employed during the main body of experiments (runs R7 to R11)

9.4 Discussion of the operational behaviour of the CFB reactor

A general remark for the five pyrolysis runs discussed in this chapter is that, unlike those conducted in the second series of experiments, Section 8.8.2, no severe plugging was encountered in the downstream equipment, a fact confirmed during inspection of the heat exchanger. It was found that 9 to 10 of the tubes were plugged after runs R7, R8 and R9 (out of 31 tubes) and 18 to 20 of the tubes were plugged after runs R10 and R11 compared to almost 30 for the commissioning runs R1 to R4, described in Chapter 8.

This fact justifies the by-passing of gas and vapors prior to steady-state and its positive effect as far as the proper operation of downstream processing is concerned.

9.4.1 Start-up procedure

The biomass flowrate, BFR, was gradually increased, as discussed in Sections 8.8.1 and 8.8.2, up to the design (=10 kg maf/h) value for all five runs discussed in this chapter. During the first 20 minutes of these runs, partially converted woodchips were captured by the inertia impinger and removed, which indicated that in the initial stages of biomass feeding biomass was only partially pyrolysed due to insufficient heat transfer rates to the biomass particles at this stage of feeding.

In the initial stages of the biomass feeding procedure, char and partially pyrolysed biomass were circulated to the combustor where they were burnt by the incoming fluidising air, heating up the sand blown up the riser section. After this initial combustor heat-up period the solid heat carrier (silica sand) had been heated to higher temperatures and so higher temperatures were attained in the riser section. The higher heat transfer rates promote fast pyrolysis reactions, so that the incoming biomass feedstock was completely converted to volatiles and char. The air flowrate (FGF) was kept constant, however, the air factor decreasing as the biomass throughput (BFR) increased continuously throughout each run.

After start-up and during steady-state (indicated by temperature fluctuations of less than 10°C in the riser section), the vapor products were directed through the liquid collection equipment, i.e. through the shell-and-tube heat exchanger, the exhaust valve V2 and the cotton wool filter, Figure 9-1, and were finally vented to the atmosphere.

The five runs R7, R8, R9, R10 and R11, lasted for approximately 170 minutes, of which approximately 30-45 minutes were in the steady-state. The duration of the steady-state

operation was limited by the gradual plugging of the heat exchanger as explicitly described in Section 8.6.1. Minor problems were encountered in these five runs and are described in detail below.

9.4.2 Temperature measurements

As explained in Section 8.7.1, the thermocouples placed adjacent to the reactor wall seriously underestimated the riser temperature, which was correctly indicated by the thermocouples facing the bulk of the gas-solids suspension. A correction factor was derived to compensate for the error. Table 9-2 identifies the thermocouples affected by this problem.

Table 9-2:TCs misplaced (Mis=X) and temperature difference (ΔT) when corrected (Corr=-)

Thermocouple ID	Run 7 Mis	Run 8 Mis	Run 9 Mis	Run 10 Mis	Run 11 Mis	Run 11		
						Mis	Corr	ΔT
TC2	-	-	-	-	-	512	512	0
TC6	X	X	X	X	-	439	502	63
TC7	X	X	X	X	-	424	479	55
TC8	X	X	X	X	-	409	459	50
TC 9	X	X	X	X	-	327	443	116
TC10	X	X	X	X	-	376	436	60
TC11	X	X	X	X	-	372	426	54
TC12	X	-	-	-	-	412	412	0
TC13	X	X	X	X	-	355	402	47
TC14	X	-	-	-	-	397	397	0
TC15	X	X	X	X	-	338	390	52
TC16	-	-	-	-	-	405	405	0
TC18	-	-	-	-	-	335	335	0

These estimates were derived by an individual run preceding R11, in which temperature indications in the preheat mode were recorded with the thermocouples both misplaced (adjacent to wall) and placed correctly after disconnection and replacement with the thermocouple tip in the middle of the reactor facing the bulk of the gas-solids suspension. The location of each thermocouple was described in Section 8.7.1 and the locations of some significant thermocouples were given in Table 8-6.

The consistently higher temperature in TC 16 is due to exit effects, while the high temperature difference in TC 9 (thermocouple just opposite biomass feeding point) is

probably due to the fact that when adjacent to the wall (misplaced), this thermocouple is partially cooled due to poor insulation in its periphery (biomass feeding point not heavily insulated, in order to avoid high temperatures and, hence, premature pyrolysis in the transport screw).

9.4.3 Specific features for Run R7

A sudden pressure tap tubing burnout during R7 gave rise to the intrusion of atmospheric air into the upper section of the riser leading to a subsequent rise of the temperature due to the induced combustion of the biomass particles and volatiles in this part of the CFB. This temperature rise is further discussed in Section 10.2.3 below. However, this problem was quickly remedied by plugging the pressure tap.

The most severe problem of run R7 was the shortage of biomass. The amount of biomass was insufficient for this particular run, since an estimation of the relatively long time interval to heat-up the reactor was not known at that time, so that an excessive amount of biomass had to be consumed before reaching steady-state. This resulted in steadily decreasing biomass flowrate to the reactor, less char produced and lower O_2 conversion in the combustor. Consequently, O_2 was breaking through up the riser, where exothermic reactions prevailed raising the riser temperature and hence causing severe deviations from the steady-state mode of operation.

9.4.4 Specific features for Runs R8 and R9

During these runs no serious problems were encountered.

9.4.5 Specific features for Run R10

An unexpected sudden increase in aeration gas flowrate (AGF) caused an increase in solids circulation rate (SCR) resulting in overloading of the standpipe. This caused, in turn, the operation of the standpipe in the packed bed flow mode which had as a consequence the cessation of solids flow and hence loss of solids circulation (as discussed in Section 5.5.4). As a result, no char was circulating through the standpipe/L-valve reinjection system and the atmospheric oxygen was escaping from the combustion chamber unconverted, promoting biomass combustion in the riser section. In addition, a substantial amount of solids, which were not captured by the solids removal configuration (cyclone and impinger), were discharged to the atmosphere.

Readjusting the AGF cured the problem. However, the effects of this disturbance were critical to the performance of the CFB reactor and are further discussed in Section 10.3.2.

This practical experience confirms the sensitivity of operation of CFB reactor to AGF and suggests the adoption of automatic control of AGF and possibly the inclusion of a suitable alarm in a scaled-up operation, a recommendation further discussed in Chapter 10.

9.4.6 Specific features for Run R11

This run was conducted with an increased initial bed inventory (IBI). A loss of solids occurred twice, once when the reactor system was in the preheat mode, which was due to the increased IBI, Table 9-1. The increased amount of solids could not be accommodated by the cyclone and solids reinjection system and were subsequently rejected. The effect of an increased IBI is further discussed in Section 10.3.2.

The amount of solids heat carrier rejected during R11 totalled 1.5 kg leaving a final solids inventory of about 11 kg. After the excess solids had been rejected, the CFB reactor operated in a reliable manner, in the same mode as that encountered for the experiments R8 and R9.

During R11 the Aeration Gas Flowrate (AGF) suddenly stopped. This resulted in the cessation of solids flow and hence loss of solids circulation (as discussed in Section 5.5.4). As a result, the oxygen escaped the combustion chamber unconverted (no char was circulating through the standpipe/L-valve reinjection system), the effects being those referred to in the previous section for R10.

This disturbance was remedied by increasing the AGF to the desired value.

9.5 Experimental mass balances

In the following, mass balances are considered both over the entire CFB reactor system as well as over the biomass pyrolysis and liquid recovery sections.

When deriving mass balances over the entire CFB reactor system it should be remembered that, as depicted from Figure 4-5, input streams are incoming air and biomass, while output streams incorporate pyrolysis liquids (including both feedstock moisture and reaction water) as well as entraining gases, i.e. N_2, CO_2 and CO (products of char combustion) and non-condensible pyrolysis gases. Hence, mass balances over the entire CFB reactor, discussed in

Section 9.5.2 below, may be obtained by measuring the incoming streams (air and biomass) as well as the outcoming ones (pyrolysis liquids and product gas). The definition of mass balances over the entire CFB reactor system at steady-state conditions is schematically shown in Figure 9-2.

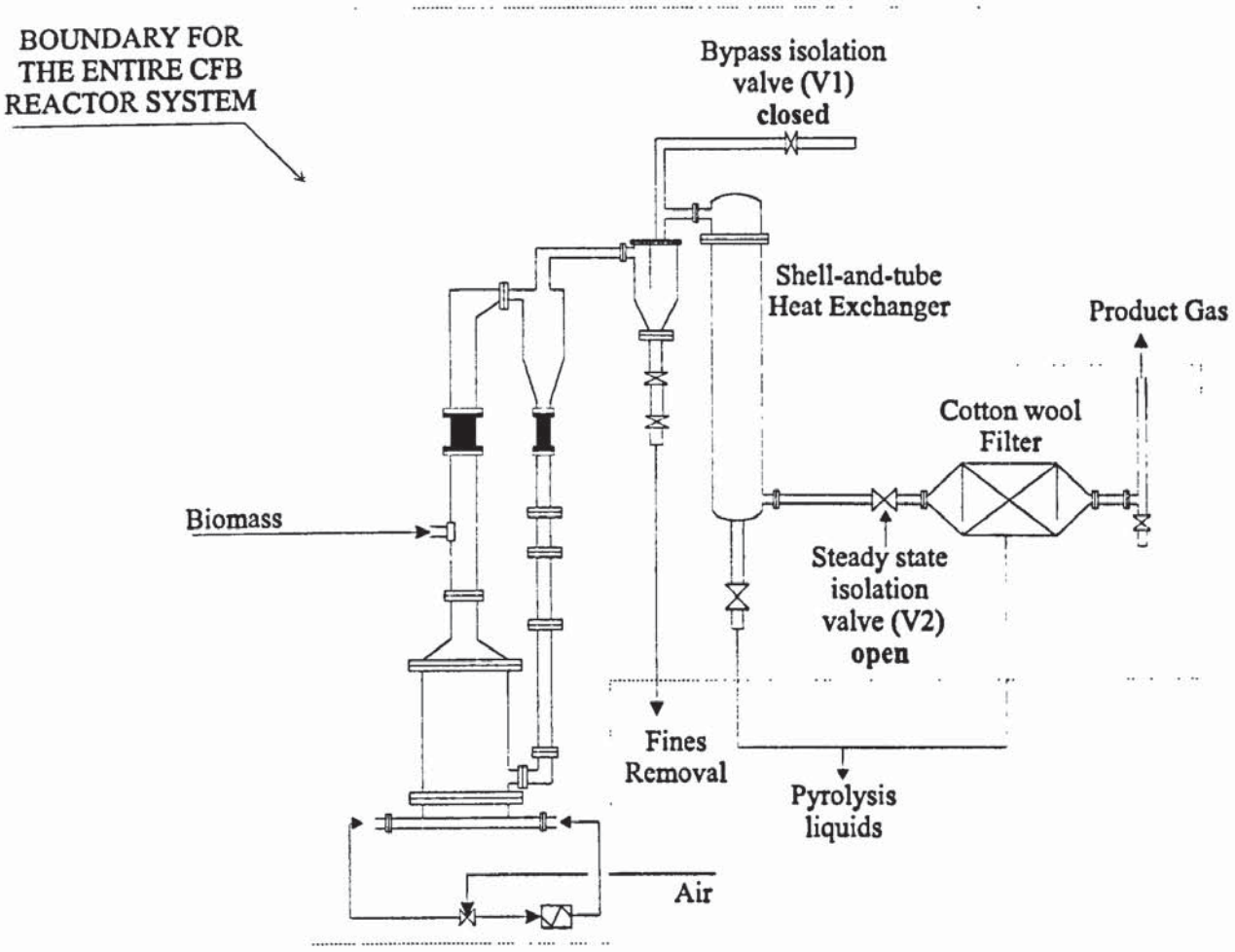

Figure 9-2: Schematic mass balance over the entire CFB reactor system at steady-state conditions

Mass balances over the pyrolysis (riser) and liquid recovery sections provide information about the distribution and yields of biomass pyrolysis products (char, pyrolysis liquids and pyrolysis gas). These mass balances are not obtained in a straightforward manner, since char is not normally a CFB reactor outcoming stream, being produced in the riser and consumed internally in the lower part of the CFB reactor (combustion chamber).

Moreover, and due to the fact that the CFB reactor product gas is the sum of pyrolysis gas and flue gas from the char combustor, the composition and yield of pyrolysis gas was estimated indirectly requiring the adoption of a multiple gas sampling and analysis approach.

The definition of mass balances over the pyrolysis section (riser) is schematically shown in Figure 9-3 below and is further discussed in Section 9.5.4.

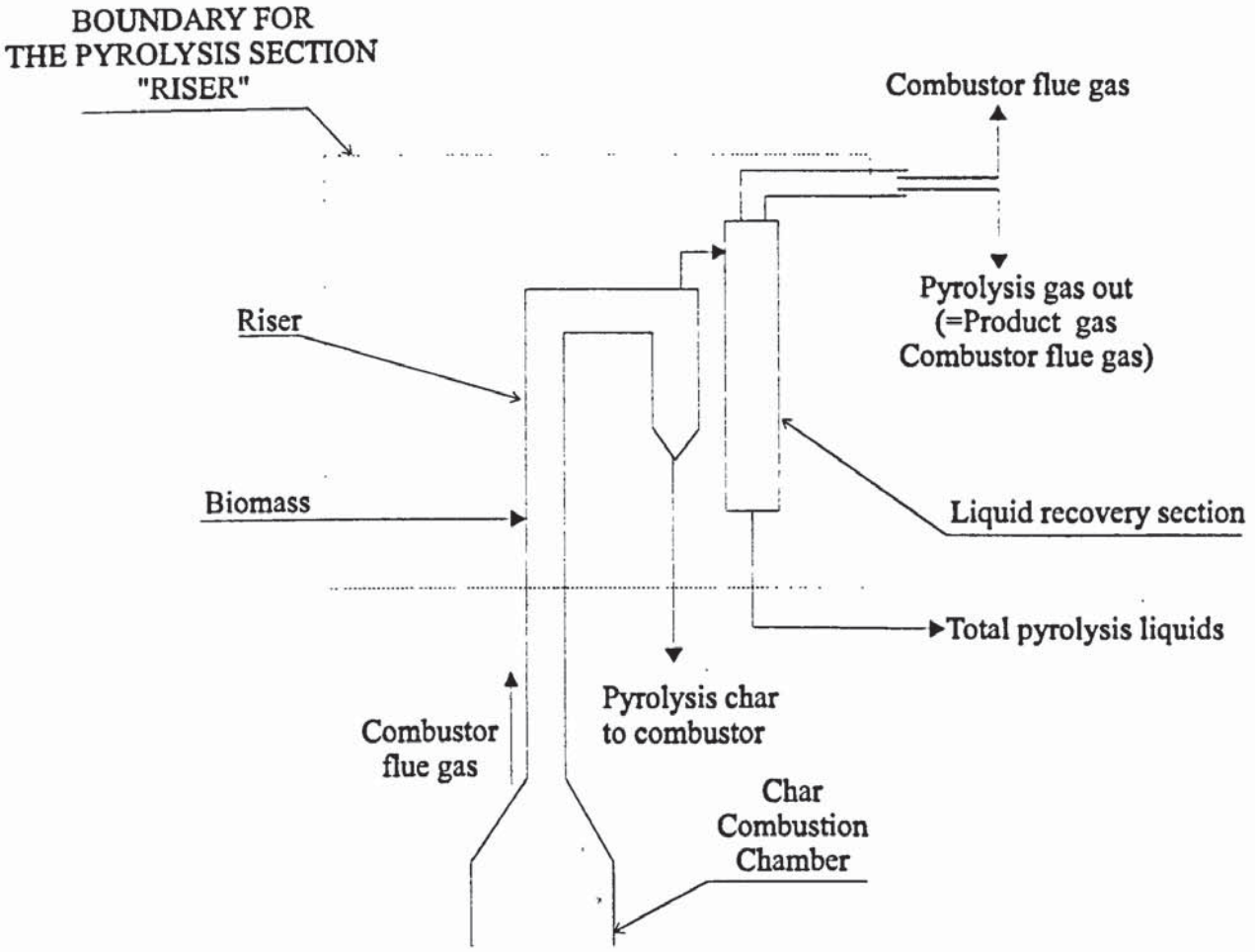

Figure 9-3: Schematic mass balance over the reactor pyrolysis (riser) and liquid recovery sections at steady-state conditions

9.5.1 Basis for the determination of product yields

In the following, the steady-state is defined as the state of operation where temperatures in the different systems of the CFB reactor system have been stabilised and product gas composition is approximately constant.

Biomass flowrate (BFR) was estimated by conducting a volumetric calibration prior to each run, correlating the metering screw rotation speed to biomass flowrate, as discussed in Section 7.3. BFR was gradually increased until the steady-state mode of operation is reached.

Incoming air is kept constant throughout each run and is directly measured by means of an air mass flowmeter, the measuring principle of which is based on thermal dispersion

technology. The air mass flowmeter was provided with an accurate (±1 % of measured value) calibration curve, see Section 7.4.1.

Outcoming products flowrates were determined after the steady-state mode of operation has been established. The pyrolysis liquids flowrate was determined experimentally, the liquids being collected directly from the bottom of the heat exchanger (recovered from HE), Figure 9-1, and by weighing the cotton wool filter (CWF) before and after each run, the weight difference assumed to be due to pyrolysis vapors escaping recovery in the HE. The liquids and solid agglomerates discussed in Section 8.6.1, retained in the heat exchanger tubes, were not taken into consideration, since their recovery was very troublesome requiring solvent extraction, solids filtering and evaporation of the solvent in a vacuum evaporator, equipment not available due to budget restrictions.

Total gas out was determined by averaging the gas composition from the GC system from samples taken during steady-state operation in the riser section and considering a N_2 balance (Schoeters, 1983; Maniatis, 1986). In the following hydrocarbons with a higher than 3 carbon atoms (C3+) are characterised as "others" and considered solely to be C_3H_6. Due to the very close conductivity of H_2 and He (GC system carrier gas), hydrogen in low concentrations (as is the case for low temperature pyrolysis of biomass), i.e. <1.0 % wt, could not be detected in the gas analysis system used. The N_2 flow in the L-valve is determined by a gas rotameter, normalised and subtracted from all calculations.

Mass balances over the entire CFB reactor, Figure 9-2, are described below in Section 9.5.2, while a mass balance over the pyrolysis (riser) and liquid recovery sections, Figure 9-3, indicating the product distribution of biomass pyrolysis and requiring multiple gas sampling and analysis, is further discussed for run R11 in Section 9.5.4.

9.5.2 Mass balances over the entire CFB reactor system - runs R7 to R11

This section presents the mass balances over the CFB reactor for runs R7 to R11. It should be emphasised here that run R7 is not considered truly representative due to the erratic feeding discussed in Section 9.4.1. A summary for the experimental mass balances over the CFB reactor for the five runs R7 to R11 is presented below in Table 9-3. All the product yields for the work described in this section are by direct measurement, recovery and experimental estimations and no yields were assumed or calculated on a "by difference" basis.

Table 9-3: Mass balances over the entire CFB reactor for the runs R7, R8, R9, R10 and R11

Run number	R7	R8	R9	R10	R11	
Operating Parameters						Section where discussed
Riser temperature [°C]	581	605	579	496	550	Section 4.5.1
Combustor temperature [°C]	678	700	645	748	740	Section 4.6.3
Run time at steady-state [min]	30	28	45	31	45	
Vapor residence time [ms]	374	388	396	458	373	Section 4.3.1
Feedstock size, d_p [mm]	$1.5<d_p<2$	$1<d_p<1.5$	$1<d_p<1.5$	$1< d_p<1.5$	$1.5< d_p <2$	Section 9.2
Nominal air factor (0<S<1)	0.296	0.236	0.229	0.226	0.214	Section 9.2
Final Bed Inventory [kg sand]	9.10	10.75	10.90	10.00	10.30	Section 9.5.1
Input Streams (reactor)						Section 9.5.1
Biomass In [kg maf/h]	8.44	10.45	10.20	8.96	10.22	
Moisture/Ash In [kg/h]	0.73	0.91	0.89	0.78	0.89	Section 9.5.1
Air In [kg/h]	16.00	14.70	13.90	12.10	13.00	
Total In [kg/h]	25.17	26.06	24.99	21.84	24.11	
Output Streams (reactor)						
Total liquids Out [kg/h]	4.12	6.60	6.95	6.24	5.99	
• recovered from HE	3.31	5.12	5.18	3.87	4.13	Section 9.5.5
• recovered from CWF	0.81	1.48	1.77	2.42	1.86	
Total gas out/Product gas [kg/h]	19.54	18.25	17.42	14.28	16.19	
Gas composition [% wt]						
• N_2	58.97	61.97	60.76	66.04	61.57	
• CO_2	20.43	24.13	28.15	26.97	27.12	
• CO	14.58	9.75	7.84	5.18	8.81	
• CH_4	1.07	0.64	1.03	0.33	0.87	Section 9.5.6
• O_2	2.75	0.91	0.88	1.24	0.86	
• C_2H_6	0.11	-	-	0.02	0.07	
• C_2H_4	0.98	0.60	0.36	0.22	0.38	
• Others (as C_3H_6)	1.11	2.00	0.08	-	0.28	
Total Out [kg/h]	23.66	24.85	24.37	20.57	22.18	Section 9.5.1
Mass balance closure [%]	94.00	95.36	97.52	94.18	91.99	
Mass balance [N_2-free, %]	88.29	91.26	95.67	89.89	86.35	Section 9.5.2
Total liquids yield [% wt maf]	40.12	54.46	57.43	61.50	49.91	

The basis for the determination of mass balances over the CFB reactor was further discussed in the previous section. Mass balances over the entire CFB reactor were obtained by simply diverting product gas from the by-pass line to the downstream processing equipment, Figure 9-2, as soon as temperatures in the riser section were stabilised, differing by less than 10°C. As soon as the pressure build-up in the heat exchanger rose to above 150 mmWC, the

product gas stream was diverted again, so that the total time between these two times constituted the duration of each run in the steady-state mode of operation.

Concerning the operating parameters in Table 9-2, it should be kept in mind that the riser temperature is the average of thermocouples TCs 12, 14 and 16. The vapor residence time (VRT, t_{res}) is the ratio of the reactor system operational volume, i.e. the volume of the riser section above biomass feeding point plus the riser of the cyclone, impinger and heat exchanger upper section, to the total gas/vapor volumetric flowrate, i.e. as defined in Eq. 4-29, Eq. 4-33 and Eq. 4-38 in Section 4.3.1.

9.5.3 Comparison of the results obtained with other fast pyrolysis processes

Mass balances for other fast pyrolysis processes, as far as total liquids yields are concerned, are given in Table 9-4 for comparison purposes. The fast pyrolysis processes presented in Table 9-4 were discussed in detail in Chapter 3.

Table 9-4: Comparison of fast pyrolysis liquid yields based on pneumatic reactors

Group[1]	Total liquids[2]	Closure	Temp (°C)	Reference	Feedstock size, d_p (mm)
ERCO	≈40	xx[4]	510	(Kosstrin, 1980)	not given
Un. of Waterloo	78	96	500	(Scott and Piskorz, 1984)	$1 \times 10^{-3} < d_p < 3 \times 10^{-3}$
Union Fenosa	65-75[3]	xx[4]	500	(Cuevas, 1995)	<3
Ensyn, Inc	72.6	100	500	(Freel and Graham, 1988)	avg. 3×10^{-3}
GTRI	78	100	550	(Knight *et al.*, 1985)	0.25
OFPP	56.8	100	482	(Bogley *et al.*, 1977)	<1.20
Egemin	54.8	100	550	(Maniatis, 1994)	$1 < d_p < 5$
This work	61.5	94.2	496	R10, Table 9-3	$1.0 < d_p < 1.5$

1) biomass fast pyrolysis processes were discussed in Chapter 3
2) on a % wt feedstock maf basis
3) results refer on a % wt feedstock wet basis - mass balance closures not available
4) not performed or not referenced

It can be seen that the total liquids yields are somewhat lower than those obtained for other biomass fast pyrolysis processes (with the exception of ERCO, OFPP and Egemin). The mass balance closures over the entire CFB reactor are generally good. However, when

considered over the pyrolysis section/riser of the CFB reactor these mass balances become significantly lower as will be discussed below in Section 9.5.4.

The deviations from 100 % mass balance closures are due to the following reasons:

- Most of the missing components in the mass balance closures are believed to be a volatile part of the organic vapors, either retained as solids-liquids agglomerates in the heat exchanger, an issue discussed in Section 8.6.1, or escaping the cotton wool filter as vapors.
- There are uncertainties connected with the reliability of the volumetric biomass feeding system.

9.5.4 Mass balance over the riser and liquid recovery sections for run R11

The mass balance over the riser and the liquid recovery sections, Figure 9-3, gives the distribution of biomass fast pyrolysis products, i.e. pyrolysis condensable vapors (including feedstock and reaction water), solid char and pyrolysis non-condensable gas. These mass balances enable the calculation of char and pyrolysis gas yields and, hence, provide an evaluation of the combined performance of the riser and liquid recovery sections as far as liquid production and recovery is concerned.

Although char is not a product stream of the CFB reactor system, its yield over the riser section may be estimated by considering a mass balance over the char combustor. To perform such a mass balance, the gas composition at the exit of the char combustor (combustor flue gas) is required. To achieve this, an additional gas sampling line for run R11 was designed and installed, shown in Figure 9-4.

The char combustor flue gases theoretically consist of N_2 and CO_2, since char is ideally burnt completely to CO_2 and O_2 is entirely consumed during the char combustion process, as discussed in Section 4.5.3. However, the gas analysis in this part of the system revealed the presence of CO and residual O_2.

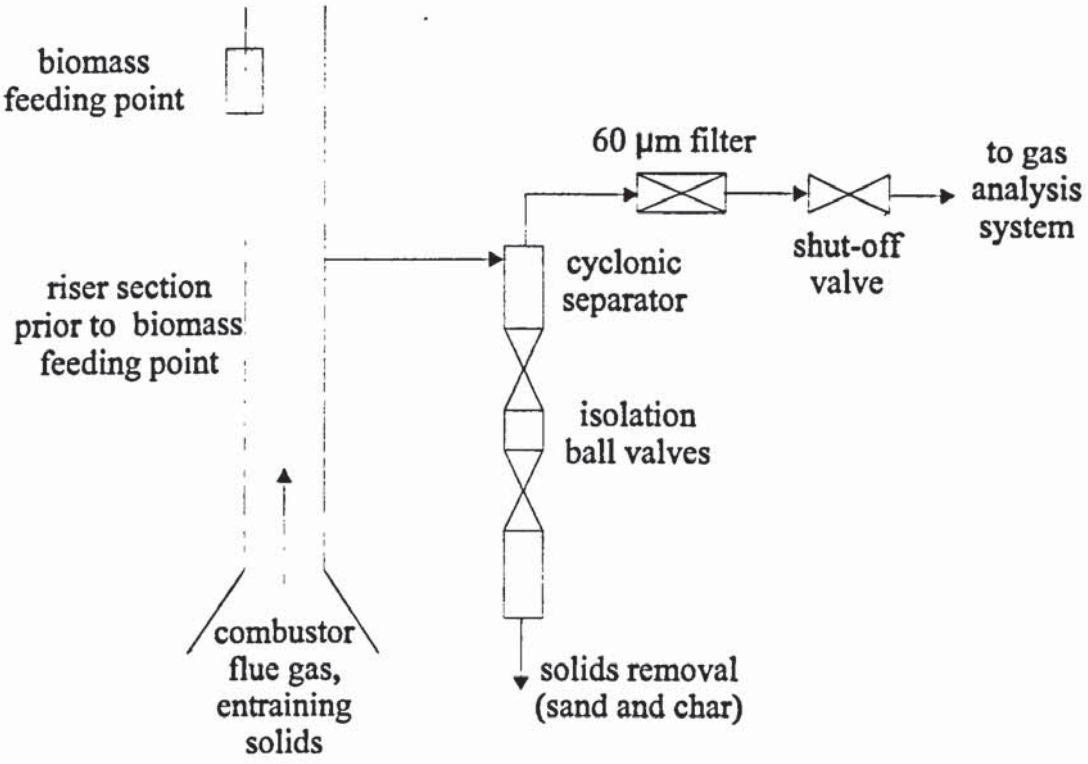

Figure 9-4: Arrangement for gas sampling from the char combustor (run R11)

During steady-state conditions for run R11, three gas-samples were periodically taken from the riser above the char combustor and below the biomass feedpoint, Figure 9-4, and were analysed with the on-line gas analysers for CO, CO_2, N_2 and O_2. The analysis of these gas samples was averaged, see Table 9-5. Flue gas flowrate was estimated by taking a N_2 balance over the char combustor (Maniatis, 1986).

Table 9-5: Gas analysis from the char combustor (at FGF=13 kg air/h => G^{in}_{O2} =3.029 kg/h) for run R11 (BFR=10.22 kg maf/h)

Gas compoment i	% v/v	% wt	G_i (kg/h)
CO	2.60	2.33	0.336
CO_2	19.59	27.55	3.970
O_2	0.91	0.93	0.133
N_2	76.90 (by diff.)	69.19	9.971
Combustor flue gas	100.00	100.00	14.410

Taking into account the mass flowrate of gaseous components as estimated in Table 9-5, the char flowrate is further estimated by considering a mass balance over the char combustor:

$$\text{Input streams} = \text{Output streams}$$

$$\Rightarrow G_{char}^{est} + G_{N2} + G_{O2}^{in} = G_{CO2} + G_{CO} + G_{O2}^{out} + G_{N2}$$

$$\Rightarrow G_{char}^{est} = G_{CO2} + G_{CO} + G_{O2}^{out} - G_{O2}^{in}$$

$$\Rightarrow G_{char}^{est} = 3.970 + 0.336 + 0.133 - 3.02$$

$$\Rightarrow G_{char}^{est} = 1.410 \text{ kg/h} \qquad \text{(Eq. 9-3)}$$

The elementary stoichiometric reactions for the formation of 3.970 kg/h CO_2 and 0.336 kg/h CO indicate a theoretically determined value for char flowrate, G_{char}^{theor}, to the combustor of 1.23 kg/h, as discussed in Section 4.5.3.

Moreover, at 541°C (riser temperature for run R11) a char yield of 10.75 % wt of maf biomass feed was experimentally determined in a bubbling fluidised bed reactor (Scott and Piskorz, 1988). Thus, the experimentally char flowrate to the combustor is estimated to be approximately:

$$G_{char}^{exp} = 0.1075 \text{ [kg char/kg maf biomass]} \times 10.22 \text{ [kg maf biomass/h]}$$

$$\Rightarrow G_{char}^{exp} = 1.099 \text{ kg char/h}$$

$$\Rightarrow G_{char}^{exp} \approx 1.100 \text{ kg char/h} \qquad \text{(Eq. 9-4)}$$

From the above findings it may be concluded that

- O_2 conversion in the combustor chamber approached 96 %, i.e. incoming O_2 was nearly all consumed in the char combustor at steady-state conditions in accordance with the hypothesis made by Nilsson (1990), Section 4.5.3
- nearly all O_2 forms CO_2 with char in accordance with assumptions made by other researchers (Liinanki, 1981; Van den Aarsen, 1984)
- $G_{char}^{exp} < G_{char}^{theor} < G_{char}^{est}$, so that the differences in the experimentally determined value (according to Eq. 9-4), the theoretically calculated value (according to the discussion held in Section 4.5.3) and the estimated, by the mass balance over the char combustor, value (according to Eq. 9-3) for char flowrate may be attributed to excess char being accumulated in the char combustor, and hence the CFB reactor, over time.

At this point the char air factor, referred to in Section 9.2, is further examined and calculated for the operating parameters of run R11. An elemental analysis of fast pyrolysis biomass derived char, incorporating data from Scott and Piskorz (1984), gives the following composition for char (on a % wt moisture-free basis): carbon 70.0; hydrogen, 2.8; nitrogen

0.3; oxygen [by difference] 20.4 and ash 6.5. Given this composition and taking into account the calculation procedure adopted by Maniatis (1986), the char air factor, S_c, according to Eq. 9-2 is correlated to fluidising gas flowrate (FGF), using the typical analysis of pyrolysis char given above as follows:

$$S_c = \frac{G_{air}}{\sum (z_i p_i^{air}) G_{char}} = 0.1232 \frac{G_{air}}{G_{char}}$$

$$\Rightarrow S_c = 0.1232 \frac{FGF}{G_{char}}$$

(Eq. 9-5)

According now to the different procedures considered for the estimation of char flowrate, different values for the char air factor, S_c, as determined by Eq. 9-5, are obtained and shown in Table 9-6 below:

Table 9-6: Char air factor according to the procedure followed for char flowrate estimation (data valid for run R11)

Char flowrate, G_{char}, estimation procedure	Flowrate [kg/h]	S_c, Eq. 9-5
Combustor mass balance estimated, Eq. 9-3	1.41	1.13
Theoretically estimated, Section 4.5.3	1.23	1.30
Experimentally calculated (Scott and Piskorz, 1988)	1.10	1.46

In all the cases considered, the char air factor value, as determined by Eq. 9-5, is greater than 1, practically allowing for complete combustion of char in the bubbling fluidised bed combustor (Desrosiers, 1979).

The above discussion shows that reference to the term "air factor" to denote the proportion of the amount of air in relation to the amount of biomass fed to the CFB combustor, should be exercised carefully, since for different parts of the system different values for the air factor are obtained. This is due to the fact that the different sections of the CFB reactor serve a different function and attention must be given to defining exactly the flowrate and composition of feedstock (biomass or char) and oxidant in each part of the system before a reference to an air factor value is given. Thus, the reference given to a nominal air factor, referring to the relation of the incoming feedstock and oxidant streams and discussed in Section 9-2 above, must only serve as a generic feature of the CFB fast pyrolysis reactor and not a specific term for the classification of the system in question in the wide range of

existing biomass energy conversion systems comprising combustors, gasifiers and pyrolysers.

The pyrolysis gas, i.e. the product gas excluding N_2, residual O_2 as well as CO_2 and CO derived from char combustion, yield and composition for run R11 may now be estimated and are given in Table 9-7, below. It is important to note that the combustor flue gases are considered inert in the temperatures (<605°C) prevailing in the riser and do not dissociate or contribute to secondary reactions according to the discussion in Section 2.4. Thus, the flowrates of CO and CO_2 in the combustor flue gases, calculated in Table 9-5, are subtracted from the respective flowrates in the product gas, the difference considered to be the CO_2 and CO produced during biomass pyrolysis in the riser section.

Table 9-7: Pyrolysis gas composition for run R11

Gas component in product gas	% wt in product gas (from Table 9-3)	G_i (kg/h) in product gas (Table 9-3)	G_i (N_2, O_2 and combustion products free, Table 9-5)	% wt in pyrolysis gas
N_2	61.57	9.9710	-	-
CO_2	27.12	4.3913	(4.3913-3.9700)	22.46
CO	8.81	1.4281	(1.4281-0.3360)	58.22
CH_4	0.87	0.1425	0.1425	8.60
O_2	0.86	0.1409	-	-
C_2H_6	0.07	0.0113	0.1130	6.02
C_2H_4	0.38	0.0615	0.0615	3.28
Others (C_2H_6)	0.28	0.0454	0.0454	1.42
Total	100.00	16.192	1.8758	100.00

This procedure allows the derivation of mass balances for the pyrolysis process, i.e. the product distribution of the gaseous (primary vapors, entraining gases and pyrolysis gas) and solid char products, i.e. the distribution of biomass pyrolysis products which leave the riser and liquid recovery sections for run R11. They are given below in Table 9-8, where the results of Scott *et al.*, (1985) have also been incorporated for comparison.

Char yield is estimated according to the theoretical calculations discussed above, Section 4.5.4, corresponding to the actual yields of CO and CO_2 in the combustor.

Table 9-8: Mass balance over riser and liquid recovery sections for run R11

(feedstock: pine wood)

Input streams (feedstock in the riser section)	Flowrate (kg/h)	Yields (% wt wet feedstock)	Yields (% wt maf feedstock)	Yields (from Scott *et al.*, 1985)[1]
Biomass In (kg maf/h)	10.22	92.00	100.00	
Moisture/Ash In (kg/h)	0.89	8.00	0.00	
Total In (biomass feedstock)	11.11	100.00	100.00	
Output streams (products out of the riser & liquid recovery sections)				
Total liquids (measured)	5.99	53.92	49.91	76.00
Pyrolysis char (estimated in R11)	1.23	12.69	13.80	10.75
Pyrolysis gas (calculated in R11)	1.88	16.88	18.35	13.25
Total Out (pyrolysis products)	9.28			
Mass balance closure (over riser & liquid recovery sections)		83.49	82.069	≈100.00

1) at 541 °C, feedstock aspen-poplar, 7.55 % wt moisture, VRT=0.445 s with N_2 as the fluidising gas

From the above results it is apparent that the mass balance closures over the pyrolysis process, in this context expressed as product yields over the riser and liquid recovery sections, are less satisfactory than those achieved for the entire CFB reactor system, Table 9-3, where mass balances are based both on 100 % recovery of fluidising gas and on a N_2-free basis.

Moreover, the total liquid yields are lower than those obtained by other researchers for similar reactor conditions, as already discussed in Section 9.5.3. The poor liquid yields might be a result of :

- Liquid recovery procedures, since in the bench scale unit incorporated in the University of Waterloo (UoW) experiments, acetone was used as solvent to remove residual reaction products from the reactor and connecting lines, while in the CFB reactor liquids and agglomerates retained in the heat exchanger were not washed out, as discussed in Section 8.6.1.
- Poor heat transfer for the 10-fold higher particle size (particle sizes, between 150 and 250 μm were incorporated in the UoW bench scale unit) employed in this work.

- Isothermal operation of the riser section, an operational feature which promotes additional primary vapor cracking, according to the discussion held in Section 4.6.1.
- Increased char accumulation in the reactor system, the excess char blown in the pyrolysis section, promoting additional heterogeneous char-vapors reactions in the hot reactor zone (at 550°C) and enhancing secondary cracking reactions, which lead, Section 2.4, to increased yields of non-condensible gases.

9.5.5 Pyrolysis liquids

Pyrolysis liquids are the sum of organic liquids, feedstock moisture and reaction water and are referred to as total liquids. Total liquid yields on a maf feedstock basis versus average riser temperature are shown in Figure 9-5, where the variation of total liquid yields as a function of temperature, based on experimental work undertaken by University of Waterloo researchers (Scott *et al.*, 1988), is also shown.

These results are in accordance with the findings of Scott and Piskorz (1982; 1983), in the temperature range 500-600°C, the total liquid yield increasing with decreasing reactor temperature. The operation of the riser in the isothermal mode promotes higher gas yields as compared to adiabatic operation (Scott and Piskorz, 1984), since secondary cracking of the primary vapors and further decomposition of char particles proceed in the riser section, promoted by the higher wall temperatures and extra heat transfer provided by the hot inert sand particles.

The highest total pyrolysis liquid yield, 61.50 % wt on a maf feedstock basis, was obtained for run R10 at approximately 500°C in the riser section, i.e. above the biomass feeding point, and a vapor residence time of 458 ms, as defined by Eq. 4-38, Section 4.6.1.

The total liquid yields obtained are rather low compared to other fast pyrolysis processes, see also Table 9-4. However, it should be kept in mind that the heavier fractions of the pyrolysis liquids were retained in the heat exchanger due to the physical/chemical mechanism, thoroughly discussed in Section 8.6.1, and leading to the formation of sticky agglomerates in the heat exchanger. The loss of the heavier organics is also reflected in the low mass balance closure over the riser and liquid recovery sections of the CFB reactor system, for run R11, extensively discussed in Section 9.5.4 above.

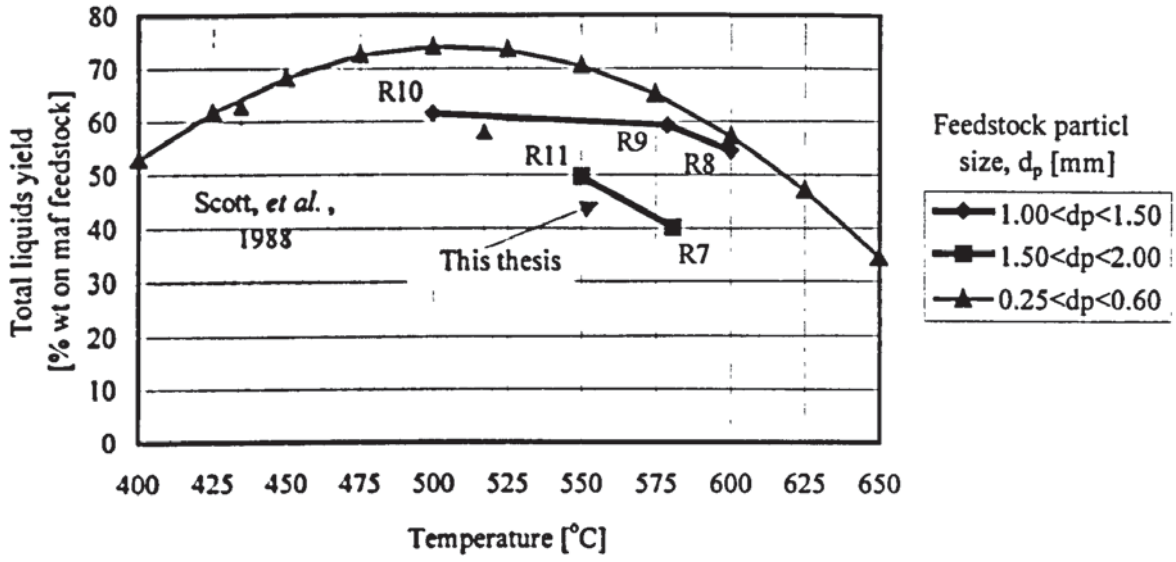

Figure 9-5: Total liquids yield, on a maf basis, versus riser temperature

Although the heavy fractions could be collected and accounted for in the mass balance closures, this was not practised since the removal of entrained solids (char and sand) from the agglomerates would require solvent washing, filtration and subsequent solvent removal in a vacuum evaporator. These procedures were considered time consuming, troublesome and costly.

Three important process parameters were varied during runs R7 to R11, namely the pyrolysis reactor (riser) temperature, the vapor residence time (VRT, t_{res}) and the feedstock particle size, d_p. The reactor temperature seems to be the most important process parameter for the total pyrolysis liquid yields, in accordance with the findings of Scott *et al.*, (1988), while the VRT does not seem to have any significant effect in the narrow range (370 ms<t_{res}<460 ms) considered. In fact, the maximum liquid yields, R10, are attained in the longer vapor residence time (VRT), Table 9-3, which exhibits the influence of pyrolysis temperature, at least in the low range of VRTs considered for this thesis. Larger particle size feedstocks result in decreased liquid yields, Figure 9-3, since larger particle sizes result in more severe heat transfer limitations, as discussed explicitly in Section 2.7.

From the limited data available it is shown that pyrolysis liquids are more difficult to recover in a single recovery step at lower temperatures, since as temperature decreases, an increasing fraction of the condensable liquids is retained in the cotton wool filter, Table 9-3. This may be due to the combined effect of the following two factors:

1. The higher formation of the vapors from depolymerisation product (anhydrosugars), favoured at lower temperatures, Section 2.3.1, are more difficult to recover than those of the fragmentation products (carbonyl compounds), favoured at higher temperatures.
2. At lower pyrolysis reactor temperatures, the condensables yields increase, as discussed above, hence the load on the heat exchanger becomes higher, so that an increasing amount of heavier organics escapes recovery due to insufficient cooling.

In Figure 9-6, the fraction of total liquids retained in the heat exchanger (HE) is plotted as a function of temperature and particle size.

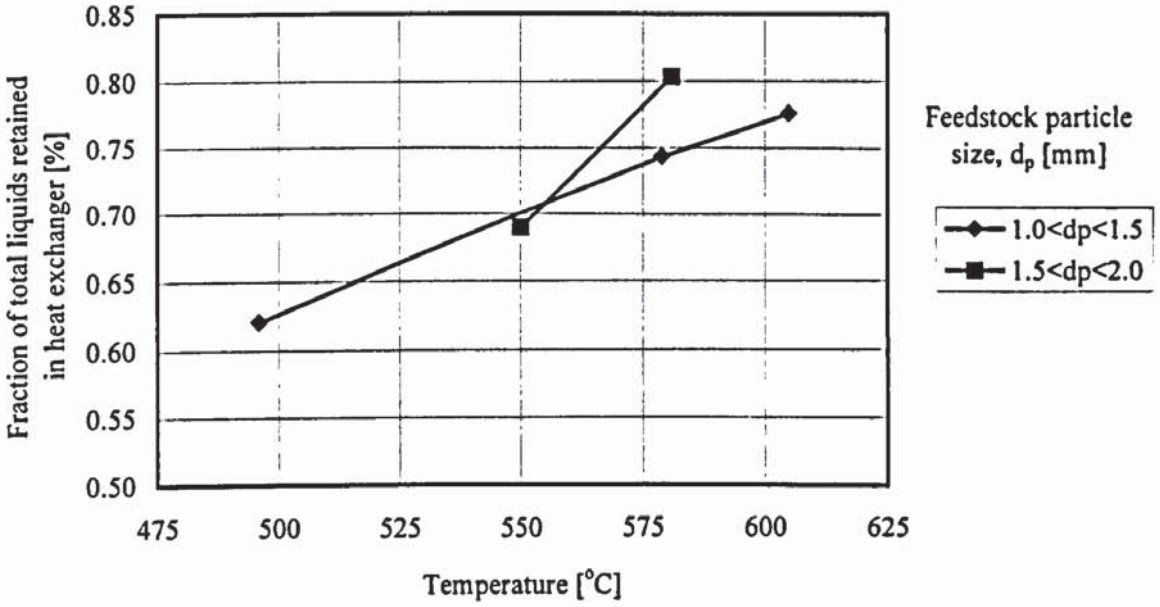

Figure 9-6: Fraction of total liquids retained over the HE and CWF as a function of temperature and feedstock particle size.

9.5.6 Product gas

Product gas is the sum of char combustor flue gas products (N_2, CO_2 and CO) as well as biomass pyrolysis gas, Figure 9-3, so pyrolysis gas yields and composition cannot be estimated by a single gas analysis of the gaseous reactor products at the reactor exit. Pyrolysis gas composition has to be estimated by subtracting the char combustor flue gas from the product gas (total gas) as discussed in Section 9.5.4.

Product gas composition was determined on-line by gas chromatography (GC), using the configuration discussed in Section 7.6.4. The sampling point was located after the cotton-wool filter. A suction pump was employed to supply a gas sample to the GC system through a series of filters to remove persistent aerosols and particulates. The combustor flue gas

flowrate was determined by continuous on-line gas analysers through a sampling procedure described above in Section 9.5.4.

In order to estimate the product and combustor gas flowrates, N_2 was used as an internal standard, a procedure also followed by other researchers (Schoeters, 1983; Maniatis, 1986). This approach was considered more reliable than using a dry gas meter (a wet gas meter was very expensive), which would require excessive protection measures against persistent aerosols escaping recovery in the liquid recovery section (heat exchanger and cotton-wool filter). The limited N_2 flow in the CFB L-valve was also accounted for (by means of a variable flow flowmeter) and subtracted from subsequent gas flowrate calculations.

It should be pointed out that the conclusions from gas analysis should be interpreted with caution, due to the limited number of experiments and to the fact that, with the exception of run R11, the product gas lumps together the pyrolysis and combustion products CO and CO_2. However, some interesting trends may be distinguished and are referred to below.

There is a constant decrease of both the CO-content and hydrocarbon gas yield with decreasing nominal air factor (decreasing temperature in the pyrolysis section, i.e. riser) for the smaller particle size and the narrow range of the nominal air factor for the three runs (runs R8, R9 and R10) considered. This trend is in accordance with the findings of Schoeters (1983) and Maniatis (1986), who dealt with the influence of the air factor on gas quality in bubbling fluidised bed gasifiers.

However, concrete conclusions cannot be derived for the larger particle size due to the limited data (runs R7 and R11) and the large range of the nominal air factor considered for these two runs. The CO content and the hydrocarbons gas yield in the product gas are plotted versus air factor in Figures 9-7 and 9-8 respectively.

The decrease of both the CO content and the hydrocarbons gas yield with decreasing gas temperature has also been demonstrated by Scott and Piskorz (1982) during experimentation with wood flour in a laboratory fluidised bed pyrolyser, Section 3.4.2.

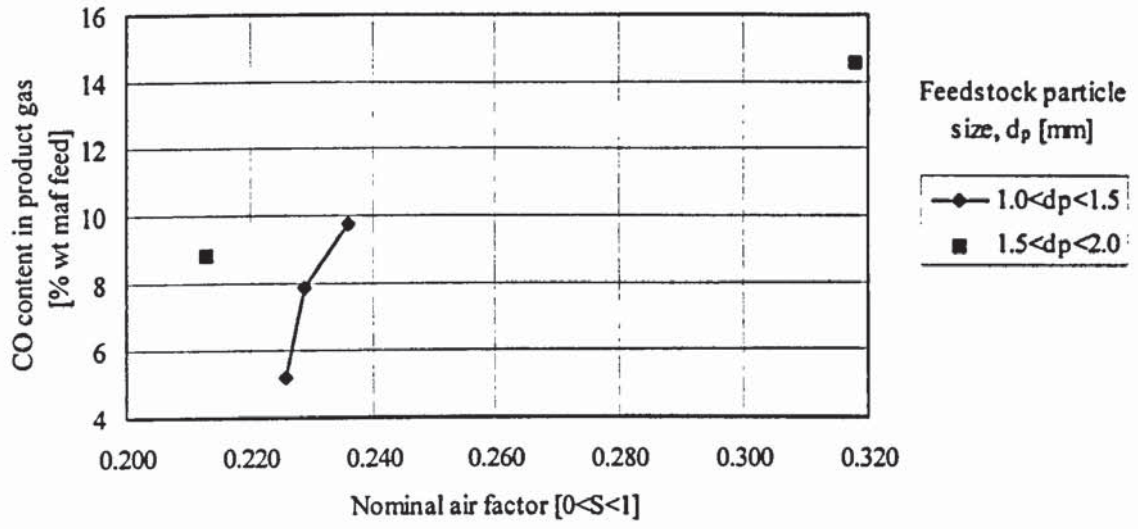

Figure 9-7: CO content in product gas versus nominal air factor

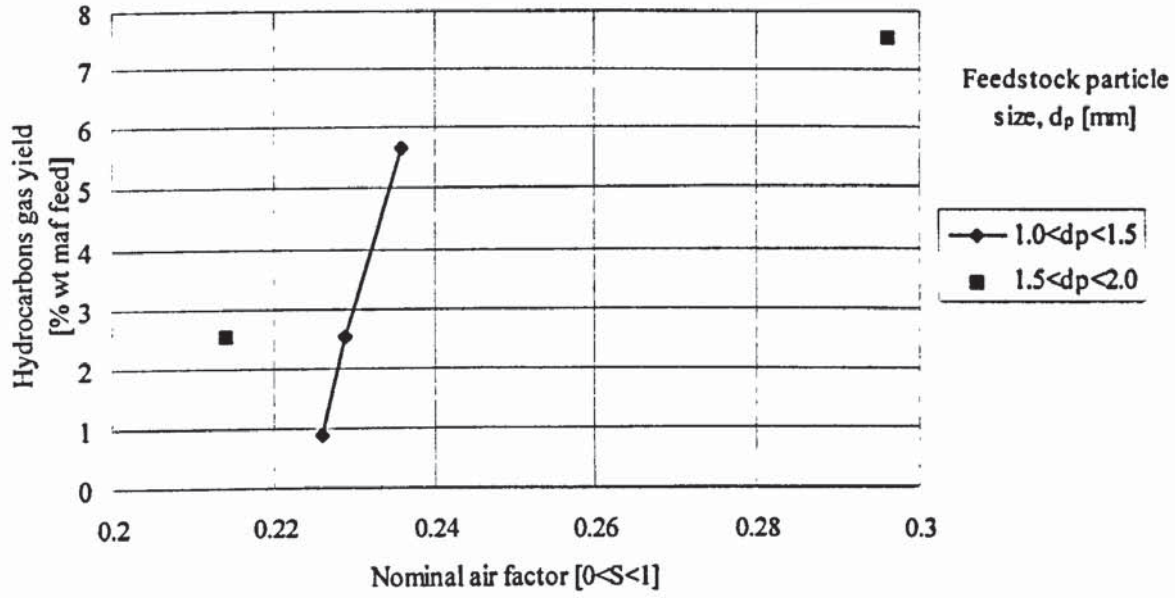

Figure 9-8: Hydrocarbons gas yield versus nominal air factor

The decrease of CO content and hydrocarbons gas yield in the product gas with decreasing nominal air factor (riser temperature) discussed above, has a direct impact on the product gas Higher Heating Value (HHV) as depicted from Figure 9-9, where the product gas HHV versus air factor is plotted. Again, there is a distinct trend of HHV decrease with decreasing nominal air factor for the smaller particle size, which is consistent with the work of other researchers based on fluidised bed fast pyrolysers (Scott and Piskorz, 1984), while for the larger particle size feedstock concrete conclusions cannot be drawn.

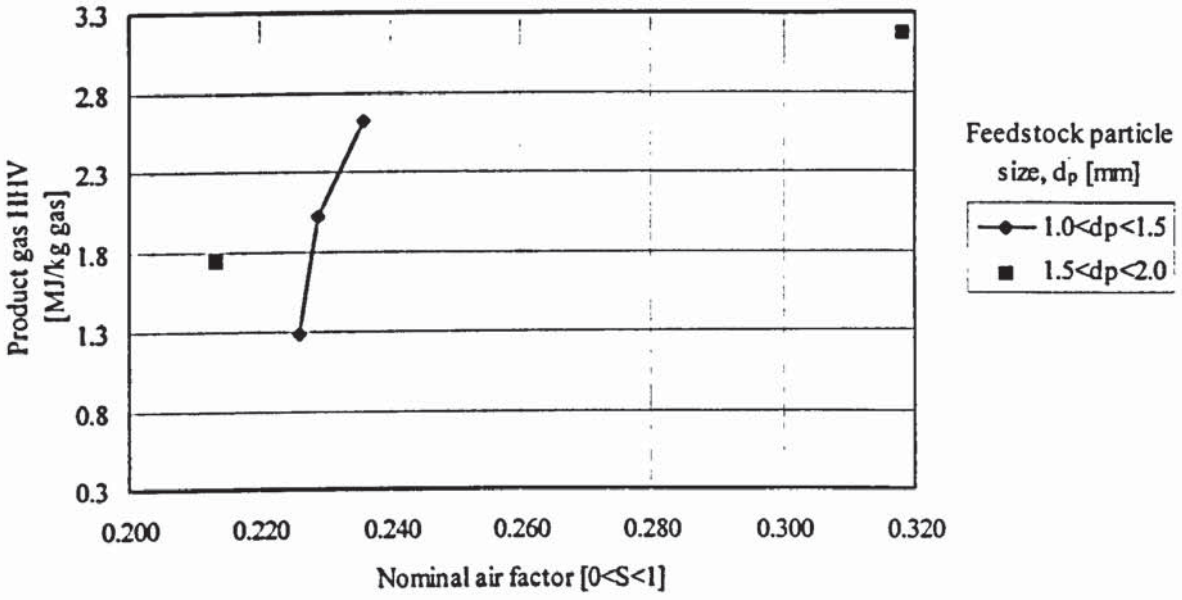

Figure 9-9: Product gas HHV versus nominal air factor

The results presented in Figure 9-9 are in contradiction with those of researchers who studied the product gas HHV versus the air factor for bubbling fluidised bed gasifiers (Schoeters, 1983; Maniatis, 1986). In these cases, the prolonged VRTs and increased temperatures involved had as a result the extensive secondary cracking of the primary vapors and the prevalence of endothermal reactions in the extended gasifier freeboard, which resulted in the formation of gaseous products at the expense of condensables.

Finally, the estimated pyrolysis gas composition for Run R11 and data derived from a bubbling fluidised bed (BFB) pyrolyser, based on the WFPP technology, Section 3.4, operated by researchers at Aston University (Peacocke *et al.*, 1996) are shown in Table 9-9.

Although it is difficult to draw any concrete conclusions due to the different reactor configurations involved, the pyrolysis gas composition in the CFB pyrolyser indicate significant organic vapor cracking, with the production of CO and hydrocarbons at the expense of CO_2. This is probably attributed to the isothermal operation in the upper riser section of the CFB pyrolyser compared to the adiabatic cooling in the freeboard of the BFB, as discussed in Section 4.6.1. The gas yield in the BFB is slightly higher than the normalized (assuming a 97 % mass balance closure for the CFB reactor) gas yield of the CFB, 23.8 to 20.4 % wt on a maf wood basis respectively, due to the slightly higher temperature in the BFB reactor.

Table 9-9: Comparison of pyrolysis gas composition between CFB and BFB pyrolysers

Component in pyrolysis gas	Pyrolysis gas composition (% wt) in a CFB (this work - R11)[1]	Pyrolysis gas composition (% wt) in a BFB (Peacocke *et al.*, 1996)[2]
CO	58.22	49.56
CO_2	22.46	40.18
CH_4	8.60	6.14
C_2H_4	3.28	2.60
C_2H_6	6.02	-
C_3H_6	1.42	1.58[3]
H_2	nd	nd
Pyrolysis gas yield[4] (%)	16.88 (on a 80.29 % mass balance closure)	23.8 (on a 97 % mass balance closure)
TOTAL	100.00	100.00

1) riser temperature: 550 °C, vapor residence time: 373 ms (Table 9-3)
2) bubbling fluidised bed temperature: 562 °C, vapor residence time: 1013 ms
3) expressed as C_3H_8
4) based on a maf wood basis

9.5.7 CFB reactor specific throughput

Another important aspect in terms of reactor scale-up is that of specific throughput. A comparison between the different reactor systems developed, as far as specific throughput and gas-to-feed ratios are concerned, is presented in Table 9-10.

As seen from the data presented in Table 9-10, the proposed CFB reactor exhibits the highest specific throughput of all the reactor systems based on atmospheric pressure tested for biomass fast pyrolysis.

Moreover, the proposed CFB reactor exhibits the lowest gas volume to be treated in the subsequent downstream processing equipment (expressed as gas-to-feed ratio). The gas-to-feed ratio of the proposed CFB pyrolyser is comparable to that encountered in non-pneumatic, conduction promoted high heat transfer ablative pyrolysis systems lying in the range 0.5-4.1 (Peacocke *et al.*, 1996).

Table 9-10: Specific throughputs and gas-to-feed ratios of some pneumatically operated biomass fast pyrolysis reactors

Fast pyrolysis system developer	Reactor diameter (m)	Achieved flowrate (kg maf/h)	Specific throughput (kg/m^2s)	Gas-to-feed ratio	Reference
Georgia Tech	0.15	13.61	0.207	5.6 - 9.2	Kovac *et al.*, (1991)
University of Waterloo	0.10	up to 3	0.104	6 - 8	Scott and Piskorz (1983); Scott (1988)
Aston University	0.075	1.5	0.094	6.2 - 8.6	Peacocke *et al.*, (1996)
Union Fenosa	0.40	160	0.354	7 - 10	Cuevas (1995)
ENSYN	0.04	2.20	0.486	not given	Graham (1988)
EGEMIN	0.40	84	0.186	3.75	Roggeman (1993).
This work	0.05	8.4 - 10.5	1.12 - 1.48	1.3 - 1.9	runs R7 - R11

9.5.8 Conclusions for experimental mass balances

The following conclusions may be drawn concerning the mass balances:

1. Good mass balance closures (better than 91 %, Table 9-5) over the entire CFB reactor system have been derived, despite the

2. Less satisfactory (worse than 84 %, Table 9-8) mass balance closure over the riser and liquid recovery sections was obtained for run R11, where multiple gas sampling and analysis, i.e. both from the product gas and the flue gas stream from the char combustor, has been exercised. The main reason is considered to be the unquantified losses of heavier organics in the heat exchanger as discussed in Section 8.6.1 and the deleterious effect of char accumulation in the CFB riser, further promoting secondary cracking reactions and increased yields of non-condensable gases at the expense of condensable organic vapors.

3. Total liquid yields (on a maf basis) lower than those reported for other biomass fast pyrolysis processes have been obtained. The main reason is believed to be the poor operation of the liquid recovery system.

4. A very high degree of incoming O_2 conversion to CO_2 (mainly) and CO is attained in the BFB char combustor. However, pyrolysis char slowly accumulates in the CFB reactor, and is then transported through the biomass pyrolysis section (riser), where reactions leading to cracking of the heterogeneous primary vapors are being promoted.

5. The total liquid yields increase with decreasing temperature and decreasing particle size, in accordance with the findings by other research groups. The highest total liquid yield, 61.50 % wt on a maf feedstock basis, was obtained at 500°C and 460 ms Vapor Residence Time (VRT).

6. The pyrolysis (riser) temperature seems to be the most important parameter influencing total liquid yields (see also Scott and Piskorz, 1984, Halling, 1987; Scott *et al.*, 1988).

7. VRT was not explored as an independent variable, but in the low range examined, i.e. between 373 and 458 ms (Table 9-3), its impact on total liquid yields seems insignificant.

8. For the smaller feedstock particle size tested, CO content and hydrocarbons gas yield in the product gas decrease with decreasing temperature, thus resulting in a lower HHV gas.

9. The product gas yield decreases with decreasing temperature. These findings are in accordance with those reported by other research groups.

10. The residence time of solid char in the BFB (char combustor) is probably inadequate, so that a near 100 % char conversion to gas products has not been achieved. Thus, an improved design of this part of the system must be provided for incorporating additional measures, further discussed in Chapter 11.

11. The proposed CFB fast pyrolysis reactor exhibits the highest specific throughput and one of the lower gas-to-feed ratios of all the two-phase systems (incl. Entrained beds) tested.

9.6 Temperature profiles versus height in the CFB reactor for Run R11

Due to the thermocouple misplacement in the riser section (discussed in previous sections) a temperature profile along the CFB reactor loop was not considered reliable, apart from run R11, in which all the thermocouples were placed correctly. The temperature profile versus height for run R11 is presented in Figure 9-10, along with a scaled drawing of the CFB reactor to facilitate the profile examination.

In the beginning of the run, at 0 min after biomass feeding (blue line) the CFB reactor operates in the hot mode. The isothermal operation of the bubbling fluidised bed is clearly shown, while the temperature gradually decreases along the riser length. At 90 min after biomass feeding (red line) higher temperatures in the combustor and the riser section have been established, while at steady-state, at 180 minutes after biomass feeding (green line) a temperature shift has been accomplished with higher temperatures in the combustor, while increased biomass flowrates (lower air factors) impose a significant thermal load in the upper riser section moving the temperature to lower levels.

The observed temperature shift is a crucial requirement that has to be achieved, if the CFB system developed is to be operated in the dual-mode presented in the objectives of this thesis, i.e. as a char combustor (lower part - high temperatures) and a biomass pyrolyser (upper part - lower temperatures).

It is also important to note that the pyrolysis section operates isothermally, which verifies the hypothesis made in Section 4.6.1, that the pyrolysis riser of the CFB reactor is operated isothermally. Temperature uniformity in the riser is achieved by the dense gas-solids suspension promoting high heat transfer rates to the incoming biomass particles.

On the other hand, it has been shown in a bench scale unit (Scott and Piskorz, 1984) that bubbling fluidised bed pyrolysers give better results, as far as pyrolysis liquid yields are concerned, due to the adiabatic quenching operation and, hence, the more effective preservation of primary vapors. Adiabatic quenching is favoured in the lean freeboard region of the BFB reactors, where the temperature drops significantly due to the lean gas-solids suspension and the dominance of homogeneous, secondary phase reactions. Similar effects are also known to occur in bubbling fluidised bed gasifiers (Maniatis, 1986). However, comparing studies in an adiabatic and an isothermal reactor (Scott *et al.*, 1988) did not present any significant differences in liquid yields, so that the above claim remains to be verified in larger scale operation, Section 2.7.2.

At this point a comparison between the CFB biomass fast pyrolysis reactor and biomass updraft gasifier, Figure 9-11, is attempted given the resemblance of these two biomass conversion systems in terms of reactor configuration and temperature profile.

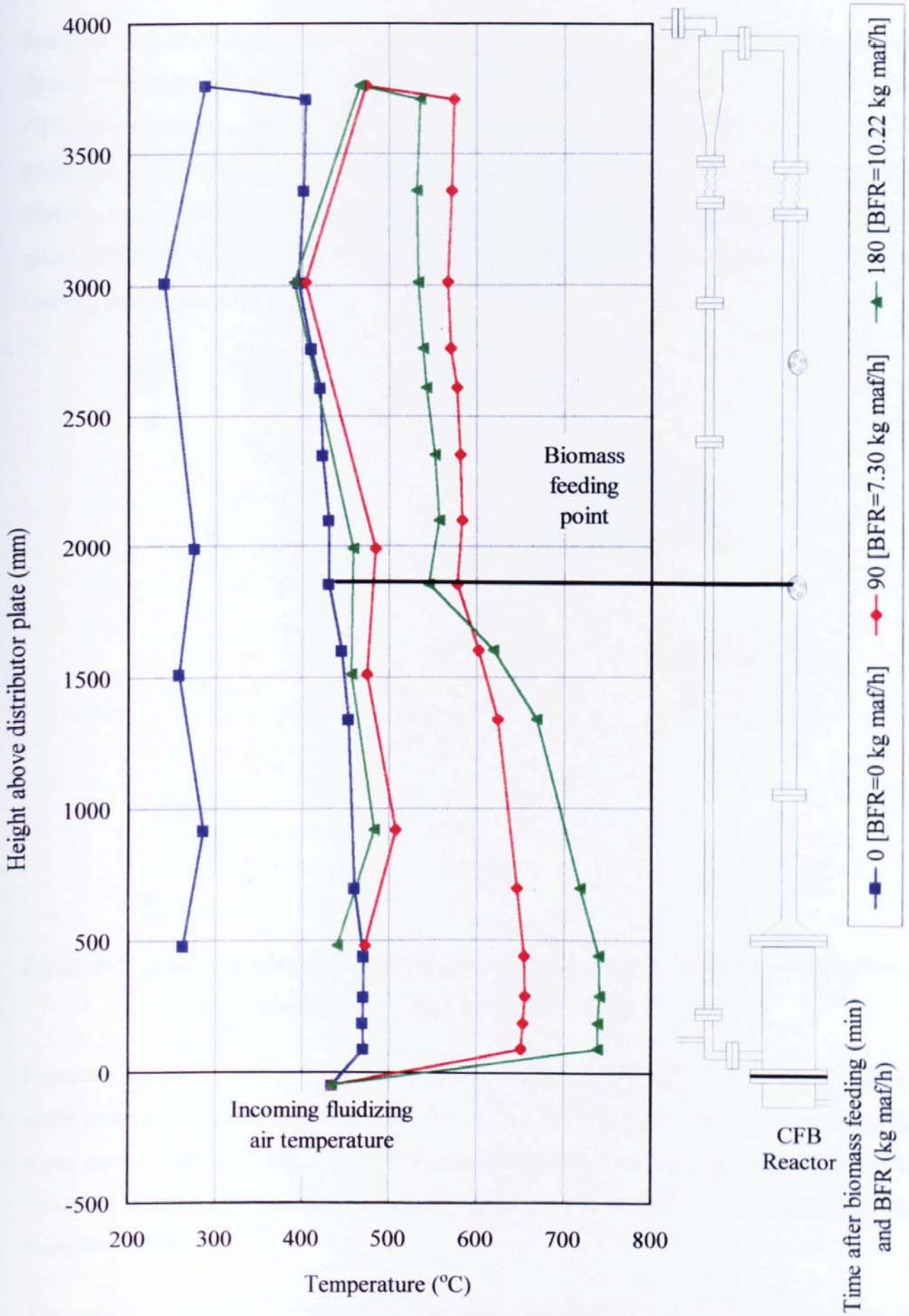

Figure 9-10: Temperature profile versus height in the CFB reactor for run R11

For both reactor configurations the nominal air factor, as defined in Eq. 9-1, is quite similar (Reed, 1981) lying between 0.2 and 0.3. Moreover, the main feature of both systems, i.e. the CFB fast pyrolysis reactor and the updraft gasifier, is the sequential occurrence of the oxidation and pyrolysis processes, which are separated spatially and therefore temporally. Finally, in both reactor configurations biomass is introduced at a high, oxygen-free reactor point, while the oxidant is introduced at the bottom of the reactor, the two streams never coming into intimate contact.

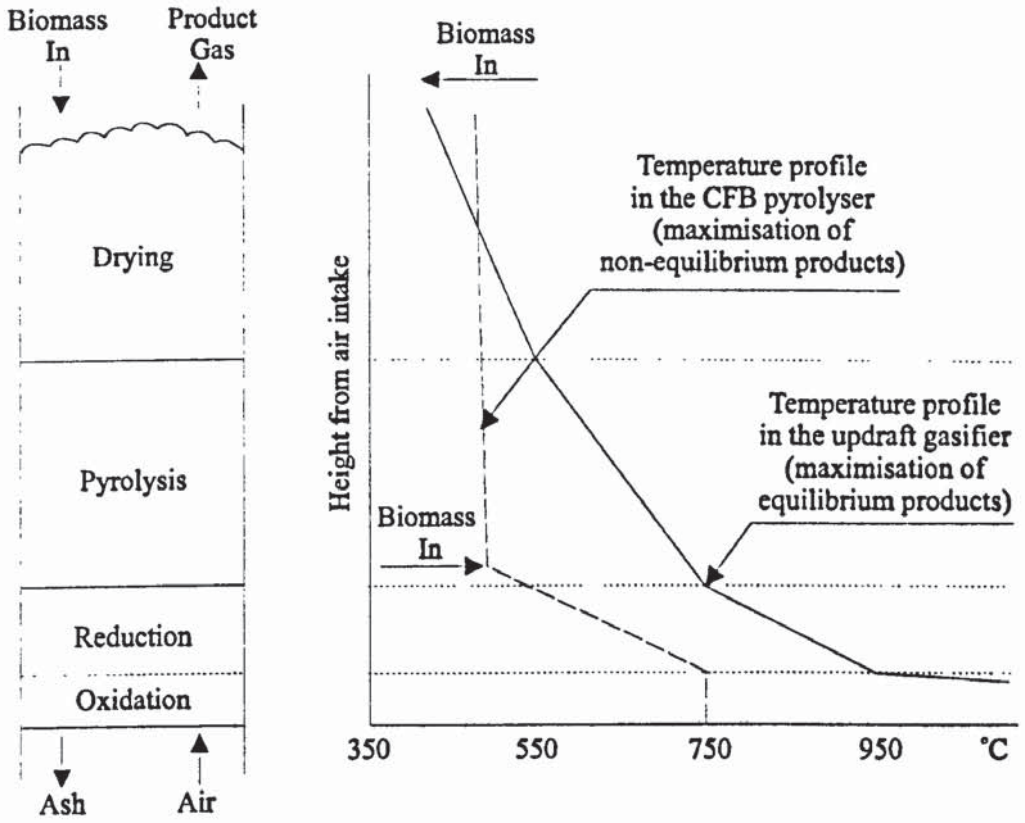

Figure 9-11: Major processes occurring in an updraft gasifier and temperature profiles in an updraft gasifier and the CFB pyrolyser (schematic)

However, these two reactor systems objectives are radically different. The updraft gasifier tends to maximise gas production while the CFB pyrolyser tends to maximise condensable vapor yields. Thus, and despite their profound similarities, the engineering design of each of these two biomass thermochemical conversion units is quite distinctive, the main differences being the following:

The updraft gasifier design strives to maximise gas production through establishment of chemical equilibrium in the upper reduction and pyrolysis zones, Figure 9-11. This is achieved by the high temperature, CO_2-rich gas stream released from the char combustion process in the lower oxidation zone.

The high temperature favours, kinetically and thermodynamically, the highly endothermic Boudouard and water-gas reactions, discussed in Section 2.4, which control the upper limit of temperature in the subsequent reduction zone, Figure 9-11. On the other hand, the CFB reactor is designed to preserve the valuable, non-equilibrium products of biomass pyrolysis at temperatures around 500°C, where gas-phase reactions are very slow, incorporating also very short gas/vapor residence times in the reaction zone and high heat transfer rates.

The CFB biomass fast pyrolyser may be considered as a drastically modified updraft gasifier, where the desired separation of char oxidation and biomass pyrolysis processes and, hence, the utilisation of char energy content, is achieved by the excess gas velocities incorporated (through the appropriate reactor design and geometry) in the pyrolysis (riser) section. The very short gas/vapor residence time and the moderate reactor temperatures incorporated in the CFB reactor configuration subsequently maximise the yields of the desired non-equilibrium condensable vapors at the expense of the high temperature-favoured equilibrium permanent gases.

9.7 Pressure drop versus time over the bubbling fluidised bed (char combustor)

The pressure drop over the char combustor (bubbling fluidised bed - ΔP_{bed}) was found to be approximately constant when performing hot experiments with no biomass feeding to the CFB reactor. However, during actual pyrolysis experiments, biomass feedrate to the CFB reactor steadily increased and at high biomass feeding rates the char constantly accumulates, as discussed above in Section 9.5.4. The char bed, i.e. the weight of char hold-up in the bubbling bed at steady state, must be seriously considered, since if the char bed attains high values, loss of fluidisation may occur due to excessive pressure drop over the bed (Maniatis, 1986). The variation of ΔP_{bed} was constantly measured for all experiments and the results and conclusions are discussed in the following.

The pressure drop over the BFB, as measured by a Fischer-Rosemount, Type DP 1151, differential pressure transmitter, is presented in Figures 9-12 to 9-16, respectively. Note that these measurements are given from the biomass feeding point for runs R7 to R10, while for run R11, pressure drop measurements are recorded 150 minutes before biomass feeding commenced. In these diagrams, the temperature in the discharge leg of the impinger (TC 33) was also recorded to illustrate any solids losses occurring in the CFB reactor system. Sudden

temperature increase at this part of the system was an indication of hot solids blown out from the CFB reactor. This solids loss necessitated the adoption of the proper corrective measures, i.e. the removal of the solids through the two-valve mechanism described in Section 8.4.4.

Figure 9-12 represents the pressure drop (ΔP_{bed}) over the bubbling fluidised bed (BFB) for run R7. In this diagram, no significant changes are shown except for the sudden decrease of ΔP_{bed}, when solids were blown from the system during the pressure tap tubing burn-out discussed in Section 9.4.1. This decrease in ΔP_{bed} was accompanied by a sharp increase in impinger temperature, indicating the capture of the hot solids blown out of the CFB reactor. As discussed above, at high air factors (characteristic for initial biomass feeding stages) no significant increase in ΔP_{bed} is shown, since all char is rapidly consumed. The only increase is shown at the end of the run, where the air factor retains its lower value, since the char bed is slowly formed.

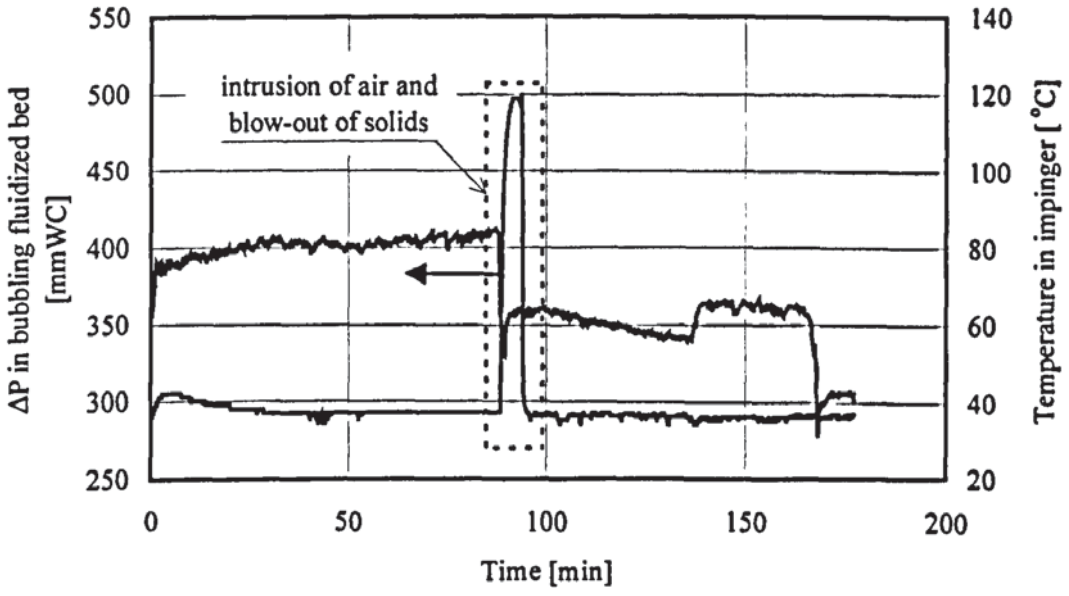

Figure 9-12: Pressure drop (ΔP_{bed}) over bubbling fluidised bed versus time for run R7

Figure 9-13 represents the pressure drop (ΔP_{bed}) over the bubbling fluidised bed (BFB) for run R8. In this run, performed at a lower air factor than that of run R7, a slow gradual increase in ΔP_{bed} is recorded, the ΔP_{bed} levelling off once biomass flowrate was cut off and the air factor attained again high values. The problem of char accumulation becomes more dominant at lower air factors, since at higher air factors the char is efficiently burnt with the excess oxygen present.

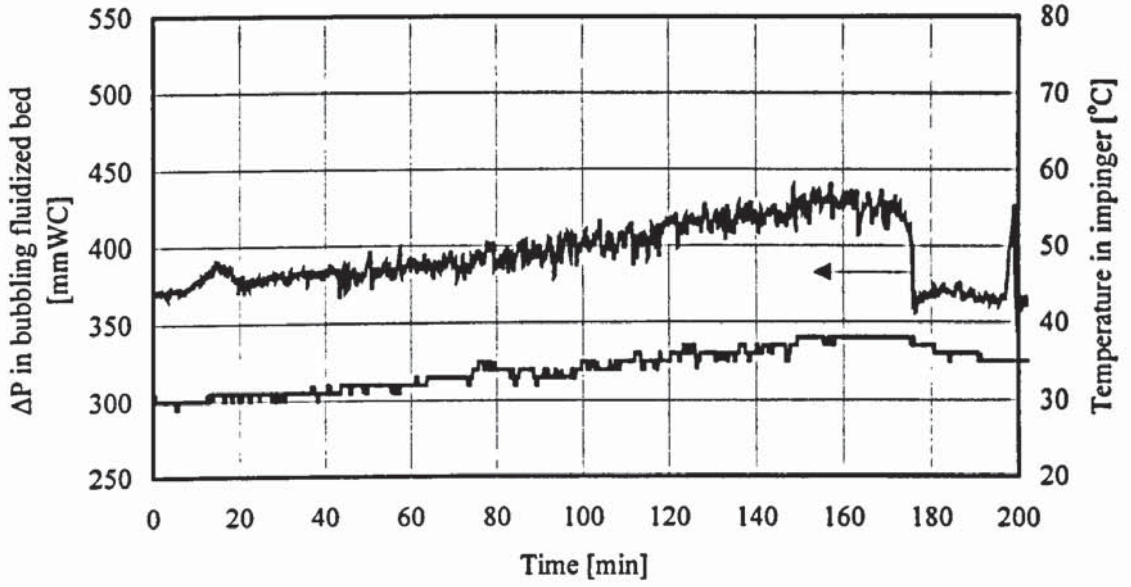

Figure 9-13: Pressure drop (ΔP_{bed}) over bubbling fluidised bed versus time for run R8

Figure 9-14 represents the pressure drop (ΔP_{bed}) over the bubbling fluidised bed (BFB) for run R9. A more rapid ΔP_{bed} increase was obtained, compared to that obtained for run R8, once more indicating the significance of the lower air factor on the accumulated char conversion (oxidation) rates at this part of the system. After biomass feeding stopped, the BFB air for this particular run was cut off instantaneously, also clearly shown in Figure 9-14.

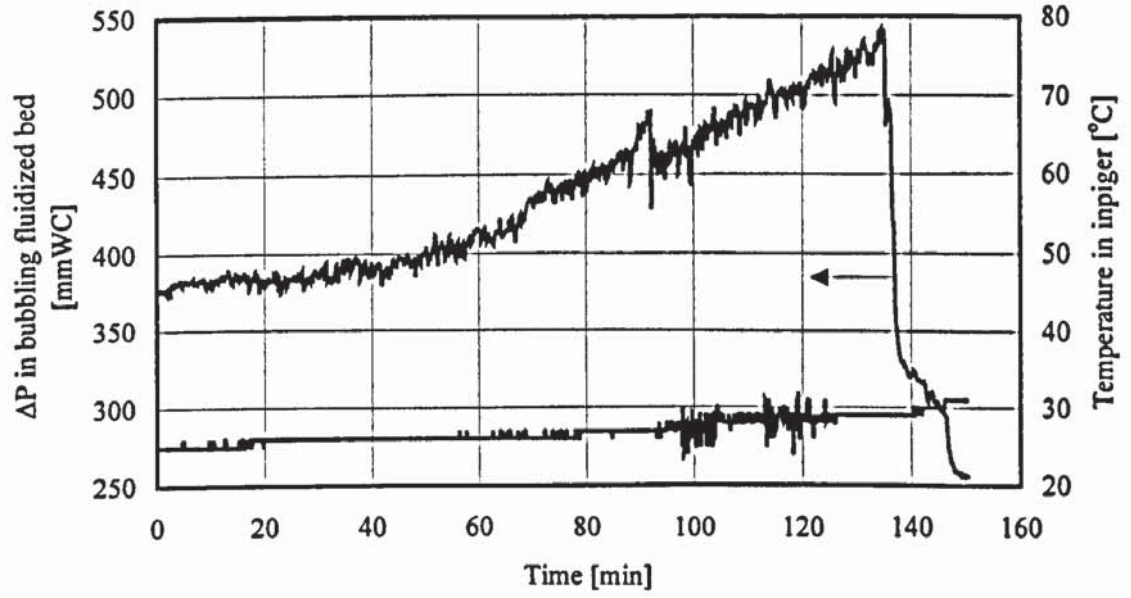

Figure 9-14: Pressure drop (ΔP_{bed}) over bubbling fluidised bed versus time for run R9

Figure 9-15 represents the pressure drop (ΔP_{bed}) over the bubbling fluidised bed for run R10. At about 70 minutes after biomass feeding commenced and due to the loss of solids

circulation discussed in Section 9.4.3, a substantial amount of solids was blown out through the by-pass line and not through the impinger. The ΔP_{bed} initially decreased, then increased rapidly once biomass flowrate was increased and a low nominal air factor prevailed.

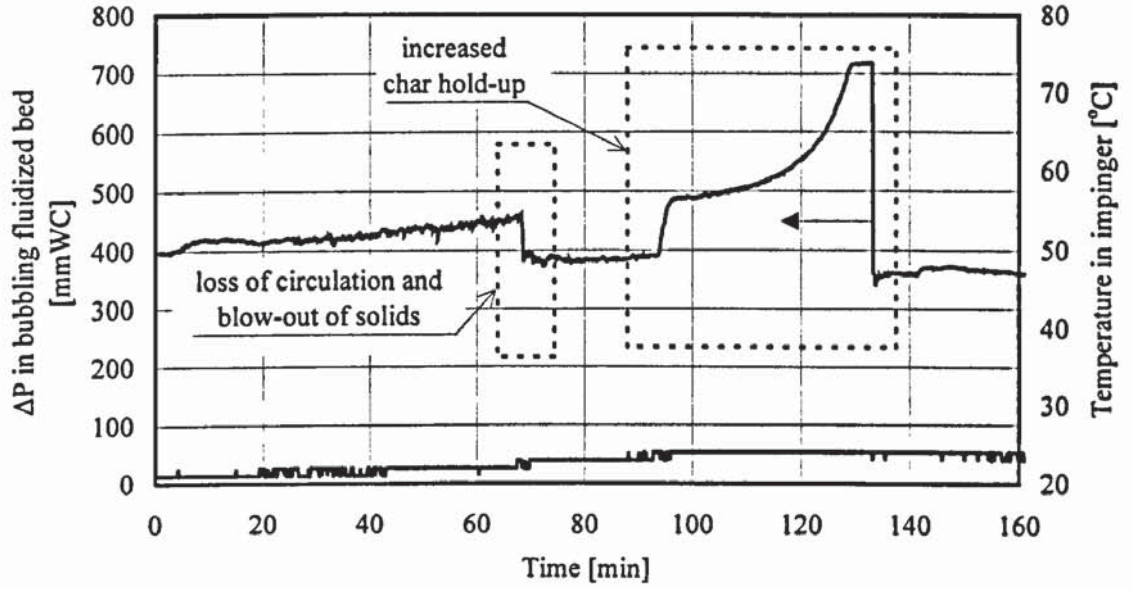

Figure 9-15: Pressure drop (ΔP_{bed}) over bubbling fluidised bed versus time for run R10

Finally, in Figure 9-16 the pressure drop (ΔP_{bed}) over the bubbling fluidised bed for run R11 is shown. Due to the two solids losses and the standpipe aeration loss (see Section 9.4.4), temperature increase in the impinger discharge leg was readily encountered.

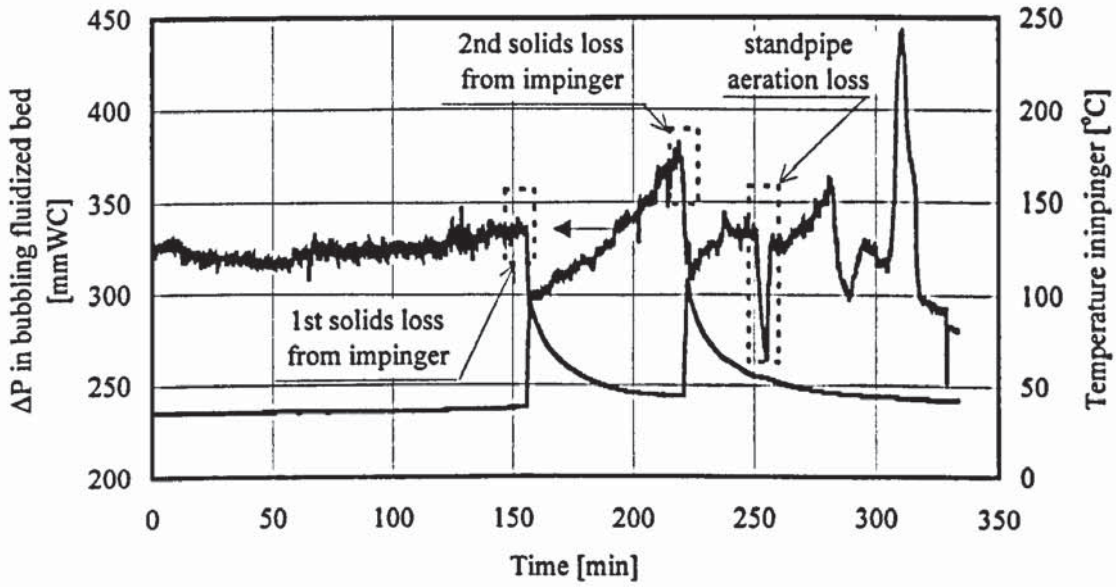

Figure 9-16: Pressure drop (ΔP) over bubbling fluidised bed versus time for run R11

In Table 9-11, the ΔP_{bed} over the BFB caused by the char bed as a percentage of the char-free bed ΔP_{sand} (sand bed) derived in the beginning of each experiment (prior to biomass feeding)

is presented, along with data extracted from Schoeters (1983) and derived from gasification of charcoal in a bench scale fluidised bed unit.

Table 9-11: Pressure drop recovery in char bed as compared with sand bed (ΔP_{sand})

Run Number	R7	R8	R9	R10	R11	Schoeters (1981)
% increase over ΔP_{sand}	<10	22.5	50	80	25	16 - 24
air factor (0<S<1)	0.318	0.236	0.229	0.226	0.214	0.35

As seen from the above table there seems to be a problem for runs R9 (excess amount of sand, Table 9-1, and lower combustor temperature, Table 9-3) and R10 (reduced amount of sand, Table 9-1, and high combustor temperature, Table 9-3). However, these two cases present an extreme, in terms of the prevailing conditions that favour high char hold-up, namely low temperatures and high char-to-sand ratio.

It is anticipated that in larger units, where the inert (heat carrier) solids storage systems are expected to be much larger, the amount of char hold-up will be considerably lower, practically posing no problem. However, in case of an emergency, i.e. conditions that favour high char hold-up values, the extra amount of char may be removed from the BFB mechanically by means of a configuration proposed in Section 8.5.3, Figure 8-5, or corrective measures may be taken, such as the temporary increase of FGF to burn off the excess char being slowly accumulated.

The pressure drop in the standpipe (ΔP_{st}) could not be evaluated during runs R7 to R11 as with the CFB cold model, described in Section 5.2. As known by other researchers who have extensively experimented with the downflow of solids in standpipes (Jones *et al.*, 1980; Knowlton, 1986), the solids downflow induces a minor gas downflow in the standpipe. This gas is entrapped in the solids (char and gas) vortex generated by the primary cyclone, Figure 9-1, and consists of both inert gases and condensables. As long as the temperature of the gas-solids downflowing suspension is kept above approximately 350°C, which is the case in all circumstances, the small amount of condensables entrapped will not condense causing problems in standpipe operation, and will either be degraded to non-condensable gases or be burnt in the subsequent passage of the gas-solids suspension in the combustion chamber.

However, when exposed to cold surfaces, like those of the pressure tap tubing, these condensables will condense locally along with fine solids, causing a clogging in this part of the pressure sampling system. This generates a much lower output reading in the signal of

the pressure transmitters, erroneously indicating a stopping of gas-solids suspension in the standpipe. A remedy for this would be to bleed some gas into the standpipe at low velocities through the taps as reported by Kraft *et al.*, (1956). However, this measure would induce extra standpipe aeration and, given the very narrow standpipe diameter and the problems caused with excessive standpipe aeration, described in detail in Section 5.3.4, it was decided to abandon pressure drop measurements in the standpipe for the hot model, with the uninterrupted flow of solids to be indicated by temperature recordings in this part of the system. Again, the thermocouples in the standpipe (TCs 20-24) were placed adjacent to the wall, thus underestimating standpipe temperature by approximately 30-50°C, in order to secure unhindered passage of the gas-solids suspension in the narrow standpipe.

9.8 Summary

The main body of experiments in the CFB reactor comprised five runs and resulted in:

- experimental mass balances both over the entire CFB reactor system and the pyrolysis riser and liquid recovery sections (for run R11)
- temperature profiles versus height (for run R11)
- pressure drop versus time in the bubbling fluidised bed combustor.

The results obtained show that the reactor configuration successfully operates as a biomass fast pyrolysis system to maximise liquid yields, with the novel feature of providing for autothermal operation by utilising the by-product char energy content in a single reactor.

The main drawbacks of the proposed system remain:

1. The poor performance of the downstream processing equipment, which is believed responsible for relatively poor mass balance closures for the pyrolysis products and substantial losses of pyrolysis liquids.
2. The necessity to perform modifications in the char combustor part and circulation loop of the CFB reactor.

CHAPTER 10 : CFB REACTOR CONTROL ISSUES

10.1 Introduction

The performance of the Circulating Fluidised Bed (CFB) biomass fast pyrolyser in terms of operability and the maximisation of pyrolysis liquids was investigated during the experimental programme, see Chapter 9. In the following the response of the CFB reactor to changes in operating parameters is discussed and issues related to stability and controllability of the CFB reactor are outlined. This chapter is structured as follows:

- CFB reactor start-up procedure, Section 10.2
- operating parameters response on CFB performance, Section 10.3
- char accumulation effect on CFB performance, Section 10.4
- CFB reactor control strategy, Section 10.5
- summary of findings, Section 10.6.

10.2 CFB reactor start-up procedure

During the start-up phase, there is no char in the combustion chamber, so that fluidising air comes into direct contact with the incoming biomass particles in the upper riser section promoting partial devolatilisation and circulation of char and partially converted biomass particles to the combustion chamber.

As depicted from the diagram in Figure 10-1 for run R7, long stages of biomass feeding cause a slow but steady temperature increase in the combustor (TC 2). When the biomass flowrate (BFR) increased to 4.5 kg maf/h, the temperature in the impinger (TC18) gradually increased, stabilising at approximately 675°C. This is an indication of gasification/combustion reactions and oxidation in this part of the CFB reactor, which are due to the high volatiles content and light particle density for the sawdust feedstock used, both factors promoting more oxidation in the upper section of the riser and in the solids recovery and separation system (the cyclone and impinger). Similar trends for CFB wood combustors in the start-up phase were also reported by Grace and Lim (1987).

High temperatures in this part of the system should be avoided since the organic vapors released from biomass in the riser section would undergo cracking reactions to permanent gases favored at higher temperatures, Section 2.4, where the desired condensable products

are destroyed. The high temperatures are reduced at lower nominal air factors, Eq. 9-1, which are achieved by increased BFRs leading to the increased production of char and the subsequent depletion of oxygen in the combustion chamber. Hence, the exothermic gasification/combustion reactions were no longer sustained and a rapid temperature decrease, i.e. from 688 to 568°C, was observed in the upper riser section.

The intrusion of air into the upper part of the riser section during run R7 due to a sudden pressure tap tubing burnout caused a sudden, sharp temperature increase in the impinger (TC 18) and riser (TC 16), discussed in Section 9.4.3, this is also indicated in Figure 10-1. This problem was quickly fixed by plugging the pressure tap.

Though shorter biomass feeding periods at lower BFRs were practiced for the subsequent run R8, in order to avoid the exothermic gasification/combustion reactions discussed above, these were still present though to a lesser extent.

The start-up procedure adopted for these two runs, R7 and R8, has shown that very long stages of biomass feeding at lower BFRs should be avoided and that, due to extended start-up times required to reach steady-state, a high inventory of biomass in the feeding system must be considered. Moreover, a high inventory of biomass should be considered since, as discussed in Section 9.4.3 for run R7, an extended operation period is required to heat-up the different parts of the CFB system until the steady-state is reached and further maintained.

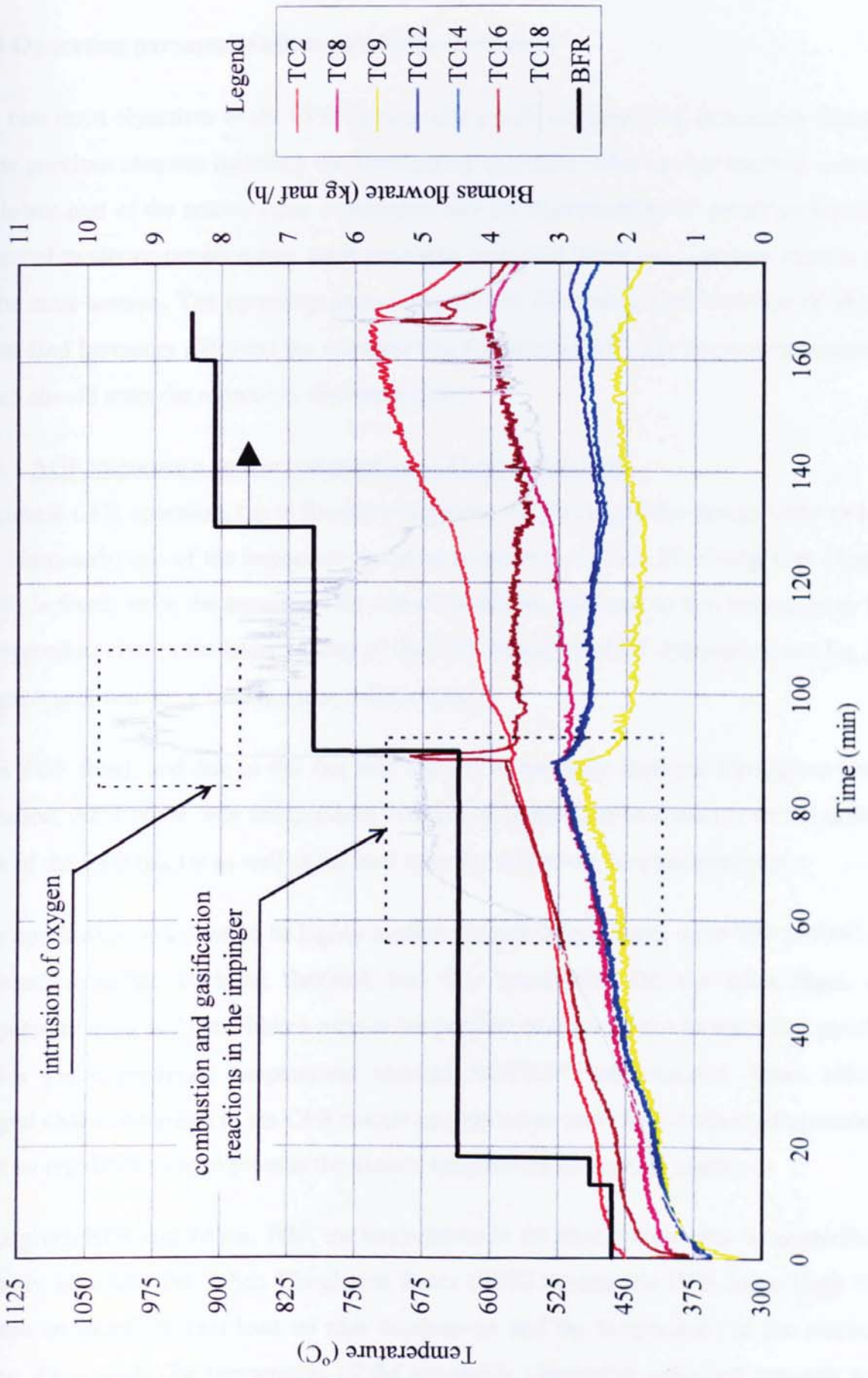

Figure 10-1: Temperature profile versus time in the combustor (TC2), riser (TCs 8, 9, 12, 14 and 16) and impinger (TC 18) for run R7

10.3 Operating parameters effect on CFB performance

The two main objectives of the CFB biomass fast pyrolyser have been thoroughly discussed in the previous chapters including the autothermal operation utilising char thermal content in the lower part of the reactor (char combustor) and the maximisation of pyrolysis liquids by means of moderate temperatures, short gas/vapor residence times and high heat transfer rates in the riser section. The operating parameters are the Fluidising Gas Flowrate (FGF), the Initial Bed Inventory (IBI) and the Aeration Gas Flowrate (AGF), the proper combination of which should meet the objectives discussed above.

10.3.1 AGF importance on riser temperature and heat transfer rate

At normal CFB operation, i.e. at Biomass Flowrates (BFR) around the design value (≈10 kg maf biomass/h) one of the important operating parameters, i.e. the Fluidizing Gas Flowrate (FGF) is fixed, since the amount of air added should be restricted to that necessary to burn the byproduct char in the lower portion of the CFB. Moreover, FGF determines, see Eq. 4-38 the gas/vapor residence time in the pyrolysis zone.

With FGF fixed, and due to the fact that the IBI is normally constant throughout reactor operation, AFG is the only independent variable to control the temperature in the different parts of the CFB reactor as well as the heat transfer rates to the biomass particles.

Char combustion is known to be highly exothermic and temperatures up to 900-1000°C may be reached in the bubbling fluidised bed char combustor. On the other hand, riser temperature must be kept within a narrow temperature window, since to maximise pyrolysis liquids yields moderate temperatures (around 500±10°C) are required. Thus, although integral char combustion in the CFB reactor configuration provides autothermal operation, it must be regulated so as to provide the desired temperature in the riser section.

For a given BFR and, hence, FGF, the temperature in the riser section may be controlled by properly adjusting the Solids Circulation Rates (SCR) around the CFB loop. High SCRs impose an increased heat load on char combustion and the temperature in the combustor drops. As a result, the temperature of the gas-solids suspension entrained upwards to the riser section is decreased, thereby achieving the required temperature control in the riser section.

Moreover, the heat transfer rates to the biomass particles in the riser section must be maximised to avoid any extensive temperature gradients within the pyrolysing particles leading to undesired charring and vapor decomposition reactions occurring in the fast pyrolysis regime, Section 2.7.1. This may be avoided by promoting high local heat transfer coefficients through the predominance of the ablative, i.e. a form of solid conductive heat transfer, pyrolysis regime as discussed in Section 4.4. The latter is achieved by a denser riser, i.e. a riser with a higher solids density or a lower voidage, promoted by high Solids Circulation Rates around the CFB loop.

As seen from the above discussion, two of the most important requisites for biomass fast pyrolysis, namely those of moderate temperatures in the pyrolysis reactor (riser) and high heat transfer rates to pyrolysing particles, are simultaneously satisfied by properly adjusting SCR. SCR is, in turn, regulated by AGF provided that the other operating parameters, namely FGF and IBI, are kept constant. The increased solids circulation around the CFB loop increases heat load in the char combustor promoting the following desirable effects:

- reduction of bubbling fluidised bed temperature
- reduction of riser (pyrolysis) temperature
- increase of heat transfer rates.

The response of the different parameters to a increase of AGF is further shown below in Figure 10-2.

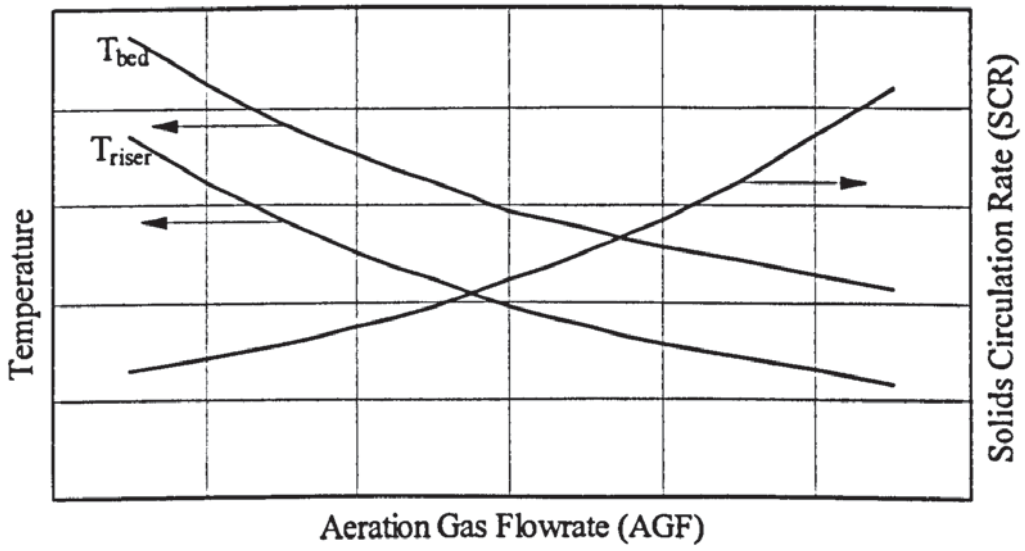

Figure 10-2: Response of temperature and Solids Circulation Rate (SCR) on stepwise changes in Aeration Gas Flowrate (AGF), for a given IBI and FGF

At low SCRs high temperatures prevail in the combustor and the hot gas-solids suspension entrained in the riser promote higher than desired temperatures. This may be controlled by increasing the SCR by properly adjusting AGF, as also seen in Figure 5-14, Section 5.3.4. The increased heat load in the combustor lowers the temperature in the bubbling bed and riser while, in the same time, increased heat transfer rates are achieved due to the increased SCRs.

In spite of the effects that the proper adjustment of SCR has on control of the pyrolysis temperature and heat transfer rates to biomass particles, efforts to exploit its advantages during the CFB hot reactor operation met with limited success due to the following reasons:

1. In contrast with the cold CFB unit tests, SCRs values could not be estimated in the hot unit, given the complexity and the increased cost associated with such an estimation. Instead, AGF was kept to a constant value, one suitable to keep the solids in the standpipe moving in the moving bed flow mode, Section 5.2.
2. The CFB reactor as designed had a limited capability to control SCR over a wide range. Whenever excess gas aeration was practised, standpipe stability problems occurred, probably due to the fact that the lean, i.e. depleted from solids, standpipe did not provide an adequate gas seal leading to loss of circulation and decreased SCRs as extensively discussed in Section 5.3.4.

In the CFB system designed, provision was not made for temporary storage of circulating solids by accommodation in a hopper or in a wider standpipe. Hence, the limited solids storage capacity of the system designed reduced the ability to control solids circulation rate and in this way decreased the flexibility of the system as far as temperature control in the different sections is concerned. The inclusion of a solids hopper and its effects on CFB operation is further discussed in Section 10.5.

10.3.2 Loss of solids circulation

In the experiments carried out loss of solids circulation in the standpipe was occasionally observed. The phenomenon gives rise to a series of undesired phenomena, namely:

- sudden temperature increase in the combustor temperature, due to the lack of the heat load imposed by the circulating solids; this in turn promotes
- depletion of char inventory in the char combustor (no renewal of char since solids are not circulating around the loop)

- intrusion of oxygen into the riser zone and promotion of gasification and combustion in the upper pyrolysis zone.

The above phenomena are clearly shown in Figures 10-3 and 10-4 for the runs R10 and R11 respectively, where such losses of solids circulation were encountered. More specifically:

The loss of solids circulation prior to steady-state, discussed in Section 9.4.3, that occurred during run R10, Figure 10-3, resulted in a substantial amount of sand being blown out of the reactor through the by-pass line. This, in turn, resulted in a decreased IBI, which led to a high rate of temperature increase in the combustor (TC 2), due to much lower heat load and leaner gas-solids suspensions. In Figure 10-3 a separation in the temperature profiles along the riser section may be observed, indicating poor heat transfer to biomass particles.

As shown in Figure 10-4 steady-state conditions, i.e. uniformity of temperature in the char combustor and riser, were reached for a BFR of 9.75 kg maf/h for run run R11. Another significant result is that after the second solids loss occurred (loss 2), approximately 120 min after biomass feeding had been initiated, the temperature in the bubbling bed (TC 2) rose to around 740°C. This is due to the fact that the solids blown out reduced once more the mass of the bed, so that the rest of the solids underwent a rapid temperature increase.

After the BFR had been re-established to the design value and, unlike the situation in run R10, where the sand inventory had also been significantly depleted, the combustor temperature (TC 2) did not exhibit the rapid temperature increase observed in this run, being instead stabilised at temperatures around 735-740°C. This may be attributed to the fact that the final bed inventory for run R11 was higher than that of run R10 (10.70 and 10 kg sand respectively, see Table 10-1 below).

Table 10-1: Sand inventory measured in the CFB reactor prior and after each run.

Run No	R7	R8	R9	R10	R11
Initial amount of sand (kg)	11.00	11.00	11.25	11.75	12.50
Remaining amount of sand (kg)	9.10	10.85	10.90	10.00	10.70
Amount of sand blown out (kg)	1.90	0.25	0.35	1.75	1.80

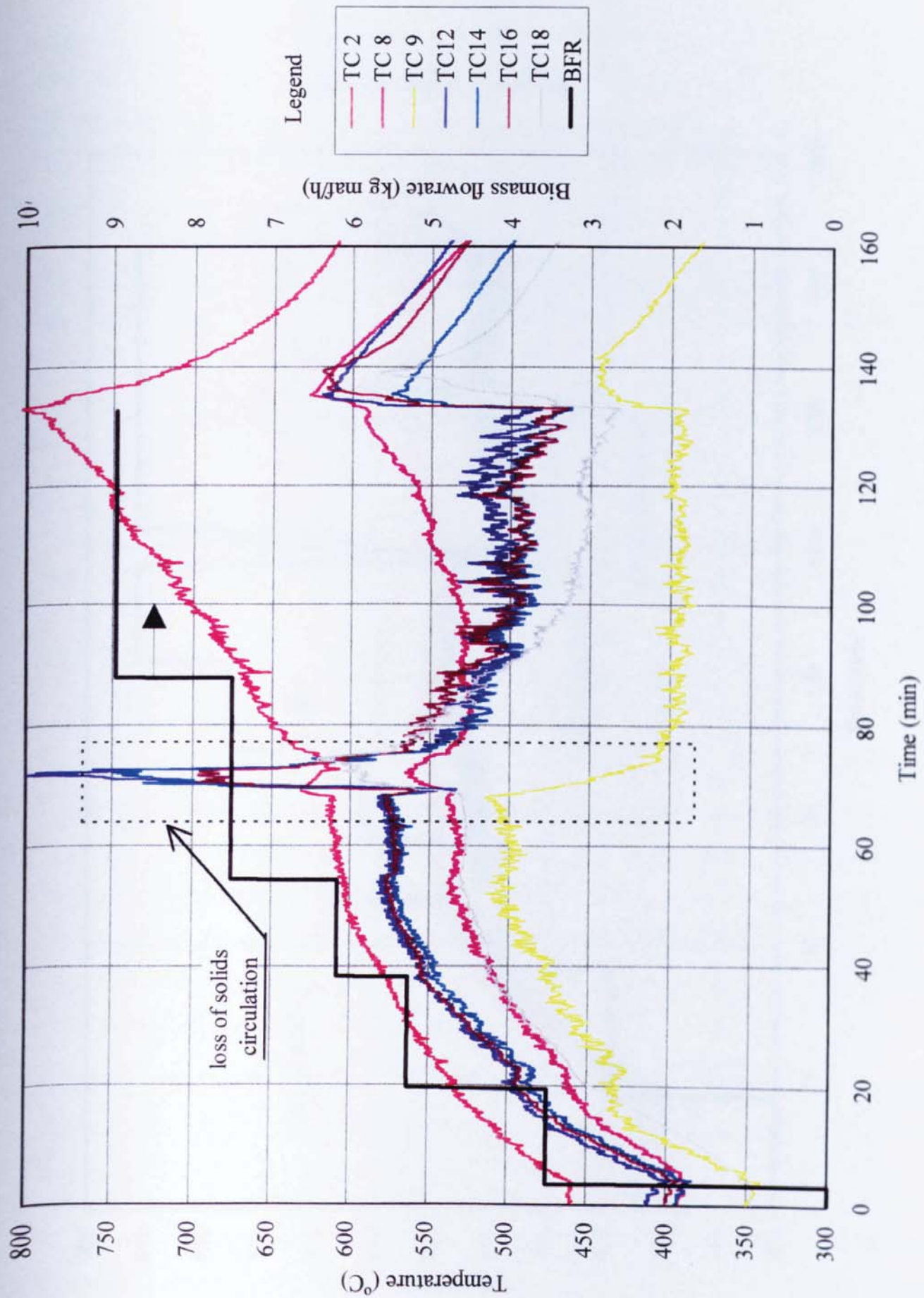

Figure 10-3: Temperature profile versus time in the combustor (TC2), riser (TCs 8, 9, 12, 14 and 16) and impinger (TC 18) for run R10

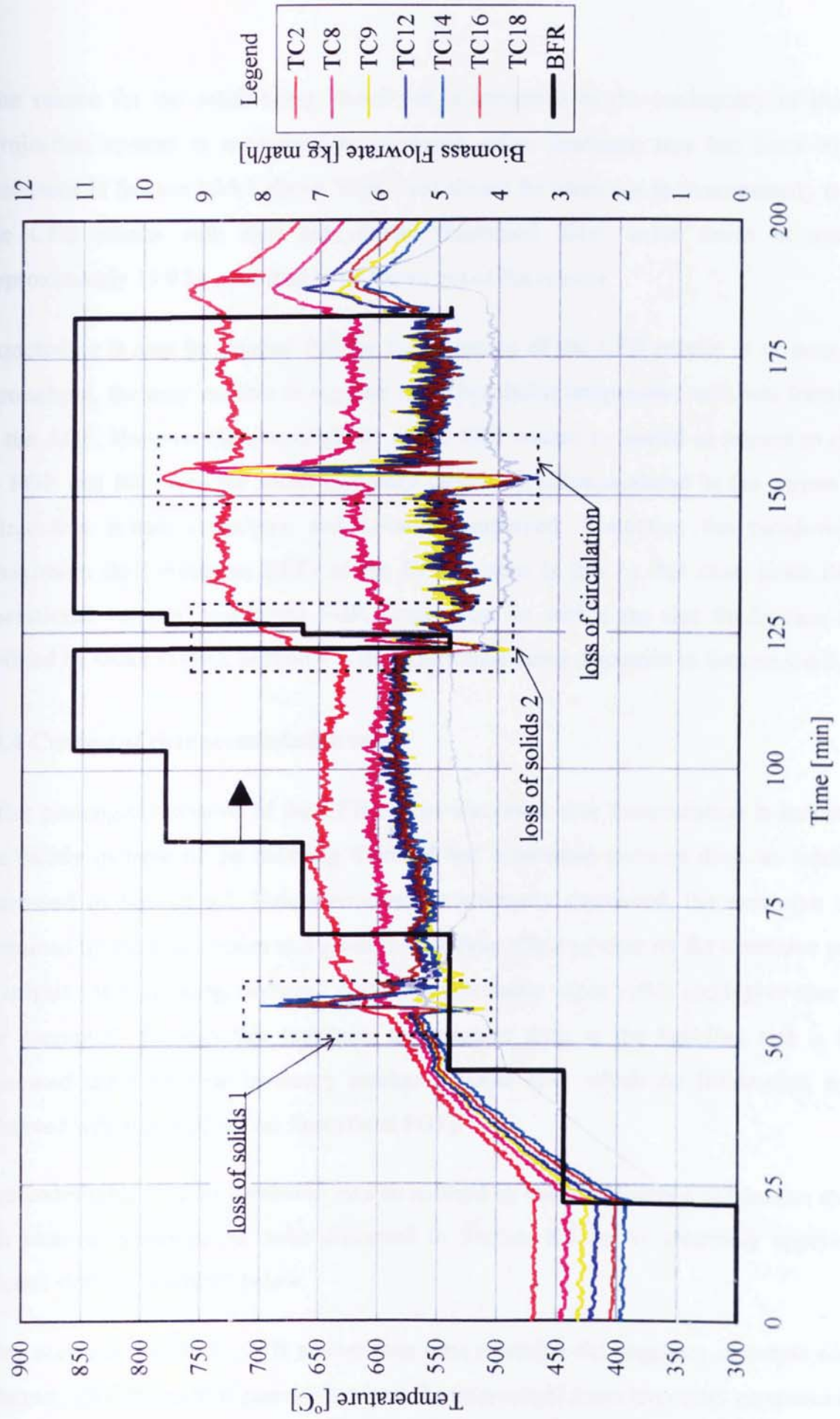

Figure 10-4: Temperature profile versus time in the combustor (TC2), riser (TCs 8, 9, 12, 14 and 16) and impinger (TC 18) for run R11

The reason for the solids being blown out is attributed to the inadequacy of the solids reinjection system to accommodate increased solids loadings, this has been explicitly discussed in Section 10.3.1 above. Thus, care should be taken not to unnecessarily overload the CFB reactor with inert heat carrier (increased IBIs), since solids in excess of approximately 11.0 kg sand tend to be blown out of the reactor.

Concluding it may be claimed that for the operation of the CFB reactor at or near design throughput, the only variable to regulate riser (pyrolysis) temperature and heat transfer rate is the AGF. However the controllability of the CFB reactor is limited in respect to changes to FGF and IBI since the solids inventory cannot be accommodated in the narrow solids reinjection system (standpipe and L-valve) employed. Moreover, the turndown ratio (maximum BFR:minimum BFR) of the CFB system is low in this case, since the riser operational velocity, and hence FGF, range must lie within the fast fluidisation regime defined by Grace (1986), Section 4.3, its significance being discussed in Section 4.6.2.

10.4 Control of char accumulation rate

After prolonged operation of the CFB reactor increased char accumulation is indicated by the steady increase of the bubbling fluidised bed combustor pressure drop, as extensively discussed in Section 9.7. Unless removed or internally consumed, the excessive char is entrained up the riser section and given the catalytic effect of char on the excessive primary pyrolysis vapor cracking, Section 2.4, lower condensable vapor yields and higher char yields are promoted. Through this sequence, the pressure drop in the bubbling bed is further increased until the char inventory reaches a value after which no fluidisation may be achieved with the available air flow (fixed FGF).

The undesirable char accumulation may be reduced by either adopting a continuous char and ash removal measures, as those discussed in Section 8.5, or by internally applying the control strategy described below.

Char accumulation in the CFB reactor over time promotes the sequence of events which is schematically shown in Figure 10-5, where the response of some important parameters, such as the temperatures in the combustor and riser as well as the bubbling bed pressure drop, on a stepwise increase of char inventory versus time is recorded.

At this point, it should be kept in mind that the description following is qualitative and further experimentation for the establishment of the proper sequence of interventions to control char accumulation rate in the CFB reactor is required.

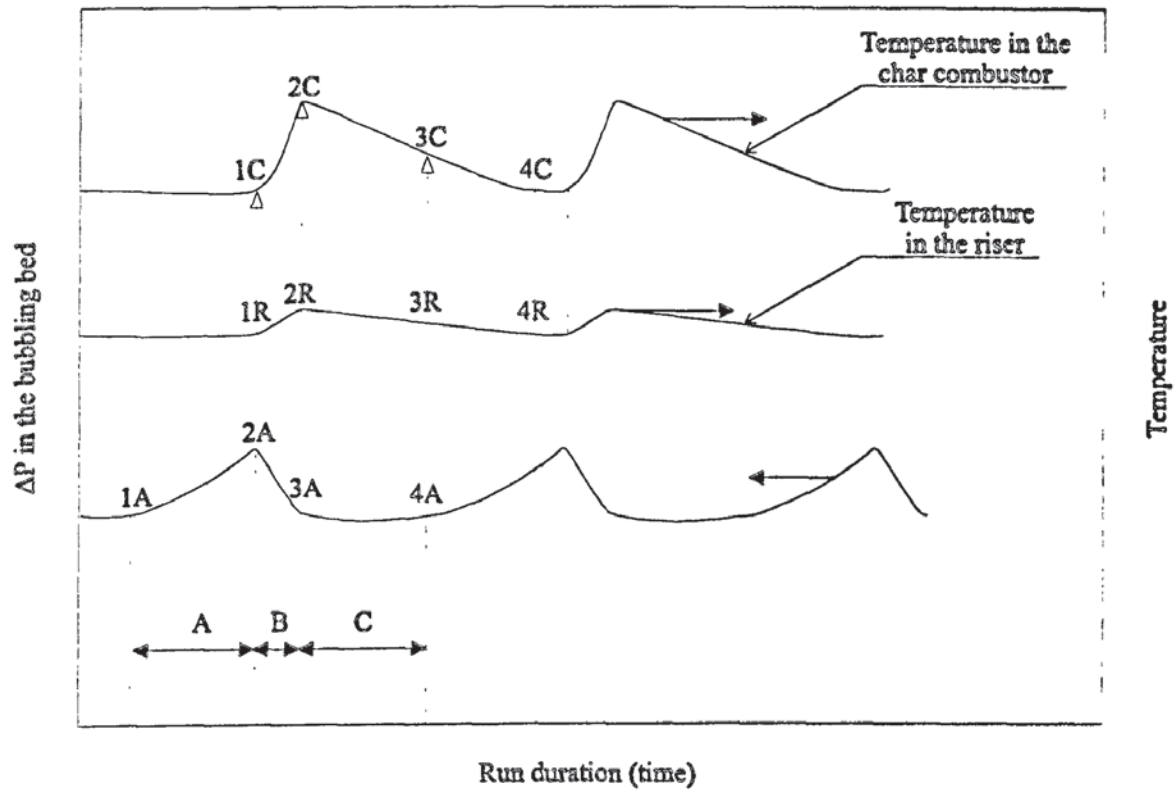

Figure 10-5: Temperature (in the combustor and riser) and combustor pressure drop profiles over time

At point 1A the pressure drop in the bubbling fluidised bed begins to increase over time due to the increased char inventory until a value is reached, point 2A, which necessitates the adoption of corrective measures. At this point, the fluidising gas flowrate (FGF) is momentarily increased from the design value, so that the char air factor is temporarily increased and the extra char is burnt.

Increased char combustion rates promote a rapid higher temperature in the bubbling bed, so that the temperature increases from 1C to 2C. At this point, all extra char had been consumed and the pressure recovery has been achieved in the bubbling bed, i.e. from point 2A to point 3A. On the other hand, the temperature in the riser increases, though at a lower rate than that of the char combustor due to the leaner gas-solids suspension, i.e. from point 1R to 2R. As a result of the increased riser temperature, less char is produced and circulated through the reaction loop, so that the char concentration in the bubbling fluidised bed, and

hence the char hold-up, are rapidly decreased, so that the pressure drop is reduced to its initial value, 3A in Figure 10-5.

After the operating point 3A has been reached, FGF is reduced to its design value, so that the char air factor, see Eq. 9-5, decreases to its initial value and the bed is left to slowly cool down, until point 3C is reached. At this point the riser temperature has also been decreased to 3R, so that the char yields again rises up to a point where char accumulation is apparent and bubbling bed pressure drop begins to increase once more, point 4A. When the combustor and riser temperatures have attained their initial value, 4C (=1C) and 4R (=1R) respectively, the pressure drop in the combustor increases steadily, so that the corrective measures (temporary increase of FGF, etc.) have again to be applied. Thus, the char accumulation rate control cycle is once more repeated and the excess char is consumed internally.

On the other hand, the reactor is somewhat self-stabilising at higher than 500°C riser temperatures. In this case, gas and organic vapors yields are maximised at the expense of char. The resulting decreased amount of char gives less fuel to the combustion chamber, which will lower the combustion temperature and hence the riser temperature. At the lower riser temperature the char production increases which again rises the combustion temperature, etc.

10.5 CFB reactor control strategy

Following the issues discussed in Sections 10.2, 10.3 and 10.4, it may be seen that the control strategy for the CFB biomass fast pyrolysis reactor is quite straightforward:

- short stages of biomass feeding at increasing BFRs values are required
- a high inventory of biomass in the feeding system, due to the extended start-up period, must be considered
- for a given IBI and FGF, the AGF is the only independent parameter to regulate, within narrow limits though, the temperature in the combustor and riser as well as heat transfer rates to biomass particles.
- char accumulation may be faced either by the continuous withdrawal of excess char, see Section 8.5, or by temporary increase of FGF to combust the extra char, see Section 10.4.2.

From the above discussion it follows that the control flexibility of the CFB system depends on whether a reservoir of solids is included or not in the circulation system as illustrated in Figure 10-6. With no reservoir of solids, Figure 16(A), one can only operate by keeping a constant solids inventory (IBI) even though the riser operational velocity, u_R, which is directly dependent on FGF (and, hence, on BFR), may change.

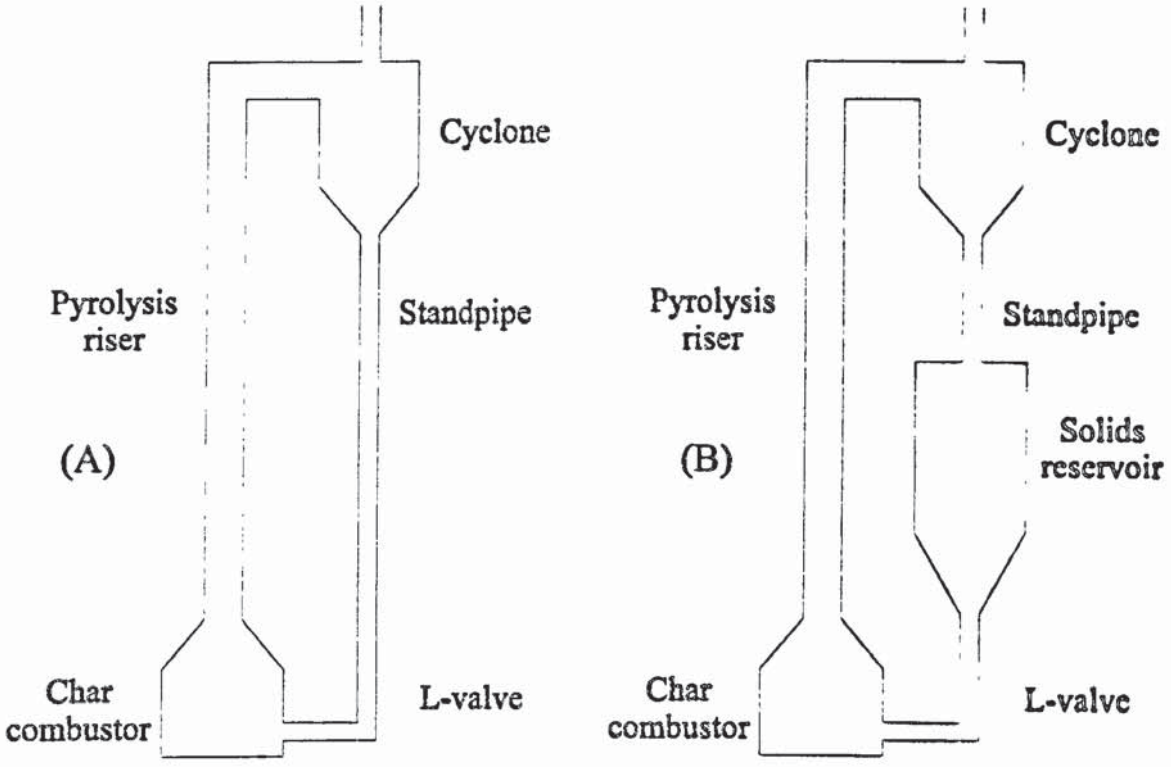

Figure 10-6: Solid circulation systems for the operation of the CFB pyrolyser in the fast fluidisation regime: (A) no reservoir of solids and (B) with reservoir of solids

On the other hand, a CFB reactor equipped with a reservoir of solids, Figure 10-6(B), may be operated in one of four ways (Kunii and Levenspiel, 1992):

- *Mode I*: Keep a constant IBI, even though the riser operational velocity may change.
- *Mode II*: Keep a constant gas flow rate, u_R, even though SCR may change.
- *Mode III*: Keep a constant SCR , even though u_R may change.
- *Mode IV*: SCR and u_R may change independently.

Without the reservoir of solids (present CFB configuration) one can only operate according to Mode I and Mode II although in this latter case standpipe stability issues restrict CFB operational flexibility. With the reservoir of solids the system becomes much more flexible in that it can operate in any mode. It should be mentioned that the sketches shown in Figure 10-6 are idealised illustrations and in practice a variety of designs for getting smooth steady

state circulation of solids are encountered (Yerushalmi and Avidan, 1985; Yerushalmi, 1986a, 1986b; Hartge *et al.*, 1986).

10.6 Summary

In this chapter, insights on issues concerning CFB control and stability are provided and the response of operating parameters on process variables is discussed. The major findings are:

- CFB reactor start-up should be given thorough attention, since long consequent preheating stages of biomass feeding promote high temperatures in the upper riser section
- the AGF is, for a given FGF and IBI, the only independent parameter to control, within narrow limits, though since the control interval is limited by standpipe stability, the temperature in the combustor and riser and heat transfer rates to biomass particles
- char accumulation rates in the CFB reactor may be controlled either by the continuous withdrawal of excess char, or by temporary increase of FGF to burn the extra char.

Finally, it has been pointed out that the controllability and stability of the proposed CFB biomass fast pyrolyser could be greatly improved if an additional reservoir of solids is incorporated, thereby significantly improving the operational flexibility of the system.

CHAPTER 11: CONCLUSIONS AND RECOMMENDATIONS

11.1 Introduction

A circulating fluidised bed (CFB) reactor for biomass fast pyrolysis incorporating integral char utilisation has been successfully designed, built and operated. The conclusions are set out below in Section 11.2, while the recommendations for future equipment modifications and process improvements are discussed in Section 11.3.

11.2 Conclusions

11.2.1 Design

In order to meet the objectives of this thesis, Section 1.3, the principles of biomass fast pyrolysis in terms of mechanisms, kinetics and heat transfer were reviewed and a number of candidate reactor schemes reviewed and evaluated.

A Circulating Fluidised Bed (CFB) reactor with integral char combustion was selected for biomass fast pyrolysis as incorporating the most desirable features to maximise pyrolysis liquids yields.

A major requirement for the desired dual-mode operation of the reactor system conceived was the close coupling of the two reactor subsystems, namely the pyrolysis riser (medium temperature) and char combustor (high temperature).

A design procedure was developed leading to the establishment of the appropriate design variables, including biomass flowrates, reactor dimensions and process parameters, such as riser temperature and VRT.

11.2.2 Cold CFB model

A cold model of similar dimensions to the proposed, hot CFB reactor was designed and tested, in order to:

1. predict the complex hydrodynamics of the proposed CFB reactor system
2. establish relationships between heat transfer and operating parameters and to
3. provide stable and unhindered reactor operation.

The conclusions drawn from this cold model operation are summarised below:

- The basic CFB reactor design proved effective in providing the high heat transfer rates (expressed as low voidage values in the riser and high solid circulation rates) to biomass particles in the very short VRTs required.
- The understanding of the complicated aspects related to two-phase gas-solids flow in the standpipe resulted in a smooth, stable transfer of solids over a wide range of operating parameters during cold CFB reactor operation.
- The mode of solids circulation adopted was obtained by means of a non-mechanical device and proved reliable. This provided a reactor system with no moving parts, in which the desired heat transfer could be easily adjusted over a wide range of operating parameters to match the heat load requirements.

11.2.3 Hot unit construction and operability

The following conclusions concerning the different components of the CFB hot reactor may be made:

- A biomass feeder with an internal stirring device, a metering device and a transport device to the CFB reactor was successfully conceived, designed, constructed and tested.
- The use of two and three cyclones in series, of which the second cyclone fed the standpipe proved inappropriate to remove char and sand fines satisfactorily, since those configurations were insufficient to capture char and unconverted wood particles, especially during the reactor start-up phase. These problems were partially faced by adopting a configuration of a primary cyclone and inertia impinger in series. Char and sand fines removal from the reactor was eventually acceptable but not satisfactory and requires further development.
- A variety of configurations for the product collection system were built and tested, the most efficient tested being a combination of a shell-and-tube heat exchanger (condenser) and a cotton wool filter. Moreover, in order to avoid an excessive burden in the liquid recovery equipment during start-up, a gas by-pass line, where all gases prior to steady-state were vented, was installed. However, the liquid recovery configuration gave rise to a number of problems, the most important being gradual plugging of the heat exchanger due to the formation of sticky solid-liquid agglomerates. This system needs substantial improvement.

11.2.4 Hot CFB reactor commissioning

The main problems to occur during reactor commissioning were related to solids capture, establishment of an appropriate start-up procedure and the liquid recovery system.

- Three separate series of experiments were conducted in the CFB reactor. The first series, commissioning experiments, was dedicated to gain experience, familiarise with CFB reactor operation as well as identify the problems related to CFB operation and adopt the necessary measures to remove them. During the second series of experiments a biomass feeding strategy was developed in order to achieve steady-state prolonged reactor operation as a pyrolyser. The main body of experiments were conducted as the third series to derive meaningful mass balances and evaluate reactor performance, as far as pyrolysis products yields are concerned.
- Although an acceptable solids capture device configuration (discussed in Section 11.2.3) was adopted, significant portions of submicron char were found in the condenser tubes, which resulted in further reduction of pyrolysis liquid yields, since char is known to be an effective tar-cracking catalyst. The submicron char is believed to be a direct result of the significant attrition and fragmentation char particles undergo in the riser due to the high turbulence during reactor operation.
- All of the product collection systems tested exhibited a serious performance problem since they were based on indirect cooling, so that the tarry deposits collected in the heat exchanger tube inlets resulting in partial plugging of the condenser tubes. This led to a restriction of flow and an increase in pressure drop to maintain steady conditions. In some cases complete plugging of the majority of the tubing causes the termination of the test. Indirect vapor cooling was proved inefficient and should be avoided whenever possible.
- A by-pass was also provided in combination with the liquid recovery configuration described, so that during start-up the gas and vapors were vented directly to atmosphere. Once steady-state was achieved, the pyrolysis products were diverted to the liquid recovery section, thereby providing better mass balances.
- The liquids collection system was not very effective:
  - Indirect cooling of gas/vapors in a shell-and-tube heat exchanger is not recommended, since deposits of heavy components in the tubes result in polymerisation reactions by which organic vapors might be converted to other products (secondary and tertiary tars).

* The tarry deposits formed in the heat exchanger tubes form a layer reducing the heat transfer coefficient and thus not cooling the gas/vapor products. This prolongs their residence time at higher temperatures which further reduces the desired product yield.
* The deposits accumulate, reducing the free area resulting in tube plugging and excess pressure build-up.

- Gradually increasing biomass feeding to the CFB reactor should be practised to avoid thermal overloading at lower temperatures and provide for sufficient char accumulation in the combustor, so that the oxygen is mainly consumed in this part of the CFB reactor configuration.

11.2.5 Hot CFB reactor operation

The following conclusions concerning hot CFB reactor operation are drawn:

- The modified liquid product recovery scheme finally adopted, comprising a by-pass line to vent gases prior to the establishment of steady-state conditions in the riser section, and a separate product recovery line consisting of a heat exchanger connected in series with a cotton wool filter as discussed in Section 8.6.4, was an acceptable compromise, recovering the majority of the pyrolysis liquid products to give acceptable mass balance closures during the duration of a run. This system, however requires substantial modifications and improvement.
- Excellent temperature uniformity is achieved in the CFB pyrolysis section. This verifies the hypothesis of high suspension densities supported from the cold model operation and thus providing adequate heat transfer rates to the incoming biomass particles.
- The system's stability and operability were improved through a series of experiments, five of which had acceptable mass balance closures over the entire CFB reactor system. Run times of up to three hours were carried out. However, the steady state maximum run times were held between 30 and 45 min, since the gradual heat up of the CFB reactor is quite time- and feedstock-consuming.
- Two biomass (pine wood) feedstock sizes were tested, a smaller size, between 1 and 1.5 mm and a larger particle size between 1.5 and 2 mm.
- Liquid yields of up to 61.5 % wt on a moisture-ash-free biomass basis (maf) have been obtained. These yields are considered low in comparison with other fast pyrolysis processes reporting yields of up to 75 % (on a maf feedstock basis). The temperature at which the highest pyrolysis were comparable with what was obtained from other fast

pyrolysis processes at approximately 500°C in the riser section. Higher yields were obtained for the smaller particle sized feedstock.

- Steady-state conditions for the CFB reactor are defined as the state where the temperature profiles in the char combustor and the riser have reached the proper values denoting combustion in the former and pyrolysis in the latter sections and remaining constant within a 10-20°C interval as well as the product gas composition is constant.
- The CFB reactor system has a rapid heat-up period from cold to the point where gradual biomass feeding begins (approximately 5 hours), whereas it requires approximately 2 hours to reach steady-state conditions after biomass feeding is initiated.
- A very high oxygen conversion (approximately 96 % wt) is achieved in the bubbling fluidised bed, while char conversion to carbon dioxide approaches 92.2 % wt, the rest being converted to carbon monoxide.
- Char accumulation rates in the combustor are slow, the additional char formed to be combusted by periodical increases in oxidant input.
- Care should be given to avoid unnecessarily overloading the bubbling fluidised with too high an initial solids inventory, since the excess solids cannot be easily accommodated in the narrow transport system, being blown out of the CFB reactor to maintain a final solids inventory. It was found that the ideal IBI would be at equal proportions of the biomass input load, i.e. approximately 10-10.5 kg sand.

11.2.6 Reactor design verification

The design procedure for the CFB pyrolysis reactor accurately predicted:

- correlations between input variables and process parameters
- basic CFB reactor dimensions
- the beneficial advantage of a high heat transfer environment in the riser section.

Moreover, the experimental procedure verified the correlations between reactor dimensions and feedstock throughputs developed during the design of the CFB reactor. As a consequence the design procedure developed may be used as a meaningful tool for reactor scale-up.

11.2.7 Analysis

The liquids obtained had a typical density of 1.10-1.15 kg/l and were acidic. The liquid samples analysed appeared less viscous than pyrolysis liquids obtained by other processes. The liquid products appeared to contain very low concentrations of high molecular weight

materials and also low level of lignin derived components. These differences are attributed to the condensation system adopted, where the heavy components were retained as described explicitly in Section 10.2.5. Although there is a clear indication that better liquid quality may be obtained after CFB reactor optimisation has taken place, there is a need for more thorough analysis of the liquids.

Gas analysis with continuous on-line analysers gave satisfactory results. Although gas analysis was hampered by problems associated with out-of-range span of the analysers, valuable information was provided, especially during reactor start-up. On-line batch sampling by a GC (applied for the first time in fast pyrolysis experiments as far as is known) was performed and the GC results proved a valuable tool for the verification of steady-state and derivation of meaningful mass balances. The main results of the gas analysis are:

- CO content and hydrocarbons gas yield in the product gas are decreased with decreasing temperature and decreasing feedstock particle size (decreasing air factor), which has a direct impact on the energy content of the product gas (lower HHV).
- The product gas yield increases with increasing riser temperature.

It should, however, be emphasised that the product gas lumps together the biomass pyrolysis and char combustion gaseous derived products as well as the entraining gas (N_2).

11.2.8 CFB reactor control and stability issues

The operation of the CFB reactor was found to be quite straightforward. More specifically:

- The AGF is, for a given FGF and IBI, the only independent parameter to regulate, within narrow limits though the control interval limited by standpipe stability, the temperature in the combustor and riser as well as heat transfer rates to biomass particles.
- Char accumulation rates in the CFB reactor may be controlled either by the continuous withdrawal of excess char, or by temporarily increasing FGF to burn the extra char.

It has also been pointed out that the controllability and stability of the proposed CFB biomass fast pyrolyser could be greatly improved if an additional reservoir of solids is incorporated, thereby significantly improving the operational flexibility of the system.

11.2.9 Overall conclusions

The overall conclusions from this work are that the Circulating Fluidised Bed reactor incorporating integral char combustion has successfully pyrolysed biomass feedstocks to give

liquids. The reactor has the highest specific throughput of all the similar configurations tested, the lowest gas-to-feed ratio, presents a good scale-up potential and has a compact design by which capital costs can be reduced. However, there are several features requiring development especially in the char combustor, solids recovery and separation system configuration and downstream processing equipment.

11.3 Recommendations

The recommendations are set out in the following:

11.3.1 Reactor design and modeling

Modeling of CFB reactor biomass pyrolyser should be directed to the incorporation of detailed analytical models which can relate the process parameters, such as temperature and gas/vapor residence time, the product distribution more accurately rather than the simple kinetic models adopted in this thesis and discussed in Section 4.5.1.

Modeling of the CFB char combustor should incorporate detailed analysis of woodchar combustion kinetics investigating the effects of excess air, fluidised bed flow mode and residence time distribution of both gas and solids. Since char combustor is considered a crucial part of the CFB design, an appropriate experimental programme is required in order to verify the theoretical findings and relate them with actual char combustor performance.

Modeling of both char combustor and biomass pyrolyser should also be improved in order to relate their critical dimensions to product yield and product distribution as well as their variation with process parameters. This modeling approach should also be related to the analytical models referred to above, resulting in more exact predictions based on kinetic data obtained from actual experimental work.

11.3.2 Design and modifications in the CFB reactor

The char combustor should be modified in order to provide for even higher char and oxygen conversion. This could be achieved by the adoption of the following measures:

- Increase of combustor height and possibly diameter (to be coupled with wood char combustion analytical models).
- Increase of gas distributor free area to avoid dead zones and enhance mass transfer between oxygen and char, thus improving gas-solid conversion.

The biomass pyrolyser should be modified in order to provide higher heat transfer to biomass particles. This can be achieved by the following:

- Further reducing the diameter of the upper riser section to increase turbulence and hence heat transfer.
- Resizing the reactor top (slightly higher) to increase the riser suspension density and promote higher heat transfer coefficients.
- Providing a small amount of inert gas (as practised in secondary air injection ports in wood/coal combustors) to adjust further gas-vapor residence time.

Furthermore, a multisolids approach could be adopted in the CFB system based on the selection of two different inert heat carrier sizes. The larger would remain in the combustor whilst the smaller would be readily entrained up the riser and recirculated through the solids reinjection system. Of course this approach would have the disadvantage that more efficient solids recovery and separation systems would be required for capturing the finer materials entrained.

11.3.3 Solids recovery and separation configuration

In spite of the relative success of the CFB reactor solids recovery system finally adopted, there is still a relatively high percentage of fine sand and char escaping the solids removal system, being entrained with the gas/vapor stream in the downstream processing equipment. The sand and ash promote the formation of the agglomerates discussed above and lead to the gradual plugging of the heat exchanger. Thus, increased efficiency, obtained through better design and modeling, is required, for development of appropriate solids recovery and separation system configuration.

A number of configurations has been proposed, Section 8.5, to minimise char and sand carry over, of which hot gas filtration of the gas/vapor-solids stream could be successfully practised, however at a higher cost and increased complexity.

11.3.4 Downstream processing equipment

Recovery of pyrolysis liquids is not a simple condensation process and rapid cooling of the product vapors leads to the formation of stable aerosols and micron-size droplets, possibly with polar molecules bonded onto the surface of water droplets.

Impingement and coalescence of the vapors must, therefore, be an essential feature in the liquids recovery process, where direct gas-liquid vapors quenching should be practised instead of indirect heat exchange. The gas/vapor recovery system should incorporate:

- a direct contact vapor-liquid (scrubber-like) device
- adequate cooling of the recirculated scrubbing medium (pyrolysis liquids, water or heavy fuel oil-not miscible with the liquid pyrolysis products)
- proper recirculation of cold scrubbing medium (selection of the liquid pump)
- separation of char fines from the recovered liquids.

A secondary gas/vapor recovery system should be installed to recover fine aerosols not yet collected, which should consist of either a mist-type eliminator and/or an electrostatic precipitator.

11.3.5 CFB reactor operation

The CFB reactor operability should be substantially improved and tested in the long-term in order to provide robust data for further scale up considerations in particular:

- Different feedstocks should be tested to optimise the reactor for each one.
- Prolonged reactor operation should be demonstrated (>100 hours), by adopting the measures discussed above for solids and vapors collection and recovery.
- Different feedstock sizes should be tested to evaluate heat transfer for larger biomass.
- Solids circulation rates should be measured by developing a proper measuring device, in order to estimate heat transfer rates to biomass particles.
- Control strategies should be adopted to account for the char accumulation in the combustor during reactor operation (for example the temporary increase of FGF in order to combust any extra char accumulated in the combustor over time).
- Ash removal procedures should be adopted to remove ash from the pyrolysis vapors and decrease inorganics content in the pyrolysis liquids as far as possible.
- Gravimetric instead of volumetric biomass feeding must be used to increase accuracy in mass balances and more controllable and reliable feeding.

11.3.6 Analysis

Modifications in the existing equipment are required, particularly:

- Reduce the span of the on-line continuous gas analysers.
- Reduce the analysis time for the GC incorporating shorter columns.

- Incorporate an FID detector (GC) analysis to allow for the detection of higher than C3+ hydrocarbons.
- Provide measures for hydrogen determination., e.g. use of alternative carrier gas in the GC system, especially at elevated temperatures.

Additional instrumentation and analysis equipment should also be installed, such as:

- Provide solids sampling procedures from the different parts of the CFB loop (standpipe and combustor).
- Install pressure transducers with faster response times to enable more thorough investigation of CFB hydrodynamics.
- Install more accurate gas analysers.
- Exercise multiple gas sampling and analysis in all subsequent runs in order to gain information on char and oxygen conversion in the combustor as well as derive mass balances for the pyrolysis section (riser), in analogy with the results obtained for run R11.

11.3.7 Overall modifications in the CFB fast pyrolysis plant

The recommendations suggested above are illustrated in Figure 10-1, which shows the areas requiring development and modifications. The necessary overall modifications are also summarised in Table 11-1 below.

Table 11-1: Areas in the pyrolysis plant requiring further modifications (as in Figure 10-1)

Area No	Modifications required in the biomass fast pyrolysis bench scale plant
A	Air-tight rotary valve to provide for prolonged reactor operation.
B	Continuous sand replenishment (B1) - Ash, sand, char removal system (B2).
C	Incorporation of a solids reservoir (enlarging the standpipe or installing a hopper) to provide for more flexible operation and avoid disturbances in IBI.
D	Incorporation of hot gas filtration to account for enhanced capture of fine sand and char particles.
E	Adoption of a liquid recovery system comprising of a direct-contact quenching system and a mist eliminator or an electrostatic precipitator.

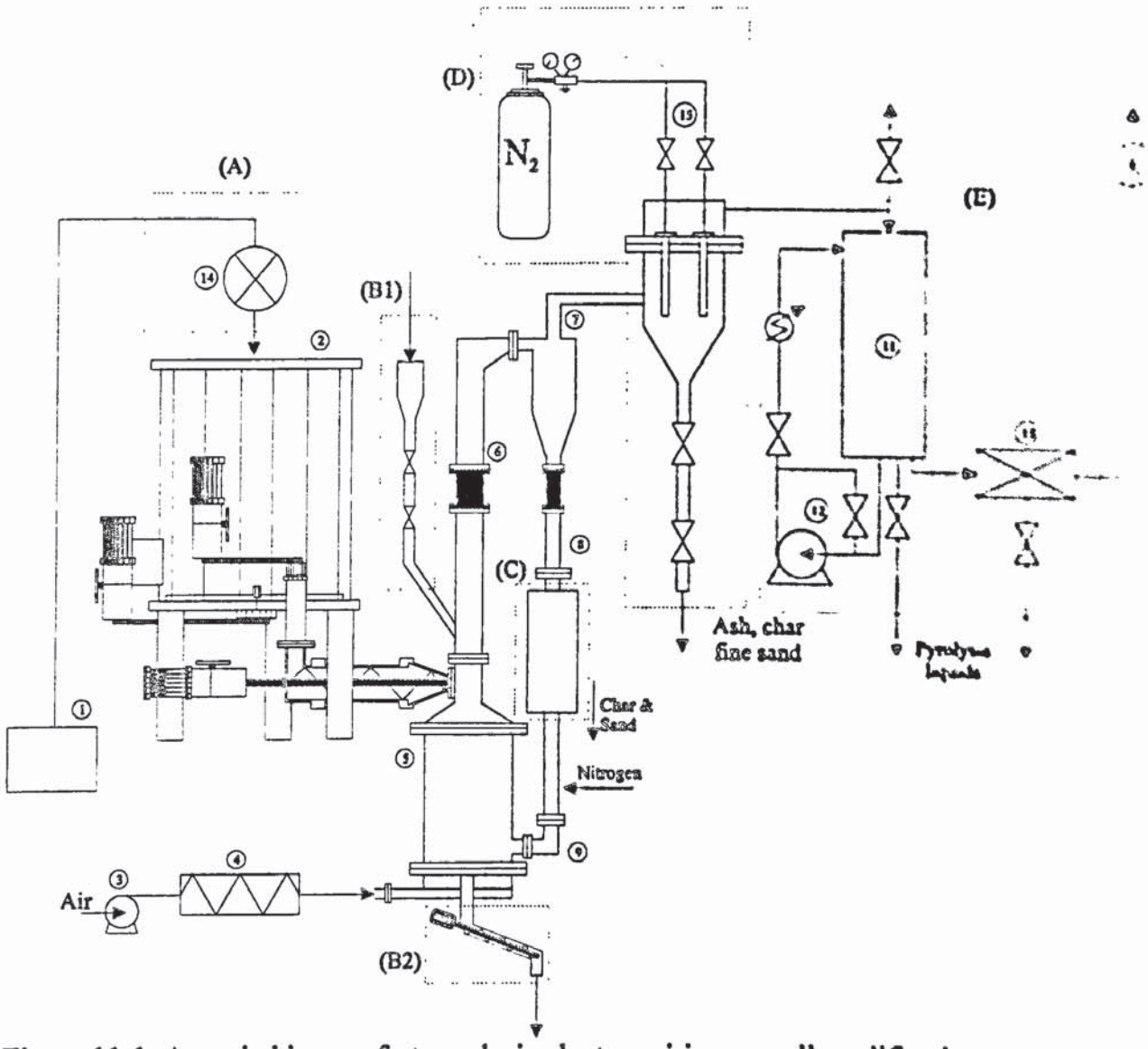

Figure 11-1: Areas in biomass fast pyrolysis plant requiring overall modifications (1-feedstock preparation, 2-biomass feeder, 3-air compressor, 4-air preheater, 5-char combustor, 6-biomass pyrolysis riser, 7-primary cyclone, 8-standpipe, 9-L-valve, 10-hot gas filter, 11-product recovery unit, 12-liquid recycle pump, 13-mist eliminator/electrostatic precipitator, 14- gas tight rotary valve, 15-pulsation valves, V1- By-pass valve, V2- steady-state valve)

11.3.8 Results

The results from the fast pyrolysis pilot plant operation are comparable with those from other fast pyrolysis processes under similar conditions. It is recommended however that mass balance data and analyses are obtained for lower temperatures of 450-500°C instead of about 500-600°C as in this thesis.

Finally, the final recommendation given is (Bridgwater, 1991) to implement the above recommendations.

NOMENCLATURE

Symbol	Description/Definition	Units
a	ash mass fraction in feedstock	[kg ash/kg feed]
A, B, C, D,	constants given in Table 4-2	[-]
A	surface area	[m^2]
A_d	cyclone inlet area	[m^2]
A_R	riser cross sectional area	[m^2]
Ar	particle Archimedes number	[-]
Bi	Biot number	[-]
c_{pw}	specific heat capacity	[kJ/kg K]
c_p^i	specific heat for component in gas stream	[kJ/kmole K]
c_{pH2O}	specific heat water(=4.19)	[kJ/kg K]
C_D	drag coefficient ($=4g(\rho_s-\rho_g)d_p/(3\rho_g u^2)$)	[-]
d^*	dimensionless particle size defined by Eq. 4-1	[-]
D_B	bed diameter	[m] or [cm]
d_p	sand particle diameter	[m]
D_R	riser diameter	[m]
E	activation energy	[kJ/kmole]
f_l	biomass mass fraction (maf) converted to char	[kg/kg]
f_c	total carbon content in char	[kg/kg]
$\overline{F_g^{tot}}$	mean gas flowrate including entraining gas	[m^3/h]
F_g^{tot}	total gas flowrate including combustion gases, air N_2 and pyrolysis condensable vapours + non-condensable gases	[m^3/h]
g	acceleration due to gravity (=9.81)	[m/s^2]
G_{air}	mass flowrate of air (=FGF, Table 9-1)	[kg/h]
G_B	biomass throughput (on a maf basis=BFR)	[kg/h]
G_{BWA}	biomass throughput	[kg/h]
G_{char}	char flowrate	[kg maf/h]

G_{cH2O}	cold water flow	[kg/h]
G_{liq}	total liquids mass flowrate	[kg/h]
$G_{g,i}^{out}$	mass flowrate of component i in entraining gas stream	[kg/h]
G_s	solids circulation rate(=SCR)	[kg/h]
G_{H2O}	water/steam mass flowrate	[kg/h]
h_t	overall (total) heat transfer coefficient	[$W/m^2 K$]
H_{mf}	height of bed at minimum fluidization	[cm]
k	reaction rate constant (oil decomposition step)	[s^{-1}]
k_o	pre-exponential factor for product i	[s^{-1}]
k_o	pre-exponential (frequency) factor	[s^{-1}]
L_R	riser length above biomass feeding point	[m]
m	mass	[kg]
MW	molecular weight	[kg/kmole]
P	reactor pressure	[N/m^2]
p_i^{air}, q_i^{air}	amount of air required for stoichiometric combustion	[kg/kg feed]
Q_l	total liquids sensible heat	[kJ/h]
Q_{ext}	externally provided heat input	[kJ/h]
Q_{pyr}	total heat requirements for biomass pyrolysis process	[kJ/h]
Q_{loss}	various heat losses along the CFB system	[kJ/h]
Re	Reynolds number	[-]
R	universal gas constant (=8.314)	[J/mole K]
T	temperature	[K]
T_2	temperature of the entraining gas stream	[K]
T_{wc}	the temperature in the centre of the wood particle	[K]
t	time	[s]
t_{res}	gas/vapour product residence time	[s]
u^*	dimensionless gas velocity defined by Eq. 4-2	[-]
u_r	numerical value of slip gas-solids velocity	[m/s]

u_{st}	solids velocity in the standpipe	[m/s]
u_g	interstitial gas velocity in the standpipe	[m/s]
$\overline{u_R}$	mean gas/vapour velocity at reactor conditions	[m/s]
u_{ms}	the minimum slugging velocity	[cm/s]
u_{mf}	the minimum fluidization velocity	[cm/s]
V	volume	[m^3]
w	water mass fraction in feedstock	[kg H_2O/kg feed]
W	initial weight fraction	[kg]
W_f	final (non-degradable) weight fraction	[kg]
$W_{cell, A, V, C \text{ and } G}$	the normalized weights of cellulose, "Active cellulose", volatiles, char and gases respectively	
x	char combustion efficiency (0<x<=1)	[-]
y_i	fraction of component i (C, H, O) in biomass	[-]
z_i	fraction of component i (C, H, O) in char	[-]

Greek symbols

α	wood thermal conductivity	[W/m K]
ΔH	enthalpy change	[kJ/kmole]
ΔH_i^0	enthalpy of the component i in entraining gas	[kJ/h]
$-\Delta H_c^o$	heat of char combustion (- for exothermic)	[kJ/h]
ΔP	pressure drop along the riser section	[N/m^2]
ΔT	T_{in} - T_{out} allowable water temperature rise	[°C]
Δz	distance between pressure measurements	[m]
ε	voidage	[-]
λ	heat of reaction	[J/g]
μ	viscosity	[Pa s]
ϱ	gas density at normal conditions	[kg/Nm^3]
ϱ_s	solids (sand) skeletal density	[kg/m^3]
ϱ_{susp}	suspended solids density	[kg/m^3]
τ_g	mean residence time of volatiles in the reactor	[s]

τ_{sL}	residence time of solids according to Lidén	[s]
Φ	yield	[% wt]
Φ^*	maximum attainable yield	[% wt]

Subscripts

c	combustor
D	Diebold
g	gas
G	Gorton
i	component i
L	Lidén
o	initial conditions
p	particle
R	riser
st	standpipe

REFERENCES

- Acres American Incorporated,*"Technical, Environmental and Economic Evaluation of the San Diego County Resource Recovery Facility at El Cahon, California"*, US EPA, Contract No. 68-01-4420, Rayleigh, NC (1979).
- Agarwal, J.C., Davis, W.L. and King, D.T., *Chem. Eng. Progr.*, 58, p. 85 (Nov 1962).
- Andrews, R., Patnaik, Q.L. and Thamburaj, R., in *Biomass Pyrolysis Oil Properties and Combustion Meeting*, 26-28 Sep 1994, Estes Park, CO, NREL-CP-430-7215, pp. 383-391 (1995).
- Antal, M.J., Friedman, H.L. and Rogers, F.E., *Comb. Sci. Techn.*, 21, p. 141-152 (1980a).
- Antal, M.J., *Annual Meeting of the AIChE*, Philadelphia, June, American Institute of Chemical Engineers, NY (1980b).
- Antal, M.J., *Bio-Energy '80 World Congress and Exposition*, Atlanta, GA. April 21-24, Bio-Energy Council, Washington DC, pp. 174-176 (1980c).
- Antal, M.J., *Report to the Office of Technology Assessment*, U.S., Congress, Washington, DC (1980d).
- Antal, M.J., in *Advances in Solar Energy*, K.W. Boer and V.A. Duffie, (eds.), American Solar Energy Society, New York, pp. 61-111 (1983).
- Antal, M.J., *Proc. Int. Conf. Fundamentals of Thermochemical Biomass Conversion*, Estes Park, CO, October 18-22, 1982, SERI, Golden, CO (1983).
- Antal, M.J., in *Advances in Solar Energy*, K.W. Boer and V.A. Duffie, (eds.), American Solar Energy Society, New York, pp. 175-255 (1985).
- Arena, U., Cammarota, A. and Pistone, L., in *Circulating Fluidized Bed Technology I*, P. Basu (ed.), Pergamon, New York, p. 119 (1986).
- Arsenau, D.F. and Stanwick, J.J., *Thermal Analysis*, 3, pp. 319-326 (1971).
- Arsenau, D.F., *Can. J. Chemistry*, 49, pp. 632-638 (1971).
- Back, E.L., *Das Papier*, 27, p. 475 (1973).
- Baeyens, J. and Geldart, D., *Chem. Engng. Sci., 29*, p. 225 (1974).
- Baeyens, J., Maniatis, K., Roggeman, G. and Peeters, H., in *Proc. of the EC Contractors' Meeting*, 7 October 1992, Florence-Italy, Report EUR 15389 EN, pp. 59-66 (1994).
- Bain, R.L., *Physical Solids Separation*, Chemical Conversion Research Branch, National Renewable Energy Laboratory, Golden, CO (1991).

- Baldauf, W., "Upgrading of fast pyrolysis liquids at Veba Oel AG", in *Biomass Gasification and Pyrolysis*, A.V. Bridgwater and M. Kaltschmitt (eds.), CPL Press (1997).
- Basu, P. and Frazer, S.A., Chapter 7 in *Circulating Fluidized Bed Boilers: Design and Operation,* Butterworth-Heinemann (1991).
- Basu, S.N. and Stangeby, P.C., *Enfor Report C-98*, Environment Canada, Ottawa (1981).
- Beall, F.C. and Eickner, H.W., *Research Paper FPL 130*, Forest Products Laboratory, Madison, WI (1970).
- Beenackers, A.A.C.M. and Bridgwater, A.V., in *Pyrolysis and Gasification*, May 1989, Ferrero, G.L., Maniatis, K., Buekens A. and Bridgwater, A.V. (eds.), Elsevier Appled Science Publishers, p 141 (1989).
- Berg, D.A. Sumner, P.J., Meunier, M., Briens, C.L. and Bergougnou, M.A., *Proc. 1st Intl.Conf. in Circ. Fluid. Bed Techn.*, Basu Pr. (ed.), Pergamon Press (1986).
- Bergougnou, M.A., deLasa, H.I., Mok, L.K.S., Graham, R.G., Freel, B.A. and Hazle,H., *ENFOR Project C-147 Final Report* - Ultrapyrolysis of Biomass and Wood Components, Environment Canada, Ottawa (1983).
- Bogley, W.J., Mixon W.R., Dean, C. and Lizdas, D.J., *"Solid Waste Utilization-Pyrolysis"*, Oak Ridge National Laboratory, Oak Ridge, TN (1977).
- Boukis, I. and Vassilatos, V., *"Flash Pyrolysis of Biomass in a Bench Scale Fluidized Bed Plant"*, Interim Report to Contract JOUB-0054C-(TT) (Dec. 1991).
- Bradbury, A., Sakai, Y. and Shafizadeh, F., *J. Appl. Polym. Sci.*, 23, pp. 3271-3280 (1979).
- Bridge, S.A., *"Flash Pyrolysis of Biomass for Liquid Fuels"*, Master Thesis, University of Aston, Birmingham (1990).
- Bridgwater, A.V. and Bridge, S.A., Ch. 2, in *Biomass Pyrolysis Liquids Upgrading and Utilization*, A.V. Bridgwater and G. Grassi (eds.), Elsevier Applied Science, London, pp. 11-92 (1991).
- Bridgwater, A.V. and Double, J.M., in *Pyrolysis as a Basic Technology for Large Agro-Energy Projects*, E. Mattucci (ed.), Commission of the European Communities, Brussels, Belgium, pp. 167-171 (1989).
- Bridgwater, A.V. and Evans, G.D., *An assessment of thermochemical conversion systems for processing biomass and refuse*, ETSU B/T1/0020/REP (1993).

- Broido, A., *et al.*, *J. Appl. Polym. Sci.*, 17, pp. 3627-3635 (1973).
- Brown, M.D., *et al.*, in *Energy from Biomass and Wastes XVI*, D.L. Klass (ed.), Institute of Gas Technology, Chicago Illinois (1992).
- Browne, F.L., *Theories of Combustion of Wood and its Control*, U.S. Forest Service, U.S. Department of Agriculture, Forest Products Laboratory, Rep. 2136 (1963).
- Browning, B.L., *The Chemistry of Wood*, Wiley (Interscience), New York (1963).
- Burkell, J.J., Grace, J.R., ZhaO, J. and Lim, C.J., *Circulating Fluidized Bed Technology II*, P. Basu and J.F. Large (eds.), Pergamon Press, Toronto, pp. 501-509 (1988).
- Byrne, G.A., Gardner, D. and Holmes, F.H., *J. of Appl. Chem.*, 16, pp. 81-88 (1966).
- Cabradilla, K.E. and Zeronian, S.H., in *Thermal Uses and Properties of Carbohydrates and Lignin*, Shafizadeh, F., Sarkanen, KV. and Tillman (Eds..) Academic Press, NY, p. 73 (1976).
- Carrasco, J.E., *Energy from Biomass - 1st Contr. Meeting*, Florence (Nov-1990).
- Clift, R., *Hot Gas Clean up: The State-of-the-Art and Prospects for the Future*, Proceedings of the VII Symposium 83: Pressurized Fluidized Bed Combustion and Gasification Power Systems, Technical Research Centre of Finland, Espoo, Finland (1988).
- Cogliati, , G., in Advanced Gasification, Series E, Vol. 8, Reidel Publishing Company, pp. 173-214 (1986).
- Coombs, J, *MacMilan Dictionary of Biotechnology*, MacMilan Press Ltd, London and Basingstoke (1986).
- Cuevas, A., Union Electrica Fenosa, Private Communication (1995).
- Dave, R., Hauzelot, J.L. and Villermaux, J., *Chem. Engng.Sci.*, 34 (6), pp. 867-876 (1979).
- de Jenga, C.I., Antal, M.J. and Jones M., *J. Appl. Polym. Sci.*, 27, p. 4313 (1982).
- Deglise, X., Morliere, P. and Sclicklin, Ph., *Proc. 1st EC Conf. Energy from Biomass*, Brighton, Nov 4-7, 1980, Applied Science Publishers, London, p. 569 (1981).
- Denloye, A.O.O. and Botterill, J.S., *Powder Technology*, 19, pp. 197-203 (1978).
- Desrosiers, R., Chapter 6 in *Survey of Biomass Gasification-Volume II*, SERI (1979).
- Desrosiers, R.E. and Lin, R.J., *Solar Energy*, 33 (2), pp. 187-196 (1984).
- Diebold, J.P., *Specialists' Workshop on Fast Pyrolysis of Biomass*, Copper Mountain, CO, SERI/CP-622-1096, pp. 3-6 (Oct-1980a).

- Diebold, J.P., in *Proceeding of Biomass Pyrolysis Oil Properties and Combustion Meeting*, Sept. 26-28, 1994, Estes Park, Colorado, NREL-CP-430-7215 , pp. 237-251 (1980b).
- Diebold, J.P.,*"The Cracking Kinetics of Depolymerized Biomass Vapours in a Continuous Tubular Reactor"*, Master of Science Thesis, Colorado School of Mines, Golden, CO (1986).
- Diebold, J.P., Czernik, S., Scahill, J.W., Phillips, S.D. and Feik, C.J., in *Proceeding of Biomass Pyrolysis Oil Properties and Combustion Meeting*, Sept. 26-28, 1994, Estes Park, Colorado, NREL-CP-430-7215, pp. 90-109 (1994).
- Diebold, J.P. and Power, A.J., *"Engineering aspects of the Vortex Pyrolysis Reactor to Produce Primary Pyrolysis Oil Vapours for Use in Resins and Adhesives"*, in Research in Thermochemical Biomass Conversion, Bridgwater, A.V. and Kuester, J.L. (eds.), Elsevier Applied Science Publishers, London and New York, pp. 609-628 (1988).
- Diebold, J.P. and Scahill, J., *Annual Report, SERI/PR-234-1456*, SERI, Golden, CO (1982).
- Diebold, J.P. and Scahill, J., *Proc. 15th Biomass Thermochemical Conversion Contractors Meet.*, Atlanta, GA, March 16-17, 1983 PNL, Batelle, Richland, WA (1983).
- Diebold, J.P. and Scahill, J.W., *Proc. of U.S. DOE 16th Thermochemical Conversion Contractor' s Meeting*, Portland, OR, May 8-9, Pacific Northwest Laboratory, Richland, WA 99352, CONF-8405157 (PNL-SA-12403) pp. 319-348 (1984).
- Diebold, J.P., Scahill, J.W. and Power, A.J., in *Research in Thermochemical Biomass Conversion*, Phoenix, Arizona, USA, April 1988, p. 609, Elsevier Appl. Sc. Publ., London and New York (1988).
- Dunlap, F., *US Dept. Agr. Bull No 110*, Washington D.C. (1912).
- Elliot, D.C., *Analysis and Comparison of Biomass Pyrolysis/Gasification Condensates - Interim Report, PNL-5555*, Pacific Northwest Laboratory, Richland, WA, (1985).
- Elliot, D.C. and Baker, E.G., *Interim Report PNL-5844*, Pacific Northwest Laboratory, Richmond, WA (1986).
- Evans, R.J., Appendix C in "*Entrained-Flow, Fast Ablative Pyrolysis of Biomass, Annual Report*", 1 Oct. 1983-30 Nov. 1984, by J.P. Diebold and J.W. Scahill, SERI, Golden, CO. SERI/PR-234-2665 (1985).

- Evans, R.J. and Milne, T.A., *Fundamental Pyrolysis Studies: Final Report*, 1 October 1980-30 December 1985, SERI/PR-234-3026, Solar Energy Research Institute, Golden, CO (1985).
- Evans, R. and Milne, T., in *Proceeding of the 17th Biomass Thermochemical Conversion Contractor's Meeting*, Minneapolis, MI, Oct 15-16 (1985).
- Evans, R.J. and Milne, T.A., *Energy and Fuels*, 1, pp. 123-137 (1987a).
- Evans, R.J. and Milne, T.A., *Energy and Fuels*, 2, pp. 311-319 (1987b).
- Evans, R., Milne, T.A. and Soltys, M., in *Proceeding of the 16th Biomass Thermochemical Conversion Contractor's Meeting*, Portland, O.R., May 8-9, U.S. DOE CONN-8405157, pp. 349-374 (1984).
- Freel, B.A. and Graham, R.G., *Papid Pyrolysis of Wood and Wood-Derived Liquids to Produce Olefins and High Quality Fuels*, Ottawa: Energy Mines and Resources Canada (1988).
- Freel, B.A. and Graham, R.G, *Report of Contract File No 5152 23216-6-6656*, Renewable Energy Branch, Energy, Mines and Resources, Canada (1988).
- Freel, B.A., Graham, R.G., Bergougnou, M.A., Orerend, R.P. and Mok, L.K., *AIChE Symp. Ser.*, 255, Vol 83, pp. 105-111 (1987).
- Freel, B.A. and Huffman, D.R., in *Biomass Pyrolysis Oil Properties and Combustion Meeting*, 26-28 Sep 1994, Estes Park, CO, NREL-CP-430-7215, pp. 383-391 (1995).
- Geldart, D., *Powder Technol.*, 7, 285 (1973).
- Gorton, C.W. and Knight, J. A., *Biotechnology and Bioengineering Symposium,* 14, pp. 15-20 (1984).
- Gorton, C.W., Kovac, R.J., Knight, J.A. and Nygaard, T.I., *Biomass*, 21, pp. 1-10 (1990). Grace, J.R., in *Proc. 1st Intl. Conf. Circulating Fluidized bed Technology II*, P. Basu (Ed.), Pergamon, Halifax, pp. 63-81 (1986).
- Grace, J.R. and Lim, C.J., *Circulating Fluidized Bed Combustion of Coal, Woodwastes and Pitch*, Final Report, Energy, Mines and Resources Canada, DSS File Number: 24ST. 23440-6-9007 (Dec 1987).
- Graham, R.G., *Rapid Pyrolysis of Wood and Wood-derived Liquids to produce Olefins and High Quality Fuels*, Energy, Mines and Resources Canada, Ottawa/Ontario/Canada, DSS Contract File No:23216-6-6656/01-S2 (1988).
- Graham, R.G., *"A Characterisation of the Fast Pyrolysis of Cellulose and Wood Biomass"*, PhD Thesis, University of Western Ontario (1993).

- Graham, R.G., Bergougnou, M.A. and Overend, R.P., *J. Anal. and Appl. Pyrol*, 6, pp. 95-135 (1984).
- Graham, R. G., Freel, B. A. and Bergougnou, M. A., "Rapid Thermal Processing (RTP): Biomass Fast Pyrolysis Overview", in *Proc. of the 1st Europe-Canada Workshop*, pp. 52-63 (1990).
- Graham, R.G., Mok, L.K., Bergougnou, M.A. and de Lasa, H.I., *Proc. 4th Bioenergy R&D Seminar*, Winnipeg, NRC Ottawa, Canada, p. 31 (Mar-1982).
- Grassi, G., in *Pyrolysis as a basic technology for large agro-energy projects*, Mattucci, E., Grassi, G. and Palz, W. (eds.), L' Aquila 15-17 October 1987, EUR 11382 EN (1989).
- Gray, M.R., "*The effects of moisture and ash content on the pyrolysis of a wood derived material*", PhD Thesis, California Institute of Technology, Pasadena, USA, (1984).
- Gulyurtlu I., Cabrita, CC., Franci, F. and Menard, H., "Pyrolysis of Forestry Wastes in a Fluidized Bed Reactor to produce Medium Calorific Value Gas", in *Research in Thermochemical Biomass Conversion*, Bridgwater, A.V. and Kuester, J.L. (eds.), Elsevier Applied Science Publishers, London and New York, pp. 597-608 (1988).
- Gust, S., "Combustion of pyrolysis liquids", in *Biomass Gasification and Pyrolysis*, A.V. Bridgwater and M. Kaltschmitt (eds.), CPL Press (1997).
- Hajaligol, M.R., Howard, J.B., Longwell, J.P. and Peters, W.A., *Ind. Eng. Chem. Process Des. Dev.*, 21, pp. 457-465 (1982).
- Hallen, R.T., Sealock, L.J. and Cuello, R., in *Proc. Intl. Conf. Fundamentals of Thermochemical Biomass Conversion*, Estes Park, CO, October 18-22, 1982, SERI, Golden, CO (1984).
- Halling, J.N., *Modelling the liquid product distribution from the Waterloo Fast Pyrolysis Process*, MSc Thesis, University of Waterloo, Canada (1987).
- Han, G.Y., Lee, G.S. and kim, S.D., *Korean J. of Chem. Eng.*, 2 (2), pp. 141-147 (1985).
- Hartge, E.U., Li, Y. and Werther, J., in *Circulating Fluidized Bed Technology I*, P. Basu (ed.), Pergamon, New York, p.153 (1986)
- Hoffman, W.L., Italligan, J.B., Peterson, R.L. and de la Garza E., *Combust. Sci. Tecnol.*, 26, p. 1977 (1983).
- Holman, J.R., *Heat Transfer*, 4th ed., McGraw-Hill, New York (1976).
- Hopkins, M.W. and Antal, M.J., *J. Appl. Polym. Sci.*, 29, p. 2163 (1984).
- International Energy Agency (IEA), *Bioenergy Agreement Newsletter*, 6(3), pp. 6-7 (1994).

- Jones, P. J., Teo, C. S. and Leung, L. S., in *Fluidization*, J. R. Grace and J. M. Matsen (eds.), p. 469 (1986).
- Kaiser, D., "Upgrading of fast pyrolysis liquids by DMT", in *Biomass Gasification and Pyrolysis*, A.V. Bridgwater and M. Kaltschmitt (eds.), CPL Press (1997).
- Kanury, A.M., *Combustion and Flame*, 18, pp. 75-83 (1972).
- Kanury, A.M. and Blackshear, Jr. P.L., *Combustion Sci. & Technology*, 2, pp. 5-9 (1970).
- Kavarov, V. V., in *Wasteless Chemical Engineering*, Mir Publishers - Moskow (1985).
- Kilzer, F. and Broido A., *Pyrodynamics*, 2, p. 151 (1965).
- Knight, J.A., Gorton, C.W. and Kovac, R.J., Entrained Flow Pyrolysis of Biomass, in *Proc. of the 15th Biom. Thermochem. Conv. Contract. Meet.*, p.409, Atlanta-Georgia, CONF-830323/PNL-SA-11306 (1983).
- Knight, J.A., Gorton, C.W. and Kovac, R.J., Entrained Flow Pyrolysis of Biomass, in *Proc. of the 16th Biom. Thermochem. Conv. Contract. Meet.*, May 8-9, 1984, Portand-Oregon, CONF-8405157/PNL-SA-12403, p. 287 (1984).
- Knight, J.A., Gorton, G.W., Kovac, R.J., Elston, L.W. and Hurst, D.R., "Oil Production via Entrained Flow Pyrolysis of Biomass", in *Proc. of the 13th Biomass Thermochemical Conversion Contractors' Meeting*, Arlington, Virginia, Oct 27-29, 1981, pp. 475-492 (1981).
- Knowlton, T.M., in *Proceedings of Powder and Bulk Solids Conference/Exhibition*, Philadelphia, PA (1979).
- Knowlton, T.M., in *Gas Fluidization Technology*, D. Geldard (ed.), Chichester, p. 406 (1986).
- Knowlton, T.M. and Hirsan, I., Paper E3, in *Proceedings of Pneumotransport 5*, BHRA Fluid Engng., London, p. 257 (1980).
- Kobro, H. and Brereton, C., in *Circulating Fluidized Bed Technology II*, P. Basu (Ed.), Pergamon, Toronto, pp. 263-272 (1986).
- Kojima, T., Ishihara, K., Kuramoto, M. and Furusawa, T., *World Cong. III of Chem. Engng.*, Tokyo (1986).
- Kosstrin, H. M., "The Mobile Fluidized Bed Pyrolysis System", in *Proc. of Bio-Energy '80 World Congress and Exposition*, April 21-24, 1980, Atlanta, GA,. The Bio-Energy Council, Washington, DC. (1980a).
- Kosstrin, H. M., in *Proc. Spec. Workshop on Fast Pyrolysis of Biomass*, Copper Mountain, Colorado, pp. 105-121 (1980b).

- Kovac, R.J., Gorton, C.W., Knight, J.A., Newman, C.J. and O' Neil, D.J., in *Research on the Pyrolysis of Hardwood in an Entrained Bed PDU*, Prepared for the USDoE under Contract DE-ACO6-76RLO 1830, PNL-7788/UC-245 (August 1991).
- Kovac, R.J., Gorton, C.W., O' Neil, D. J. and Newman, C.J., "Low Pressure Entrained Flow Pyrolysis of Biomass to Produce Liquid Fuels", in *Proc. of the 1987 Biom-Thermochem. Conv. Contr. Meet.*, p.23, Atlanta-Georgia (1987).
- Kraft, W. W., *et al.*, in *Fluidization*, D. F. Othmer (ed.), Van Nostrand Reinhold, New York (1956).
- Kuester, J.L., *Trip Report (Japan)*, US Dept. of Energy Report No C00-2982-65 (Jan-1981).
- Kunii, D. and Levenspiel, D., in *Fluidisation Engineering*, First Edition, Wiley, New York, (1969).
- Kunii, D. and Levenspiel, O., in *Fluidisation Engineering*, Second Edition, H. Brenner (ed.), Butterworth-Heinemann (1991).
- Larson, E.D. and Svenningsson, P.M., *Energy from Biomass and Wastes XIV*, Klass, D.I. (Ed.), Institute of Gas Technology, Chicago, Illinois (1990).
- Lèdè, J., Li. H.Z., Villlermaux, J., Moyne, C. and Degiovanni, A., *Int. J. Heat & Mass Transfer*, 29, pp. 1407-1415 (1985).
- Lèdè, J., Panagopoulos, J., Li, H.Z. and Villermaux, J., *Fuel*, 64, p. 1514 (Nov-1985).
- Lèdè, J., Verzaro, F., Antoine, B. and Villlermaux, J., *Chem. Engng. and Proc.*, 20(6), pp. 309-317 (1986).
- Leech, J., "Running a dual fuel engine on pyrolysis oil", in *Biomass Gasification and Pyrolysis*, A.V. Bridgwater and M. Kaltschmitt (eds.), CPL Press (1997).
- Levelton, B.H. & Associates Ltd., *Status of Biomass Feeder Technology*, ENFOR Project C-259, B.H. Levelton & Associates Ltd. (Dec-1982).
- Levy, S.J., San Diego County Demonstrates Pyrolysis of Solid Wastes, *Report SW-80d.2*, US Environmental Protection Agency (1975).
- Lewellen, P.C., Peters, W. A., Howard, J.B., *16th Int. Symp. Combust. Proc.*, pp. 1471 - 1480 (1977).
- Lidén, A. G. *"A Kinetic and Heat Transfer Modelling Study of Wood Pyrolysis in a Fluidized Bed"*, Master Thesis, University of Waterloo, Waterloo, Ontario (1985).
- Lidén, A.G., Berruti, F. and Scott, D.S., *Proc. of the 37th Com. Chem. Engng. Conf.*, Montreal, Que., pp. 473-476 (1987).

- Lidén, A.G., Berruti, F. and Scott, D.S., *Chem. Eng. Comm.*, 65, p. 207 (1988).
- Luengo, C.A. and Censig, M.O., "Biomass Pyrolysis in Brazil: Status Report", in *Biomass Pyrolysis Liquids Upgrading and Utilization*, A.V. Bridgwater and G. Grassi (eds.), Elsevier Applied Science, London, pp. 11-92 (1991).
- MacLean, J.D., *Transactions of the American Society of Heating and Ventilating Engineers*, 47, pp323-354 (1971).
- Maniatis, K., "*Fluidized Bed Gasification of Biomass*", PhD Thesis, Aston University (1986).
- Maniatis, K., Personal communication (1995).
- Maniatis, K., Baeyens, J., Roggeman, G. and Peeter, H., *"Flash Pyrolysis of Biomass in an Entrained Bed Reactor"*, Final Report to the EEC, Contract JOUB-0025 (1993).
- Marinelli, L. and Carson, J.W., *Chem. Engng. Prog.*, pp. 22-28 (Jul-1992).
- Massaquoi, J.G.M. and Riggs, J.B., *AIChE J.*, 29, p. 975 (1983).
- Matsen, J.M., in *Fluidization Technology*, Vol. 2, D.L. Kearns (ed.), Hemisphere, Washington, D.C., p. 135 (1976).
- McGinnes, E.A., Jr., *et al.*, *Scanning Electron Microscopy*, Part II, pp. 469-476 (1974).
- McGinnes, E.A., Jr., *et al.*, *Scanning Electron Microscopy*, Part III, pp. 543-548 (1976).
- McKeough, P. *et al.*, *IEA Co-operative Project D1: Biomass Liquefaction Test Facility Project*, Vol. 5, App. J, DOE/NBM-1062 (1988).
- Milne, T.A. and Soltys, M. N., *Quarterly Report, SERI/PR-234-1617*, SERI, Golden, CO (1983).
- MoK, L. K., "*Kinetic Studies of the Flash Pyrolysis of Wood Bark*", Master Thesis, Mc Gill University, Montreal, Quebec (1984).
- Mok, L..K. and Antal, M.J., in *14th Thermochemical Conversion Contractor's Meet.*, Washington D.C., Jun. 23 - 24 1982, PNL, Batelle, Richland WA, p. 403 (1982).
- Mok, L.K., Graham, R.G., deLasa, H.I. and Bergougnou, M.D., *AIChE Symp. Ser.*, 244, Vol. 80, pp. 70-79 (1984).
- Mok, L.K., Graham, R.G., Freel, B.A. and Bergougnou, M.D., *J. Anal. Appl. Pyrol.*, 8, pp. 391-400 (1985).
- Nunn, T.R., Howard, J.B., Longwell, J.P. and Petera, W.A., *Conf on Fund. Therm. Biom. Conv.*, Estes Park, Colorado, pp. 293-314 (1982).
- Nunn, T.R., Howard, J.B., Longwell, L.P. and Peters, W.A., *Ind. Eng. Chem. Prod. Res. Dev.*, 24(1), pp. 836-844 (1985).

- O' Neil, P.J., Kovac, P.J. and Gorton, C.W., *XIII Conf. on Energy from Biomass and Wastes*, Institute of Gas Technology, pp. 829-850 (1989).
- Paisley, M.A., Creamer, K.S., Tewksbury, T. L. and Taylor, D.R., *Gasification of Refuse Derived Fuel in the Battelle high Throughput Gasification System*, USDoE Contract DE-ACOG-76RLO 1830, Pacific Northwest Laboratory, Richland, WA (1989).
- Pan, W.P. and Richards, G.N., *J. Anal. Appl. Pyrolysis, 16,* p. 117 (1989).
- Panton, R.L. and Rittmann, J.G., in *13th Symposium on Combustion*, Combustion Institute, pp. 781-801 (1970).
- Parker, J.W., in *Proc. of the 2nd Int. Symp in Fire Safety Science.*, Hemisphere Publ. Co., Tokyo, pp. 337-346 (1988).
- Patience, G.S. and Chaouki, J., *Circulating Fluidized Bed Technology II*, P. Basu and J.F. Large (Eds.), Pergamon Press, Toronto (1988).
- Patnaik, P.C., "Industrial gas turbine tests using a biomass derived fuel", in *Biomass Gasification and Pyrolysis*, A.V. Bridgwater and M. Kaltschmitt (eds.), CPL Press (1997).
- Patterson, P.A. and Munz, R. J., *Can. J. of Chem. Engng.*, 5, pp. 321-328 (Apr-1989).
- Peacocke, C.V.C., *"Ablative Pyrolysis of Biomass"*, PhD Thesis, Aston University UK (Oct-1994).
- Peacocke, G.V.C., Personal Communication (1995).
- Perry, R.H. and Green, D., in *Perry's Chemical Engineers' Handbook*, Chapter 20, 6+4 Edition/4th Printing, McGraw Hill (1984).
- Peters, W.A., in *Proc. 6th Int. Symp. Anal. Pyrolysis*, Vail, CO, September 26-30, 1982, K.J. Voorbees (ed.), Butterworths, New York (1983).
- Piskorz, J., Radlein, D., Scott, D.S., *J. Anal. Appl. Pyrolysis*, 9, pp. 121-137 (1986).
- Piskorz, J., Radlein, D., Scott, D.S. and Czernik, S., *J. Anal. Appl. Pyrolysis*, 16, p 127 (1989).
- Piskorz, J. and Scott, D.S., in *Pyrolysis Oils from Biomass, Producing, Analyzing and Upgrading*, Soltes, E.J. and Milme, T.A. (eds.), *ACS Symposium Series 376*, American Chemical Society, Washington D.C, pp. 1667-178 (1988).
- Piskorz, J., Scott, D.S. and Radlein, D., *ACS Symp. Ser.*, 376, Ch. 16, pp. 167-178 (Apr-1987).
- Pouwels, A.D., Tom, A., Eijkel, G.B. and Boon, J.J., *J. Anal. Appl. Pyrolysis*, 11, p. 417

(1987).

- Pouwels, A.D., Tom, A., Eijkel, G.B. and Boon, J.J., *J. Anal. Appl. Pyrolysis*, 14, p. 237 (1989).
- Pyle, D.L. and Zaror C.A., *Chem. Eng. Sci.*, 39, pp. 147-158 (1984).
- Radlein, D., "Production of chemicals from bio-oil", in *Biomass Gasification and Pyrolysis*, A.V. Bridgwater and M. Kaltschmitt (eds.), CPL Press (1997).
- Radlein, D., Piskorz, J. and Scott, D.S., *J. Anal. Appl. Pyr.*, 19, pp. 41-63 (1991).
- Reed, T. B., *Biomass Gasification: Principles and TechnologyEnergy Technology Review No. 67*, Noyes Data Corporation, N.J., USA (1981).
- Reed, T. B. and Cowdery, C.D., *American Chemical Society, Division of Fuel Chemistry*, 32(2), pp. 68-81 (1987).
- Reed, T. B., Diebold, J.P and Desrosiers, R., in *Specialists' Workshop on Fast Pyrolysis of Biomass, Copper Mountain*, CO, SERI/CP-622-1096, pp. 7-19 (Oct-1980).
- Richards, G.N., *J. Anal. Appl. Pyrolysis*, 10, pp. 251-255 (1987).
- Richardson, D. R., *Chem. Eng.*, 68, p.83 (May 1961).
- Roberts, A.F., *Combustion and Flame*, 17, p.p. 79 - 86 (1961).
- Roggeman, G., in *An Assessment of Thermochemical/Conversion Systems for Processing Biomass and Refuse*, A.V., Bridgwater and G.D. Evans, Contract ETSU B/T1/00207/REP (1993).
- Roman P., Walawender, W., Ran L.T. and Chang, C.C., *Ind. Eng. Chem. Proc. Des. Dev.*, 20, p. 686 (1981).
- Roy, C., de Caumia, B., Plante, P. and Menard, H., *Proc. Conf. Energy from Biomass and Wastes VII*, Lake Buena Vista, FL, January 24-28, 1983, Inst. Gas Techn., Chicago, IL, p. 1147 (1983).
- Salazar, C.M. and Connor, M.A., *Chemeca 83*, 4-7 Sep 2983, pp. 753-761 (1983).
- Salmen, N.L. and Back, E.L., *Tappi*, 60, p. 137 (1977).
- Samolada, M.C. amd Vasalos, I.A., *Fuel*, 70, pp. 883-889 (1991).
- Samolada, M and Vasalos, I., in *Advances in Thermochemical Biomass Conversion*, Vol. 2, A.V. Bridgwater (ed.), Chapman and Hall, Interlaken, 11-15 May 1992, Switzerland (1993)
- Schulten, H.R. and Gortz, W., *Anal. Chemistry, 50,* p. 428 (1978).
- Schoeters, J., *"The Fluidized Bed Gasification of Charcoal"*, PhD Thesis, Free University of Brussels (1983).

- Schoeters, J. and Buekens, A., *Proc. Fluidized Bed Combustion Conference*, Cape Town, South Africa (Jan. 1981).
- Scott, D.S., *Technical Evaluation of the Waterloo Fast Pyrolysis Process*, Alternate Energy Division, Energy-Mines-Resources Canada, Ottawa (1986).
- Scott, D.S., *Assessment of Waterloo Flash Pyrolysis Process to obtain Liquid Fuels from Canadian Peat*, Energy, Mines and Resources Canada, Ottawa/Ontario/Canada, DSS Contract File No:24ST 23216-5-7138 (June 1988).
- Scott, D.S., Private Communication (1995).
- Scott, D.S. and Piskorz, J., *Can. J. Chem. Eng.*, 60, pp. 666-674 (Oct-1982).
- Scott, D.S. and Piskorz, J., *Energy from Biomass and Wastes VII*, D.L. Klass (ed.), IGT, Chicago, pp. 1123-1146 (1983).
- Scott, D.S. and Piskorz, J., *Can. J. Chem. Eng.*, 62, pp. 404 -412 (Jun-1984).
- Scott, D.S., Piskorz, J., Bergougnou, M.A., Graham, R.G. and Overend, R.P., *Ind. Eng. Chem. Res.*, 27, pp. 8-15 (1988).
- Scott, D.S., Piskorz, J., Grinspun, A. and Graham, R.G., in *American Chemical Society, Division of Fuel Chemistry*, 32(2), pp. 1-11 (1987).
- Scott, D.S., Piskorz, J. and Majerski, D., in *Pyrolysis as a Basic Technology for Large Agroenergy Projects*, Matucci, E., Grassi, G. and Palz, W. (eds.), CEC-EUR 11382 EN, pp. 115-124 (1989).
- Scott, D.S., Piskorz, J. and Radlein, D., *Ind. Eng. Chem. Process Des. Dev.*, 24(3), pp.581-588 (1985).
- Scott, P.S., Piskorz, J. and Radlein, D., "*Pyrolysis as a basic technology for large agro-energy projects*", in *Proc. of a Workshop held in L' Aquila (Italy)*, Mattucci, E., Grassi, G. and Palz, W. (eds.), pp. 115-124 (1987).
- Scott, D.S., Piskorz, J and Radlein, D., in *Energy from Biomass and Wastes XVI*, D.L. Klass (ed.), IGT, Paper No 28 (1992).
- Scott, D.S., Radlein, D., Piskorz, J. and Majerski, P., "Potential of Fast Pyrolysis for the Production of Chemicals", in *Meeting on Biomass Liquefaction*, Alternate Energy Branch, Canmet, Energy-Mines-Resources, Ottawa, pp. 171-178 (1991).
- SERI, *Specialists' Workshop on Fast Pyrolysis of Biomass*, SERI/TR-33-239, Sol. Energy, Res. Inst., Golden, CO (1980).
- Shafizadeh, F., *Adv. in Carbohydr. Chem.*, 23, p. 419 (1968).

- Shafizadeh, F., *Proc. Specialists' Workshop on Fast Pyrolysis of Biomass, Copper Mountain*, CO, October 19-22, 1980, SERI, Golden, CO, p. 79 (1980).
- Shafizadeh, F., *J. Anal. Appl. Pyrolysis*, 3, p. 283 (1982a).
- Shafizadeh, F., *Proc. Int. Cont. Fundamental Thermochemical Biomass Conversion*, Estes Park, CO, SERI, Golden, CO (1982b).
- Shafizadeh, F. and Bradbury, A.G.W., *J. Appl. Polym. Sci.*, 23, p. 1431 (1979).
- Shafizadeh, F. and Chin, P.S., *Proc. 172nd Nat ACS Meet.*, American Chemical Society, 43, Washington, DC, p. 57 (1976).
- Shafizadeh, F., Cochran, T.G. and Sakai, Y., *AICHE Symp. Series*, 75, pp. 24-34 (1979).
- Shafizadeh, F. and DeGroot, W.F., *Fuels and Energy from Renewable Resources*, Academic Press, New York, p. 93 (1977).
- Shafizadeh, F. and Fu, Y.L., *J. Org. Chem.*, 37, p. 278 (1972).
- Shafizadeh, F. and Fu, Y.L., *Carbohyd Res.*, 29, p. 113 (1973).
- Shingles, T., *et al.*, *Chem. South Africa*, 12, p.79 (1986).
- Simmons, G.M. and Lee, W.H., in *Fundamentals of Thermochemical Biomass Conversion*, Overend, R.P., Milne, T.A. and Mudge, T.L. (eds.), Elsevier Applied Science Publishers, London, pp. 385-395 (1985).
- Simons Resource Consultants and Levelton, B.H. and Associates Ltd., *A Comparative Assessment of Forest Biomass Conversion to Energy forms. Phase I - Proven and Near Proven Technology*, Volume VI - Data Book of Unit Processes for Modification and Upgrading of Energy Forms, ENFOR Project C-258, Bioenergy Development Program, Alternative Energy Technology Branch, Canmet, Energy, Mines and Resources Canada, Ottawa (1983).
- Sjöström, E., *Wood Chemistry Fundamentals and Applications*, Academic Press Inc., NY (1981).
- Solantausta, Y., Nylund, N-O, Oasma, A., Westerholm, N. And Sipilä, K., (1995).
- Stevens, D., *Review and Analysis of the 1980-1989 Biomass Thermochemical Conversion Program*, National Renewable Energy Laboratory, NREL/TP-421-7501, p. 101 (Sep-1994a).
- Stevens, D., in *Biomass Pyrolysis Oil Properties and Combustion Meeting*, 26-28 Sep 1994, Estes Park, CO, NREL-CP-430-7215, pp. 383-391, pp. 96-99 (Sep-1994b).
- Stromberg, L., *Arch. Combust.*, 1, pp. 95-107 (1981).

- Stromberg, L., in *Proc. 7th Intern. Fluidized Bed Combust. Conf.*, vol. 2, pp. 1152-1163 (1982).
- Tang, W. and Neill, W.K., "Effect of Flame Retard ants on Pyrolysis and Combustion of Cellulose", *Journal of Polymer Science part C*, 6. pp. 65 - 81 (1964).
- Tillman, D.A., "Energy from Wastes: An Overview of Present Technologies and Programs", in *Fuels from Wastes*, Anderson, L.L. and Tillman, D.A. (eds.), Academic Press, Inc., NY, pp. 17-40 (1977).
- Trebbi, G. and Rossi, C., *Integrated Leben Project Umbria-Progress Report*, Contract JOUB-0059-I(A), Biomass Contractors' Meeting, June 1-2, 1993, Athens (1993).
- Varhegyi, G. and Szabo, P., in *Advances in Thermochemical Biomass Conversion*, A.V. Bridgwater (ed.), Blackie Academic and Professional, Glaskow, pp. 760-770 (1994).
- Vovelle, C., Mellottee, H. And Delfan, J.L., Internal Report-"*Kinetics of Thermal Degradation of Wood and Cellulose by TGA, Comparison of Calculation Techniques*", CNRS, France.
- Walavender, W. P., Hoveland, D. A. and Fan, L. T., in *Proc. Int. Conf. In Fundamentals of Thermochemical Biomass Conversion, Estes Park*, CO, October 18-22. 1982, SERI, Golden, CO (1984).
- Wenzl, H.F.J., in F.J. Herman (Editor), *Chemical Technology of Wood*, Academic Press, New York, p. 253 (1970).
- Williams, P.T. and Besler, S., in *Advances in Thermochemical Biomass Conversion*, A.V. Bridgwater (ed.), Blackie Academic and Professional, Glaskow, pp. 771-783 (1994).
- Yagi, S. and Muchi, I., *Chem. Engng. Japan, 16*, p. 307 (1952).
- Yerushalmi, , J., in *Gas Fluidization Technology*, Geldart, D. (ed.), Wiley, New York, p. 155 (1986a).
- Yerushalmi, J., *Powder Technology*, 24, p.187 (1986b).
- Yerushalmi, J. and Avidan, A., in *Fluidization*, 2nd ed., J.F. Davidson, *et al.* (eds.), Academic Press, New York, p.226 (1985).
- Yerushalmi, , J. and Cankurt, N.T., *ChemTech*, pp. 564-572 (1978).
- Zaror, C.A., Hutchings, I.S., Pyle, D.L., Stiles, H.N. and Kandiyoti, R., *Fuel*, 64, pp. 990-994 (1985).
- Zheng, Q.Y., Wang, X. and Li, X., in *Circulating Fluidized Bed Technology III*, P. Basu, M. Horio and M. Hasatani (eds.), Pergamon Press, Nagoya-Japan, pp. 263-268 (1990).

Appendix 1: Data on kinetic considerations

In this appendix, kinetic models incorporating both primary and secondary pyrolysis rate expressions and constants are considered, since they were found to be the most reliable ones for predicting the pyrolysis liquid yields for a variety of operating parameters, such as pyrolysis temperature and gas/vapor residence time.

Samolada and Vasalos' (1992) and Lidén's (1985) kinetic models for the dependence of pyrolysis liquids from temperature are based on polynomial fits of experiments conducted on laboratory scale fluidised bed systems.

Lidén's model (1985)

The experiments performed in the laboratory and bench scale fluidised bed units in the University of Waterloo, Section 3.4, led to the following proposed model for pyrolysis liquids (tar) yield:

$$CY=0.542 + 0.215CT - 0.956CT^2$$

where

CY = (Yield - 60)*0.2, the centered yield

CT=(Temp - 500)*0.2, the centered temperature

Samolada and Vasalos' model (1992)

The experiments performed at Chemical Process Engineering Research Institute, Thessaloniki, Greece, led to the following proposed model for pyrolysis liquids (tar) yield:

$$Y_{liquid}(\%\text{ wt maf})=55.19 -11.5X-21.69X^2$$

where

X = (T-560)/160, dimensionless pyrolysis temperature

T= pyrolysis temperature, bed temperature (°C)

The predictions from the polynomial models of these two research groups are further summarised in Table 1A-1 below.

Table 1A-1: Polynomial model prediction based on data from Samolada and Vasalos (1992) and Lidén (1985)

Temperature		Samolada and Vasalos (1992)		Lidén (1985)	
(°C)	(K)	Centerred Temperature	Pyrolysis liquids yield (maf)	Centerred Temperature	Pyrolysis liquids yield (maf)
400	673	-1.000	0.45	-2.00	0.41
425	698	-0.844	0.49	-1.50	0.50
450	723	-0.688	0.53	-1.00	0.57
475	748	-0.531	0.55	-0.50	0.61
500	773	-0.375	0.56	0.00	0.63
525	798	-0.219	0.57	0.50	0.62
550	823	-0.063	0.56	1.00	0.59
575	848	0.094	0.54	1.50	0.54
600	873	0.250	0.51	2.00	0.46
625	898	0.406	0.47	2.50	0.36
650	923	0.563	0.42	3.00	0.23
675	948	0.719	0.36		
700	973	0.875	0.29		

The results from the model developed by model, Lidén (1985), Figure 2-17, and Lidén *et al.*, (1988), discussed extensively in Section 2.6.3, are summarized in Table 1A-2, where the pyrolysis liquid yields versus reactor temperature for gas/vapor residence times between 0.3-0.8 s have been calculated.

The expressions used to estimate liquid yields have been given in Eq. 2-8, Section 2.6.3.

Finally, the effect of temperature on liquid yields estimated by different researchers for a given vapor residence time (0.5 s) and elevated (>500°C) temperatures, where secondary vapor decomposition (Section 2.4) becomes important, are presented in Table 1A-3.

For further details the reader is referred to Figure 2-21, Section 2.6.5.

Table 1A-2: Kinetic model proposed by Lidén (1985) and Lidén *et al.*, (1988)

Table 1A-3: Kinetic parameters and tar yields for first-order vapor-phase cracking reactions as given by various investigators

Temperature		Lidén (1985)			Diebold (1985)		Scott (1988)		Graham (1993)	
(^{0}C)	(K)	k	k_{2L}	Pyrolysis liquids yield	k_{2D}	Pyrolysis liquids yield	k_{2S}	Pyrolysis liquids yield	k_{2G}	Pyrolysis liquids yield
500	773	4.104	0.233	0.664	0.186	0.745	0.109	0.684	0.059	0.693
525	798	10.030	0.393	0.638	0.284	0.727	0.184	0.672	0.100	0.686
550	823	23.216	0.643	0.601	0.425	0.703	0.301	0.653	0.164	0.675
575	848	51.142	1.022	0.550	0.620	0.671	0.478	0.625	0.260	0.659
600	873	107.677	1.582	0.486	0.884	0.630	0.739	0.588	0.403	0.637
625	898	217.504	2.389	0.410	1.238	0.582	1.116	0.539	0.608	0.606
650	923	422.929	3.528	0.330	1.701	0.525	1.649	0.479	0.899	0.566
675	948	794.029	5.105	0.254	2.299	0.464	2.386	0.411	1.300	0.517
700	973	1443.26	7.248	0.189	3.059	0.399	3.387	0.339	1.846	0.459
725	998	2545.98	10.110	0.138	4.013	0.336	4.724	0.270	2.575	0.395
750	1023	4368.35	13.876	0.101	5.195	0.278	6.484	0.208	3.534	0.330

Appendix 2: Determination of Minimum Fluidisation Velocity

The onset of fluidization, i.e. the transition from the fixed bed to fluidised bed flow, occurs when the drag force by upward moving gas counteracts the weight of the particles. At this point, the minimum fluidizing conditions have been achieved and the superficial gas velocity is then defined as the minimum fluidisation velocity (MFV).

In a packed bed, the pressure drop is approximately proportional to gas velocity and reaches a maximum value, Δpmax, after which the packed bed suddenly unlocks, i.e. it becomes fluidised. With gas velocities beyond MFV the bed expands and gas bubbles are seen to rise. Despite the rise in gas flow, the pressure drop remains practically unchanged, since the dense gas-solid phase is well aerated and deforms easily without appreciable resistance.

The MFV is a critical parameter for a fluidised bed, since it provides a rough indication of the quality of fluidisation and its estimation is essential for the calculation of other important parameters, see Section 4.6.3.

In order to determine the MFV for the sand used in the experiments, the pressure drop versus velocity diagram was investigated in three different experiments conducted in the cold model. The results of these experiments conducted for three bed heights are presented in Figures 2A-1 to 2A-3 below.

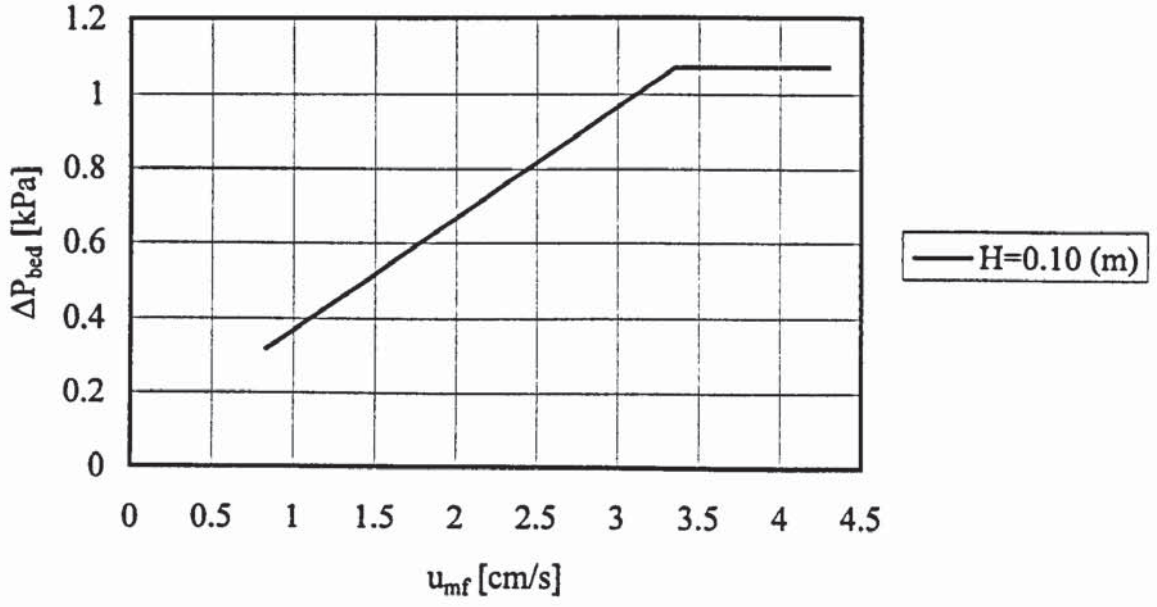

Figure 2A-1: Determination of MFV for a bed height (H) of 0.10 m

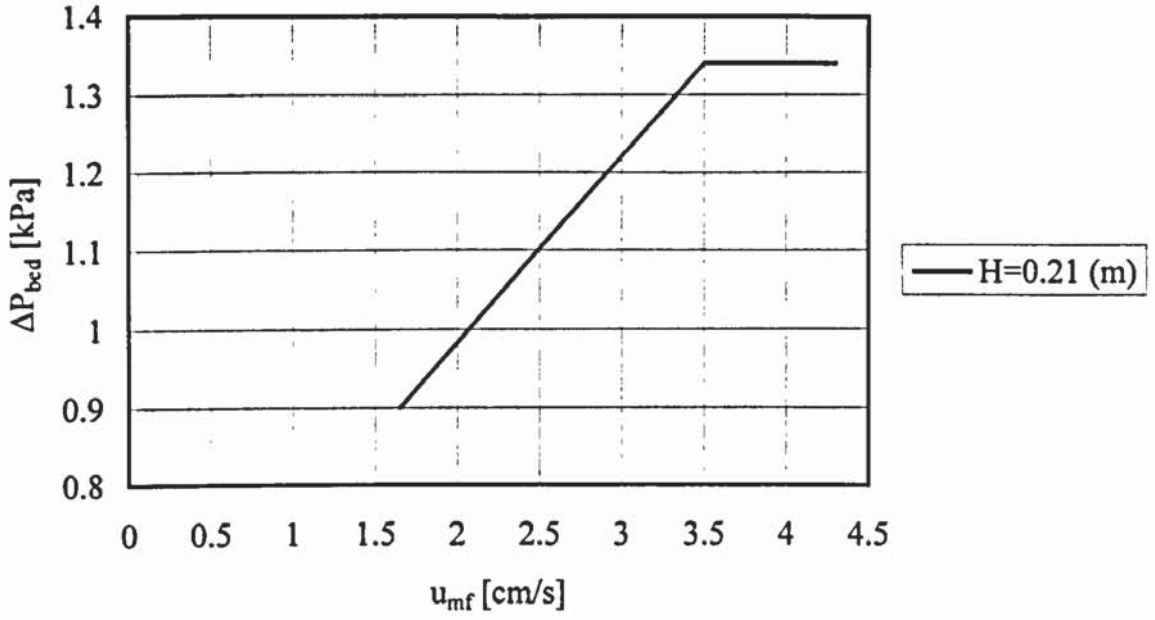

Figure 2A-2: Determination of MFV for a bed height (H) of 0.21 m

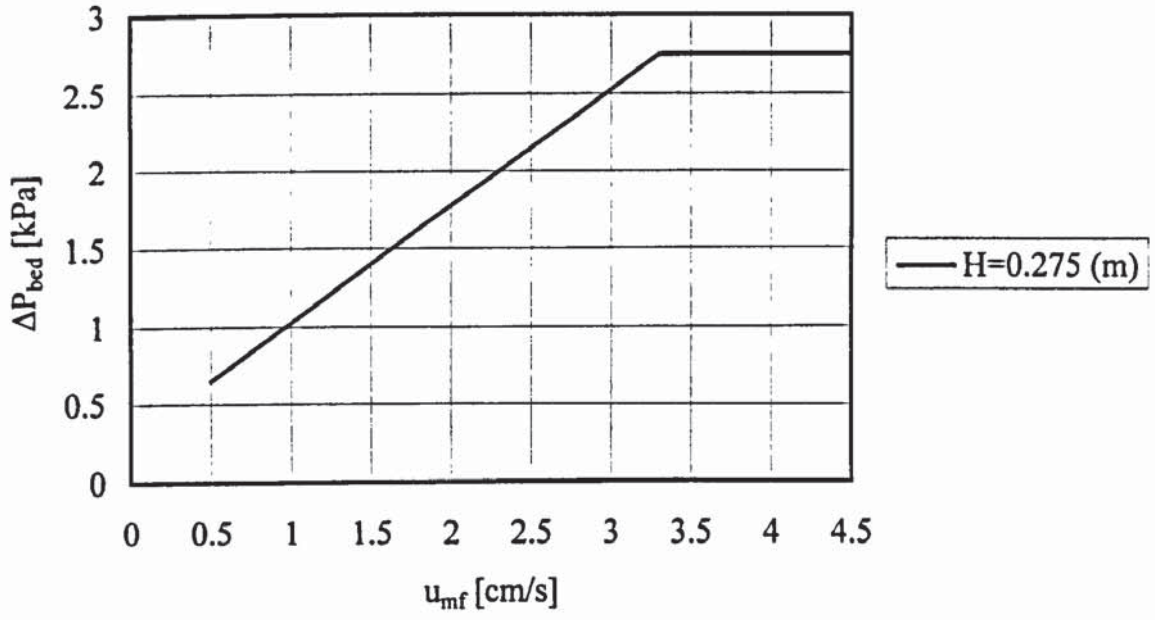

Figure 2A-3: Determination of MFV for a bed height of 0.275 m

The mean MFC for these three experiments is 0.03375 m/s. For the various practical calculations in this thesis an approximate value of 0.35 cm/s was employed.

Appendix 3: Design of air distributor

Experience shows that gas distributors should have a sufficient pressure drop to achieve equal flow through the openings. It is necessary therefore that the pressure drop accross the distributor be considerably larger than the inherent resistance to rearrangement of the incoming gas (Kunii and Levenspiel, 1969). As a generous estimate, the rearrangement resistance can be taken to be in the order of magnitude of the expansion loss when the flow passes from the inlet connection into the vessel. Richardson (1961) suggests that the ratio of distributor to expansion loss be taken as 100.

Agarwal *et al.*, (1962) recommended in addition that pressure drop across the distributor plate be roughly 10 % of pressure drop across the bed, Δp_{bed}, with a minimum in all cases of about 35 cm H_2O.

Summarising the above conditions, the pressure drop, $\Delta P_{d,min}$, across the distributor of orifice or slit type is given by Eq. 3A-1 as described by Kunii and Levenspiel (1969):

$$\Delta P_{d,min} = \text{Max}\,(0.1\,\Delta P_{bed};\ 35\text{ cm } H_2O;\ 100\,\Delta P_{\text{expansion into vessel}}) \qquad \text{(Eq. 3A-1)}$$

The above equation can be used as a design criterion for the minimum recommended pressure drop across distributors of the orifice or slit type.

Assuming no preheating of the fluidizing air, the pressure drop over the bed, ΔP_{bed}, is given by (Kunii and Levenspiel, 1969):

$$\Delta P_{bed} = H\,(1-\varepsilon_{mf})\,(\rho_s-\rho_g) \qquad \text{(Eq. 3A-2)}$$

where

H	bed height at minimum fluidization conditions	[m]
ε_{mf}	voidage at minimum fluidization conditions	[-]
ρ_s	sand density	[kg/m^3]
ρ_g	air density	[kg/Nm^3]

Assuming H=0.40 m, ε_{mf}=0.5, ρ_s=2500 kg/m^3, ρ_g=1.293 kg/Nm^3, Eq. 3A-2 becomes:

$$\Delta P_{bed}=0.40 \text{ x } (1-0.5) \text{ x } (2500-1.293) \Rightarrow$$

$$\Delta P_{bed}=500 \text{ kg-wt/m}^2 \Rightarrow 0.1\Delta P_{bed}=50 \text{ kg-wt/m}^2 \qquad \text{(Eq. 3A-3)}$$

This value is well below the minimum acceptable recommended one by Eq. 3A-1. It is thus decided to apply the second term of Eq. 3A-1 as the limiting condition:

$$\Delta P_{d,min}=35 \text{ cm } H_2O \Rightarrow \Delta P_{d,min}=350 \text{ kg-wt/m}^2$$

(Eq. 3A-4)

The third term of Eq. 3A-1 is rarely applied for two reasons:

a. The expansion loss in circular and even conical inlets is very small and hence the rearrangement resistance is negligible.

b. In order to determine the pressure drop due to the expansion into the vessel, the velocity of gas in the orifice must be known.

The Reynolds number for the total flow approaching the plate will now be calculated

$$Re = D_B \rho_s u_o/\mu_g$$

(Eq. 3A-5)

where

D_B	bubbling fluidized bed diameter (=0.172)	[m]
ρ_g	gas (air) density (=1.293)	[kg/Nm^3]
u_0	superficial gas velocity	[m/s]
μ_g	gas (air) viscosity (=1.8 x 10^{-5})	[kg/ms]

Assuming a value of u_o=0.35 m/s, Eq. 3A-5 becomes:

$$Re = 0.17 \times 1.293 \times 0.35/(1.8 \times 10^{-5}) \Rightarrow Re=4274$$

This value of Reynolds number corresponds to an orifice coefficient, see Figure 3A-1, of 0.6 (C_d=0.6), which indicates that the gas flow is in the transition range, i.e. from laminar to turbulent flow (2000<Re<10000).

Figure 3A-1: Orifice coefficient versus Reynolds number (Perry, 1963)

The velocity of air through the orifices, u_{or}, measured at gas approach density (ρ_s=1.293 kg/Nm^3) and temperature (20° C), will now be determined.

$$u_{or}=C_d(2g_c\Delta P_d/\rho_g)^{1/2} \qquad \text{(Eq. 3A-6)}$$

where

g_c	conversion factor(=9.81)	[m^2/s]
ΔP_d	pressure drop over the distributor	[cm H_2O]
C_d	orifice coefficient, Figure 3A-1	[-]

Combining Eq. 3A-4 and Eq. 3A-6 u_{or} is obtained:

$$u_{or}=0.6 \text{ x } (2 \text{ x } 9.80 \text{ x } 350/1.293)^{1/2} \Rightarrow u_{or}=43.7 \text{ m/s} \qquad \text{(Eq. 3A-7)}$$

The ratio of the gas velocity upstream, u_o, over gas velocity through the orifices, (u_o/u_{or}) gives the fraction of open area in the distributor plate. This open area is an empirical parameter, signifying the total surface area of the orifices in relation to the surface area of the distributor. In normal applications it is less than 10 % in order to ensure sufficient pressure drop over the distributor. Considering Eq. 3A-7, the following relationship is derived:

$$u_o/u_{or}=0.35/43.7=0.008 \Rightarrow u_o/u_{or}=0.8\ \% \qquad \text{(Eq. 3A-8)}$$

Hence, the above, i.e. less than 10 % free fraction area in the distributor palate, limitation is met.

The number of orifices per unit distributor area, N_{or}, can now be calculated by using the following equation:

$$u_o = A_{or} u_{or} N_{or} \qquad \text{(Eq. 3A-9)}$$

where

A_{or}	cross sectional area of an orifice($=\pi d_{or}^2/4$)	[m^2]
N_{or}	number of orifices per unit distributor area	[number/m2]

Eq. 3A-9 is further modified to give:

$$u_o = u_{or} N_{or} \Rightarrow N_{or} = 4(u_o/u_{or})/(\pi\, d_{or}^2) \qquad \text{(Eq. 3A-10)}$$

The relationship between the number and size of orifices is further estimated from Eq. 3A-10. The actual number of orifices in the distributor plate, $N_{or,d}$, may now be estimated by:

$$N_{or,d} = N_{or} A_B \Rightarrow N_{or,d} = N_{or}(\pi D_B^2/4) \qquad \text{(Eq. 3A-11)}$$

Finally, combining equations Eq. 3A-10 and Eq. 3A-11, a correlation between, is obtained:

$$N_{or,d} = (u_o/u_{or}) \times (\pi D_B/d_{or})^2 \qquad \text{(Eq. 3A-12)}$$

Tabulating d_{or}, N_{or} and $N_{or,d}$, the possible combinations shown in Table 3A-1 below may be derived.

Table 3A-1: Combinations between d_{or}, N_{or} and $N_{or,d}$

d_{or} (orifice diameter)	0.5	1	1.5	2	2.5	3	3.5	4
N_{or} (number/m^2)	40744	10186	4527	2546	1630	1132	832	637
$N_{or,d}$ (actual number of orifices)	925	232	103	58	37	26	19	15

Orifices which are too small (<1 mm) are liable to become clogged, whereas those which are too large (>3 mm) may cause uneven distribution of gas. Taking into account these considerations, the orifice diameter, d_{or}, was chosen to be 1.5 mm, which gives a number, $N_{or,d}$, of orifices in the distributor plate.

Finally, a gas distributor with 109 1.5 mm diameter orifices was constructed, shown in Figure 3A-2.

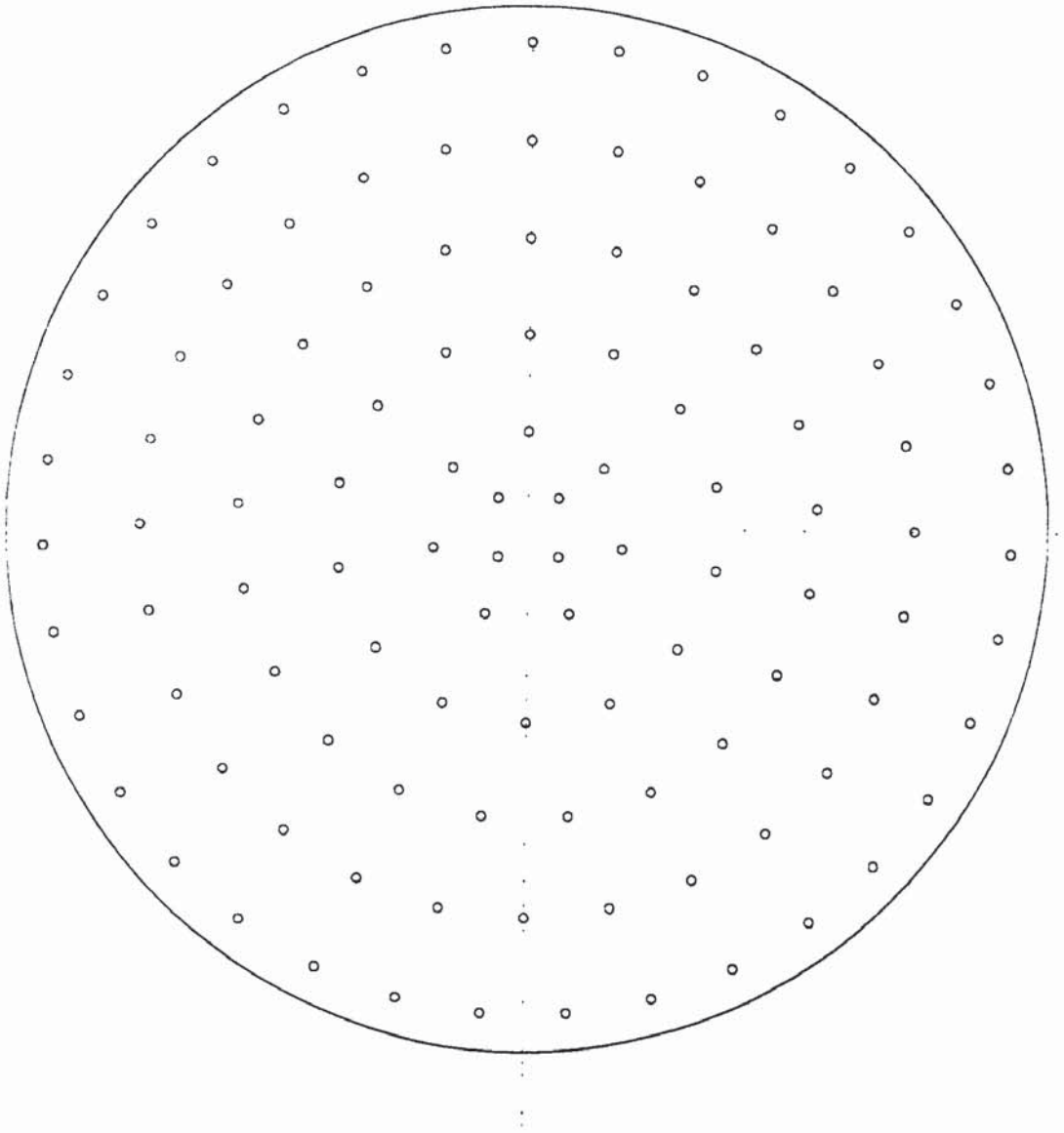

Figure 3A-2: The gas distributor of the CFB system (shown in scale 1:1)

Appendix 4: Detailed design of the CFB fast pyrolysis reactor

In this appendix the detailed drawings of the Circulating Fluidised Bed reactor, the char combustor and the solids recovery system (2 cyclones in series) is shown in Figures 4A-1, 4A-2 and 4A-3 respectively.

The construction material was AISI 316 L and the thickness of the equipment between 3-4 mm in order to achieve an acceptable resistance to the abrasion phenomenon, readily encountered in CFB reactors.

Details about the design and construction of the gas distributor plate have already been given in Appendix 3.

Biomass was fed into the CFB riser section via the lower feeding port, Figure 4A-1. Although alternate feed ports for biomass feeding have been considered, the upper feeding port was never used because of the very low gas/vapour resistance time already achieved when the lower feeding port was employed, Table 9-3 in Chapter 9.

The CFB reactor was heavily equipped with thermocouples and pressure transmitters as well as with a number of electrical resistances which allowed rapid heat-up periods. The location of these devices as well as additional comments concerning their performance may be found in Chapter 7.

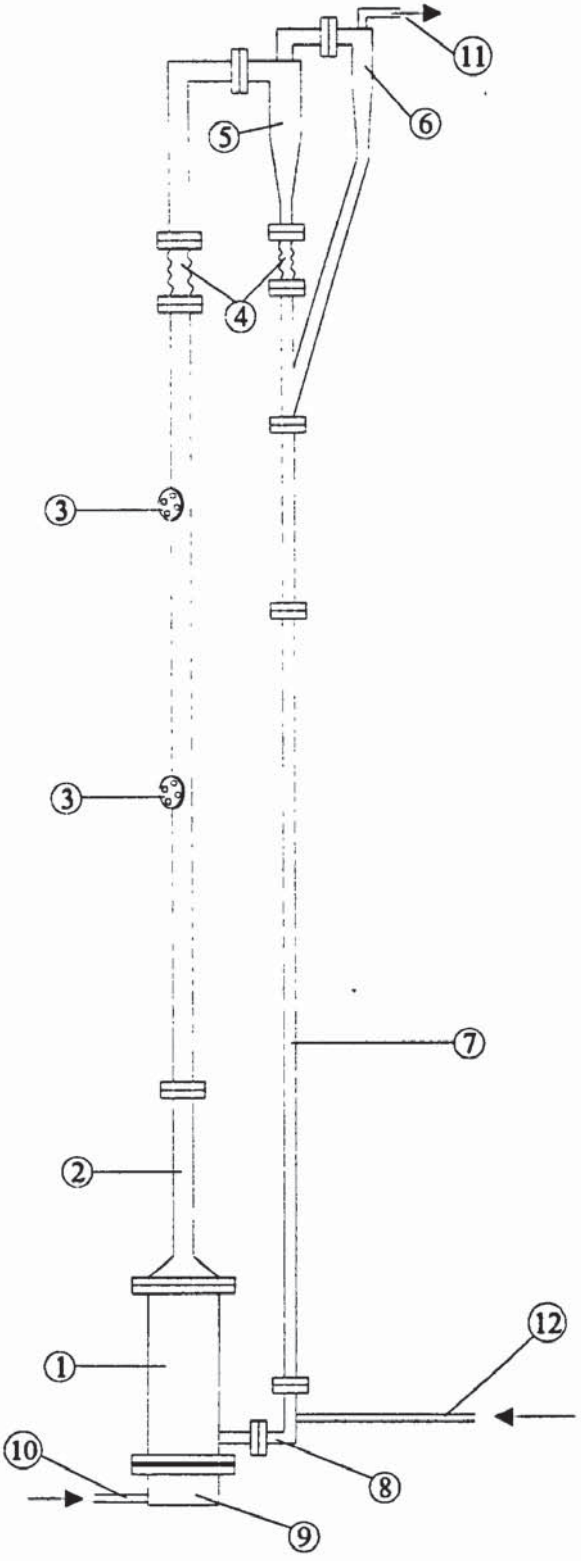

Figure A4-1: The Circulating Fluidized Bed (CFB) fast pyrolysis reactor (scale 1:20)
(1-combustion chamber, 2-riser (pyrolysis reactor), 3-alternate feed ports, 4-expansion joints, 5-primary cyclone, 6-secondary cyclone, 7-standpipe, 8-L-valve, 9-windbox, 10-fluidizing gas inlet, 11-product gas outlet, 12-aeration gas inlet)

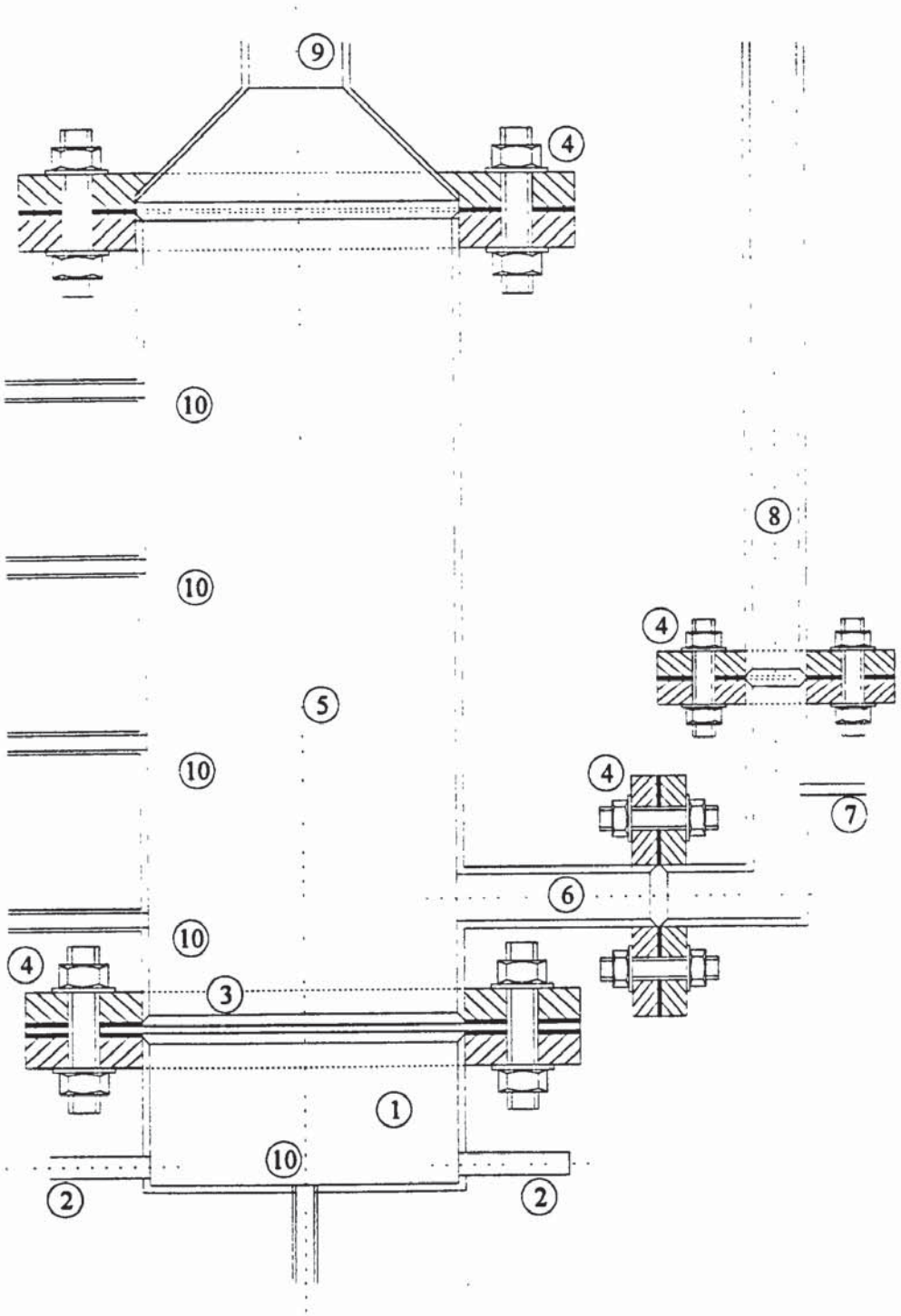

Figure 4A-2: The char combustion chamber (Scale 1:4)

(1-windbox, 2-fluidizing gas (air) inlets, 3-distributor, 4-flange, 5-char combustion chamber (bubbling fluidized bed), 6-L-valve, 7-aeration gas inlet, 8-standpipe, 9-riser, 10- thermocouple port)

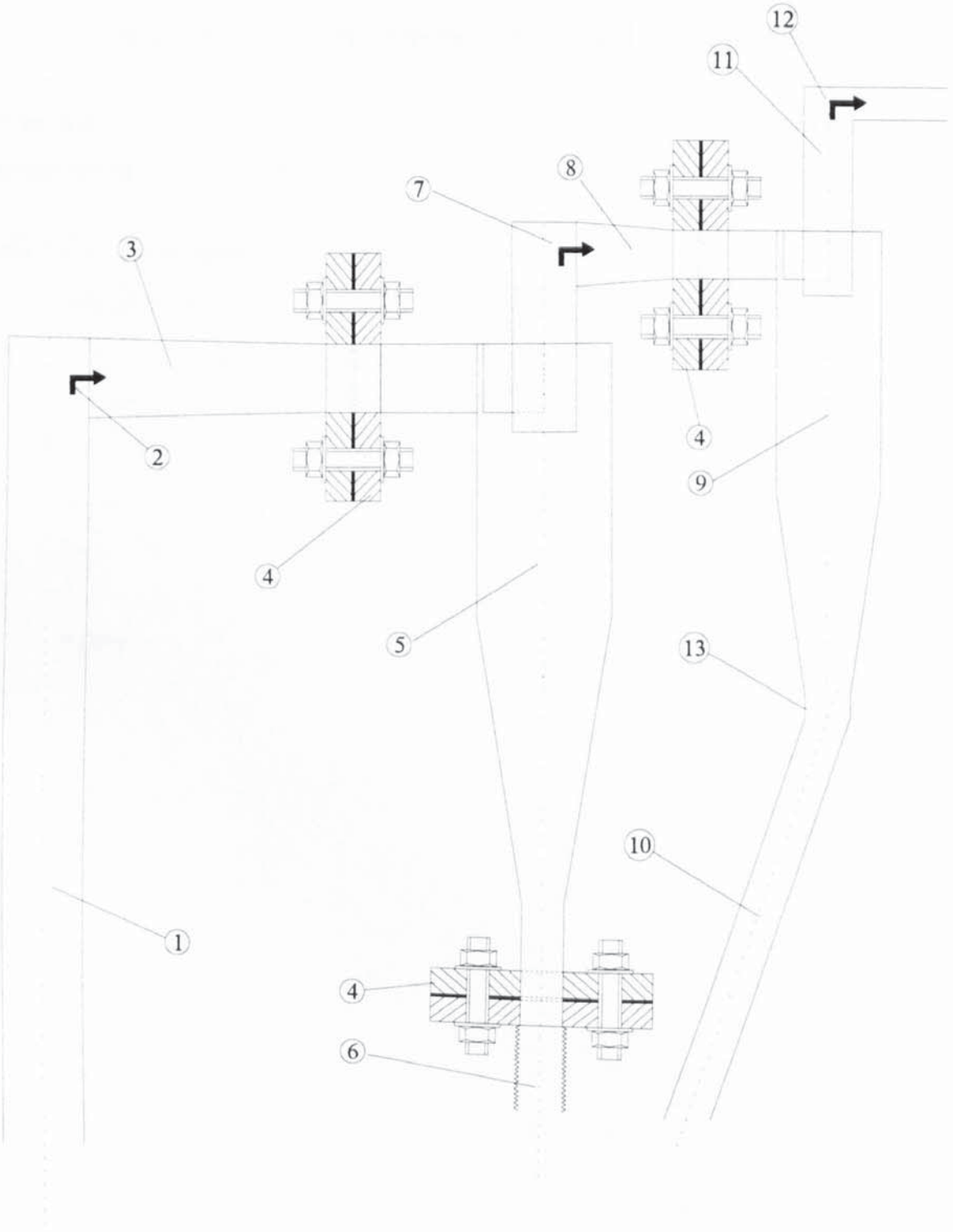

Figure 4A-3: Gas/vapour outlet and solids recovery system (Scale 1:4)

(1-riser, 2-sand, char and product gas suspension to cyclones, 3-riser exit, 4-flange, 5-primary cyclone, 6-expansion joint, 7-fine char and product gas stream, 8-primary cyclone exit, 9-secondary cyclone, 10-inclined solids return standpipe, 11-secondary cyclone exit, 12-product gas to downstream processing)

Appendix 5: Screen separator technical characteristics

The technical characteristics of the screen separators used for biomass screening are summarised in Table 5A-1 below.

Table 5A-1: Sieve separator characteristics

Manufacturer	SWECO-Belgium
Power Consumption	0.33 HP
Operating Voltage	380V/50 Hz
Protection Class	IP 55
Rotation velocity	1500 rpm
Max. Torque	8kgm
Screen diameter	24 in (600 mm)
Bottom motor weight	4.115 kg

Appendix 6: Publications

A list of publications which were completed during the course of the thesis are given below. Most of the publications have been incorporated into the thesis as chapters or parts of chapters.

Fully referreed

1. I. Boukis, K. Maniatis, A.V. Bridgwater, V. Vassilatos and Sp. Kyritsis, "Design Concept and Hydrodynamics of an Air-Blown Circulating Fluidized Bed Reactor for Biomass Flash Pyrolysis", in *Advances in Thermochemical Biomass Conversion*, A.V. Bridgwater (ed.), Interlaken, Switzerland (11-15 May, 1992).

Non-refereed

1. I. Boukis, K. Maniatis, Sp. Kyritsis, Ch. Sooter, "Flash Pyrolysis of Biomass", in *Energy from Biomass Contractors' Meeting*, Florence, Italy (20-22 Nov. 1990).
2. I. Boukis, K. Maniatis, Sp. Kyritsis, Ch. Sooter, "Flash Pyrolysis of Biomass in a Circulating Fluidized Bed", in *6th European Conference on Biomass for Energy*, Industry and Environment, Athens, Greece, (22-26 April 1991).
3. I. Boukis, K. Maniatis, Sp. Kyritsis, V. Vassilatos, I. Filtris and Ch. Sooter, "Development of a Novel Reactor for Biomass Flash Pyrolysis", in *3rd European Symposium-Soft Energy Action at the Local Level*, Chios-Greece (11-14 April 1991).
4. I. Filtris, I. Boukis and V. Vassilatos, "Pressure Measurements at a Tool for the Prediction of Hydrodynamics in a Circulating Fluidized Bed", BPU-1, in *1st General Conference of the Balkan Physical Union*, Thessaloniki, Greece, (26-28 Sep. 1991).
5. I. Boukis, K. Maniatis and Sp. Kyritsis, "Flash Pyrolysis of Biomass in a Bench Scale Fluidized Bed Plant", in *Thermochemical Biomass Conversion Coordination Contractors' Meeting*, Gent, Belgium (29-31 Oct. 1991).
6. I. Boukis and A.V. Bridgwater, "Design Concept and Hydrodynamics of an Air-Blown Circulating Fluidized Bed Reactor for Biomass Flash Pyrolysis", in *Proceedings of the Biomass Pyrolysis Oil Properties and Combustion Meeting*, Sep. 26-28, 1994, Estes Park, Colorado, NREL-CP-430-7215 pp. 137-150 (1994).

7. I. Boukis, L. Gabriel, V. Vassilatos and Sp. Kyritsis, "Biomass Flash Pyrolysis in a Circulating Fluidized Bed Reactor", in *Proc. of 8th EC Conference on Biomass for Energy, Environment, Agriculture and Industry*, 3-5 Oct., 1994, Vienna, Austria, Chartier, Ph., Beenackers, A.A.C.M. and Grassi, G., (eds.), Pergamon, pp. 1887-1893 (1995).

8. I. Boukis, "Practical Implications during Operation of a CFB Air-Blown Pyrolyser", in *Proc. of 2nd EC-Canada Workshop on Thermal Biomass Processing*, 4-5 October, 1995, Toronto, Canada, A.V., Bridgwater and E.N. Hogan (eds.), CPL Press, pp. 49-65 (1995).